Parameterization of *In Silico* Oral Disposition Models: Focus on Pediatrics

by

Anil Maharaj

A thesis
presented to the University of Waterloo
in fulfillment of the
thesis requirement for the degree of
Doctor of Philosophy
in
Pharmacy

Waterloo, Ontario, Canada, 2017

Examining Committee Membership

The following served on the Examining Committee for this thesis. The decision of the Examining Committee is by majority vote.

External Examiner	Dr. Jane Alcorn
Supervisor	Dr. Andrea Edginton
Internal Member(s)	Dr. Nikoletta Fotaki Dr. David Edwards
Internal-External Member	Dr. George Dixon

Author's Declaration

I hereby declare that I am the sole author of this thesis. This is a true copy of the thesis, including any required final revisions, as accepted by my examiners.

I understand that my thesis may be made electronically available to the public.

Abstract

Owing to their biologically relevant design, physiologically-based pharmacokinetic (PBPK) models require quantitative knowledge of organism anatomy and physiology to facilitate appropriate parameterization. Within such models, an intrinsic relationship exists between the quality of input parameters and the confidence bestowed upon simulated outputs. Therefore, in order to instil confidence in PBPK model predictions of pediatric pharmacokinetics (PK), a fundamental understanding of age-specific changes in anatomy and physiology is required. However, due to a lack of consensus and general paucity of biological data denoting pediatric gastrointestinal (GI) physiology, parameterization of mechanistic oral disposition models in this population is quite challenging. The current dissertation expands our understanding of the ontogeny of key physiological aspects regulating oral drug disposition and serves to highlight differences between children and adults. In addition, the thesis describes essential processes involved in the development of pediatric PBPK models as well as demonstrates the use of such models as tools for identification of human physiological values – a utility that is of potential interest particularly for children, where several biological knowledge gaps persist.

To illustrate the key processes involved in the rational development of pediatric PBPK models, a structured workflow was proposed and subsequently utilized to develop age-specific PK predictions for the benzodiazepine, lorazepam. Literature-based assessments of the age-dependency of small intestinal transit time (SITT), GI solubility, and α-1-acid glycoprotein (AAG) employed different methodologies. To discern the influence of age on SITT, random-effects meta-regression models were employed. Investigations assessing age-specific changes in GI fluid parameters (i.e. pepsin, bile acids, pH, osmolality, etc.) were collected from the literature and served to define the composition of a novel set of pediatric biorelevant media representative of the stomach and upper small intestine. Solubility assessments were conducted for seven BCS Class II compounds within the developed pediatric media and a set of reference adult media. Plasma AAG concentrations were assessed in both healthy subjects and those suspected of infection. The analysis evaluated use of linear, power, exponential, log-linear, and sigmoid Emax models to describe the ontogeny of AAG. Predictive performance of the most suitable ontogeny model was evaluated with regards to its ability to estimate pediatric fraction unbound in plasma ($f_{u,p}$). Predictive performance was measured using average-fold error (AFE) and absolute average-fold error (AAFE) as measures of bias and precision, respectively. To demonstrate the use of PBPK modeling to facilitate predictions of human physiology, plasma concentration-time data depicting oral administration of acyclovir and chlorothiazide in adults were utilized to generate model-

based estimates of small intestinal water volume (SIWV). Estimates were based on a framework that consisted of a whole-body PBPK model integrated with a compartmental absorption and transit (CAT) model.

Use of the proposed workflow permitted for the development of age-specific PBPK models that provided relatively accurate estimates of lorazepam PK in children in comparison to a competing modeling technique (i.e. Population PK modeling). For SITT, age was not found to be a significant modulator. With regards to the age-dependency of GI solubility, for six of the seven BCS class II compounds investigated, solubility fell outside an 80-125% range from adult values in at least one of the developed pediatric media. The ontogeny of AAG was best approximated using a sigmoid Emax model in both healthy and infected subjects. For estimation of pediatric $f_{u,p}$, the AAG ontogeny equation derived from this work (AFE 0.97; AAFE 1.24) provided a superior predictive performance in comparison to a previously proposed equation (AFE 0.74; AAFE 1.45). Model-based predictions of SIWV (~116 mL) closely approximated experimentally determined *in vivo* estimates, demonstrating the utility PBPK modeling as a rational method for investigating aspects of human physiology. The presented work serves to improve the parameterization of PBPK models tasked with simulating oral drug disposition in children; however, more research is still required to address additional knowledge gaps associated with pediatric GI physiology.

Acknowledgements

I would like to acknowledge my doctoral supervisor, Dr. Andrea Edginton, for her ongoing support throughout my graduate studies. The work presented in this dissertation is, in large part, a testament to her mentorship and guidance. The time and effort Dr. Edginton has invested into ensuring my success as a future researcher is unmeasurable, and for this, I am truly grateful.

I would like to thank Dr. Nikoletta Fotaki for her guidance over the last few years. Due to her support and leadership, my time at the University of Bath was both academically successful as well as personally rewarding. I will always look back with great adoration at my time in Bath.

Finally, I would like to acknowledge my mother, Molly Maharaj, for her continued support and love over the course of my life. It was through her encouragement that I decided to pursue a graduate degree at the University of Waterloo. She represents a consistent driving force in my life that inspires me to take chances, try new things and, above all, to always be mindful of others.

Dedication

I dedicate this thesis to my grandmother, Sarjudayia Bansee. Despite not being formally educated, my grandmother instilled in me the importance of higher education from a young age. Throughout the years, she's encouraged me to pursue my interests and offered unwavering support towards my ever-changing list of hobbies. To me, she is the true embodiment of both strength and kindness.

Table of Contents

List of Figures

List of Tables

List of Abbreviations

AAFE - absolute average fold-error

AAG - alpha-1-acid glycoprotein

AAG_{max} - maximum alpha-1-acid glycoprotein (sigmoid Emax model)

ABC - ATP-binding cassette

ACAT - advanced compartmental absorption and transit

ADAM - advanced dissolution, absorption, and metabolism

ADME - absorption, distribution, metabolism, and excretion

AFE - average fold-error

AIC - Akaike information criterion

$AUC_{0\text{-}inf}$ - area under the plasma concentration-time curve from 0 to infinity

B:P – blood-to-plasma ratio

BCRP - breast cancer resistance protein

BCS - Biopharmaceutics Classification System

BPCA - Best Pharmaceuticals for Children Act

Caco-2 - human colon carcinoma cell line

CAT - compartmental absorption and transit

CL - clearance

C_{last} - last observed drug concentration

Cl_{int} - intrinsic clearance

C_{max} - maximum drug concentration

C_{min} - minimum drug concentration

C_{peak} – maximum drug concentration post-dose

C_{trough} – minimum drug concentration post-dose

CRM - certified reference material

C_s - compound specific saturation solubility

CV - coefficient of variation

CYP - Cytochromes P450

D/S - dose-to-solubility ratio

ER_h – hepatic extraction ratio

F - bioavailabilitly

F_a - fraction of oral dose absorbed within the intestine

FaSSGF- fasted-state simulated gastric fluid

FaSSIF- fasted-state simulated intestinal fluid

FDA – United States Food and Drug Administration

FDAMA – Food and Drug Administration Modernization Act

FDASIA - Food and Drug Administration Safety and Innovation Act

fe - fraction of dose excreted renally unchanged

FeSSGF- fed-state simulated gastric fluid

FeSSIF- fed-state simulated intestinal fluid

FFA – free fatty acids

F_g - fraction of absorbed dose escaping gut wall metabolism

F_h - fraction of dose escaping hepatic metabolism

fm - fraction of dose metabolised

$f_{u,b}$ – fraction unbound in blood

$f_{u,p}$ – fraction unbound in plasma

GA – gestational age

GET - gastric emptying time

GFR - glomerular filtration rate

GI – gastrointestinal

H - hematocrit

H_2 – hydrogen

HPLC - high performance liquid chromatography

HPLC-UV - high performance liquid chromatography with ultraviolet detector

ICU - intensive care unit

IV - intravenous

IVIVC – *in vitro* – *in vivo* correlations

ka - absorption rate constant

Kd - first order dissolution rate constant

Km - Michaelis constant; substrate concentration yielding half maximal velocity

Kp - Tissue: plasma partition coefficients

LITT - large intestinal transit time

logP - octanol–water partition coefficient

LW - liver weight

MAD - maximum absorbable dose

MCT - monocarboxylate transporter

MDR2 - multi-drug resistance-associated protein 2

MLE - maximum likelihood estimation

MRI - magnetic resonance imaging

mRNA - messenger ribonucleic acid

MRT – mean residence time

MWCO - molecular weight cut-off

NaTc - sodium taurocholate

NCA - non-compartmental analysis

NEC – necrotizing enterocolitis

NICU - neonatal intensive care unit

NIH - National Institutes of Health

OATP - organic anion-transporting polypeptide

OCT - organic cation transporter

OCTT - orocecal transit time

OSF - ontogeny scaling factor

P - hill coefficient (sigmoid Emax model)

PAMPA - parallel artificial membrane permeability assay

P-BCS - Pediatric Biopharmaceutics Classification System

PBPK - physiologically-based pharmacokinetic

PD - pharmacodynamics

P_{eff} – effective intestinal permeability

PEPT - oligopeptide transporter

P-FaSSIF-150% - pediatric FaSSIF formulated with bile salt concentrations 150% of adult levels

P-FaSSIF-50% - pediatric FaSSIF formulated with bile salt concentrations 50% of adult levels

P-gp - P-glycoprotein

PICU - pediatric intensive care unit

Pi-FaSSGF- pediatric FaSSGF representative of infants (1-12 months)

Pi-FeSSIF – pediatric FeSSIF representative of infants (1-12 months) fed cow’s milk-based formula

PK - pharmacokinetics

PMA - postmenstrual age

PNA - postnatal age

Pnb-FeSSIF – pediatric FeSSIF representative of neonates fed breast milk

Pnc-FeSSGF – pediatric FeSSGF representative of neonates fed cow's milk-based formula

Pnc-FeSSIF – pediatric FeSSIF representative of neonates fed cow's milk-based formula

Pn-FaSSGF- pediatric FaSSGF representative of neonates

Pns-FeSSGF – pediatric FeSSGF representative of neonates fed soy-based formula

PopPK – population pharmacokinetic

PREA – Pediatric Research and Equity Act

PxSA - permeability x surface area product

Q_h – hepatic blood flow

r - Pearson's correlation coefficient

R^2 - coefficient of determination

REML - restricted maximum likelihood

RMSE - root mean squared error

SA – intestinal surface area

SD - standard deviation

SE_{LN} - log-normal standard error

SEM – standard error of the mean

SITT - small intestinal transit time

SIWV - small intestinal water volume

SR - sustained-release

TM_{50} - age at half-maximal alpha-1-acid glycoprotein levels (sigmoid Emax model)

t_{max} – time of where maximum concentration is observe

UGT - uridine 5'-diphospho-glucuronosyltransferase

USNRP - United States National Reference Preparation for Serum Proteins

Vmax – enzymatic maximum velocity

VPC - visual predictive checks

V_{ss} – steady-state volume of distribution

$\frac{P_{ped}}{P_{adult}}$ - ratio of pediatric-to-adult plasma protein concentrations

λz - elimination rate constant

τ^2 - between-study variance

Chapter 1: Introduction and Background

Portions of this chapter are reflective of an original manuscript published by the Ph.D. candidate (Anil R Maharaj) in the journal CPT: Pharmacometrics & Systems Pharmacology. All pertinent dialogue included in this chapter was written by the Ph.D. candidate.

Maharaj AR, Edginton AN. Physiologically based pharmacokinetic modeling and simulation in pediatric drug development. CPT Pharmacometrics Syst Pharmacol. 2014;3:e150. doi:10.1038/psp.2014.45.

1.1 Pediatric Age Groups

Children represent a heterogeneous group in terms of growth and maturation and are typically subdivided based on their stage of development. For example:

i) Neonate (birth to 1 month)
ii) Infant (1 month to 2 years)
iii) Child (2 years to 12 years)
iv) Adolescent (12 years to 18 years)

The above terms resemble those employed by the United States Food and Drug Administration (FDA) [1] and are qualitatively utilized throughout this thesis with one notable exception. Within chapter 4 (Assessment of Age-Related Changes in Pediatric Gastrointestinal Solubility), the term ‘infant’ is truncated to only include subjects between the ages of 1 month to 1 year.

1.2 Legislation regulating pediatric drug development

The relative disparity of drug information among children in comparison to adults has long been noted by the medical community [2]. The reasons behind this trend are multifactorial but essentially correspond to ethical (e.g. obtainment of consent) and logistic issues (e.g. recruitment of patients, limitations on the number of biological samples per child) associated with conducting pediatric interventional research [3, 4]. With recent data indicating only 46% of drug products with potential pediatric implications being adequately labelled for use in children [5], practitioners are often compelled to treat children using off-label drug therapies. Off-label medication use among pediatric inpatients is particularly high. For example, some institutions have denoted rates as high as 60% of

prescriptions [6, 7]. These rates are of particular concern due to a well-established positive association between adverse drug events and off-label drug usage [8, 9]. The relative lack of pediatric drug information represents a systemic problem and, as such, is not only confined to inpatient institutions. Recently, medications available to children on an outpatient basis have raised concerns among regulatory authorities. In 2008, Health Canada issued an advisory indicating that common over the counter cough-and-cold medications be relabelled to indicate that such products not be used by children below the age of 6 [10]. In the issued advisory, Health Canada recognized that although these medications have had a long history of use in children, there was still only limited evidence to support their effectiveness.

In recognition of the knowledge gap associated with pediatric drug research, the FDA introduced the FDA Modernization Act (FDAMA) and the Pediatric Rule in 1997 and 1998, respectively. The FDAMA represented the first piece of legislation which offered financial incentives to drug companies in the form of six additional months of patent exclusivity for performing pediatric research [11]. Unlike the FDAMA, which was voluntary, the Pediatric Rule mandated pharmaceutical companies to conduct pediatric research for applications involving new active ingredients, dosage forms, routes of administration, dosing regimens, or indications [12]. In 2002, the FDAMA was extended by the Best Pharmaceuticals for Children Act (BPCA) [13], which added provisions by which off-patent drugs could be investigated. Furthermore, the Pediatric Rule was replaced in 2003 by the Pediatric Research Equity Act (PREA) [14]. Both the BPCA and PREA were permanently reauthorized in 2012 by the FDA Safety and Innovation Act (FDASIA) [15] and represent the current legislation pertaining to pediatric drug research in the United States. Furthermore, the FDASIA expanded the PREA to include a provision requiring sponsors to submit a pediatric study plan to the regulatory body by the end of Phase 2 trials. Plans should provide a prospective outline of pediatric studies the sponsor plans to conduct in support of their application. The directive towards early implementation of pediatric investigations is also iterated by the European Medicines Agency, which advises sponsors to submit a pediatric investigation plan as early as the completion of healthy subject pharmacokinetic (PK) studies (i.e. Phase 1 trials) [16].

Due the abovementioned legislative directives, the past decade has seen an unprecedented increase in pediatric focused drug research, advancing the state of medical care amongst children [17]. To balance this increased demand for pediatric research with the desire to protect study participants from risks associated with clinical investigations, the use of modeling and simulation has been supported as a rational means for informing the design of pediatric clinical studies [18]. Modeling and

simulation can support several aspect of pediatric trial design including estimation of pediatric specific dosages, identification of optimal PK or pharmacodynamic (PD) sampling schemes, and tabulation of appropriate sample sizes (i.e. number of participants) [19]. Overall, modeling and simulation permits for the development of informative pediatric trials that maximize information gathered while reducing the burden imposed on study subjects (e.g. minimizing the number of biological samples per patient, reducing the number of pediatric study participants). In recognition of these benefits, the FDA's Advisory Committee for Pharmaceutical Science and Clinical Pharmacology unanimously voted in a March 2012 meeting (National Harbor, MD) to support the motion that modeling and simulation be considered for all pediatric drug development programs. During the same meeting, the committee also assessed whether the routine use of physiologically-based pharmacokinetic (PBPK) modeling, when possible, be incorporated into the pediatric drug development process. Although the committee expressed concerns regarding limitations and knowledge gaps surrounding pediatric PBPK modeling (i.e. ontogeny of transporters), the motion passed with a slim majority by members who felt PBPK modeling offered an enhanced ability for predicting and understanding age-related changes in PK amongst children.

1.3 Physiologically-based pharmacokinetic models

This section will provide a brief description of whole-body PBPK modeling and its applicability to pediatric drug development. Whole-body PBPK models strive to provide a comprehensive depiction of compound PK throughout the entire body. A general schematic depiction of the structure of a whole-body PBPK model is illustrated in Figure 1.1 [20]. Dissimilar to empirically derived compartmental PK models (Figure 1.2) where compartments represent the sum of kinetically similar tissues, whole-body PBPK models segregate compartments based on anatomical considerations. Model structure is comprised of multiple compartments each representing a defined organ/tissue space. Drug movement is facilitated by assigning flow rates to each compartment reminiscent of a circulatory system. Flow is unidirectional, permitting movement of drug from the arterial pool, through the tissues, and into the venous pool. Typically, systems operate in a loop, permitting venous blood to be recycled back into the arterial pool via the lung. Within the model, clearance (metabolism or excretion) can be ascribed to any relevant tissue compartment. Commonly, the body's two main eliminatory organs, the liver and kidney, play predominant roles in modulating drug clearance. To computationally account for clearance as well as the rate of drug exchange between blood and tissue compartments, models utilize a series of

differential equations. Therefore, provided models are programmed appropriately, simulations should exhibit preserved mass balance throughout the entire time course.

Figure 1.1 Schematic depiction of a whole-body PBPK model

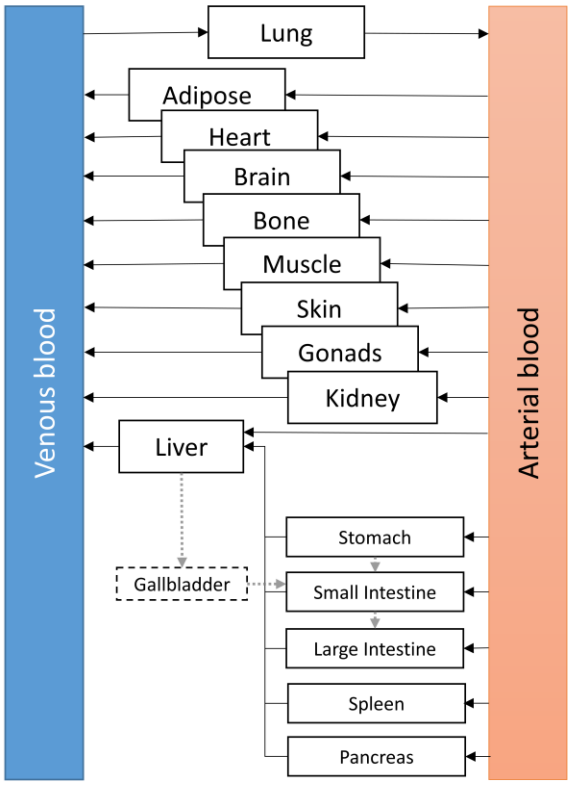

Figure 1.2 Schematic depiction of an empirically derived compartmental model (e.g. two compartment model) [V_1 and V_2 denote the volumes of the central and peripheral compartments, respectively; k_{12} and k_{21} represent the distributional rate constants; and k_{10} denotes the elimination rate constant]

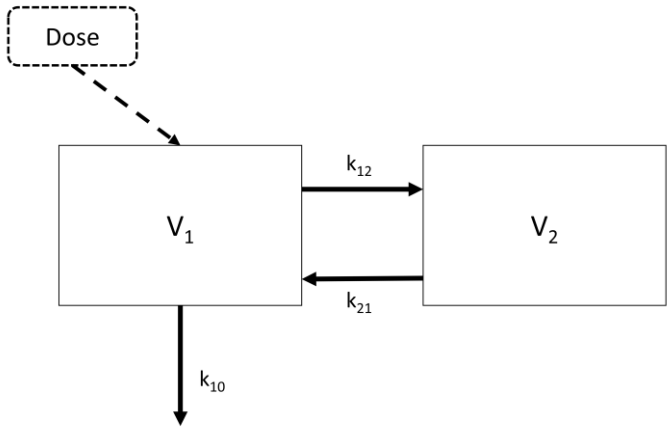

The rate of distribution into tissue compartments may be defined as either perfusion-limited or permeability-limited. For smaller lipophilic compounds, distribution into compartments is typically a function of the rate of blood flow to the tissue (i.e. perfusion-limited). For larger hydrophilic molecules, distribution across tissue membranes may be restricted. In these cases, the rate of tissue distribution must be described using permeability-limited kinetics [20].

PBPK models provide an integrative platform for incorporating several levels of information: physicochemical, *in vitro*, preclinical, and clinical. These various data sources serve to inform model parameterization. Model parameters can be defined as either system or drug-specific. System-specific parameters pertain to the anatomy and physiology of the organism under study. Examples include organ volume, composition and blood flow; enzyme/transporter localization and abundance; and plasma protein concentrations. Drug-specific parameters pertain to drug physicochemical properties (e.g. lipophilicity, molecular weight, pKa, solubility, etc.) and their biological binding affinities (e.g. towards plasma proteins, enzymes, and transporters). Based on the inter-relationship between system and drug-specific parameters, tissue-to-plasma partition coefficients (Kp) and quantitative measures of specific clearance pathways (e.g. whole organ intrinsic clearance - CL_{int}) can be derived. Owing to its physiologically-based structure and parameterization, PBPK models permit for extrapolation of PK estimates between developmentally unique age groups as well as different species. As models are

mechanistic, extrapolations can be conducted by modifying system-specific parameters towards the organism or age group of interest while maintaining an understanding that drug-specific parameters remain constant. This is dissimilar to empirically derived compartmental models where compartments typically do not maintain a physiologic basis, limiting their applicability for fostering predictions of PK outside the range of data used in model development. The ability of PBPK models to extrapolate knowledge between age groups is highly advantageous towards the field of pediatric drug development. The platform permits for PK data from adults, which is relatively abundant, to be leveraged to provide rational estimates of PK in children.

PBPK modeling is frequently described as a 'bottom-up' approach as its design quantitatively incorporates preexisting information regarding anatomic/physiologic parameters and their influence on the processes governing PK [21]. By maintaining these relationships within its structure, PBPK models provide pediatric researchers with an innovative approach to assess the ramifications of developmental changes in anatomy/physiology on compound PK in an *a priori* manner. Based on the utility of PBPK models to garner informative predictions of pediatric PK, interest amongst the pharmaceutical industry has increased. This is demonstrated by the proportion of Investigational New Drug and New Drug Applications containing pediatric PBPK modeling techniques received by the FDA between 2008 and 2013 [22]. Of the 84 applications which incorporated PBPK modeling into their submissions, 21% were utilized to investigate PK amongst children.

1.4 Structured workflows

The key steps associated with the development of pediatric PBPK models have been described in two recently published workflows [21, 23]. These workflows denote relevant information requirements for pediatric PBPK model development as well as a general methodology for their creation. Notably, both workflows denote the importance of development and evaluation of an adult PBPK model prior to extrapolation towards children. Based on this retrospective methodology, the relative wealth of adult PK information can be leveraged in the development of pediatric models. The use of such workflows can potentially impact the pediatric drug development process by ensuring pediatric PBPK models are developed in a systematic and rational fashion. This would permit for standardization of regulatory submissions and allow for expedited regulatory reviews.

Chapter 2 of this thesis will demonstrate how such workflows can be utilized to support pediatric research and development. The chapter will propose a workflow for facilitating the

development of pediatric PBPK models and utilize it to develop age-specific predictions of lorazepam PK amongst children. Lorazepam, an intermediate acting benzodiazepine, is administered for a variety of 'off-label' indications in children including status epilepticus, chemotherapy induced nausea and vomiting, anxiety, sedation, and procedural amnesia [24]. Despite extensive use among pediatric patients [25, 26], further information is still needed to adequately define its safety, efficacy, and PK, as demonstrated by lorazepam's inclusion on the National Institutes of Health (NIH) priority list of medications requiring urgent pediatric studies in 2003 [27]. The chapter provides the reader with a detailed description of each step in the model development process using a functional example. The work will demonstrate how multiple levels of information (e.g. *in vitro* microsomal studies, *in vivo* adult PK data) can contribute towards the development of informative pediatric PBPK models. Furthermore, the workflow proposed within the chapter reflects the currently accepted paradigm of how PBPK models should be developed to support pediatric drug development research.

1.5 Mechanistic oral absorption modeling

PBPK models tasked with simulating intravenous (IV) drug administration are associated with higher levels of accuracy in comparison to models simulating oral drug delivery. This notion has been previously corroborated by Poulin et al. [28] who compared the predictive accuracy of adult PBPK models (IV and oral) at recapitulating plasma concentration-time profiles for a set of 16 compounds. Based on an aggregated metric that combined elements of curve shape and non-compartmental descriptors (i.e. $AUC_{0\text{-}inf}$ and C_{max}), the authors found that PBPK models simulating IV administration were able to achieve a medium to high degree of accuracy in 69% of the modeled compounds; whereas, models simulating oral drug absorption were only able to achieve this level of accuracy in 20% of the studied drugs. This pattern of decreased predictive capacities of PBPK models describing oral drug administration is not confined to adults. Three recent publications pertaining to the development of pediatric PBPK models for voriconazole and sotolol have denoted inaccuracies associated with predictions of oral drug disposition, especially in younger subjects such as neonates [29-31].

This discrepancy in predictive performance associated with PBPK models simulating oral drug administration can be linked to the complex milieu of physiological and environmental factors that interact within the gastrointestinal (GI) tract to facilitate oral absorption. In order to predict the rate and extent of oral absorption, a fundamental understanding of several processes including drug dissolution, drug degradation, gastric emptying, intestinal transit, drug diffusion/permeation, and first pass

metabolism is required. [32]. Within the context of PBPK models, oral absorption is typically accommodated via the incorporation of sub-models tasked with providing mechanistic descriptions of the abovementioned processes. For example, to facilitate *a priori* predictions of oral drug absorption, most commercially available modeling platforms (i.e. Gastroplus®, PK-Sim®, SimCyp®) have integrated a derivation of the compartmental absorption and transit (CAT) model, as originally described by Yu et al. [33], into their whole body PBPK model structure.

The CAT model was originally developed to describe the transit kinetics of the small intestine, which is generally regarded as the primary site of oral compound absorption [34]. Based on small intestinal transit data derived via scintigraphy from over 400 human subjects, Yu et al. [33] found that a multi-compartment model incorporating 7 compartments provided the best fit with observed data. Compartments were linked by a unified first-order transit function to describe flow along the small intestine. In a subsequent publication, the authors demonstrated the capacity of the CAT model to facilitate predictions of oral compound absorption (Figure 1.3) [35]. When combined with data from regional intestinal permeability studies in adults, the CAT model provided a good agreement between predicted and observed fractions absorbed in humans for ten compounds.

Figure 1.3 Schematic depiction of a CAT model used to facilitate predictions of oral compound absorption [ks – first-order gastric emptying rate; kt – first-order intestinal transit rate; and ka – first-order absorption rate constant]

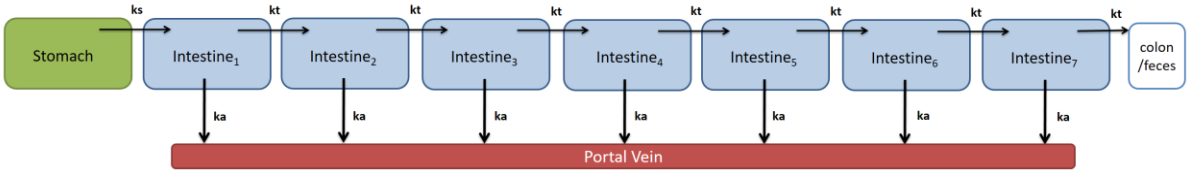

Contemporary oral absorption models (e.g. ACAT model) have expanded the scope of the original CAT model to accommodate additional compartments to describe transit within the stomach as well as transit and absorption within the large intestine. Current models permit for compartments to be uniquely parameterized with dissimilar pH values, fluid volumes, transit rates, and surface areas based on regional specific (e.g. jejunum vs. ileum) anatomic/physiologic values. Unlike the original CAT model, where drug could only persist within the dissolved state, current models permit drug to persist in several forms including unreleased, undissolved, dissolved, degraded, metabolized, and

absorbed [36]. With the inclusion of empiric as well as mechanistic dissolution functions, models can now simulate a variety of drug release profiles.

Unless contrary evidence suggests otherwise, PBPK models assume oral absorption of dissolved drug transpires via passive absorption [20]. Estimates of intestinal permeability can be attained using a variety of approaches including *in vivo* based regional perfusion systems (i.e. Loc-I-Gut), *in vitro* based assays (i.e. PAMPA, Caco-2), or *in silico* based algorithms which derive estimates based on compound physico-chemistry [37]. Models can also include phenomena such as luminal degradation by including compartment specific degradation rate constants [36]. Lastly, with the addition of enterocytic compartments adjacent to the above-illustrated luminal compartments, models can incorporate processes such as gut metabolism and active transport (influx/efflux), provided data regarding regional distribution of intestinal enzymes and transporters are available.

Based on their mechanistic design and physiologic relevant parameterization, PBPK models establish an intuitive link between the quality of input parameters (e.g. human anatomic/physiologic data) and the accuracy of model predictions. Correspondingly, the poor precision of oral PBPK models, as described above, speaks to both the complexity and the lack of quantitative information regarding GI physiology in humans.

Prediction of pediatric oral absorption using a PBPK based approach adds an extra layer of complexity owing to the need to parameterize models in an age-specific manner. Notably, development of such models requires an innate understanding of how GI physiology changes as a function of age from birth to adulthood. For example, effective parameterization of a pediatric oral absorption model would require information characterizing age-dependent changes in GI pH, luminal fluid composition, intestinal fluid volume, gut surface area and length, transit times, and enzyme/transporter localization and abundance. Unfortunately, many of these parameters have yet to be fully elucidated within pediatrics. In the context of pediatric PBPK modeling, many researchers will simply assume that parameters such as gastric emptying time (GET) [30], small intestinal transit time (SITT) [29] and intestinal solubility [38] in children are comparable to that of adults. Due to a lack of consensus and general paucity of biological data denoting pediatric GI physiology, many of these assumptions have yet to be confirmed. As a result, there is a need for high quality research examining developmental differences in the processes governing oral absorption. By improving our understanding of pediatric GI physiology, such research will permit for effective PBPK model parameterization and subsequent improvements in pediatric PK predictions.

1.6 Establishing confidence in PBPK model predictions

Based on a 2010 guidance document pertaining to the characterization and application of PBPK models in risk assessment published by the International Programme on Chemical Safety (IPCS) [39], establishment of confidence in PBPK model predictions should incorporate three aspects: comparisons between simulations and observed data, evaluation of the biological basis of the model, and assessments of model uncertainty and sensitivity. Comparisons between model simulations and observed data can be instituted using a variety of metrics. For evaluating precision with regards PK measures such as $AUC_{0\text{-}inf}$, C_{max} and t_{max}, metrics such as absolute average fold error (AAFE), root mean squared error (RMSE), the mean ratio (obs/pred), and proportion of estimates falling within a specified fold-error (i.e. 2-fold, 3-fold etc.) have been utilized [28, 29, 40]. Additionally, assessments of model predictive performance for simulating concentration-time values can include qualitative measures such as visual predictive checks (VPC) [40]. In children, the development of PBPK models may serve as the initial exploration of pediatric PK. In such cases, *in vivo* PK data to appraise the accuracy of simulations will likely be nonexistent among children. However, a key process in the development of pediatric PBPK models, which will be described in more detail in Chapter 2, involves initial development and evaluation of an adult model. In this regard, available PK data in adults can be utilized to assess the predictive accuracy of simulations generated from the adult PBPK model. This evaluation provides information regarding the model's suitability for performing pediatric extrapolations. Models that display good agreement with observed adult data are perceived to have an increased reliability for fostering predictions of pediatric PK. In contrast, models that depict deviations from observed data sets are perceived to be of low reliability. Such models should not be utilized for pediatric model development but instead be reevaluated for the etiology of their poor predictive performance. Based this methodology, evaluations using adult PK data can serve to inform the subsequent development of pediatric PBPK models.

Evaluation of the biological basis of the model assesses fidelity of the model's structure and parameters. Regardless of a model's ability to recapitulate observed *in vivo* datasets, PBPK model structure and parameterization should remain biologically realistic. For example, adult models that incorporate parameter values that are biologically unrealistic (e.g. glomerular filtration rate (GFR) that exceeds the upper limit of normal) are of questionable reliability for the subsequent development of pediatric PBPK models. Confidence in model predictions is, therefore, contingent on a structure and parameterization that are biologically representative of the organism of interest. This concept highlights the pivotal need for research in defining the developmental physiology of the GI tract in pediatrics.

Without a clear understanding how GI parameters responsible for modulating oral disposition change as a function of age, we cannot be assured that pediatric PBPK models are parameterized in physiologically relevant manner.

Lastly, assessments of model uncertainty and sensitivity can also serve to characterize the reliability of model predictions. Uncertainty analyses focus on the spread or distribution of simulated outputs due to the ambiguity surrounding input parameters and model structure. For sensitivity analyses, the emphasis is shifted towards quantitatively describing the influence of model parameters on modulating simulated outputs. Uncertainty analyses can be conducted in an iterative manner by incorporating the potential range of ambiguous parameter values into simulations. The level of uncertainty is then determined based on the ratio of the 95^{th} percentile to the median value for the selected output metric (e.g. AUC, C_{max}, etc). Quantitative measures of sensitivity can be attained by varying individual model parameters by 1% and evaluating the impact on simulated outputs. Based on the relationship between uncertainty and sensitivity, inferences regarding model reliability can be attained. For example, models possessing parameters with high uncertainty and high sensitivity are presumed to have a low reliability. In contrast, models possessing parameters with either low uncertainty or low sensitivity are considered to possess a high reliability. Key parameters postulated to have sensitivity (i.e. high sensitivity) towards oral compound absorption are highlighted by the maximum absorbable dose (MAD) equation [41].

$$MAD = P_{eff}\ x\ SA\ x\ SITT\ x\ C_s \quad \text{(Equation 1.1)}$$

Briefly, the equation denotes that the upper limit of oral absorption can be attributed to intestinal permeability (P_{eff}), intestinal absorptive surface area (SA), small intestinal transit time (SITT), and intestinal solubility (C_s). With regards to pediatric oral absorption modeling, such parameters have yet to be appropriately defined in an age-specific manner (e.g. high uncertainty). As such, the reliability of PBPK models at simulating oral absorption among children may be of questionable reliability.

1.7 Literature-based assessments of the ontogeny of biological parameters affecting oral compound disposition

Chapters 3, 4, and 5 of this thesis serves to provide focused assessments of the ontogeny of key physiologic parameters responsible for modulating oral drug disposition. The assessments utilize the current literature to quantitate age-specific differences in physiology between children and adults.

Chapter 3 focusses on the parameter small intestinal transit time (SITT). The small intestine is of particular importance as it represents the region where the majority of nutrient and xenobiotic absorption transpires [42]. Correspondingly, knowledge of the time a xenobiotic spends traversing the small intestine is essential towards fostering predictions of oral compound absorption. This is particularly true for poorly absorbed compounds, where the extent of absorption is highly mediated by the time of contact between the compound and the small intestinal epithelium [43].

Chapter 4 provides a comprehensive assessment of age-specific changes in GI fluid composition. The analysis examines changes in luminal bile salt concentrations, pH, osmolality, buffering capacity, and concentrations of fat digestion products between children and adults. Differences in GI fluid composition can translate into alterations in compound luminal solubility [44] - a key parameter influencing oral absorption. As such, quantification of the relationship between age and GI fluid composition is inherently required to facilitate appropriate predictions of pediatric oral absorption. After providing a literature-based assessment of age-related differences in GI fluid composition, the chapter extends these findings by formulating a set of novel pediatric biorelevant media. Biorelevant media attempt to simulate the complex physicochemical nature of *in vivo* GI fluids. When used in conjunction with *in vitro* test (e.g. USP apparatus II -paddle assembly), biorelevant media can provide suitable *in vitro/in vivo* correlations (IVIVC) of oral drug absorption [45, 46]. Developed pediatric media were utilized to perform solubility assessments for 7 Biopharmaceutics Classification System (BCS) Class II compounds. The BCS (Figure 1.4) categorizes compounds based on two properties: aqueous solubility and permeability [47]. Accordingly, compounds can be classified as either BCS I (high solubility, high permeability), II (low solubility, high permeability), III (high solubility, low permeability), or IV (low solubility, low permeability). For BCS Class II compounds, limitations in the extent of oral drug absorption are primarily attributed to inadequate solubility. Therefore, changes in the luminal solubility of such compounds may be suggestive of alterations in oral drug performance [48]. To assess the impact of developmental changes in fluid composition, solubility values determined in age-specific biorelevant media reflective of children and media representative of adults were compared.

Figure 1.4 The Biopharmaceutics Classification System

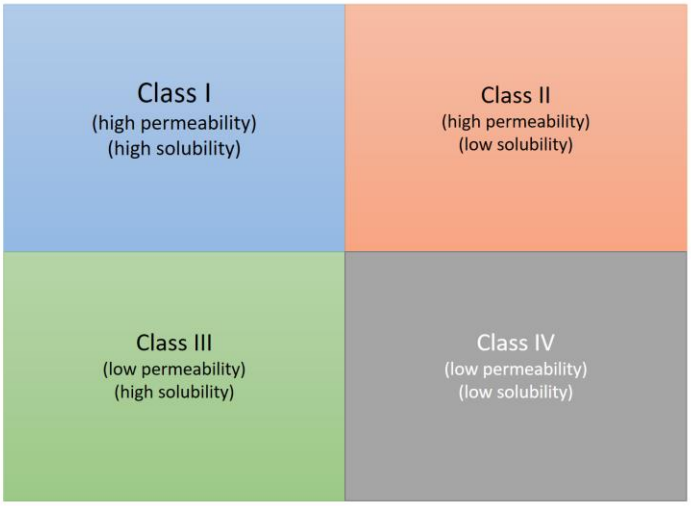

Chapter 5 evaluates the ontogeny of a key plasma protein, α-1-acid-glycoprotein (AAG). AAG exhibits high affinity towards a variety of basic lipophilic compounds, including several exogenously administered xenobiotics [49, 50]. Between children and adults, developmental differences in plasma protein concentrations have been documented [51]. As the extent of xenobiotic-protein binding exhibits a direct relationship to the concentration of plasma proteins, differences in drug-protein binding between children and adults are expected [52]. Within the context of PBPK modeling, the magnitude of xenobiotic-protein binding is parameterized using the fraction unbound in plasma ($f_{u,p}$). This critical parameter can exert profound influences towards the processes of clearance and distribution [49], thus modulating estimates of systemic xenobiotic exposure.

In addition to its effects on systemic PK parameters (e.g. clearance and distribution), alterations in $f_{u,p}$ can influence the availability of orally administered compounds by modulating the degree of hepatic first-pass. Oral bioavailability is primarily contingent on three processes: intestinal absorption, gut metabolism, and hepatic first-pass. The contributions of these processes towards overall bioavailability (fraction of administered drug that reaches the systemic circulation) can be succinctly described using the following equation:

$$F = F_a \, x \, F_g \, x \, F_h \qquad \text{(Equation 1.2)}$$

where F, F_a, F_g, and F_h denote the overall bioavailability, fraction of drug absorbed within the intestine, fraction of drug escaping intestinal metabolism, and the fraction of drug evading liver metabolism, respectively. The effects of liver extraction on F is particularly relevant for high extraction ratio (ER) compounds [53]. ER describes the fraction of drug presented to an eliminatory organ (e.g. liver or kidney) that is removed during a single pass. High ER drugs refer to those compounds that are efficiently removed by an eliminatory organ (ER > 0.7) [54]. The influence of hepatic extraction on F can be described using a simple substitution to the equation depicted above:

$$F = F_a \, x \, F_g \, x \, (1 - ER_h) \quad \text{(Equation 1.3)}$$

where ER_h denotes the hepatic ER. Based on this equation, for compounds with high ER_h, hepatic first-pass metabolism will pose a major limitation towards achieving appropriate oral bioavailability. With regards to the relevance of developmental changes in $f_{u,p}$ to oral bioavailability, the relationship between these two parameters can be illustrated using the following equation [53]:

$$F_h = \frac{Q_h}{Q_h + Cl_{int} \cdot f_{u,b}} \quad \text{(Equation 1.4)}$$

where Q_h is the hepatic blood flow, Cl_{int} is the intrinsic clearance of the liver, and $f_{u,b}$ is the fraction unbound in blood (note: exhibits a proportional relationship to the fraction unbound in plasma). In the case of low ER_h compounds, the $C_{lint}*f_{u,b}$ component of equation 1.4 is minute, allowing the denominator to be simplified as just Q_h. Therefore, changes in $f_{u,b}$ are likely to be inconsequential to the bioavailability of low ER_h compounds. However, for high ER_h compounds, the magnitude of $Cl_{int}*f_{u,b}$ is larger and, thus, cannot be simplified within the denominator. As a result, alterations in $f_{u,b}$ will inversely effect the oral bioavailability of high ER_h drugs. Based on this rationalization, developmental differences in AAG concentrations amongst children may potentiate the presence of age-specific differences in oral bioavailability.

1.8 Utilization of PBPK modeling for optimization of physiological parameters

Chapter 6 demonstrates an alternative use of PBPK models as a platform for parameter optimization rather than its traditional role for generating PK predictions of compound exposure. Within the literature, publications depicting adult PBPK models simulating oral drug absorption have employed CAT sub-models that vary widely in terms of the amount of fluid allocated to the small intestine (e.g. from 250 to 600 mL) [55-58]. Conversely, *in vivo* estimates of small intestinal water volume (SIWV) within adults denote a central tendency between 86-167 mL [59-61]. Since only dissolved drug is permitted to permeate the intestinal membrane, defining of the amount of fluid available within the small intestine is imperative to facilitate predictions of oral drug disposition. As previously iterated in the section pertaining to the use of structure workflows for the creation of pediatric PBPK models, the initial development and evaluation of an adult PBPK model is an essential step for subsequent development of informative pediatric models. Aside from ensuring adult models can recapitulate observed PK data, evaluations should also include an assessment of the model's physiologic fidelity [39]. Adult models incorporating parameters not consistent with known *in vivo* measures are considered to be of low confidence and are, therefore, limited in terms of performing extrapolations towards pediatrics. The methodology employed within Chapter 6 exploits the mechanistic and physiologic basis of PBPK models. Observed plasma concentration-time data following oral drug administration were utilized as an input, subsequently allowing the model to approximate the most appropriate SIWV. The work seeks to define an optimal value for SIWV within adults. Furthermore, comparison of this simulation-based SIWV to physiologically determined values in adults will provide an evaluation the biological relevance of the CAT model. The results of this evaluation will serve to establish a level of confidence attributed to such models and their applicability to perform extrapolations towards children. In addition, the depicted work will clearly define how the small intestinal water is distributed within the context of multi-compartmental absorption models (i.e. CAT models) - an aspect that is also of interest to the parameterization of pediatric absorption models.

1.9 Overarching Thesis Objective

To increase the knowledge base associated with aspects of pediatric physiology that influence oral compound absorption, allowing for effective PBPK model parameterization and increased confidence in model predictions.

1.10 Objectives

a) Propose a structured workflow for scaling PK information from adults to pediatrics using PBPK modeling based techniques and provide a functional example of how such a workflow can be utilized to support pediatric drug development.
b) Conduct critical appraisals of the literature to increase the current state of knowledge surrounding pediatric physiology pertinent to oral drug disposition
c) Demonstrate how systemic exposure data following xenobiotic administration can be utilized to inform PBPK model parameterization

1.11 Hypotheses

a) Utilization of structured workflows for the development of pediatric PBPK models provide a rational means of leveraging adult PK data to foster predictions of pediatric PK
b) Critical evaluations of the current literature can be used to improve the parameterization of pediatric PBPK models tasked with simulating oral drug disposition
c) Human systemic exposure data can be utilized to inform PBPK model parameterization in cases where human anatomical/physiological information is unavailable

Chapter 2: A Workflow Example of PBPK Modeling to Support Pediatric Research and Development: Case Study with Lorazepam

The contents of this chapter are reflective of an original manuscript published by the Ph.D. candidate (Anil R Maharaj) in the American Association of Pharmaceutical Scientists (AAPS) Journal. All pertinent research analyses was conducted by the Ph.D. candidate.

Maharaj AR, Barrett JS, Edginton AN. A workflow example of PBPK modeling to support pediatric research and development: case study with lorazepam. The AAPS journal. 2013;15(2):455-64. doi:10.1208/s12248-013-9451-0

2.1 Introduction

The Food and Administration Drug (FDA) enacted the Pediatric Research Equity Act (PREA) in 2003, requiring pharmaceutical companies to assess pharmacokinetics (PK), safety and efficacy of new drug products in pediatric subjects. Recently, several FDA pediatric submissions have incorporated physiologically-based pharmacokinetic (PBPK) models, stimulating an interest in their utility among regulatory authorities [23]. In a March 2012 meeting, the majority of the FDA's Pharmaceutical Science and Clinical Pharmacology Advisory Committee voted to support the use of PBPK modeling for pediatric drug development; a decision with potential implications towards the manner in which pediatric drug information is derived.

PBPK modelling is characterized by the use of mathematical algorithms to predict the interplay between drug specific characteristics, and organism anatomy and physiology. Similar to empirically derived compartmental models, the structure of PBPK models includes compartments in order to describe the processes of absorption, distribution, metabolism and excretion (ADME). In a PBPK model, however, compartments are based on actual organs with inherent volumes and blood flows linked through the vasculature. The mechanistic nature of PBPK models permit rational scaling between organisms (i.e. rat to human) as well as developmental stages (i.e. adult to child). This is the result of defining ADME as a function of anatomy, physiology and biochemistry; components not accounted for in traditional compartmental models.

Use of pediatric PBPK models offer researchers an *a priori* approach to predict a compound's PK behavior in children, with or without prior PK data in humans, though knowledge of the drug

substance's physicochemical characteristics is essential. The developmental processes involved in the creation of pediatric PBPK models has been documented by several researchers and typically include defining physiology and anatomy, protein binding, and clearance, all as a function of age [62-64]. Amongst the literature, pediatric PBPK models have been utilized in several different capacities: suggesting starting doses for children of different age groups, predictions of environmental contaminant exposure, optimization of clinical drug trial design (sampling schedule, number of patients, etc.), and assessment of potential drug-drug interactions [23, 64-66].

Lorazepam, an intermediate acting benzodiazepine, is administered for a variety of 'off-label' indications in children including status epilepticus, chemotherapy induced nausea and vomiting, anxiety, sedation, and procedural amnesia [24]. Despite extensive use among pediatric patients [25, 26], further information is still needed to adequately define its safety, efficacy and PK, as demonstrated by lorazepam's inclusion on the National Institutes of Health (NIH) priority list of medications requiring urgent pediatric studies in 2003 [27]. Most published literature regarding lorazepam PK parameters (Table 2.1) is primarily focused on an adult patient population. In humans, lorazepam exhibits an affinity for albumin with a bound fraction in plasma of approximately 89% [67-69]. Hepatic metabolism and renal filtration represent the major and minor pathways of clearance, respectively [70-72].

This study will use a systematic workflow to demonstrate how adult drug data is leveraged in the development of pediatric PBPK models. Using lorazepam as an example, a rational prediction of lorazepam PK will be computed as a function of age and further compared to PK data from a pediatric clinical study.

Table 2.1 Physicochemical, ADME, and Anatomic/Physiologic Data for Initial Parameterization of the Adult Lorazepam PBPK Model

Physicochemical	LogP[a]	2.39 [73]
	pKa[b]	1.3 (base), 11.5 (acid) [74]
ADME	fu_p[c]	0.11 [67-69]
	$CL_{int(hep\text{-}UGT2B7)}$[d]	0.439 ml/min/g_{liver} [68, 71, 75-77]
	CL_{GFR}[e]	0.01 ml/min/kg [70-72]
	B:P[f]	0.642 [78]
Anatomic/Physiologic	Organ Size	Generated using simple demographic information (Sex: M, Age: 26.6 yrs, Wt: 68 kg) by methods described in Willman et al 2007 [79].
	Organ Blood Flow	
	Tissue Composition	

Tissue:plasma (Kp) were estimated using the methods described by Rodgers and Rowland [80-82]
Hepatic (plasma) clearance was estimated using a well stirred liver model (equation 2.3)
a: logarithm of the octanol-water partition coefficient (lipophilicity)
b: negative logarithm of the acid dissociation constant
c: plasma fraction unbound
d: intrinsic clearance of hepatic isozyme UGT2B7
e: renal (plasma) clearance due to glomerular filtration
f: blood-plasma partition coefficient

2.2 Methods

2.2.1 Model Building Workflow

Model building workflow: Following the proposed workflow (figure 2.1), the development of a pediatric population PBPK model is presented using lorazepam as an example. The derived model will be used to assess PK differences between children (age 0 – 18 years) and adults.

Figure 2.1 Proposed workflow for scaling adult PBPK models towards children

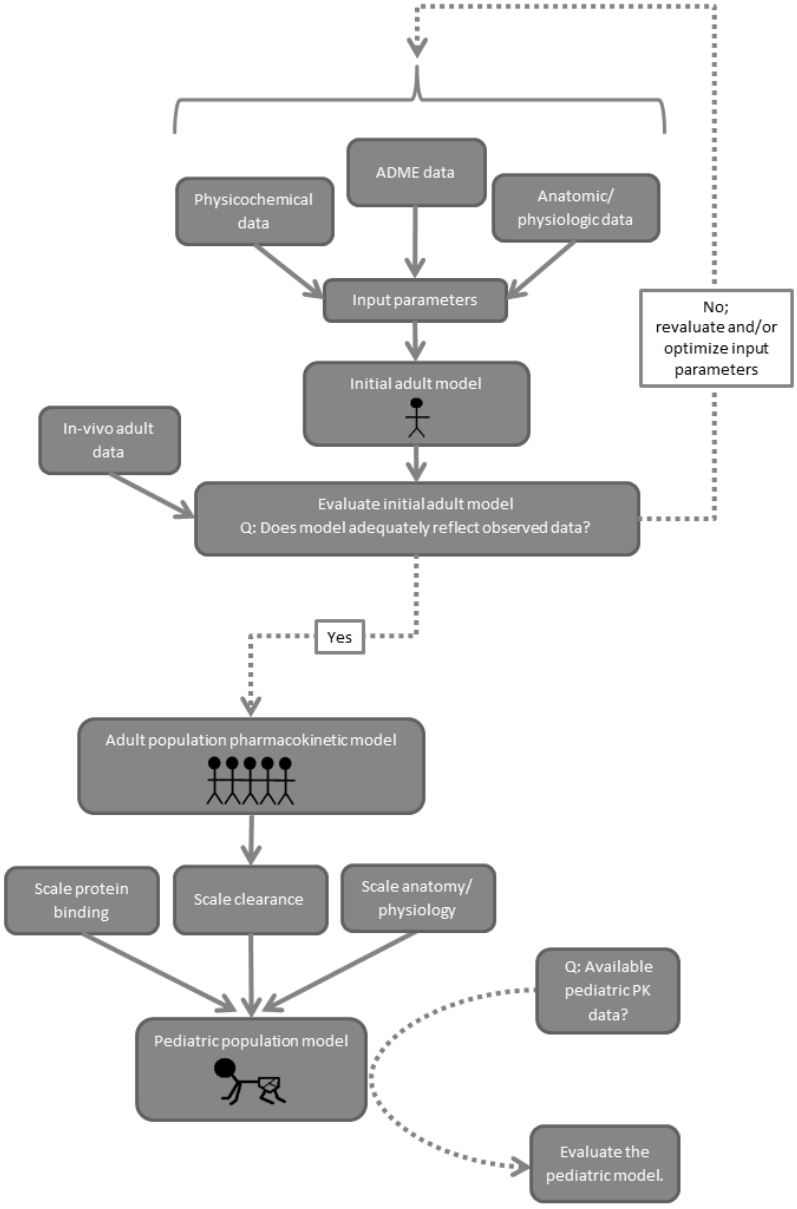

2.2.2 Development of the adult PBPK model

Model structure and parameterization

All simulations (adult and pediatric) were completed using PK-Sim® v 4.2 (Bayer Technology Services, Leverkusen, Germany), which implements a whole-body PBPK model consisting of 15 organs. Due to the physicochemical nature of lorazepam (low molecular weight - < 500 g/mol, moderate lipophilicity and neutral at physiologic pHs) all organs were considered kinetically equivalent to well-stirred compartments with the exception of the brain. PK-Sim® utilizes a permeation barrier between the plasma and interstitial fluid of the brain to simulate the physiologic equivalent of the blood-brain-barrier. Specific physicochemical, ADME, and anatomic/physiologic data used for initial parameterization of the adult lorazepam model are presented in Table 2.1. Tissue: plasma partition coefficients (Kp) were predicted using the *in silico* tissue composition approach proposed by Rodgers and Rowland [80-82]. Using the abovementioned characteristics, an initial adult model was generated.

Optimization of the adult model

Concentration-time data from four separate adult PK studies [71, 75-77] were dose normalized to 2mg and compared to the output of the initial adult PBPK model. Outputs were generated using the average observed clearance in conjunction with the mean age and weight of participants in the studies to define anatomical and physiological values [79]. A visual check was used to evaluate predictive accuracy between simulated (PBPK model) vs. observed concentration-time data and appropriateness of line shape. Subsequently, the model parameters of intrinsic hepatic clearance ($CL_{int(hep\text{-}UGT2B7)}$) as well as lipophilicity (logP), a direct predictor of Kp(s), were optimized using the MoBi® Toolbox for MATLAB® (Bayer Technology Services GmbH, Leverkusen, Germany/ The Mathworks Inc., Natick, MA), an integrative modeling tool that permits parameter analysis. Parameters were iteratively optimized to achieve values which minimized the error between observed and model derived concentration-time points.

Adult Population Model

A virtual population of 100 adult individuals was created using PK-Sim®'s Population Module in order to simulate the effect of anthropometric and intrinsic clearance variability on the PK behavior of lorazepam. The module incorporates the work conducted by Willmann et al. 2007 [79] to create a population of individuals with associated variability consistent with real life observations.

Demographic constraints (sex, age, weight) of the simulated population were reflective of the adult subjects included among the lorazepam PK studies [71, 75-77]. All subjects received a 2 mg intravenous dose, representing a commonly prescribed adult dosage. Inter-patient variability associated with UGT2B7 intrinsic activity, the hepatic enzyme responsible for lorazepam metabolism [83], was estimated from an *ex-vivo* metabolism study for the probe substrate zidovudine using human liver microsomes [84]. As a result, UGT2B7 intrinsic clearance was varied based on a log-normal distribution with a geometric standard deviation of 1.34. The average area under the plasma concentration-time curve to infinity ($AUC_{0\rightarrow\infty}$), a measure of systemic exposure, was tabulated to comparatively assess dosage equivalency between adults and children. Extrapolation to infinity occurred by dividing the final concentration (C_{last}) by the elimination rate constant (λz), where λz was calculated based on a linear regression of the final 10% of predicted time points transformed on the natural log scale. To evaluate the range of PK variability amongst the virtual population, 5% and 95% prediction intervals for concentration-time values were generated and compared to dose normalized observed values (assuming linear PK) from each of the four lorazepam PK studies [71, 75-77].

2.2.3 Age-dependent scaling of PBPK model parameters

Protein binding

Prediction of pediatric protein binding was estimated using equations presented by McNamara and Alcorn [51]. The authors successfully predicted the fraction of protein binding in infants for several compounds using fraction unbound in adults and compound specific plasma protein affinity. For lorazepam, literature data indicates an affinity for albumin and an average fraction unbound (plasma) of 0.11 in adults [67-69].

Clearance

Total clearance of a compound is calculated as the sum of its individual clearance pathways. For lorazepam, the clearance in children was calculated as the sum of scaled hepatic and renal clearances using a physiologically-based approach. The process of physiologic hepatic clearance scaling relies on the following underlying assumptions [83]:

1. pathways of clearance in children are the same as those observed in adults

2. well-stirred model conditions hold (hepatic uptake of the compound is a function of blood flow - not permeability across cell membranes.)
3. enzyme metabolism follows first order kinetics (concentrations are within linear range – no enzyme saturation)

Hepatic UGT2B7 enzyme activity is on average 5% of the adult value at term, increases to 30% by the age of 3 months and reaches adult activity by 1 year of age. To quantify the relationship between age and enzyme activity a cubic spline function, as derived by Edginton et al. [83], was utilized. Scaled intrinsic clearance in pediatric subjects can be calculated from adult values using the following formula [85],

$$CL_{\text{int UGT2B7 (child)g liver}} = OSF_{UGT2B7} \text{ x } \text{CL}_{\text{int UGT2B7 (adult)g liver}} \qquad \text{(Equation 2.1)}$$

where $CL_{\text{int UGT2B7 (child)g liver}}$ is the scaled intrinsic clearance due to UGT2B7 per gram of liver, OSF_{UGT2B7} is the ontogeny scaling factor for UGT2B7 specific to the age of the child, and $\text{CL}_{\text{int UGT2B7 (adult)g liver}}$ is the intrinsic clearance due to UGT2B7 per gram of liver in adults. Total hepatic plasma clearance can be derived from intrinsic clearance using the well-stirred model,

$$CL_{\text{int (child)}_{\text{total liver}}} = \text{CL}_{\text{int UGT2B7 (child)g liver}} \text{ x } \text{LW}_{\text{child}} \qquad \text{(Equation 2.2)}$$

$$CL_{\text{hepatic (child)}} = \frac{\text{Q}_{\text{h (child)}} \text{ x } \text{f}_{\text{u,p(child)}} \text{ x } \text{CL}_{\text{int (child)}_{\text{total liver}}}}{\text{Q}_{\text{h (child)}} + \left(\text{f}_{\text{u,p(child)}} \text{ x } \text{CL}_{\text{int (child)}_{\text{total liver}}}\right) / \text{ B : P}_{\text{(child)}}} \qquad \text{(Equation 2.3)}$$

where $CL_{\text{int (child)}_{\text{total liver}}}$ is the whole liver intrinsic clearance in the child, LW_{child} is the liver weight of the child, $CL_{\text{hepatic (child)}}$ is total hepatic clearance in the child, $\text{Q}_{\text{h (child)}}$ is liver blood flow in the child, $\text{f}_{\text{u,p(child)}}$ is the scaled unbound fraction (plasma) in the child, and $\text{B : P}_{\text{(child)}}$ is the blood:plasma ratio in the child. The B:P ratio is affected by both changes in protein binding and hematocrit and can be tabulated using equations derived by Rodgers and Rowland [82],

$$Kp_{rbc,u} = \frac{B:P_{(adult)} - 1 + H_{(adult)}}{H_{(adult)} \times f_{u,p(adult)}} \quad \text{(Equation 2.4)}$$

$$B:P_{(child)} = 1 + [H_{(child)} \times (f_{u,p(child)} \times Kp_{rbc,u} - 1)] \quad \text{(Equation 2.5)}$$

where $Kp_{rbc,u}$ is the unbound partition coefficient of red blood cells (assumed to be constant between adults and children), $B:P_{(adult)}$ is the blood:plasma ratio in adults, $H_{(adult)}$ is the hematocrit in adults, $f_{u,p(adult)}$ is the fraction unbound (plasma) in adults, and $H_{(child)}$ is the hematocrit of the child [86].

The effects of maturation and growth on renal function were examined in a seminal paper by Hayton [87]. The study proposed a series of equations to estimate renal function parameters, such as glomerular filtration rate (GFR) and active secretion, in children as a function of age and weight. To scale adult renal clearance values towards pediatric patients the estimated GFR of the child, as determined using Hayton's algorithm, was used in conjunction with the following equation proposed by Edginton et al. [83],

$$CL_{GFR\,(child)} = \frac{GFR_{(child)}}{GFR_{(adult)}} \times \frac{f_{u,p(child)}}{f_{u,p(adult)}} \times CL_{GFR\,(adult)} \quad \text{(Equation 2.6)}$$

where $CL_{GFR\,(child)}$ is the child's clearance due to glomerular filtration, $GFR_{(child)}$ is the estimated GFR of the child, $GFR_{(adult)}$ is the GFR in adults (assumed to be 110 ml/min), and $CL_{GFR\,(adult)}$ the clearance due to glomerular filtration in adults.

Anatomy/Physiology

The age dependence of body weight, height, organ weights and blood flows were obtained from Edginton et al. [63] and represent those values currently used as default values in PK-Sim®. The above parameters were derived based on the mean value for European children ranging from neonates to 18 years old.

2.2.4 Age-dependent PK simulations

Pharmacokinetic variability among pediatric populations of various age-groups was assessed by creating virtual populations of 100 individuals aged 0, 3, 7, and 14 days; 1, 2, 3, 6 and 9 months; and 1, 1.5, 2, 3, 4, up to 18 years. All patients received a single 0.05 mg/kg dose of intravenous lorazepam, representing a common pediatric dosage. Inter-patient variability associated with hepatic UGT2B7 intrinsic clearance was assumed to be identical to that of adults. Dosage equivalency between adults and children, the dose (mg/kg) required to achieve an $AUC_{0\rightarrow\infty}$ similar to the average value obtained in the adult population model, was calculated for each simulated population. In addition, to demonstrate the potential utility of this modelling technique, mean tissue concentration-time profiles for targeted organs (adipose, muscle, brain) were simulated for a population of 2 year old patients (n = 100) following a 0.05 mg/kg intravenous dose.

2.2.5 Assessment of model accuracy

The predictive accuracy of the derived pediatric lorazepam model at estimating concentration-time values and PK parameters was evaluated using an observed data set provided by Chamberlain et al. [88]. Concentration-time data from 63 pediatric patients, ranging from 5 months to 17 years of age, who received intravenous lorazepam either electively or part of routine treatment of status epilepticus were included in the sample [88]. Forty of the 63 pediatric subjects received a single intravenous dose of lorazepam. Of these subjects, 15 received lorazepam electively. Pediatric PBPK model concentration estimates were based on simulations incorporating the age, weight, and height for each child, in addition to the dose administered. The predictive accuracy of the pediatric PBPK model for estimating observed concentration-time values for each individual patient was assessed by tabulating the average-fold error (AFE).

$$AFE = 10^{\frac{1}{n}\sum \log\left(\frac{predicted}{observed}\right)} \qquad \text{(Equation 2.7)}$$

Observed PK parameters derived from non-compartmental analysis (NCA) were determined for elective patients (n=15) in whom intense serial sampling was performed following intravenous lorazepam administration [88]. Lorazepam total body clearance (CL) was calculated as Dose/ $AUC_{0\rightarrow\infty}$, where $AUC_{0\rightarrow\infty}$ was determined using the linear-log trapezoidal rule up to the final sample time with extrapolation to infinity based on $C_{last}/\lambda z$. Non-compartmental extrapolation of $AUC_{0\rightarrow\infty}$

was analogous to the approach used for PBPK model assessment but differed in the algorithm used to estimate λz, which was computed based on regression of the natural logarithm of concentration values during the post-distributive phase. The volume of distribution (V_{ss}) was calculated as V_{ss} = MRT*CL, in which MRT is the mean residence time. MRT was calculated as $AUMC_{0\rightarrow\infty}$/ $AUC_{0\rightarrow\infty}$, where $AUMC_{0\rightarrow\infty}$ is the area under the first moment curve from zero to infinity. These parameters were similarly calculated from PBPK model simulations. The relative accuracy of predicted CL and V_{ss} values, as determined by physiologic scaling, were assessed against observed values (NCA) for each patient using fold error.

$$\text{fold error} = \frac{\text{predicted}}{\text{observed}} \qquad \text{(Equation 2.8)}$$

As a final evaluation, the PK variability associated with ontogeny and anthropometrics among a virtual pediatric patient population after receiving a single 0.05 mg/kg intravenous (bolus) dose of lorazepam was compared with individual observed data. Five percent and 95% concentration-time prediction intervals were generated for the entire age range (0-18 years) of the virtual pediatric population with equal representation from each age. The simulated profile was evaluated using individual observed concentration-time data (normalized to 0.05 mg/kg) for 40 of the 63 pediatric patients who received a single intravenous dose of lorazepam [88].

2.3 Results

Mean adult hepatic intrinsic clearance and lipophilicity (logP) values were optimized to 0.416 ml/min/g_{liver} and 2.43, respectively. Figure 2.2A compares the concentration-time profile derived from the optimized adult population model to dose-normalized observed data from 4 PK studies [71, 75-77]. Observed data in the initial phase of distribution were over predicted by the model; however, subsequent data were well described. The range of PK variability for lorazepam associated with a simulated pediatric population (0-18 years) is displayed in figure 2.2B. Approximately 72% of dose-normalized observed lorazepam concentration-time values from a subset of 40 pediatric patients fell within the 90% prediction interval of the simulated population.

The dosage (mg/kg) required to achieve similar $AUC_{0\rightarrow\infty}$ as those observed in adults after a 2 mg intravenous dose of lorazepam varied as a function of age (figure 2.3 A,B). Newborns (0 days old) required approximately $1/10^{th}$ of the weight normalized dose given to adults, whereas infants between

the ages 1 and 3 years required dosages (mg/kg) that exceeded those of adults. After 3 years of age, the weight normalized dose slowly decreased towards adult requirements.

Predicted tissue specific concentrations from the pediatric PBPK model were calculated for a virtual population of 2 year old patients following a 0.05 mg/kg dose of lorazepam (figure 2.4). Estimates indicate that muscle and adipose tissue equilibrate with plasma concentrations at a much faster rate compared to the brain.

The predictive accuracy of concentration-time estimates derived by our pediatric PBPK model was assessed using individual patient AFE values for all 63 sample patients (figure 2.5A). Forty-four percent, 73%, and 92% of patients had AFE values within 1.25, 1.5, and 2 fold deviation from observed values, respectively.

PBPK estimates of CL and V_{ss} were compared to observed values obtained by NCA from the 15 elective patients (figure 2.5 B,C). For CL, 40%, 60%, and 80% of predictions were within 1.25, 1.5 and 2 fold deviation from observed values, respectively. Comparatively, predictions of V_{ss} were relatively more accurate with 53%, 80%, and 100% of estimates within 1.25, 1.5, and 2 fold error from observed values, respectively.

Figure 2.2 (A) Predicted (*solid line* corresponds to geometric mean; *dashed lines* corresponds to 5thand 95thpercentiles; virtual population n=100) versus observed (*symbols* [71, 75-77]) plasma concentration versus time data following a 2-mg IV lorazepam bolus in adults. Log (concentration) versus Log (time) plot is displayed in insert. (B) Predicted (*solid line* corresponds to geometric mean; *dashed lines* corresponds to 5th and 95thpercentiles; virtual population n=1140) versus observed (*symbols* [88]) plasma concentration versus time data following a 0.05 mg/kg IV lorazepam bolus in children aged 0 to 18 years. Log (concentration) versus Log (time) plot is displayed in insert.

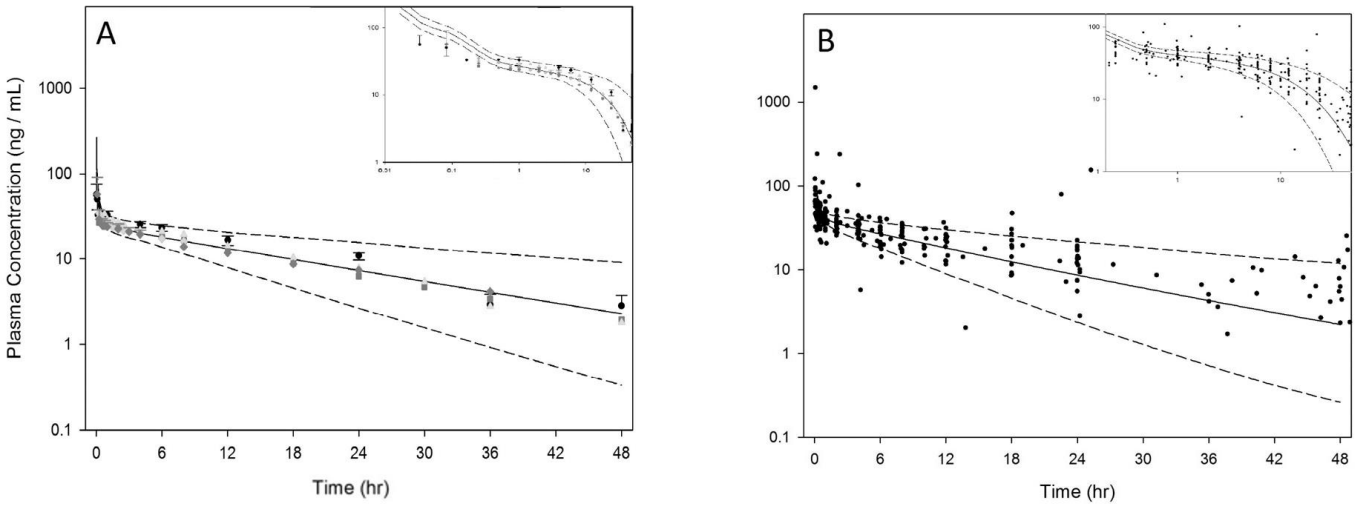

Figure 2.3 Pediatric dose (mg/kg) required to achieve an equivalent $AUC_{0\rightarrow\infty}$ of a 2 mg dose in adults. (A) entire pediatric age-range. (B) children between 0 and 1 years old.

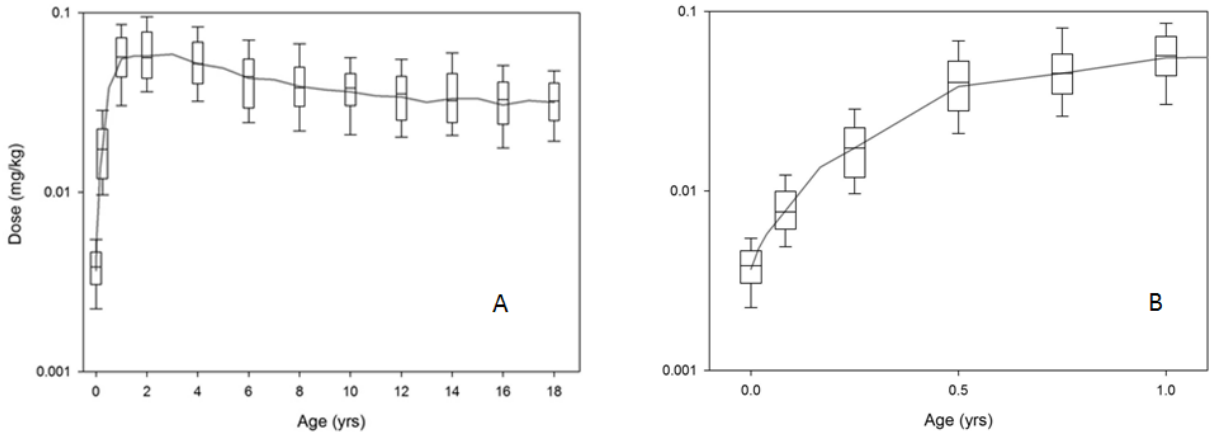

Figure 2.4 Mean tissue concentration-time profiles for selected organs among a virtual population (n = 100) of 2 year old subjects

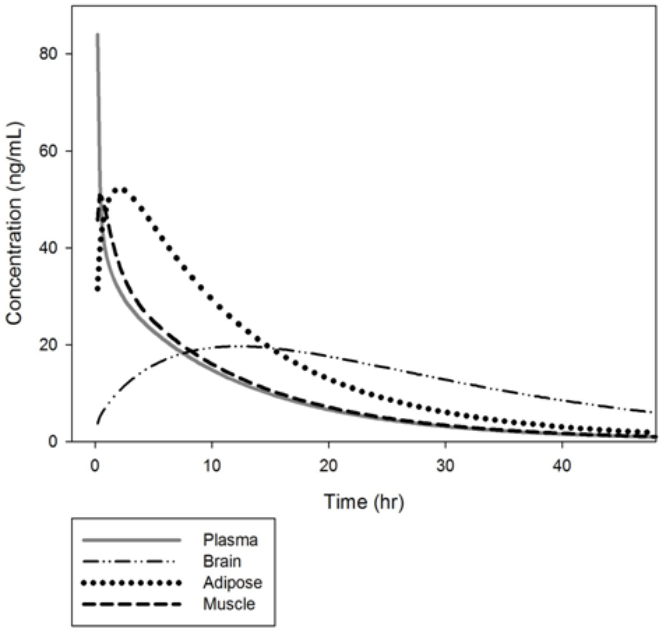

Figure 2.5 Predictive accuracy plots - Individual AFE values for PBPK model concentration-time predictions for the 63 pediatric patients (plot A), fold error associated PBPK model clearance predictions for the 15 elective patients (plot B), and fold error associated PBPK model volume of distribution predictions for the 15 elective patients (plot C). ***(Dotted line represents 1.5-fold error. Dashed line represents 2-fold error)***

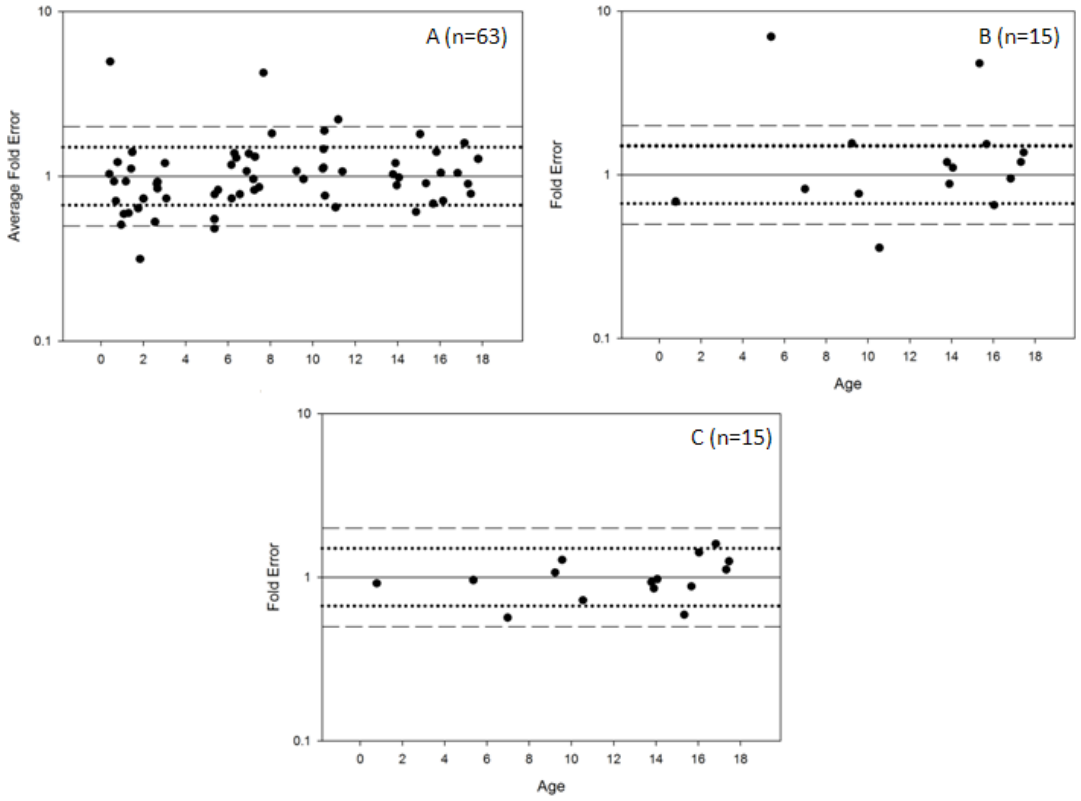

2.4 Discussion

Integration of PBPK modelling with pediatric drug research has been illustrated by five recent FDA submissions [89]. Common applications of modelling in the aforementioned submissions include optimizing study design, recommending starting doses for different age groups, and facilitating covariate analysis. The workflow presented in Figure 2.1 ensures pediatric PBPK models are developed using physiologically rationale approach and incorporates elements from two recently proposed workflows. Similar to Figure 2.1, Leong et al [23] and Edginton [21] both presented workflows which included an evaluation of appropriateness of the adult model prior to scaling. Refinement (optimization) of the adult model was also included by Leong et al. Edginton's use of virtual populations to assess

PK variability among simulated adult and pediatric populations was similar to the approach adopted in this study.

The workflow's evaluation process ensures that the derived adult model adequately reflects *in vivo* PK data. A major underlying assumption involved in physiologic scaling necessitates pathways of clearance in children are the same as those observed in adults. This ensures that physiologic processes accounted for in the adult model will be mirrored in the pediatric model. As such, models displaying poor predictive accuracy in adults should be re-evaluated for missing drug specific information that may explain the discrepancy (i.e. additional transporter affinities, alternative clearance pathways, etc.). Scaling to pediatrics should only be considered for adult models found to be in general agreement with observed data. In order to better represent *in vivo* PK, the modeler may opt to refine the adult model based on observed data prior to scaling towards pediatrics. Input parameters, such as lipophilicity and intrinsic clearance are generally chosen as targets for optimization as a result of uncertainty surrounding literature values of lipophilicity and variability of clearance values between PK studies.

Physiologic scaling also relies on another key assumption in order to extrapolate adult models towards pediatrics: enzyme metabolism follows first-order kinetics. Validation of this assumption would normally require *in vivo* dose escalation studies in pediatric patients; data which is simply unavailable for most compounds. Consequently, we are reliant on adult PK data to estimate the likelihood of enzyme saturation occurring among children. For lorazepam, exposure ($AUC_{0\rightarrow\infty}$) in adults has previously been shown to increase proportionately with intravenous dosage increases from 2 to 4 mg, indicating a lack of saturable metabolism [71].

The derived adult population PK model (figure 2.2A) exhibited an acceptable fit for the majority of observed data with the exception of concentration-time points during the initial phase, post-administration. This lack of fit may be attributed to an unrealistic assumption made by most PK models: initial mixing of blood in the central compartment is instantaneous. As a result, initially simulated concentration-time points may appear erroneously high as they fail to account for the lag time associated with the introduction of the compound to the systemic circulation and its presence at a peripheral sample site [90]. Potential issues related to drug-IV catheter binding may present an alternative explanation for the lack of initial data fit. Reversible binding of drug to the IV catheter would result in delayed administration of the entire dose, resulting in a PK profile similar to a short-term IV infusion as opposed to a bolus dose. Slight over-prediction of initial concentration-time points were also observed in the pediatric population PK model (figure 2.2B), a finding which exemplifies the congruent relationship between the adult and pediatric model.

During the first year of life, increasing UGT2B7 enzyme activity corresponds with increases in weight normalized lorazepam clearance. With dosage rate being directly proportional to clearance, it is not surprising that the dosage (mg/kg) required to maintain a similar $AUC_{0\rightarrow\infty}$ as adults after a 2mg intravenous dose increases during the first year (figure 2.3B). The average dosage requirement in term neonates, where enzyme activity is estimated to be only 5% of adult values, was 0.0037 mg/kg; whereas, adults received approximately 0.03 mg/kg. For pediatric subjects between the ages of 1-3 years, the average weight-normalized clearances exceeded that of adults and, as a result, required increased relative dosages to maintain similar exposure rates. These findings have been corroborated in the literature by studies examining the age-dependence of lorazepam clearance [68, 83]. Using the process of physiologic scaling as outlined in this study, the increased weight-normalized lorazepam clearance simulated in young children aged 1-3 years was a function of complete hepatic UGT2B7 maturation and a higher liver weight: body weight ratio compared to adults.

Current intravenous dosing recommendations for preoperative administration of lorazepam in adults, 0.044 mg/kg (max 2mg/dose) 15-20 minutes before surgery, and in infants and children, 0.05 mg/kg (range: 0.02-0.09 mg/kg) [24], were compared to dosage requirements derived from our simulated pediatric populations. While the suggested pediatric dosing range relates to the majority of the simulated children, neonatal dosing (0 days - 1 month) does not appear to follow the same regimen. Furthermore, the recommendations provided do not incorporate an age-dependence to dosing. Results from our simulations indicate that neonates require substantially lower doses than suggested for infants and children (i.e. 0.05 mg/kg). For example newborns (0 days old) require approximately $1/10^{th}$ (0.0037 mg/kg) of adult doses; whereas, one month old neonates require approximately $1/4^{th}$ (0.0077 mg/kg) of adult doses. Accordingly, dosing recommendations derived from population PBPK models circumvent the use of inexact dosing ranges by assigning a unique dosage to particular age groups.

The utility of PBPK models at estimating concentrations values within specific organs is demonstrated in figure 2.4. These estimates highlight the potential future of PBPK models to create targeted dosing regimens based on *a priori* estimates of drug distribution within specific compartments of interest (i.e. site of action). The plasma concentration simulated by the model is reflective of the overall mass-transfer between all organs. As a result, larger organs to which the drug permeates into (ie. muscle and adipose) will play a larger role in influencing the overall plasma profile compared to smaller organs (brain). By simply evaluating the PBPK model estimates using plasma concentration-time data we are unable to confirm the reliability of individual organ estimates, especially smaller organs which only influence plasma levels minutely. Consequently, in order to increase reliability in

specific compartment estimates, experimental data assessing tissue concentration or effect biomarkers that can link to target concentrations is inherently needed.

Using the presented workflow, retrospective assessment of the derived pediatric model may only take place once sufficient observed data is available. To evaluate our pediatric lorazepam model, concentration-time data from a cohort of 63 pediatric patients was obtained [88]. For the majority of sample patients (approximately 73%), PBPK model concentration estimates were within a 1.5 fold prediction error on average. Additionally, the predicative performance of the pediatric PBPK model at estimating CL and V_{ss} was determined among elective patients (n =15) included in Chamberlain et al.'s study [88]. For CL, 60% of model estimates were within 1.5 fold deviation from observed values. Comparatively, model estimates of V_{ss} were associated with a greater predictive accuracy with 80% of estimates lying within 1.5 fold error.

When attempting to estimate individual subject parameters (i.e. CL and V_{ss}), PBPK models normally incorporate superficial biometric data such as age, weight, and height, to derive a complete physiologic/anatomic depiction of the subject. All physiologic/anatomic values (i.e. organ weights, % enzyme activity) denote values that would be expected from a mean individual of a particular age, weight and height. What this approach does not account for is the intrinsic (inter-patient) variability that underpins biological research (i.e. not all 8 year olds, weighing 35kg, and measuring 120cm will have the same organ weights). Consequently, the accuracy of individualized PBPK model derived parameter estimates will be affected by the magnitude of the inherent inter-subject variability that exists. Data driven population PK estimation techniques represent an alternative approach to estimating individualized PK parameters. Chamberlain et al. [88] found no covariates which were statistically significant to necessitate inclusion into their final PK model. Subsequently, estimates of CL and V_{ss} were predicted using 0.14 L/hr/kg$^{0.75}$ and 1.37 L/kg, respectively. When used to estimate individual PK parameters among the elective group (n=15), this method predicted 47%, 67%, and 80% of CL values within a 1.25, 1.5, and 2 fold deviation from observed values, respectively. For V_{ss}, 33%, 87%, and 100% of estimates fell within 1.25, 1.5, and 2 fold error, respectively. These values are quite similar to ones obtained via PBPK modelling. One major difference being that PBPK model estimates were generated independent of PK data from children; whereas, Chamberlain et al.'s study derived estimates based on data obtained through *in vivo* experimentation with pediatric subjects. As such, PBPK modelling provided a relatively accurate approach for estimating individualized PK parameters compared to the estimates generated by Chamberlain et al. Despite the previous finding, a large proportion of subjects had CL and V_{ss} estimates associated with greater than 1.25 fold error which

indicates, in an absolute sense, individualized predictions generated through PBPK modelling still requires further development.

With predictions directed towards a mean individual, it not surprising that PBPK modelling can be used to estimate average parameter values among specific populations. For 14 of the 15 pediatric subjects among the elective group greater than the age of 5 years, the PBPK model produced mean estimates of CL and V_{ss} that exhibited a 14% and -6% relative error, respectively, from the mean observed values calculated by NCA. One patient who was approximately 1 years old was excluded from this analysis as the mean clearance was judge to be significantly different than the rest of the group, which was comprised of older children. This assertion was based on the increased dosing requirements for children between the ages of 1-3 years due to increased weight normalized clearances, as depicted in figure 2.3 A,B.

PBPK models also display a unique ability to estimate the magnitude of variability that surrounds PK parameters. Many PBPK modelling applications are capable of generating virtual populations in order to estimate PK variability associated with anthropometric differences between individuals. These populations can also be manipulated to encompass the range of inter-individual variability that exists around each physiological/anatomical value. As such, PBPK population-based modelling techniques may be used to provide *a priori* estimates of variability associated with PK parameters such as CL and V_{ss} for a given population. For example, the coefficient of variation associated with observed clearance values, determined by NCA, for 14 of the 15 elective group patients greater than 5 years of age was 53%. To generate an *a priori* estimate of variability using PBPK modelling, a uniform virtual population of 1300 children between the ages of 5 and 17 years (100 children per year) was created with associated variability around organ sizes, tissue blood flows, and metabolizing enzyme activity. The coefficient of variation of associated with PBPK model estimates of clearance among this population was 43%. Although this estimate under predicts the observed variability, it does provide a preliminary estimate of the magnitude of variation that may be observed within the population. Estimates of high degrees of CL and V_{ss} variability among a population for drugs with narrow therapeutic indexes may indicate the need for individualized dosing regimens; whereas, drugs with wider therapeutic indexes may be administered using fixed dosing levels (ie. 60 mg for 1-2 year olds, 80 mg for 2-5 year olds, etc.).

Although evaluation of the derived PBPK model represents a crucial step in the workflow process, a clear metric has yet to be proposed to aid researchers in classifying a particular model as “good” vs. “bad”. As such, acceptable tolerances of predictive performance of the pediatric model

should be established on a drug by drug basis based on current information available in adults: PK-PD relationship, safety profile, and therapeutic index.

The derived pediatric population PBPK model was able to account for approximately 72% of the variability associated with concentration-time points observed in a subset of 40 pediatric patients. The inability of the model to fully account for the variability observed is likely a result of the uniform nature of age groups included in the simulated population. One thousand one hundred and forty pediatric patients, between the ages of 0 days to 18 years, were simulated with 60 patients being selected per year. As a result, PK variability associated with the simulated population was skewed towards the large majority of patients whose clearance values were similar to that of adults (i.e., patients greater than 3 years of age). Patients with relatively lower and higher clearance values, neonates and children aged 1-3 years, respectively, comprised a small portion of the simulated population and, therefore, only minimally contributed to the PK variability amongst the total population. Consequently, the total range of simulated variability may have been understated with use of a uniformly aged population.

2.5 Conclusion

Since lorazepam's inclusion on NIH's priority list in 2003, two clinical pediatric studies have been completed under the sponsorship of National Institute of Child Health and Human Development (NICHD) with one additional study in the recruitment phase. With future advancements in model development there is the potential for PBPK models to shift from being used as a compliment to clinical PK studies to a partial replacement. For example, PBPK models may be used to decrease the amount of clinical trials required in children by functioning as the primary exploratory investigation of drug PK. This could potentially eliminate the need for exploratory PK studies in children and permit clinical investigations to function on a confirmatory basis. With the recent FDA recommendation, interest in the use and development of pediatric PBPK models will inevitably increase. The current study demonstrates the fundamental processes required for development of a pediatric PBPK model incorporating existing adult drug data. Using this approach, the model was able to predict lorazepam PK in children as a function of age. With the rise in use of PBPK modelling software in the field of pediatric drug development, the use of procedural workflows, similar to the one presented, will ensure consistency in model outputs and potentially permit for expedited reviews of such research by regulatory bodies.

Chapter 3: Examining Small Intestinal Transit Time as a Function of Age – Is There Evidence to Support Age-Dependent Differences Among Children?

The contents of this chapter are reflective of an original manuscript published by the Ph.D. candidate (Anil R Maharaj) in the journal Drug Metabolism & Disposition. All pertinent research analyses was conducted by the Ph.D. candidate.

Maharaj AR, Edginton AN. Examining Small Intestinal Transit Time as a Function of Age: Is There Evidence to Support Age-Dependent Differences among Children? Drug Metab Dispos. 2016;44(7):1080-9. doi:10.1124/dmd.115.068700.

3.1 Introduction

Estimation of bioavailability following oral compound administration is an inherently complex procedure, requiring a fundamental understanding of the interplay between compound and formulation properties and the dynamic nature of the alimentary canal. Within the gastrointestinal (GI) tract a multitude of physiological parameters can exert an influence on both the rate and extent of compound absorption including gastric emptying time (GET), small intestinal transit time (SITT), regional differences in pH and permeability, relative abundances of intestinal transporters and enzymes, and GI fluid volumes. As developmental changes in any of the aforementioned parameters may impart differences in oral absorption between children and adults, there is an inherent need to identify which parameters change as a function of age and by how much. The small intestine is of particular importance as it represents the region where the majority of nutrient and xenobiotic absorption transpires [42]. This is due to the presence of several morphological features on the luminal surface such a folds (valves of Kerckring), villi, and microvilli which serve to significantly expand the absorptive surface area [91]. Correspondingly, knowledge of the time a xenobiotic spends traversing

the small intestine is essential towards fostering predictions of oral compound absorption. This is particularly true for poorly absorbed compounds, where the extent of absorption is highly mediated by the time of contact between the compound and the small intestinal epithelium [43].

Conceptually, the widely utilized maximum absorbable dose (MAD) equation as proposed by Johnson and Swindell [92] offers a simplistic overview of how small intestinal transit time (i.e. SITT) can influence the extent of compound absorption. The equation (3.1) utilizes the absorption rate constant (ka), compound specific saturation solubility (C_s), small intestinal water volume (SIWV), and SITT to garner estimates of the MAD following oral compound administration.

$$MAD = ka * C_s * SIWV * SITT \quad \text{(Equation 3.1)}$$

Based on equation 3.1, shorter SITT (i.e. ↓SITT) would translate to lower compound availability following oral administration; whereas, longer SITT (i.e. ↑SITT) would result in the opposite. Owing to the influence of intestinal transit on oral drug absorption, there exists an inherent need to identify specific subpopulations exhibiting differences in SITT [93].

In humans, estimates of SITT have been determined using a variety of techniques including lactulose H_2 (hydrogen) breath tests, scintigraphy and wireless pH/pressure monitoring devices [94-96]. Scintigraphy, however, is generally regarded as the 'gold standard' for SITT assessment. Amongst adults, SITT is generally assumed to be independent of feeding state, age, gender, weight, and compound formulation (i.e. tablet vs. solution) [33]. In an analysis of over 400 adult small intestinal transit times compiled over multiple investigations utilizing scintigraphy, Yu et al. [33] estimated the average (±SD) SITT to be 199 min ± 78 min. However, as data pertaining to children were not formally assessed by the analysis, the applicability of these values towards pediatric subjects, who are developmentally immature, remains questionable.

Based on previously published literature reviews, which are non-quantitative in nature, it has been postulated that older children may possess shorter (i.e. faster) intestinal transit times compared to adults [97, 98]. This assertion originates, in part, from clinical investigations in asthmatic children administered sustained-release (SR) theophylline. Children frequently demonstrated large inter-individual differences in the percent fluctuation between maximum and minimum steady-state theophylline plasma concentrations (i.e. $[C_{peak}\text{-}C_{trough}/C_{trough}] \times 100$) [99, 100]. As such, they generally require more frequent dosage administration times in order to maintain appropriate therapeutic concentrations [101]. In addition to higher weight normalized clearances compared to adults [102], the

etiology of this variability among children has also been attributed to inconsistent theophylline SR absorption due to variability in parameters such as intestinal transit time [103].

Since intestinal transit has the capacity to influence the extent of absorption (i.e. bioavailability) of certain xenobiotics [104], an understanding of the differences in SITT between children and adults is critical to deriving age appropriate dosage regimens. This article will serve to examine the relationship between age and mean SITT based on available literature and provide a current assessment of small intestinal transit in children and adults. In addition, the pharmacokinetic (PK) influence of alterations in intestinal transit among children will be examined using a model-based approach for the compound theophylline.

3.2 Methods

3.2.1 Literature-based assessment of SITT as function of age

Primary literature sources documenting SITT from children to adults were acquired from the PubMed database (last accessed June 2015). In addition, secondary [105, 106] and tertiary [107] literature sources were utilized as focal points from which further primary investigations were obtained. Data were limited to subjects free of pathologies that may influence intestinal motility. As such, subjects with GI disorders such diarrhea, constipation, ileus and Crohn's disease were excluded. The analysis included data pertaining to various formulations (solutions, single unit capsules, multi-unit pellets) as well as different feeding states (i.e. fasting and fed).

Methods employed to measure SITT were wide ranging and included H_2 breath tests, scintigraphy, wireless pH/pressure capsules, lactose-[13C]ureide breath tests, fluoroscopy (X-ray), and magnetic tracking systems. Upon initial evaluation of the data, two separate investigations reported by Fallingborg et al. in which fluoroscopy (X-ray) was utilized purported the two longest SITT compared to other investigations (7.5h and 8h) [108, 109]. Transit times recorded by this method traced the GI movement of an orally administered capsule through the use of bony landmarks and gaseous outlines. Consequently, subtle movements such as displacement of the dosage form from the ileum to the caecum may not have been easily discerned. In addition, as the use of fluoroscopy was exclusively confined to these two investigations from the same research group, supplementary studies conducted by separate investigators were unable to assess the validity of these findings. As a result, data pertaining to the two aforementioned studies were removed from the analysis.

Lactulose H_2 breath tests report intestinal transit in terms of orocecal transit time (OCTT) rather than an exact measurement of SITT. Furthermore, among adults, lactulose has been demonstrated to dramatically accelerate normal small intestinal transit while reducing associated inter-subject variability [96]. As the focus of this analysis was to define the effects of age on SITT under normal conditions, inclusion of studies where intestinal transit was altered would appear counterintuitive. Unfortunately, a large majority of pediatric investigations exclusively employed lactulose H_2 breath testing. Exclusion of such data would notably decrease the power of the analysis towards recognizing developmental differences in intestinal transit among the youngest cohort of patients. As a result, the analysis did not exclude studies in which intestinal transit was measured via lactulose H_2 breath tests; however, data from these investigations were segregated and analyzed separately.

To discern the influence of age on SITT based on separate investigations acquired from the literature, the analysis utilized meta-regression [110]. Briefly, meta-regression is a technique by which weighted data from separate investigations can be combined to provide an assessment of the influence of specific covariates on a given outcome or effect. Unlike the more familiar regression analyses typically employed within primary investigations, which examines relationships at the level of individual subjects, meta-regression examines the relationship between study-level covariates (i.e. age) and aggregated measures of effect (i.e. mean intestinal transit time) among separate investigations. In this context, mean intestinal transit time parallels the concept of a dependent variable used in conventional linear regression.

For each study, the aggregated measure of effect was recorded as the mean SITT, or mean OCTT for studies employing breath tests. Variances associated with each measure of intestinal transit were calculated based on the following formula:

$$Variance_i = \left({SD_i}/{\sqrt{n_i}} \right)^2 \quad \text{(Equation 3.2)}$$

where SD_i is the study-specific standard deviation associated with intestinal transit and n_i is the number of subjects examined within the specific study. Since the analysis compiles SITT (or OCTT) data as measured among separate subject groups by different investigators, heterogeneity of intestinal transit between studies was expected. Therefore, a random-effects model with between-study variability was adopted. Using this method, weights associated with each intestinal transit measure were tabulated as the reciprocal of the sum of within-study variance (i.e. $Variance_i$) and between-study variance (τ^2).

Between-study variance was approximated using a restricted maximum likelihood (REML) estimation technique [111].

Since meta-regression requires study specific effect measures (e.g. SITT) to be summarized in the form of mean and standard deviation, supplementary estimation techniques were employed for studies that summarized data using alternative statistics. For studies where SITT (or OCTT) were represented by the median, maximum and minimum, estimates of mean and standard deviation were computed as described by Hozo et al. [112]. For studies where SITT were summarized using the interquartile range (i.e. 25th percentile, median, and 75th percentile), the estimation techniques denoted by Wan et al. were employed [113]. In several investigations multiple SITT determinations were conducted on the same participants under various conditions (i.e. fasted vs. fed or transit of tablet vs. transit of solution). In such cases, data provided by each treatment arm were considered to be highly correlated (i.e. Pearson's correlation coefficient (r) ≈ 1). Inclusion of correlated data into the analysis as though it represents separate independent entities would inappropriately bias parameter estimates. To circumvent this issue, the analysis aggregated data to provide a single estimate of SITT (or OCTT) represented by the mean and pooled standard deviation (equation 3.3) between separate treatment conditions for such studies [110].

$$SD_i = \frac{1}{2}\sqrt{s_1^2 + s_2^2 + (2r \cdot s_1 \cdot s_2)} \qquad \text{(Equation 3.3)}$$

Equation 3.3 depicts the formula for the pooled standard deviation (SD_i) where s_1 is the standard deviation associated with the first treatment arm, s_2 is the standard deviation associated with the second treatment arm, and r is the correlation coefficient between measures of intestinal transit from each treatment arm (assumed to be 1 for this analysis).

Examination of the influence of age on mean intestinal transit time was conducted using two separate analyses. The first analysis was restricted to studies that employed lactulose H_2 breast tests, where intestinal transit was postulated to be accelerated due to the effects of lactulose. A random-effect meta-regression was conducted using age as the sole modulator. For the remaining studies that employed scintigraphy, wireless pH/pressure capsules, lactose-[13C]ureide breath tests, H_2 breath tests (without lactulose) and magnetic tracking systems, data was also analyzed using a random-effect meta-regression model, but with both age and measurement method as modulators. As scintigraphy represents the anecdotal 'gold standard' method, the variable 'measurement method' was coded as either 0 or 1: 0 pertaining to studies utilizing scintigraphy and 1 pertaining to studies employing other

measurement techniques. Age was quantified by the mean age as depicted from each investigation. If mean values were not specified but alternative summary statistics were available, the mean age was estimated in a similar manner as depicted for intestinal transit times. For some adult investigations, only the range (i.e. minimum and maximum) of ages of the study participants were described. In these studies age was denoted by the middle of the age range. In two adult investigations [114, 115] no ages were specified. For these studies a mean of 45 years was utilized, which represents the approximate middle of the adult age range from our collected cohort of studies. Both linear and curve-linear relationships between age and intestinal transit were investigated based on the following models:

$Linear$:

$$SITT = B_0 + (Measurment\ Method * B_1) + (Age * B_2) \quad \text{(Equation 3.4)}$$

$2nd\ Order\ Polynomial$:

$$SITT = B_0 + (Measurment\ Method * B_1) + (Age * B_2) + (Age^2 * B_3) \quad \text{(Equation 3.5)}$$

$3rd\ Order\ Polynomial$:

$$SITT = B_0 + (Measurment\ Method * B_1) + (Age * B_2) + (Age^2 * B_3) + (Age^3 * B_4)$$

(Equation 3.6)

where the estimated regression coefficients for the model intercept, the binary variable 'measurement method', and the continuous variables age, age^2, and age^3 are denoted by B_0, B_1, B_2, B_3, and B_4, respectively.

To reduce collinearity and mitigate computational errors associated with polynomial regression models, the explanatory variable, age, was centered (i.e. $x_i - \bar{x}$) within each analysis [116]. Tables are subsequently presented using centered data; however, figures are presented using actual age (i.e. uncentered) to ease interpretation. In addition to the models depicted above, models that included interaction terms between age and measurement method were also explored for studies where intestinal transit was measured by scintigraphy and other auxiliary techniques. All analyses were conducted using the metafor package [117] in conjunction with R statistical software (v3.1.2). Modulating variables (age and measurement method) were deemed significant contributors to the model if associated parameter estimates attained p-values of ≤ 0.05. For studies where results were presented graphically, data was quantified using GetData Graph Digitizer (v2.26).

3.2.2 Model-based assessment of the influence of intestinal transit on theophylline pharmacokinetics in children

To assess the impact of alterations in intestinal transit on the PK of theophylline among children, a physiologically-based pharmacokinetic (PBPK) modeling approach was utilized. Simulations were parameterized based on a previously conducted *in vivo* PK study conducted by Pedersen and Steffensen [118]. Briefly, the study investigated the absorption of a SR once-daily theophylline preparation in children ranging from 8 to 14 years. Plasma concentration values were ascertained from 14 children on days 6 and 7 following multi-dose administration.

Simulations were conducted using PK-Sim® v5.2 (Bayer Technology Services, Leverkusen, Germany). Development of pediatric specific PBPK models followed a well-accepted modeling paradigm [23] whereby adult models are first developed and evaluated prior to scaling models towards a younger population. The adult model was parameterized utilizing drug-specific properties obtained from the literature (e.g. molecular weight, logP, pKa, solubility). System-specific parameters (e.g. organ weights and blood flows) were provided within the software platform. Tissue: plasma partition coefficients (Kp) were estimated using *in silico* tissue composition-based algorithms published by Rodgers and Rowland [80-82]. Albumin was denoted as the principle binding protein of theophylline in plasma with an average fraction unbound of approximately 0.58 in healthy adults [119, 120]. Human intestinal permeability was estimated for theophylline by scaling from *in vitro* Caco-2 data [121]. Correspondingly, simulations utilized an intestinal permeability of 4.4×10^{-4} cm/s, a value that is qualitatively associated with high permeability compounds [122].

In adults, theophylline clearance is a combination of hepatic metabolism (CYP1A2 and CYP2E1) and glomerular filtration [83, 123]. Utilizing the PBPK model framework, literature-based PK studies depicting concentration-time profiles following administration of theophylline either intravenously [124, 125] or orally [126] as an immediate release formulation (assuming fraction absorbed = 1) were utilized to obtain specific estimates of hepatic and renal clearance in healthy adults. This method of parameter obtainment has been previously described in literature [127]. In addition, using a similar modality, tissue: plasma partition coefficients were refined using a single global scalar value to ensure simulated results from the adult PBPK model adequately represented observed PK data.

Following development and refinement of the adult model, pediatric model development commenced. A population of n = 50 was generated [79] in order the match the demographics (age, weight, %females) of children examined by Pedersen and Steffensen [118]. Simulations utilized an oral dose of 15.5 mg/kg/q24h, representing the average dose administered during the study. Plasma sample

time points within the simulation were congruent to those depicted by the study. *In vivo* release characteristics of the SR theophylline preparation was simulated based on fraction absorbed vs. time data obtained from PK evaluations following single-dose administration to a similar subset of children investigated within the same study. Using this approach, it was inherently assumed that theophylline release from the formulation was the principle rate-limiting factor for absorption. To explore the influence of intestinal transit on theophylline PK, pediatric models were parameterized using separate intestinal transit rates: [1] SITT and large intestinal transit time (LITT) were held at the reference adult values, [2] SITT was decreased by 25% compared to adult values (i.e. faster) while LITT was held at the reference, [3] SITT was decreased by 50% compared to adult values (i.e. faster) while LITT was held at the reference, [4] both SITT and LITT were decreased by 25% compared to adult values (i.e. faster), and [5] both SITT and LITT were decreased by 50% compared to adult values (i.e. faster). Simulated estimates of C_{max}, C_{min}, and percent fluctuation between peak and trough plasma concentrations [$(C_{max} - C_{min})/C_{min}$] after 1 week of dosing were compared to observed data presented by Pedersen and Steffensen [118].

3.3 Results

Estimates of SITT and OCTT were compiled over 40 separate investigations obtained from the literature (Figure 3.1) [94-96, 114, 115, 128-162] and pertained to subject groups ranging in average age between 20 days to 67 years. OCTT was measured via lactulose H_2 breath testing in 14 subject groups [96, 128-137] while estimates of intestinal transit time were ascertained via scintigraphy in 28 groups [94, 96, 115, 138-156] and other measurement techniques in 10 subject groups [95, 114, 134, 135, 157-162]. Correspondingly, 52 subject groups were included within the analysis. The analysis included 11 investigations [138, 140, 142-145, 148, 150, 152-154] where estimates of intestinal transit were pooled between test conditions (e.g. fasted vs. fed). For each of these investigations, mean intestinal transit times were not found to be significantly different between treatment arms as either denoted by the authors' or independently confirmed using a paired student's t test (p-value > 0.05 – two tailed test). One investigation by Clarke et al. [141] examined GI transit kinetics of pellets of varying sizes (0.5 and 4.75 mm) and densities (1.5 and 2.6 g/cm^3) in a single group of adult subjects using scintigraphy. A statisically significant difference in SITT was denoted between pellets of different sizes ($p \leq 0.05$). Conseqently, data concerning this study was analyzed as two separate subject groups pertaining to each pellet size rather than combining data across both formulations.

As an initial assessment, differences between the separate measurement methods was examined with a preliminary meta-regression run with the entire data set using measurement technique (i.e. lactulose H_2 breath test vs. other vs. scintigraphy) as the sole modulator of mean intestinal transit time (Figure 3.2). Compared to investigations employing the 'gold standard' measurement technique scintigraphy, studies utilizing lactulose H_2 breath tests displayed mean intestinal transit times that were approximately 133 mins faster (i.e. smaller). This result is consistent with previous literature denoting lactulose's ability to accelerate intestinal transit [96]. Moreover, intestinal transit time estimates determined using other measurement methods (i.e. wireless pH/pressure capsules, lactose-[13C]ureide breath test, H_2 breath tests [without lactulose] and magnetic tracking systems) were on average 60 mins slower (i.e. greater) when compared to investigations utilizing scintigraphy.

Data pertaining to intestinal transit studies employing lactulose H_2 breath tests [96, 128-137] are displayed as a function of age in Figure 3.3. Fitted estimates based on a linear meta-regression model are superimposed and depict a negative correlation between age and OCTT. However, the estimated parameter associated with age did not attain statistical significance, indicating a lack of evidence to support the notion that age influences OCTT (Table 3.1). Second and 3rd order polynomial models (Appendix A Figure 1) exhibited slightly more complex relationships between age and OCTT, but similar to the linear model, age was not considered a significant modulator (Appendix A Tables 1 and 2).

For studies utilizing scintigraphy in addition to other measurement techniques [94-96, 114, 115, 134, 135, 138-162], data are displayed in Figure 3.4. Separate regression lines based on a linear meta-regression model have been superimposed according to the measurement technique employed (higher order polynomial models are displayed in Appendix A Figure 2). Parameter estimates pertaining to the linear model are displayed in Table 3.2 while those pertaining to the 2nd and 3rd order polynomial models are denoted within Appendix A Tables 3 and 4, respectively. For all tested models (linear, 2nd order polynomial, 3rd order polynomial), the coefficient associated with measurement method was found to be a significant modulator of mean small intestinal transit. However, similar to the previous assessment, age was not found to be significantly associated with mean intestinal transit time. For models which included interaction terms between age and measurement method, parameter estimates associated either age or the interaction term(s) were not significant modulators of mean SITT within the linear and 2nd order polynomial models (Appendix A Tables 7 & 8 and Figures 4 & 5). For the 3rd order polynomial model, the interaction term associated with 'Age^3*Measurement method' did attain statistical significance (p-value = 0.0391) (Appendix A Table 9 and Figure 6). However, this result was

not thought to convey a meaningful relationship between age, measurement technique and SITT as the adjusted R^2 (R^2_{adj}), which normalizes for the effects of the additional interacting parameters, was similar between 3rd order polynomial models with and without interaction terms (R^2_{adj} 0.266 vs. 0.259, respectively). In addition, highly parameterized models, such as the abovementioned interaction models, increase the risk of type I errors (false positives) [163] and, as such, covariates which display significance within this context should be interpreted with caution.

Simulations of theophylline SR in children (8-14 years) utilizing adult intestinal transit values provided a mean C_{max} along with an associated estimate of variability, as denoted by the coefficient of variation (CV%), that were similar to those observed by Pedersen and Steffensen [118] (Table 3.3). However, simulations over-predicted the mean C_{min} by approximately 1.2 mcg/mL, whereas percent fluctuation between C_{max} and C_{min} was under-predicted by approximately 20% when compared to observed data. Changes to SITT in isolation (i.e. without changes to LITT) did not appear to affect simulated outcomes as C_{max}, C_{min}, and the percent fluctuation were essentially identical to those simulations where SITT was held at adult values. C_{max}, C_{min}, and percent fluctuation were also unchanged in simulations where total intestinal transit time was decreased (i.e. both SITT and LITT) by 25%. However, a decrease in total intestinal transit by 50% resulted in a notable decrease to all indices.

Figure 3.1 Mean intestinal transit time (SITT or OCTT) estimates pertaining to each study group included within the analysis. Data is reflective of transit values from normal subjects, free of GI disease.

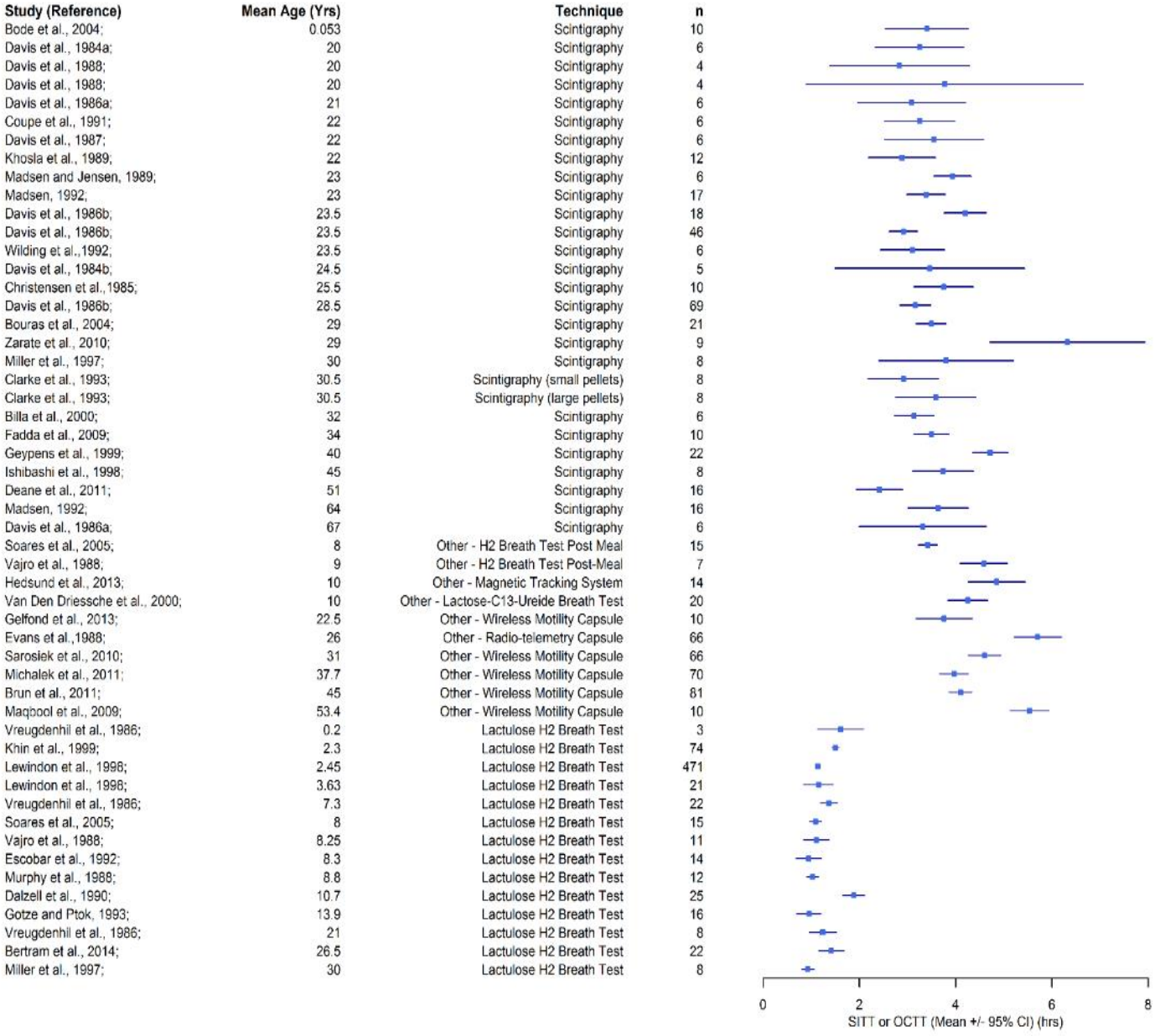

Figure 3.2 SITT or OCTT segmented according to measurement method for all investigations [94-96, 114, 115, 128-162] (i.e all age groups) documenting intestinal transit in normal subjects free of GI disease (open circles). The diameter of each circle is proportional to the $1/(Variance_i)^{1/2}$. Mean values, as estimated according to a meta-regression model employing measurement method as the sole modulator, are displayed for reference (-).

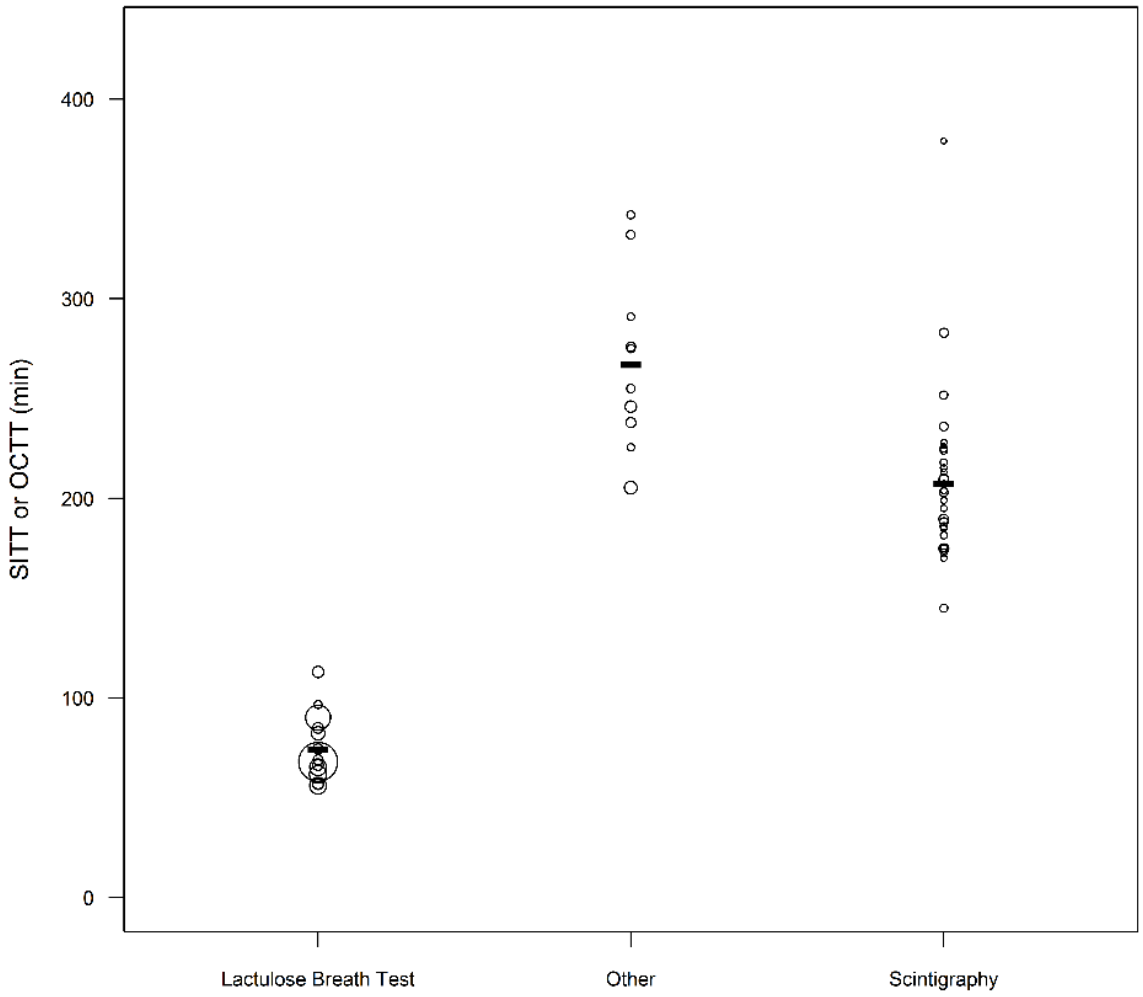

Table 3.1 Lactulose H_2 Breath Tests – Linear Meta-Regression Model

Summary Statistics	k [a]=14	$Q_{M\ (df=1)}$ [b]= 0.5296 (p =0.4668)		I^2 [c]= 92.53%	R^2 [d] = 0.00%
	Estimate	Standard Error	p–Value	95% CI (lower)	95% CI (upper)
Fixed Effects					
Intercept (B_0)	73.8142	4.5321	**<0.0001**	64.9315	82.6969
Age (B_1)	-0.3663	0.5034	0.4668	-1.3529	0.6203
Random Effects					
Between study variance (τ^2)	239.7203	116.7795	-	-	-
Tau (τ)	15.4829	-	-	-	-

[a] k = number of subject groups
[b] Q_M = heterogeneity statistic (Cochran's Q) – tests whether any coefficient (not including the intercept) is significantly different than 0
[c] I^2 = % of total variability due to heterogeneity
[d] R^2 = % of total heterogeneity explained by the covariate(s)

Figure 3.3 OCTT as a function of age for investigations employing lactulose H_2 breath testing [96, 128-137] in normal subjects free of GI disease (open circles). The diameter of each circle is proportional to the $1/(\text{Variance}_i)^{1/2}$. Estimates of OCTT based on a meta-regression model with age as a linear regressor have been superimposed for reference (mean – solid line; 95% CI – dotted lines).

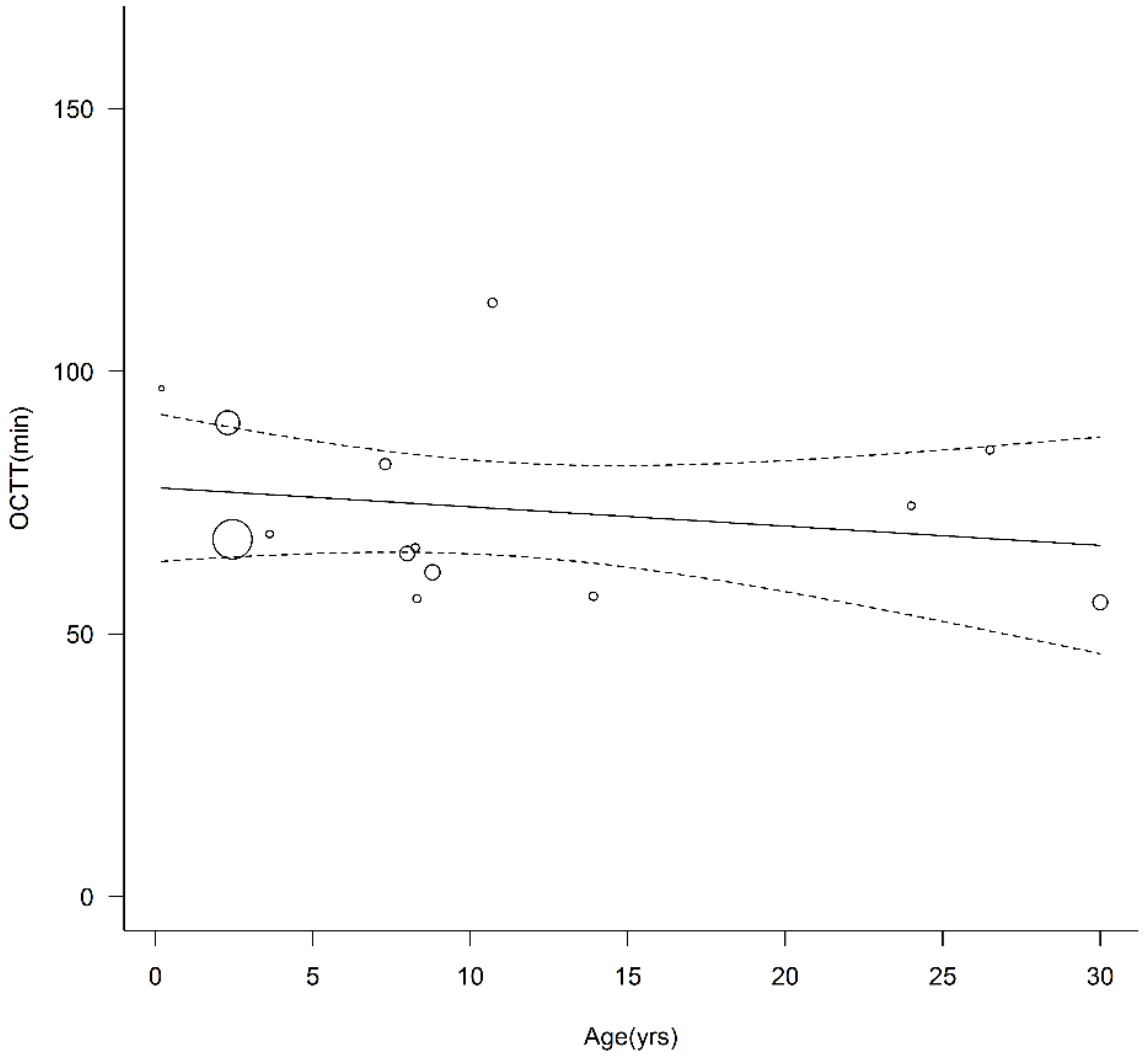

Table 3.2 Scintigraphy and Other Techniques – Linear Meta-Regression Model

Summary Statistics	k^a=38	$Q_{M\ (df=2)}{}^b$= 19.1664 (p < 0.0001)		$I^{2\ c}$= 84.57%	$R^{2\ d}$= 39.63%
	Estimate	Standard Error	p–Value	95% CI (lower)	95% CI (upper)
Fixed Effects					
Intercept (B_0)	206.9675	7.8990	**<0.0001**	191.4857	222.4493
Measurement Method (B_1)	61.5907	14.0951	**<0.0001**	33.9648	89.2166
Age (B_2)	0.4183	0.4689	0.3723	-0.5006	1.3373
Random Effects					
Between study variance (τ^2)	1165.4337	370.2652	-	-	-
Tau (τ)	34.1384	-	-	-	-

[a] k = number of subject groups
[b] Q_M = heterogeneity statistic (Cochran's Q) – tests whether any coefficient (not including the intercept) is significantly different than 0
[c] I^2 = % of total variability due to heterogeneity
[d] R^2 = % of total heterogeneity explained by the covariate(s)

Figure 3.4 SITT or OCTT as a function of age for investigations employing scintigraphy [94, 96, 115, 138-156] (black circles) and other measurement techniques [95, 114, 134, 135, 157-162] (open circles) in normal subjects free of GI disease. The diameter of each circle is proportional to the $1/(\text{Variance}_i)^{1/2}$. Estimates of mean intestinal transit time based on a meta-regression model with age as a linear regressor have been separately superimposed for studies utilizing scintigraphy (solid line) and other measurement techniques (dotted line).

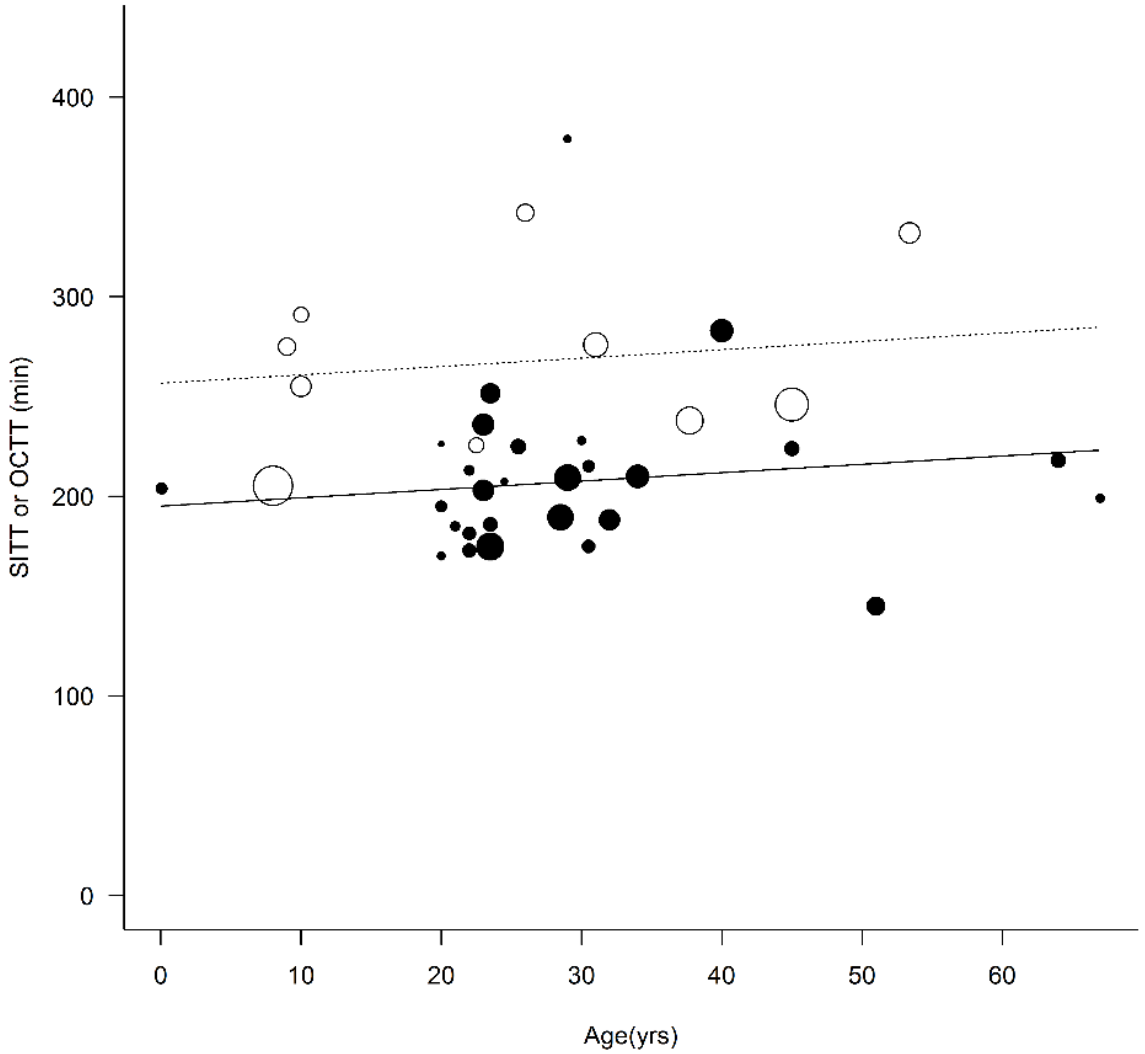

Table 3.3 Simulated vs. Observed Theophylline Absorption PK at 1 Week Following Daily Administration of a Sustained Release Formulation in Older Children (8-14 yrs)

	Source	Mean C_{max} [mcg/mL] (CV%[a])		Mean C_{min} [mcg/mL] (CV%)		Mean Percent Fluctuation (%)[b] (CV%)	
		i[c]	ii[d]	i	ii	i	ii
Observed	Pedersen and Steffensen [118]	12.86 (24.84%)	12.18 (26.07%)	6.79 (33.03%)	7.29 (31.69%)	95.78 (26.77%)	72.80 (40.34%)
Simulated - PBPK	SITT (adult) LITT (adult)	12.53[g] (27.15%)		8.48 (37.68%)		52.39 (25.60%)	
	SITT (↓ 25%)[e] LITT (adult)	12.53 (27.16%)		8.48 (37.68%)		52.38 (25.63%)	
	SITT (↓ 50%) LITT (adult)	12.53 (27.15%)		8.48 (37.68%)		52.38 (25.63%)	
	SITT (↓ 25%) LITT (↓ 25%)[f]	12.53 (27.14%)		8.48 (37.68%)		52.40 (25.65%)	
	SITT (↓ 50%) LITT (↓ 50%)	11.15 (29.01%)		7.81 (38.66%)		46.91 (24.49%)	

a - coefficient of variation

b - percent fluctuation between peak and trough plasma concentration values over a given dosing interval (i.e. [peak – trough]/trough).

c – Data reported by Pedersen and Steffensen on Day 6 following oral maintenance (q24h) therapy with a sustained release theophylline formulation (Noctelin – Riker Labs Inc.) [n = 14].

d - Data reported for 10 of 14 children investigated by Pedersen and Steffensen on Day 7 following oral maintenance (q24h) therapy with a sustained release theophylline formulation (Noctelin – Riker Labs Inc.) [n = 10 – same study group as depicted above; data for 4 children was unavailable]

e - 25% reduction in small intestinal transit time (SITT) from adult values. SITT for normal adults was parameterized as 2.1h - the default PK-Sim® v5.2 value. This represent the time span between gastric emptying of 63% of a nonabsorbable marker and localization of 90% of the marker within the caecum.

f - 25% reduction in large intestinal transit time (LITT) from adult values. LITT for normal adults was parameterized as 44.2h - the default PK-Sim® v5.2 value. This represent the time span between 90% of a nonabsorbable marker reaching the caecum and localization of 70% of the marker within the feces.

g- PBPK models were not parameterized to include intradose variability. (i.e. once steady-state was achieved, concentration-time values were congruent between dosing intervals). As such, simulated data is only provided as a single value obtained on day 7 of theophylline maintenance dosing [n = 50].

Table 3.4 Capsule Endoscopy Studies – Linear Meta-Regression Model

Summary Statistics	k [a]=16	$Q_{M\ (df=1)}$ [b]= 7.6931 (p =0.0055)		I^2 [c]= 93.76%	R^2 [d]= 41.58%
	Estimate	Standard Error	p–Value	95% CI (lower)	95% CI (upper)
Fixed Effects					
Intercept (B_0)	270.3442	8.8046	**<0.0001**	253.0875	287.6009
Age (B_1)	-1.0695	0.3856	**0.0055**	-1.8252	-0.3137
Random Effects					
Between study variance (τ^2)	908.1523	432.9293	-	-	-
Tau (τ)	30.1356	-	-	-	-

[a] k = number of subject groups
[b] Q_M = heterogeneity statistic (Cochran's Q) – tests whether any coefficient (not including the intercept) is significantly different than 0
[c] I^2 = % of total variability due to heterogeneity
[d] R^2 = % of total heterogeneity explained by the covariate(s)

Figure 3.5 SITT as a function of age for investigations employing capsule endoscopy (open circles). The diameter of each circle is proportional to the $1/(\text{Variance}_i)^{1/2}$. Estimates of SITT based on a meta-regression model with age as a linear regressor have been superimposed for reference (mean – solid line; 95% CI – dotted lines).

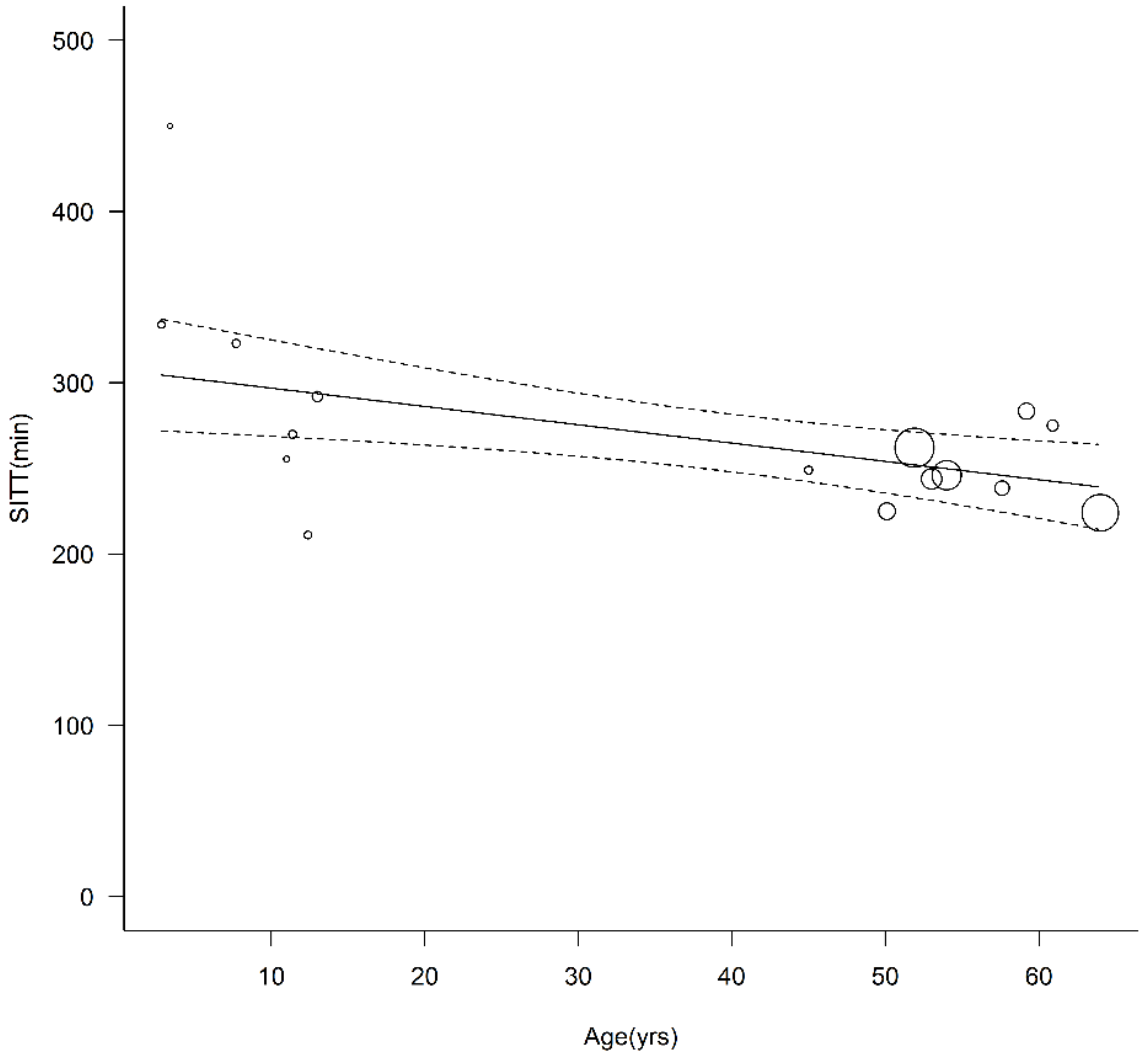

3.4 Discussion

Owing to the importance of the small intestine towards the absorption of nutrients and xenobiotics, knowledge of its transit kinetics is of key interest to pharmaceutical researchers. Though estimates of small intestinal transit have been conducted by several investigators, typically subjects are confined to a specific demographic cohorts (e.g. children, adult, elderly). The presented work sought to summarize the literature pertaining to small intestinal transit in order to assess for differences between children and adults. The analysis included data from several studies employing a variety of measurement techniques (i.e. lactulose H_2 breath tests, scintigraphy, wireless pH/pressure capsules, etc.). To evaluate the influence of age on SITT across the diverse array of collected investigations, meta-regression was utilized. Based on this analysis of the current literature, age was not found to significantly influence SITT.

Within the analysis, studies were specifically confined to subjects free of GI pathology to mitigate the potential effects of disease or altered health statuses on intestinal transit. This criterion ensured the analysis provided an assessment of the influence of age on mean SITT within the context of normal human development. To provide an example of the potential bias that can be introduced into such an analysis if patients were not stratified accordingly, a separate evaluation of SITT was conducted using data derived from capsule endoscopy investigations. Capsule endoscopy is a diagnostic procedure that permits for imaging of the small bowel while minimizing the degree of invasiveness and patient discomfort typically associated with traditional endoscopic procedures. Subjects are required to swallow a wireless video transmitting capsule that transverses the GI tract through the actions of intestinal peristalsis. Images are transmitted to a portable recording device and capsule location is determined using the obtained images [164]. Literature data pertaining to capsule endoscopy is primarily focused towards disease diagnosis with information regarding GI transit commonly reported as a secondary outcome. Such studies typically include patients with known or suspected GI disease for indications such as obscure GI bleeding, undiagnosed abdominal pain, suspected Crohn's disease, ulcerative colitis, celiac disease, and small bowel tumors [165]. Based on 11 capsule endoscopy studies [165-175], which provided information on 16 unique subject groups with mean ages ranging from 2.9 to 64 years, a meta-regression was performed using a similar methodology as described above. The analysis depicted a negative correlation between age and mean SITT using a linear model (Figure 3.5). In contrast with the previous analyses which focused on healthy/normal subjects, this analysis denoted age to be a significant modulator of mean SITT (Table 3.4). In addition, 2^{nd} and 3^{rd} order polynomial regression models also found parameters associated with either age, age^2, or age^3 provided significant

contributions towards reducing the heterogeneity associated with SITT (Appendix A Tables 5 and 6 & Figure 3) . The etiology of this association is unclear, but may be linked to differences in disease prevalence between children and adults.

The results of the analyses in healthy/normal subjects which indicate no significant effect of age towards SITT contrasts with previously held assertions that older children exhibit faster intestinal transit times than adults [97, 98]. This notion has been linked to previous pharmacokinetic investigations of SR theophylline in asthmatic children who typically display large degrees of inter-individual variability in terms of systemic concentrations [99, 100]. However, large degrees of inter-subject variability in absorption have also been denoted in adults administered SR formulations of theophylline [176]. Within our analysis, theophylline absorption among older children was examined using a model-based approach. From this assessment it was found that alterations of SITT lacked influence on the oral absorption of SR theophylline. Of note, discernable changes in theophylline absorption were only observed when total intestinal transit time (i.e. SITT and LITT) was greatly altered (i.e. ↓ 50%). Consequently, the results of these simulations downplay decreased SITT as a primary factor contributing to pharmacokinetic variability of SR theophylline in older children.

Although not formally addressed in this investigation, simulations in younger pediatric cohorts provided a similar outcome to those depicted for older children (i.e. changes in SITT failed to influence the PK of SR theophylline). The reasons behind this observation are two-fold. First, mechanistic pediatric oral absorption models are rather underdeveloped due to limited information surrounding age-specific differences in intestinal permeability, luminal fluid volumes and composition, and abundance of intestinal transporters. As a result, pediatric oral absorption models are commonly parameterized in a similar manner to those of adults. Secondly, theophylline is considered a BCS Class I compound (high solubility, high permeability) with adequate levels of absorption attainable throughout the entire GI tract (i.e. small bowel and colon) [177]. When formulated as an SR preparation, the limiting factor modulating theophylline absorption can be attributed to its rate of release. Consequently, simulations failed to depict any changes in oral absorption of SR theophylline except in extreme cases where total intestinal transit time is shorter than formulation release time (i.e. total intestinal transit time ↓ 50%).

In studies where the effects of separate formulations (solution vs. tablet) or different feeding conditions (fasted vs. fed) were explored in the same study participants, the analysis assumed SITT estimates were highly correlated (i.e. $r \approx 1$). This permitted for SITT to be summarized between treatment arms using the overall mean and pooled standard deviation. Similarity of intestinal transit kinetics between separate dosage forms and different feeding conditions was assumed based on data

presented by Davis et al [146]. The study examined 201 SITT estimates as measured by scintigraphy among normal adult subjects for single unit dosages, pellets, and solutions under various feeding conditions. The results conveyed no statistical difference in the transit behavior between formulations and a lack of effect of feeding status.

The current investigation segregated data measured by lactulose H_2 breath testing due to the propensity of lactulose to accelerate intestinal transit. In addition, lactulose H_2 breath tests typically report reduced degrees of inter-subject variability in transit times compared to studies where lactulose was not administered [96]. These findings prevented the amalgamation of intestinal transit data obtained from scintigraphy and other auxiliary techniques with lactulose H_2 breath tests into a single analysis, as reductions in intestinal transit time variability due to lactulose may have unfairly weighted the meta-regression analysis towards these investigations. Dissimilar to scintigraphy, which provides isolated measures of small bowel transit, lactulose H_2 breath tests provides composite estimates of oral to cecal transit. Thus, in order to assess the effects of age on SITT using such studies, both esophageal and gastric transit must be considered. For liquids, esophageal transit transpires in the realm of seconds and is not considered to vary with age [178]. However, gastric emptying varies between fasted and fed states and can be influenced by factors such as feed composition and osmolality [107]. In a recent assessment of gastric transit data from neonates to adults, it was found that gastric emptying was not significantly influenced by age [179]. In addition, the time at which increased levels of H_2 are first detected in expired air, denoted as the OCTT, correlates with the foremost portion of lactulose reaching the caecum rather than a specific quantity (i.e. 10% of lactulose entering the caecum) [107]. Consequently, for breath testing, differences in gastric emptying times (i.e. fasted vs. fed states) should not exert a substantial influence on OCTT. Based on this assessment, OCTT as measured by lactulose H_2 breath testing should provide a suitable surrogate for SITT, albeit in an accelerated state.

The analysis included data pertaining to 52 normal/healthy subject groups, 16 of which were representative of children less than 18 years old. The frequency of pediatric subject groups stratified according specific to developmental age ranges were as follows: 1 neonate (0-30 days), 1 infant (1 month -2 years), 3 young children (2 – 5 years), 10 children (6-12 years), and 1 adolescent (12-18 years). Accordingly, it can be seen that data pertaining to the youngest cohorts of children, especially those less than 2 years of age, are disproportionately underrepresented within the analysis. This pattern is concerning as the youngest subjects (i.e. neonates) are considered to be the most functionally immature and, therefore, the most likely to display developmental differences in comparison to adults. Consequently, the findings presented by this analysis are contingent on currently available literature

and, as such, are malleable to change if additional investigations, especially in neonates and infants, are prospectively conducted.

In one investigation, SITT within a single subject group was found to be statistically different (p-value ≤ 0.05) between administration of pellets of varying size (0.5 vs. 4.75 mm pellets) [141]. Rather than combine the measurements into to single outcome, the data was analyzed as separate groups. Although this clearly introduces the small degree of bias into our analysis, the presented results are similar to that if the investigation was simply excluded from the analysis altogether. A major limitation associated with meta-regression or any other technique where data is summarized over trials as opposed to individual subjects is aggregation bias (i.e. ecological fallacy). This bias describes the loss of information that occurs when data is averaged across trials, resulting in an inability to detect correlations that would be present if individual study subjects were assessed [180]. Unfortunately, the majority of literature investigations summarize data over all study subjects as opposed to denoting individualized measures of age and SITT. Consequently, despite the potential for aggregation bias, meta-regression was still deemed the most appropriate analysis technique.

3.5 Conclusion

The essential role of the small intestine towards facilitating absorption of nutrients and xenobiotics highlights the inherent need to appropriately define its transit kinetics. Within the literature, SITT has been reported using a variety of measurement methods by several research groups. Previous investigations have summarized SITT reflective of adult subjects, but the relevance of these values towards children remained questionable. The present study employed meta-regression in order to summarize the effect of age on SITT. Based on this analysis, there is no evidence to suggest that mean SITT differs between children and adults.

Chapter 4: Assessment of Age-Related Changes in Pediatric Gastrointestinal Solubility

The contents of this chapter are reflective of an original manuscript published by the Ph.D. candidate (Anil R Maharaj) in the journal Pharmaceutical Research. All pertinent research analyses was conducted by the Ph.D. candidate.

Maharaj AR, Edginton AN, Fotaki N. Assessment of Age-Related Changes in Pediatric Gastrointestinal Solubility. Pharmaceutical research. 2016;33(1):52-71. doi:10.1007/s11095-015-1762-7.

4.1 Introduction

The use of *in vitro* tests to forecast oral drug performance can serve to identify compounds displaying inadequate or unfavorable absorption profiles during early stages of drug development. To facilitate such *in vitro* – *in vivo* correlations (IVIVC), test media utilized should reflect the complex physiochemical nature of human gastrointestinal (GI) fluids. Accordingly, several formulas of biorelevant media have been developed based on the intraluminal conditions of the GI tract in adults [181-183]. For immediate release dosage forms, where drug release is expected to occur within the upper region of the GI tract, biorelevant media depicting the stomach and proximal small intestine are typically formulated.

Compared to compendial media, use of biorelevant media within *in vitro* dissolution experiments has been demonstrated to provide IVIVC that better predict oral drug absorption in adults [45, 46]. Despite these favorable results, the use of biorelevant media for establishing IVIVC within pediatric populations is contentious. This is because contemporary biorelevant media [181, 182] are formulated based on gastrointestinal conditions of an adult human. Consequently, their applicability towards pediatric populations, who are developmentally distinct in terms of gastrointestinal anatomy/physiology, remains questionable. Of most interest are children belonging to the youngest age groups (i.e. neonates and infants) who display the greatest developmental differences in comparison to adults [184, 185].

In recognition of the potential impact that developmental differences in GI anatomy/physiology can exert on oral drug absorption, a Pediatric Biopharmaceutics Classification System (P-BCS)

Working Group was assembled to assess whether a similar classification system as utilized in adults could be developed for children [186]. The Biopharmaceutics Classification System (BCS) categorizes drugs based on two properties, aqueous solubility and permeability [47]. Accordingly, compounds can be classified as either BCS I (high solubility, high permeability), II (low solubility, high permeability), III (high solubility, low permeability), or IV (low solubility, low permeability). The classification system supports several aspects of oral drug development in adults, including assessment of generic biowaiver applicability, lead compound selection, and formulation development [186]. Based on their findings in a 2012 publication, the P-BCS Working Group concluded that in order to have merit, substantial knowledge gaps with regards to pediatric GI physiology, intestinal permeability, and ontogeny of drug metabolizing enzymes/transporters needs to be addressed prior to establishing of a pediatric-focused BCS [186]. To enhance its applicability towards pediatric populations, it is clear that development of a P-BCS would require considerable modification of the current system. Of interest is how developmental changes in GI fluid composition affects compound solubility in relation to adults.

In addition to age-related changes, the composition of GI luminal fluids undergoes positional changes from the stomach to the colon. Changes in composition including bile salt concentration, pH, osmolality, buffer capacity, and presence of fat digestion products, can impart changes in compound specific solubility [44]. Therefore, to discern whether relevant differences in luminal solubility exist between pediatrics and adults, quantification of the relationship between age and GI fluid composition is inherently required.

This study serves to assess the impacts of growth and maturation on gastrointestinal solubility. Pediatric biorelevant media representative of the stomach and proximal small intestine were developed based on an assessment of the available literature. Developed pediatric media were utilized to perform solubility assessments for seven BCS Class II compounds. To assess the impact of developmental changes in fluid composition, solubility values were compared between the different age-specific media including media representative of adults.

4.2 Methods

4.2.1 Materials

Acetic acid (>99.7%), acetonitrile, dapsone, fenofibrate, indomethacin, hydrochloric acid 36.5-38%, methanol, pepsin (from porcine), phenytoin acid and sodium oleate were obtained from Sigma-Aldrich

Company Ltd., Dorset, England. Griseofulvin, maleic acid, sodium acetate, sodium chloride, sodium hydroxide, orthophosphoric acid and spironolactone were acquired from Fisher Scientific UK Ltd., Loughborough, England. Ammonium acetate (FSA Laboratory Supplies, Loughborough, UK), carbamazepine (Fagron UK Ltd, Newcastle upon Tyne, England), sodium taurocholate (Prodotti Chimici Alimentari S.P.A., Basaluzzo, Italy), egg lecithin - Lipoid EPCS (Lipoid GmbH, Ludwigshafen, Germany) and glyceryl monooleate - Rylo Mg 19 (Danisco, Brabrand, Denmark) were obtained from the sources specified. Ultra-high-temperature treated whole cow's milk standardized to less than 4% fat was acquired from Sainsbury's, London, England. Two infant formulas manufactured by Cow & Gate, Trowbridge, England were utilized in the study: First Infant Milk (cow's milk-based formula) and Infasoy (soya-based formula). Water was ultra-pure (Milli-Q) laboratory grade. Dialysis tubing (12-14000 Da MWCO) was acquired from Medicell Membranes Ltd., London, England. Equipment utilized in the current investigation included a Buchi R114 Rotavapor (Flawil, Switzerland), a Beckman Coulter J2-MC centrifuge (High Wycombe, England), a Mettler Toledo SevenCompact S210 pH meter (Schwerzenbach, Switzerland), an Advanced Instruments Inc. micro-osmometer Model 3300 (Norwood, MA) and an Agilent Technologies 1200 series HPLC system (Santa Clara, CA): binary pump (G1212A), autosampler (G1329A), thermostatted column compartment (G1316A), and diode array detector (G1315D).

4.2.2 Media development

Biorelevant media as characterized by Jantratid et al. [182] were selected as the focal points from which subsequent age-specific media were developed. The authors described four separate media reflective of the physiology of the stomach and proximal small intestine in adults in fasting and fed states: Fasted-State Simulated Gastric Fluid (FaSSGF), Fed-State Simulated Gastric Fluid (FeSSGF), Fasted-State Simulated Intestinal Fluid v2 (FaSSIF.v2), and Fed-State Simulated Intestinal Fluid v2 (FeSSIF.v2) (Table 4.1). Based on relative differences between adult and pediatric GI physiology, components of the reference adult media were modified to generate age-specific media.

Table 4.1 Composition of adult biorelevant media

Component	FaSSGF	FeSSGF	FaSSIF.v2	FeSSIF.v2
Sodium Taurocholate	80 (uM)	-	3 (mM)	10 (mM)
Lecithin	20 (uM)	-	0.2 (mM)	2 (mM)
Pepsin (mg/mL)	0.1	-	-	-
Sodium Chloride (mM)	34.2	237.02	68.62	125.5
Acetic Acid (mM)	-	17.12	-	-
Sodium Acetate (mM)	-	29.75	-	-
Maleic Acid (mM)	-	-	19.12	55.02
Sodium Hydroxide (mM)	-	-	34.8	81.65
Glyceryl Monooleate (mM)	-	-	-	5
Sodium Oleate (mM)	-	-	-	0.8
Milk:Buffer	-	1:1		-
HCl/NaOH qs	pH 1.6	pH 5	pH 6.5	pH 5.8
pH	1.6	5	6.5	5.8
Osmolarity (mOsm/kg)	120.7	400	180	390
Buffering Capacity (mEq/L/ ΔpH)	-	25	10	25

*adult media compositions as described in Jantratid et al. [182]

Investigations assessing developmental changes in gastrointestinal fluid composition were collected from the literature. For studies where information was displayed graphically, data was quantified using GetData Graph Digitizer (v2.26). Dependent on the specific media being formulated (i.e. FaSSGF), information pertaining to different physiological parameters were required:

(a) FaSSGF – pepsin concentrations, pH, osmolality, and bile salt/lecithin concentrations
(b) FeSSGF – feed type (i.e. cow's milk-based vs. soy-based formula), pH, osmolality, and buffering capacity
(c) FaSSIF – pH, bile salt/lecithin concentrations, osmolality, and buffering capacity
(d) FeSSIF – pH, osmolality, bile salt/lecithin concentrations, fat digestion products, and buffering capacity

Parameter values were compiled and, where suitable, graphically displayed as a function of age as an initial evaluation. If changes in GI fluid parameters between pediatric age groups and adults were noted, differences were computed based on a simplistic measure, the arithmetic mean. As the propensity of developmental effects were expected to be most prominent within the earliest stages of life, media reflective of the following age groups were formulated: neonates (0 – 28 days) and infants (1 – 12 months). When data pertaining to specific parameters were unavailable in children, either a default value representative of adult media or an inference based on current physiological knowledge was adopted.

Based on this analysis, biorelevant media reflective of pediatric physiology were defined. Media preparation was conducted using the methods depicted in Jantratid et al [182]. Measures of osmolality and pH were instituted to ensure prepared media conformed to desired values. Osmolality was measured using freezing point depression (Micro-osmometer - Advanced Instruments Inc.). Discrepancies between measured and desired osmolality were corrected by adjusting media sodium chloride concentrations as described in the literature [182]. Media pH was titrated using 1M HCl or 1M NaOH, if necessary. Buffering capacity of pediatric formula (cow's milk-based and soy-based) was determined based on the methodology presented by Hentges et al [187]. Values presented represent the amount of acid or base (i.e. mEq) required to induce of pH change of 1 unit per litre of formula [188].

4.2.3 Solubility assessment

4.2.3.1 Compound selection

Solubility assessments were conducted using BCS class II compounds. Compounds were further restricted to include only those with documented usages, including investigational uses, in both children and adults. Based on the above criteria, seven compounds were selected including carbamazepine, dapsone, fenofibrate, griseofulvin, indomethacin, phenytoin and spironolactone. Compound physicochemical properties are displayed in Table 4.2.

Table 4.2 Compound physicochemical properties

Compound	Molecular Weight (g/mol)	LogP	pKa (acid/base)
Dapsone	248	0.97	2.4 (base)
Griseofulvin	353	2.18	-
Carbamazepine	236	2.45	-
Phenytoin	252	2.47	9.5 (acid)
Spironolactone	417	2.78	-
Indomethacin	358	4.27	3.8 (acid)
Fenofibrate	361	5.3	-

*physicochemical data obtained from DrugBank [189]

4.2.3.2 Solubility experiments

Compound specific solubility assessments were conducted in each of the developed pediatric media as well as in the reference adult media to assess for age-related differences. Experiments were conducted within a shaking water bath set to 37^{O}C and 200 strokes/min.

Compound specific solubility values in aqueous-based media (FaSSGF, FaSSIF and FeSSIF) were determined based on the following procedure. A mass of solid (powdered) compound to saturate 10 mL of biorelevant media was added to borosilicate glass tubes. Next, 10 mL of freshly prepared age-specific media (pediatric or adult) was added. Tubes were covered with parafilm and placed in the shaking water bath. Solubility assessments for all compounds, with the exception of fenofibrate, were conducted following a 24 hour dwell period. For fenofibrate, previous investigations have employed

longer dwell periods (i.e. 48-72 hours) in order to achieve equilibrium solubility [190, 191]. Correspondingly, a dwell period of 72 hours was utilized in this investigation. Saturated media samples were filtered through 0.45 μm regenerated cellulose filters and diluted with fresh media prior to assessment. HPLC-UV was utilized to quantify solubility. Analytical HPLC procedures were based on modifications of methods depicted in the literature and are denoted in Table 4.3. Solubility assessments were conducted in triplicate for each test media (pediatric and adult). Calibration curves were constructed using five standard concentrations. Standards were formulated as mobile phase dilutions of a concentrated stock solution consisting of compound dissolved in an organic solvent (i.e. methanol). All dilutions were conducted using volumetric glassware.

Due to the addition of either milk or infant formula, fed-state gastric media exists as a complex multiphase system [192]. Proteins within the media deter direct filtration of samples through 0.45 μm filters. As a result, the investigation utilized equilibrium dialysis to assess compound solubility within all fed-state gastric media, which negated the need for sample filtration to remove excess drug. To ensure restrictions in the rate of membrane permeation did not delimit solubility determinations, samples were permitted to dwell for an additional 24 hours compared to aqueous-based media. A mass of solid compound required to saturate 25 mL of media was added to separate 50 mL plastic centrifuge tubes. Twenty mL of freshly prepared media was then added. Next, a dialysis membrane (MWCO 12-14000 Da) containing 5 mL of fresh media was placed in each tube. Tubes were capped and placed in a shaking water bath. Solubility assessments were conducted after a 48 hour dwell period with the exception of fenofibrate, which was assessed after 96 hours. For assessment, tubes were taken from the water bath, the dialysis membrane was removed, and its contents were extracted. One mL of media from the within the membrane was combined with 2 mL of methanol and vortexed for 5 seconds. The mixture was centrifuged at 8000 rpm and 4^{o}C for 15 minutes. The resulting supernatant was filtered through 0.45 μm regenerated cellulose filters (Cronus) and diluted in mobile phase prior to analysis. Solubility values were quantified using HPLC-UV under the conditions specified in Table 4.3. Calibrations curves with five standard concentrations were constructed for each test media. Standards were created by dilution of a stock solution, as described above, with fresh media using volumetric glassware. Solubility assessments were conducted in triplicate.

Table 4.3 HPLC-UV analytic conditions

Column	Compound	Mobile	Q[a] (ml/min)	Temp (^{0}C)	Inj Vol (µL)	λ[b] (nm)	R_t[c] (min)	Reference
1	Carbamazepine	MeOH/ Water (60:40)	1	20	50	285	6.6	[193]
2	Dapsone	Water with ammonium acetate 0.0286M / MeOH (70:30)	1	20	10	295	5.6	[194]
2	Fenofibrate	MeOH/ Acetate buffer 0.010M pH=3.7 (82:18)	1	25	80	286	6.5	[195]
2	Griseofulvin	MeOH/ Water (65:35)	1	20	20	292	4.5	[196]
2	Indomethacin	MeOH/ Water with 1.67% orthophosphoric acid (70:30)	1	23	100	270	9.9	[197]
2	Phenytoin*	Water/ AcN (50:50)	0.5	20	10	210	5.6	[198]
2	Spironolactone	MeOH/ Water (70:30)	1	20	40	237	5.7	[199]

Column 1: Hypersil (Thermo) BDS -C18 250 x 4.6mm - 5 µm
Column 2: Zorbax SB-C18 150 x 4.6mm – 3.5µm
a - Q = flow rate; b - λ = UV wavelength; c - Rt = retention time
* - HPLC conditions altered for solubility assessments with FeSSGF media due to interference with media components. Mobile phase (Water/AcN – 60:40), Q (1ml/min) and Rt=4.8 mins.

One-way analysis of variance (ANOVA) with a post-hoc Tukey's test was applied to identify statistically significant differences in solubility between various age-specific media (i.e. neonate-infant-adult). All statistical analyses were conducted using R statistical software (v 3.1.2). The investigation utilized a significance level of $p \leq 0.05$. Average solubility differences between developed pediatric media and the corresponding reference adult media were expressed as a ratio % ($\mu_{\text{pediatric}} / \mu_{\text{adult}}$ x 100). Values greater than 100% indicate compound solubility within the pediatric media exceeded the solubility observed in adults, whereas values less than 100% conveyed the opposite. To denote relevant discrepancies in solubility, reference points corresponding to ratios of 80% and 125% were used. These values parallel the 80-125% bioequivalence criterion as specified by the US-Food and Drug Administration (US-FDA) [200]. Within the analysis, statistically significant mean ratios falling outside the pre-specified boundary range were estimated to be at an increased risk for exhibiting alterations in oral drug performance between children and adults. In contrast, when mean ratios were within the 80-125%, boundary, age-specific solubility differences were not expected to alter oral drug performance.

The influence of bile salts (NaTc) on modulating compound solubility within the developed biorelevant media was approximated using the equations presented by Mithani et al. [201],

$$logSR = 2.09 + (0.64 \cdot logP) \quad \text{(Equation 4.1)}$$

$$SC_{bs} = SR \cdot SC_{aq} \quad \text{(Equation 4.2)}$$

$$C_{sx} = C_{so} + (SC_{bs} \cdot MW \cdot [NaTc]) \quad \text{(Equation 4.3)}$$

where SR is the solubilization ratio, logP is the logarithm of the octanol-water partition coefficient, SC_{bs} is the bile salt solubilization capacity, SC_{aq} is the solubilization capacity of water, C_{sx} is the estimated compound solubility (mcg/mL) in the presence bile salts, C_{so} is the aqueous solubility (mcg/mL), MW is the compound specific molecular weight and [NaTc] is the media concentration (mM) of sodium taurocholate (bile salt). The equations, which describe the quantitative relationship between bile acids and compound solubility within aqueous based systems, incorporated bile salt concentrations for each age-specific media formulated with NaTc (FaSSGF, FaSSIF and FeSSIF). For neutral compounds (griseofulvin, spironolactone, carbamazepine and fenofibrate), experimentally determined aqueous solubility values served as inputs. For ionizable compounds (phenytoin-acid, indomethacin-acid, and dapsone-base), pH specific aqueous solubility values, as estimated by the

Henderson-Hassalbach equation, were utilized. The ratio of compound solubility, relative to adults, was estimated for each of the developed pediatric media (i.e. $pediatric_{pred}/adult_{pred}\ x\ 100$). A comparison between these predictions, which solely account for the effect of bile acids, and measured values, which account of the influence of all media components, was instituted using the root mean square error (RMSE).

$$RMSE = \sqrt{\frac{1}{n}\sum_{j=1}^{n}\left(\left(\frac{\mu_{\ pediatric\ solubility(measured)}}{\mu_{\ adult\ solubility(measured)}}x100\right) - \left(\frac{pediatric\ solubility(predicted)}{adult\ solubility(predicted)}x100\right)\right)^2}$$

(Equation 4.4)

Here, the RMSE provides a quantitative assessment of the influence of media bile salts on modulating compound solubility. For example, high agreement between predicted and measured solubility ratios, as indicated by lower RMSE values, infers NaTc is primarily responsible for observed solubility changes.

4.3 Results

Literature data utilized to define age-specific GI parameters were primarily sequestered from studies examining healthy/normal children in order to mitigate the confounding effects of altered health statuses. For example, several investigations examining fasting gastric pH in children focused on pre-operative subjects with no known GI disease undergoing elective surgery. However, due the scarcity of pediatric data, some investigations examining critically ill subjects (i.e. NICU, PICU, or ICU patients) as well as preterm neonates were included in the analysis. Such studies were additionally scrutinized to ensure their appropriateness towards defining GI parameters reflective of normal children. Investigations of gastric pH including critically ill subjects were restricted to studies where acid reducing agents (i.e. H2 antagonists) were withheld [202-204]. Two pediatric studies assessing fasting gastric pepsin levels included subjects deemed as critically ill [205, 206]. As pepsin concentrations were presented as a percentage of adult values, data from these studies were compared to reference data [207] derived from critically ill adult subjects to normalize for any potential effects of illness. Similar to term neonates, preterm neonates by a gestational age of 34 weeks are expected to

possess the ability to suckle and swallow to facilitate oral nutrition [208]. Consequently, to minimize the effects of immaturity within the analysis, studies were delimited to those where the average postmenstrual age (gestational age + postnatal age) of subjects was approximately ≥ 34 weeks.

4.3.1 Pediatric Fasted-State Simulated Gastric Fluid (P-FaSSGF)

Studies depicting gastric pepsin concentrations in pediatric subjects are presented as a percentage of adult values in Figure 4.1A. Reported concentrations were measured in a fasting state with or without histalog stimulation. Values derived from histalog stimulation tests were compared to adult subjects referenced within the same study [209]. For other studies, reference adult values were ascertained from separate investigations by the same research group or investigations utilizing a similar assay technique. A segmented analysis towards neonatal subjects was only conducted in a single study [209]. The investigation showed gastric pepsin concentrations approached infantile (1m-12m) levels after the first week of postnatal life. For example, neonates between 1-8 days postnatal age exhibited mean pepsin concentrations of ~15% of adult values while older neonates (10-32 days) and infants (67-110 days) both expressed similar mean concentrations of ~41% of adult values. Neonatal FaSSGF was developed based on the youngest cohort of subjects (i.e. those within the 1st week of life) to depict a state where the effects of development are most pronounced. Infant FaSSGF was formulated using pepsin concentrations summarized over several investigations. Concentrations of 15% and 25% of adult reference values (FaSSGF) were utilized for neonatal and infant FaSSGF, respectively.

Investigations depicting fasting gastric pH values in pediatric subjects are summarized in Figure 4.1B. Adult values represented by the mean from separate investigations, as summarized by Di Maio and Carrier [210], are displayed for reference. After the first day of life, fasting gastric pH rapidly normalizes towards adult values. Correspondingly, pediatric media (neonate and infant) representative of the fasted gastric state maintained the same pH as denoted by the reference adult media (i.e. FaSSGF - pH = 1.6).

Figure 4.1 (A) Fasting gastric pepsin concentrations amongst pediatrics [205, 206, 209, 211] is expressed as a percentage of adult values [207, 209, 212]. Investigations where pepsin concentrations were quantified over a specific age range without denoting the group's mean age were graphically depicted as the middle of the age range. Average (mean) values pertaining to neonates (0-28days) and infants (1m-12m) are illustrated for reference (red – x's). (B) Fasting gastric pH amongst pediatrics (black circles) is depicted as the central tendency, either mean or median, from separate investigations [202-204, 213-232]. Studies where gastric pH values was quantified over specific age range without denoting the group's mean age were graphically depicted using the middle of the age range. Adult data is depicted by mean pH values from separate studies, as summarized by Di Maio and Carrier [210]. Dashed reference lines correspond to the maximum and minimum mean pH values observed within the presented adult studies.

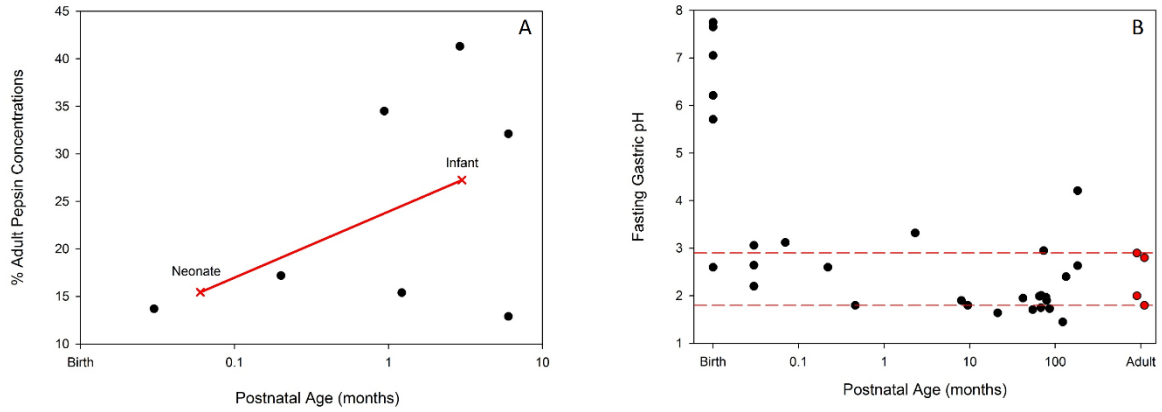

A single pediatric study was identified that investigated fasting gastric osmolality in 40 postoperative infants with a mean age of approximately 8 months [232]. The investigation depicted an average osmolality of 253 mOsm/L, which is more than twice the value of adult FaSSGF (120 mOsm/L). However, these finding may not be entirely reflective of healthy infants. In postoperative subjects, administered medications and patient induced stress during surgery can effect gastric secretions and, thus, osmolality. Consequently, owing to the lack of appropriate data to establish a relationship between age and fasting gastric osmolality, the pre-established value from adults was employed to develop pediatric media.

Literature-based assessments of gastric bile acids and phospholipids (i.e. lecithin) in the fasting state were not available for pediatric subjects. As the gastric mucosa does not contain the capacity to produce or excrete bile, the presence of gastric bile acids are primarily the result of duodenogastric reflux, a normal physiological phenomenon documented in adults [233, 234]. Therefore, it was postulated that intestinal bile levels would influence the magnitude of bile acids present within gastric fluids. With frequent feeding schedules, neonates and infants are often maintained within the fed-state during waking hours. As such, bile acid (i.e. NaTc) values within pediatric FaSSGF were derived using fed-state intestinal bile levels. The following formula was used to quantify NaTc concentrations in pediatric FaSSGF,

$$pFaSSGF_{[NaTc]}\ (uM) = \frac{pFeSSIF_{[NaTc]}}{FeSSIF_{[NaTc]}} \cdot FaSSGF_{[NaTc]} \quad \text{(Equation 4.5)}$$

where $pFaSSGF_{[NaTc]}$ is the bile acid (NaTc) concentration in pediatric FaSSGF, $pFeSSIF_{[NaTc]}$ is the NaTc concentration in pediatric FeSSIF, $FeSSIF_{[NaTc]}$ is the NaTc concentration in the reference adult FeSSIF media (10 mM), and $FaSSGF_{[NaTc]}$ is the NaTc concentration in reference adult FaSSGF media (80 uM). Bile acid values within pediatric FeSSIF media are presented in a forthcoming section. For lecithin, pediatric FaSSGF was formulated to maintain the same ratio of [NaTc]/[lecithin] as depicted by adult FaSSGF. Compositions of the developed neonatal and infant FaSSGF media are presented in Table 4.4.

Table 4.4 Pediatric Fasted-State Simulated Gastric Fluids (P-FaSSGF)

Component	Pn-FaSSGF[a]	Pi-FaSSGF[b]
Sodium Taurocholate (uM)	20	60
Lecithin (uM)	5	15
Pepsin (mg/mL)	0.015	0.025
Sodium Chloride (mM)	34.2	34.2
HCl qs	pH 1.6	pH 1.6
pH	1.6	1.6
Osmolarity (mOsm/kg)	120.7	120.7
Buffering Capacity (mEq/L/ ΔpH)	-	-

a - Pn-FaSSGF – pediatric fasted-state gastric media representative of neonates (0-28 days)

b - Pi-FaSSGF – pediatric fasted-state gastric media representative of infants (1-12 months)

4.3.2 Pediatric Fed-State Simulated Gastric Fluid (P-FeSSGF)

The composition of FeSSGF is largely influenced by added meal components. In adult FeSSGF, cow's milk is typically incorporated as it contains similar ratios of carbohydrate/protein/fat as a typical breakfast meal and avoids logistic difficulties associated with the use of homogenized solid meals [235, 236]. To institute the most physiologically relevant depiction of gastric contents in children, pediatric media were formulated using two types of commonly marketed infant formula: Cow & Gate First Infant Milk (cow's milk-based formula) and Infasoy (soya-based formula). Development of separate pediatric FeSSGF media comprised of different formulas permitted for forthcoming solubility assessments to investigate the influence of pediatric diet on biorelevant solubility.

Gastric pH within the fed-state is dependent of several factors including feed composition and time of measurement [237, 238]. Since many pediatric investigations administer various feeds (i.e. breast milk, infant formula, or D5W) and measure postprandial pH at selective time intervals, defining age-specific pH values was quite challenging. Adult FeSSGF represents a snapshot of the 'middle' phase of gastric digestion between 75 and 165 minutes post-meal ingestion [182]. The pH of adult FeSSGF was derived from Kalantzi et al.'s study, where a liquid meal consisting of 500mL Ensure

plus® was administered to 20 healthy subjects [238]. The study denoted a pH of 5 as the approximate average over the abovementioned time period. However, in a separate investigation by Dressman et al. [239], where gastric pH was monitored following ingestion of a standard solid meal (1000 Kcal), postprandial pH values differed from the results attained by Kalantzi et al. Following administration of a solid meal, gastric pH decreased towards fasting values at a faster rate compared to subjects administered a liquid meal. For example, median pH values persisted above 3 for approximately 60 minutes vs. > 180 minutes following solid meal vs. liquid meal ingestion, respectively [238, 239]. As solid foods are anecdotally the most common form of meals consumed by adults, comparison of postprandial pH changes between children, administered a typical meal (i.e. formula), and adults, administered a solid meal, were used to define pH for the developed pediatric FeSSGF. Sondheimer et al. investigated the influence of postnatal age (PNA) on gastric pH in healthy preterm neonates [240]. In-situ pH monitoring was conducted following administration of infant formula in two groups of neonates aged 2-6 days and 7-15 days PNA. Comparing pH values at approximately 120 minutes post-meal (i.e, mid-point of the 75-165 minute time frame) between the cohort of older preterm neonates and adults, as reported by Dressman et al., pH was found to be higher (0.7-1.8 units) among neonates. As a result, neonatal FeSSGF was formulated to adopt a slightly higher pH (pH = 5.7) as compared to the reference adult FeSSGF (pH = 5).

Osmolality of pediatric FeSSGF was defined by two investigations. The first, conducted by Billeaud et al. [241], characterized gastric osmolality among 15 low birth weight neonates with a mean PNA and gestational age (GA) of 8 days and 35.4 weeks, respectively. Eight test feeds, each differing in osmolality, were administered. The study noted a positive linear relationship between feed and gastric osmolality over the 3 hour study period. In a separate investigation by Thatrimontrichai and Janjindamai [242], three separate expressed breast milk feeds, which ranged in osmolality due to the addition of mineral/vitamin supplements, were tested in 26 neonate/infant subjects with a median PNA and GA of 30 days and 30 weeks, respectively. Within the study, meals with higher osmolalities were found to be associated with comparatively higher gastric osmolalities over the 1 hour test period. A linear regression model depicting the degree of association between feed osmolality and 60 minute postprandial gastric osmolality was developed based on the results of Billeaud et al.'s [241] investigation (Figure 4.2). Although a 60 minute sampling point was not obtained during the original study, the value was estimated as the average between the 45 and 90 minute sampling intervals. The validity of the derived regression equation was tested by comparing gastric osmolality predictions to the data presented within Thatrimontrichai and Janjindamai's study [242]. The results of this

comparison are depicted in Table 4.5. Estimates from the regression equation were within 8% of measured values. As such, the equation was deemed appropriate for defining osmolality in neonatal FeSSGF. Although a sampling point of 60 minutes was clearly outside the time frame used to define adult FeSSGF (75-165 minutes), children, especially those within the youngest age groups, are typically fed on a more consistent basis during waking hours (i.e. every 2-3 hours). Correspondingly, defining gastric osmolality in children based on one hour postprandial values may provide an age appropriate representation of the 'middle' phase of gastric digestion, which adult FeSSGF is formulated to mimic.

Figure 4.2 Neonatal gastric osmolality 60 minutes post-meal expressed as a function of feed osmolality. Data (black circles) represent average gastric osmolality values recorded amongst neonatal subjects as described by Billeaud et al [241]. A linear regression model (red line) was fit to the data.

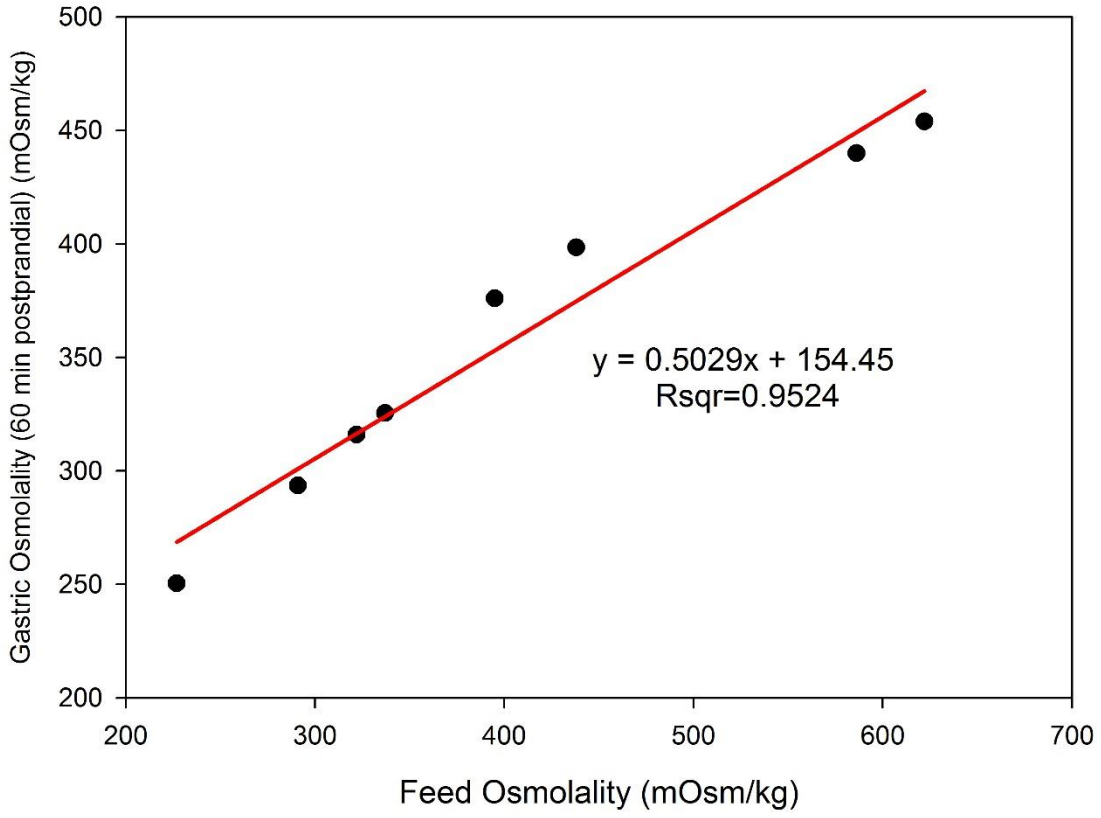

Table 4.5 Predictive performance of the osmolality regression equation

Feed Osmolality (Median - mOsm/kg)[a]	Measured Gastric Osmolality - 60 min postprandial (Median - mOsm/kg)[a]	Predicted Gastric Osmolality – 60 min postprandial (mOsm/kg)[b]	% Prediction Error ((Pred– Obs) / Obs) x 100
344	354	327	-7.6 %
426	383	368	-3.9 %
315	315	313	-0.6 %

a - Values derived from Thatrimontrichai and Janjindamai [242]

b - Predictions based on regression model, as derived from Billeaud et al. [241]

Since basal gastric volumes in infants are minute [226], the composition of gastric fluids postprandially can likely be attributed to the properties of the ingested meal. As such, the buffering capacity of pediatric FeSSGF was determined based on the buffering capacity of infant formula incorporated into the media. Since two separate neonatal media, one based on cow's milk formula and the other based on soy formula, were developed, buffering capacity determinations for each respective formula were required. Determinations were conducted at pH 5.7, the desired pH of neonatal FeSSGF. The buffering capacity (mean ± SD) of cow's milk formula at pH 5.7 was 14.03 ± 0.164. Soy-formula at pH 5.7 displayed similar a buffering capacity (14.94 ± 0.318 mEq/L/ΔpH). For simplicity, neonatal FeSSGF based on cow's milk formula and soy formula were prepared to target a buffering capacity of 15 mEq/L/ΔpH. Compositions of the developed P-FeSSGF media are depicted in Table 4.6.

Table 4.6 Pediatric Fed-State Simulated Gastric Fluids (P-FeSSGF)

Component	Pnc-FeSSGF[a]	Pns-FeSSGF[b]
Sodium Chloride (mM)	100.35	94.79
Acetic Acid (mM)	7.25	7.25
Sodium Acetate (mM)	64.65	64.65
Milk:buffer	1:1	1:1
HCl/NaOH qs	pH 5.7	pH 5.7
pH	5.7	5.7
Osmolarity (mOsm/kg)	340	240
Buffering Capacity (mEq/L/ ΔpH)	15	15

a - Pnc-FeSSGF – pediatric fed-state gastric media representative of neonates (0-28 days) fed cow's milk-based formula

b - Pns-FeSSGF – pediatric fed-state gastric media representative of neonates (0-28 days) fed soy-based formula

Appropriate information to define infantile fed-state gastric fluids (i.e. 1-12m) was not attained from the literature. As a result, an infant FeSSGF media was not developed. However, as the composition of FeSSGF is primarily attributed the contents of the added meal component, assessments conducted in neonatal media which incorporate infant formula should provide a general indication of expected solubility changes in infants consuming similar feeds. In addition, comparisons between neonatal media that are similar in all respects with the exception of the type of meal component added (i.e. cow's milk-based formula vs. soy-based formula) provide an assessment of the impact of feed composition on biorelevant solubility.

4.3.3 Pediatric Fasted-State Simulated Intestinal Fluid (P-FaSSIF)

Intestinal pH values depicted in the literature are summarized as a function of postnatal age in Figure 4.3A. The majority of pediatric data were attained from the distal duodenum though a few studies that sampled from the proximal jejunum were also included. Adult pH is depicted as mean values from

separate investigations, as summarized by Fuchs and Dressman [243]. Studies investigating intestinal pH in children, especially in the youngest age groups, were not widely published in the literature. In addition, data obtained from adults encompassed a large degree of variability. Consequently, no distinct relationship between age and fasted-state intestinal pH was observed. Pediatric media were subsequently formulated using the same pH as denoted for the adult reference media (i.e. FaSSIF – pH = 6.5).

Fasting bile salt concentrations from the proximal small intestine are depicted as a function of age in Figure 4.3B. A large degree of variability was apparent in both children and adults as denoted by the spread of data. Discernable differences between pediatric age groups (i.e. neonates, infants) and adults were not visually evident. Furthermore, the linear association between the logarithm of age and bile acid concentrations was negligible (R^2=0.05) among pediatrics. Due the substantial degree of variability between pediatric studies, P-FaSSIF was developed to assess two potential scenarios. In one media, bile salt concentrations were formulated to be 150% of adult values. In the second media, concentrations were formulated to be 50% lower than adults. A pediatric media where bile salt concentrations were similar to adult values did not necessitate development of a new media as this scenario was already depicted by the adult reference. Developed media represent hypothetical depictions of bile acid concentrations within a biologically plausible range. Correspondingly, the magnitude of compound specific solubility differences denoted in such media provides an indication of whether additional pediatric investigations are required to define bile acids within the fasted-state intestine.

Figure 4.3 (A) Pediatric fasting intestinal pH (black circles) is depicted as the central tendency, either mean or median, from separate investigations [109, 204-206, 244-246]. Studies where pH was summarized over a specific age range without denoting the group's mean age were graphically depicted using the middle of the age range. The majority of data was derived from distal duodenum, though studies which included sampling sites from the proximal jejunum were also included. Adult duodenal bile acid concentrations (red circles) are depicted as mean values from separate studies, as summarized by Fuchs and Dressman [243]. (B) Fasting duodenal bile salt concentrations amongst pediatrics (black circles) are depicted as the central tendency, either mean or median, from separate investigations [247-257]. Studies where bile acids were summarized over a specific age range without denoting the group's mean age were graphically depicted using the middle of the age range. Adult duodenal bile acid concentrations (red circles) are depicted as mean values from separate studies, as summarized by Fuchs and Dressman [243].

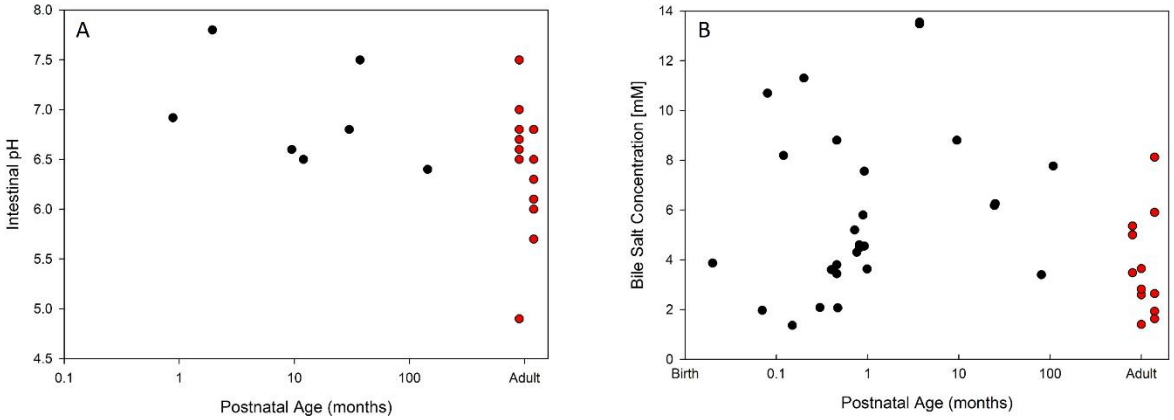

No pediatric data pertaining to phospholipids (i.e. lecithin), buffering capacity, and osmolality of intestinal fluids in the fasted-state were ascertained. Pediatric media were therefore formulated to maintain the same [NaTc]/[lecithin] ratio as depicted in the adult reference media (FaSSIF). Buffering capacity and osmolality were also defined using adult values. Compositions of the proposed P-FaSSIF media are presented in Table 4.7.

Table 4.7 Pediatric Fasted-State Simulated Intestinal Fluids (P-FaSSIF)

Component	P-FaSSIF-50%[a]	P-FaSSIF-150%[b]
Sodium Taurocholate (mM)	1.5	4.5
Lecithin (mM)	0.1	0.3
Maleic acid (mM)	19.12	19.12
Sodium hydroxide (mM)	34.8	34.8
Sodium Chloride (mM)	68.62	68.62
pH	6.5	6.5
Osmolarity (mOsm/kg)	180	180
Buffering Capacity (mEql/L/ ΔpH)	10	10

a - P-FaSSIF-50% – pediatric fasted-state intestinal media formulated with bile salt concentrations 50% (i.e. 1.5mM) of adult levels

b - P-FaSSIF-150% – pediatric fasted-state intestinal media formulated with bile salt concentrations 150% (i.e. 4.5 mM) of adult levels

4.3.4 Pediatric Fed-State Simulated Intestinal Fluid (P-FeSSIF)

Fed-state duodenal pH values from separate pediatric and adult investigations are presented in Figure 4.4A. Of the few studies presented amongst pediatrics, pH values appear to overlap with those depicted from adults. Owing to the disparate nature of available data, pH differences between each age group (neonate, infants, and adult) could not be fully elucidated. Pediatric FeSSIF media were therefore formulated using the same pH as the adult reference (i.e. pH = 5.8).

Assessments of postprandial intestinal osmolality amongst pediatrics were also scarcely published within the literature. A single study conducted by Billeaud et al. [241], which was also utilized to define pediatric FeSSGF osmolality, was identified. Duodenal osmolality was assessed in 15 low birth weight neonates following administration of a variety of feeds, each varying in osmolality. A positive linear association between feed and duodenal osmolality was found. A regression model was constructed using a congruent approach as previously discussed for defining FeSSGF osmolality

(Figure 4.4B). Although a suitable coefficient of determination (R^2 = 0.92) between feed osmolality and 60 minute postprandial duodenal osmolality was attained, a second study from which the model could be evaluated within pediatrics was unavailable. As an alternative assessment, the model was utilized to estimate to duodenal osmolality in two adult studies. Mean duodenal osmolality values of approximately 405 and 392 mOsm/kg were observed 1 hour following administration of liquid meals containing 610 and 670 mOsm/kg in separate investigations conducted by Kalantzi et al. [238] and Clarysse et al. [258], respectively. The proposed regression model provided duodenal osmolality estimates of 430 (6% over-prediction) and 454 (16% over-prediction) mOsm/kg for each respective adult investigation. Although derived from a cohort of neonatal subjects, the model exhibited an adequate predictive capacity in adults. By extension, its use for estimating intestinal osmolality amongst pediatrics (neonates and infants) was considered to be appropriate. The osmolality of neonatal FeSSIF was formulated to reflect two separate feed types, breast milk, with a reported osmolality of ~300 mOsm/kg [241, 259], and cow's milk-based formula with a measured osmolality of 368 mOsm/kg (Cow & Gate First Infant Milk). For FeSSIF reflective of older children (i.e. infants) where weaning is commonly instituted, only a single feed type was investigated, cow's milk formula. Using the aforementioned regression equation, osmolality of the developed pediatric FeSSIF was defined as 300 and 330 mOsm/kg post-administration of breast milk and cow's milk-based formula, respectively.

Fed-state duodenal bile salt concentrations among pediatrics and adults are summarized in Figure 4.4C. A positive linear association between the logarithm of age and duodenal bile acid concentrations was denoted among children (R^2 = 0.54). Bile acid concentrations among adults displayed variability, but for the most part studies depicted a mean value of approximately 10 mM, corresponding to the concentration of the reference adult media (FeSSIF v2). Mean bile acid concentrations among neonates (0-28 days) and infants (1-12m) were approximately 25% (i.e. 2.5 mM) and 75% (i.e. 7.5 mM) of adult values, respectively. Pediatric FeSSIF were subsequently formulated using these bile acid concentrations.

Figure 4.4 (A) Fed-state duodenal pH from separate pediatric investigations (black circles) is depicted by the central tendency, either mean or median [244, 260-262]. Studies where pH was summarized over a specific age range without denoting the group's mean age were graphically depicted using the middle of the age range. Adult pH values (red circles) are presented as the central tendency (mean or median) from separate investigations [238, 239, 244, 258, 263]. (B) Neonatal duodenal osmolality 60 minutes post-meal expressed as a function of feed osmolality. Data (black circles) represent average duodenal osmolality values recorded amongst neonatal subjects as described by Billeaud et al [241]. A linear regression model (red line) was fit to the data. (C) Fed-state duodenal bile salt concentrations amongst pediatrics (black circles) is depicted as the mean from separate investigations [250, 252, 254, 256, 261, 264, 265]. Studies where data was summarized over a specific age range without denoting the group's mean age were graphically depicted using the middle of the age range. Adult duodenal bile acid concentrations (0.5-1hr postprandially) (red circles) are depicted as the mean value from the various publications [210, 238, 258, 266, 267].

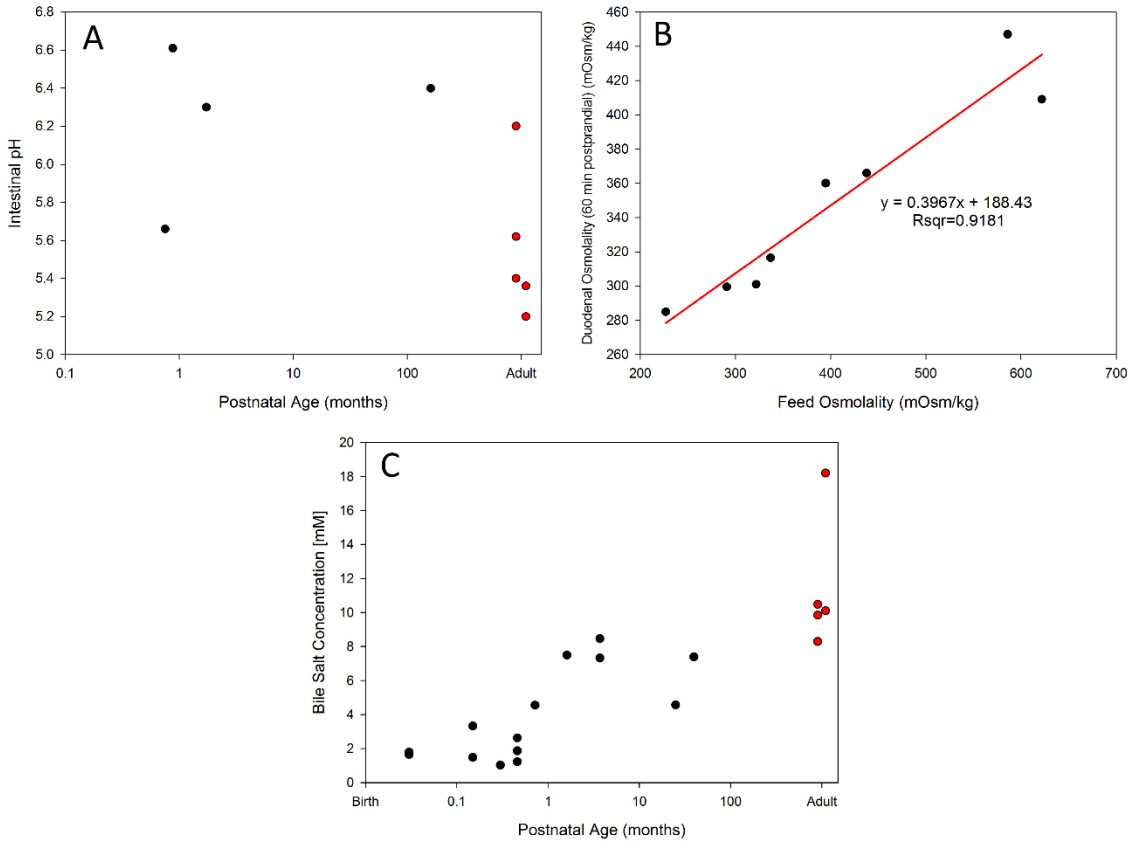

Pediatric studies characterizing concentrations of fat digestion products in the intestinal lumen have not been reported in the literature. However, since the quantity of such products is dependent on the interrelationship between fat digestion and absorption, an examination of these processes was instituted in order to derive age-dependent estimates. In newborns, concentrations of pancreatic colipase-dependent triglyceride lipase, the enzyme primarily responsible for lipid metabolism in adults, is decreased [268]. Despite this, the presence of auxiliary enzymes such as human gastric lipase, pancreatic lipase-related protein 2 and bile salt-stimulated lipase, are postulated to provide an efficient means of lipid digestion for newborns [268]. In terms of absorption, breast-fed neonates exhibit fat absorption coefficients reminiscent to that of adults despite lower duodenal bile acid concentrations [253]. It was therefore inferred that the developmental capacity of both fat digestion and absorption were comparable to adults amongst this pediatric cohort. FeSSIF media reflective of breast-fed neonates were correspondingly formulated using the same concentrations lipid digestion products (glyceryl monooleate and sodium oleate) as defined for the adult reference media (i.e. FeSSIF).

However, among formula-fed neonates, fat absorption coefficients are notably lower compared to their breast-fed counterparts as well as adults [253, 256]. Unlike breast-fed neonates, intestinal bile concentrations in formula-fed neonates were found to exhibit a positive linear correlation with percent fat absorption [253, 256]. To decipher whether a deficiency in lipid absorption or lipid digestion was the primary factor limiting internalization of fats in formula-fed neonates, pathophysiological information pertaining to necrotizing entercolitis (NEC) was used. NEC is a debilitating inflammatory GI condition occurring typically in preterm neonates but also uncommonly in term neonates. In both groups, the incidence of NEC is substantially higher in formula-fed subjects as compared to those receiving enteral feeds with breast milk [269, 270]. Though the mechanism of pathogenesis of NEC is not completely understood, one theory as described by the work published by Penn et al. [271] identified the presence of elevated concentrations of free fatty acid (FFA) as the culpable factor. The study found lipase digestion of formula, but not human milk, exhibited a cytotoxic effect in three different cell types. Furthermore, digested formula displayed significantly greater levels of FFA compared to lipase digested human milk. Based on this finding in conjunction the prevalence of NEC amongst the youngest cohort of neonates, it was inferred that the process of lipid digestion was not developmentally impaired in formula-fed neonates. Hence, the decreased capacity for fat internalization was attributed to an inadequate lipid absorptive capacity in such subjects. Correspondingly, formula-fed neonates would be expected to exhibit higher luminal concentrations of lipid digestion products. Using 75% as the average coefficient of fat absorption in formula-fed neonates [253, 256, 268], the

concentration of lipid digestion products (glyceryl monooleate and sodium oleate) was estimated to be 1.33x (i.e. 1/0.75) greater in the intestinal lumen of neonates that are formula-fed compared those that are breast-milk fed. P-FeSSIF media pertaining to formula-fed neonates was developed based on the above assertion. In infants, where luminal bile acid concentrations are higher, fat absorption is not expected to exhibit developmental impairment. Pediatric FeSSIF reflective of formula fed infants was therefore formulated using the same concentrations of fat digestion products as depicted for the adult reference media.

No pediatric studies investigating buffering capacity and concentrations of phospholipids (i.e lecithin) within the fed-state intestinal lumen were obtained. Buffering capacity of the developed pediatric media were consequently formulated using a value of 25 mEq/L/ ΔpH, the adult reference value. Using a similar approach as employed for P-FaSSGF and P-FaSSIF, lecithin concentrations were fixed to provide the same ratio of [NaTc]/[lecithin] as expressed by the reference adult media (i.e. FeSSIF.v2). The compositional details of developed P-FeSSIF media are depicted in Table 4.8.

Table 4.8 Pediatric Fed-State Simulated Intestinal Fluids (P-FeSSIF)

Component	Pnb-FeSSIF[a]	Pnc-FeSSIF[b]	Pi-FeSSIF[c]
Sodium Taurocholate (mM)	2.5	2.5	7.5
Lecithin (mM)	0.5	0.5	1.5
Glyceryl monooleate (mM)	5	6.65	5
Sodium oleate (mM)	0.8	1.06	0.8
Maleic acid (mM)	55.02	55.02	55.02
Sodium hydroxide (mM)	81.65	81.65	81.65
Sodium Chloride (mM)	95	111.73	107.35
pH	5.8	5.8	5.8
Osmolarity (mOsm/kg)	300	330	330
Buffering Capacity (mEq/L/ ΔpH)	25	25	25

a - Pnb-FeSSIF – pediatric fed-state intestinal media representative of neonates (0-28 days) fed breast milk

b - Pnc-FeSSIF – pediatric fed-state intestinal media representative of neonates (0-28 days) fed cow's milk-based formula

c - Pi-FeSSIF – pediatric fed-state intestinal media representative of infants (1-12 months) fed cow's milk-based formula

4.3.5 Solubility assessments

Solubility determinations for six of the seven compounds (carbamazepine, dapsone, griseofulvin, indomethacin, phenytoin and spironolactione) were conducted in age-specific media representative of all four gastrointestinal states: FaSSGF, FeSSGF, FaSSIF and FeSSIF (Figure 4.5). For fenofibrate, use of the predefined equilibrium dialysis method did not serve as a suitable technique for solubility determinations in fed-state gastric media. Penetration of fenofibrate through the dialysis membrane was inefficient during the selected study interval (96 hours) and, as a result, solubility could not be

quantified. Figure 4.6 depicts solubility determinations of fenofibrate in age-specific media reflective of the remaining three gastrointestinal states: FaSSGF, FaSSIF and FeSSIF.

For pediatric media representative of the fasted gastric state (i.e. P-FaSSGF), three compounds (carbamazepine, indomethacin and fenofibrate) exhibited mean solubility values below the 80 to 125% reference range, relative to adults. However for indomethacin, this difference was not statistically significant. Relative solubility changes depicted between neonatal and infant FaSSGF were consistent in terms of direction and magnitude for six of seven compounds. Only one compound, carbamazepine, displayed a statistically significant difference in solubility between neonatal and infant FaSSGF.

Solubility assessments in neonatal fed-state gastric media (i.e. P-FeSSGF), developed using cow's milk-based or soy-based formula, were compared to solubilities attained in adult FeSSGF formulated with cow's milk. Five compounds (carbamazepine, dapsone, griseofulvin, phenytoin and indomethacin) exhibited changes in solubility that fell outside the aforementioned reference range in at least one of the developed neonatal media. A trend towards lower solubility values in neonatal media was found for four of the compounds (carbamazepine, dapsone, griseofulvin and phenytoin). For indomethacin, a weak acid (pKa = 4.5), an increase in solubility compared to adult media was observed that was attributed, in part, to the higher pH of neonatal FeSSGF. Statistically significant differences in solubility between neonatal media formulated using either cow's milk-based or soy-based formula was observed in 4/6 compounds. For carbamazepine, solubility values in media comprised with cow's milk formula was greater than that of media comprised with soy formula. For dapsone, phenytoin and indomethacin the opposite was observed. In contrast, for spironolactone and griseofulvin, no statistically significant difference in compound solubility was noted between the respective neonatal media.

Since a consensus regarding differences in bile salt concentrations between children and adults within the fasted-state intestine was not achieved, compound solubility was investigated based on two theoretical media that incorporated bile salt concentrations of 150% (4.5 mM) and 50% (1.5 mM) of those in adults. For the majority of compounds (6/7), solubility determinations in both media fell within an 80% to 125% range when compared to adult values. However, for fenofibrate (logP = 5.3), solubility in P-FaSSIF-50% media was 56% of the value observed in the adult reference.

Solubility determinations conducted in pediatric media reflective of the fed-state intestine (i.e. P-FeSSIF) were compared to values attained in adult FeSSIF. For three of seven compounds (fenofibrate, griseofulvin and phenytoin), mean solubilities of less than 80% of adult values were observed in at least one of the formulated P-FeSSIF. These relevant solubility alterations were

exclusively found in neonatal media. In comparison, mean solubility values in infant FeSSIF fell within 80-125% of adult values for all compounds investigated. A general trend towards statistically significant lower solubilities in neonatal media compared to infant FeSSIF was observed in five of seven compounds. Statistically significant solubility differences between neonatal media formulated to depict intestinal fluids following administration of cow's milk-based formula (Pnc-FeSSIF) or breast milk (Pnb-FeSSSIF) were denoted for three compounds (griseofulvin, spironolactone, and phenytoin). A higher solubility was observed for griseofulvin in Pnc-FeSSIF though in both neonatal media, values were below the 80-125% reference range. Solubility was also greater in Pnc-FeSSIF for spironolactone but, in this case, solubility values in both media fell within the 80-125% reference range. In contrast, for phenytoin, a higher solubility was observed in Pnb-FeSSIF. Solubility in Pnb-FeSSIF fell within 80-125% of adult values, but for media depicting formula-fed neonates (Pnc-FeSSIF), the mean solubility was well below the 80% reference point.

Changes in compound solubility between pediatric and adult media induced by alterations in bile salt concentrations were estimated according to the equations proposed by Mithani et al [201]. These values are displayed in Figures 4.5 and 4.6 (red dots) for media formulated with NaTc (i.e. FaSSGF, FaSSIF, and FeSSIF). Table 4.9 displays RMSE values between predicted and measured solubility ratios for the developed pediatric media in order of increasing compound lipophilicity. For the two least lipophilic compounds investigated (dapsone and griseofulvin), predictions made using Mithani el al.'s equations were within a RMSE of 10%. In these cases, the equations provide an acceptable approximation of the direction and magnitude of solubility changes observed in pediatric media. As compound lipophilicity increased, a departure between predicted and measured solubility ratios was observed as indicated by larger RMSE values. For such compounds, the predicted magnitude of solubility changes due to alterations in media NaTc content were typically overstated when compared to measured values.

Figure 4.5 Measured solubility in age-specific biorelevant media expressed as the mean solubility ratio (bars) between each respective pediatric and adult media (i.e. Pi-FaSSGF / $FaSSGF_{Adult}$). Predicted solubility ratios due to differences in media bile acid content were calculated for P-FaSSGF, P-FaSSIF, and P-FeSSIF according Mithani et al.'s equations (red line, dots) [201]. Dashed lines (---) characterizing the bioequivalence criterion (80-125%) are displayed for reference. Media are denoted as follows: Pi-FaSSGF (Infant FaSSGF), Pn-FaSSGF (Neonate FaSSGF), Pnc-FeSSGF (Neonate FeSSGF comprised of cow's milk-based formula), Pns-FeSSGF (Neonate FeSSGF comprised of soy-based formula), P-FaSSIF-150% (Pediatric FaSSIF comprised with 4.5 mM NaTc), P-FaSSIF-50% (Pediatric FaSSIF comprised with 1.5 mM NaTc), Pi-FeSSIF (Infant FeSSIF), Pnb-FeSSIF (Neonatal breast-fed FeSSIF), and Pnc-FeSSIF (Neonatal formula-fed FeSSIF). Statistically significant solubility differences ($p \leq 0.05$) compared to (a) adult media, (i) infant media, (n) neonatal media, and (b) P-FaSSIF-150% were depicted using the symbols indicated.

(see next page)

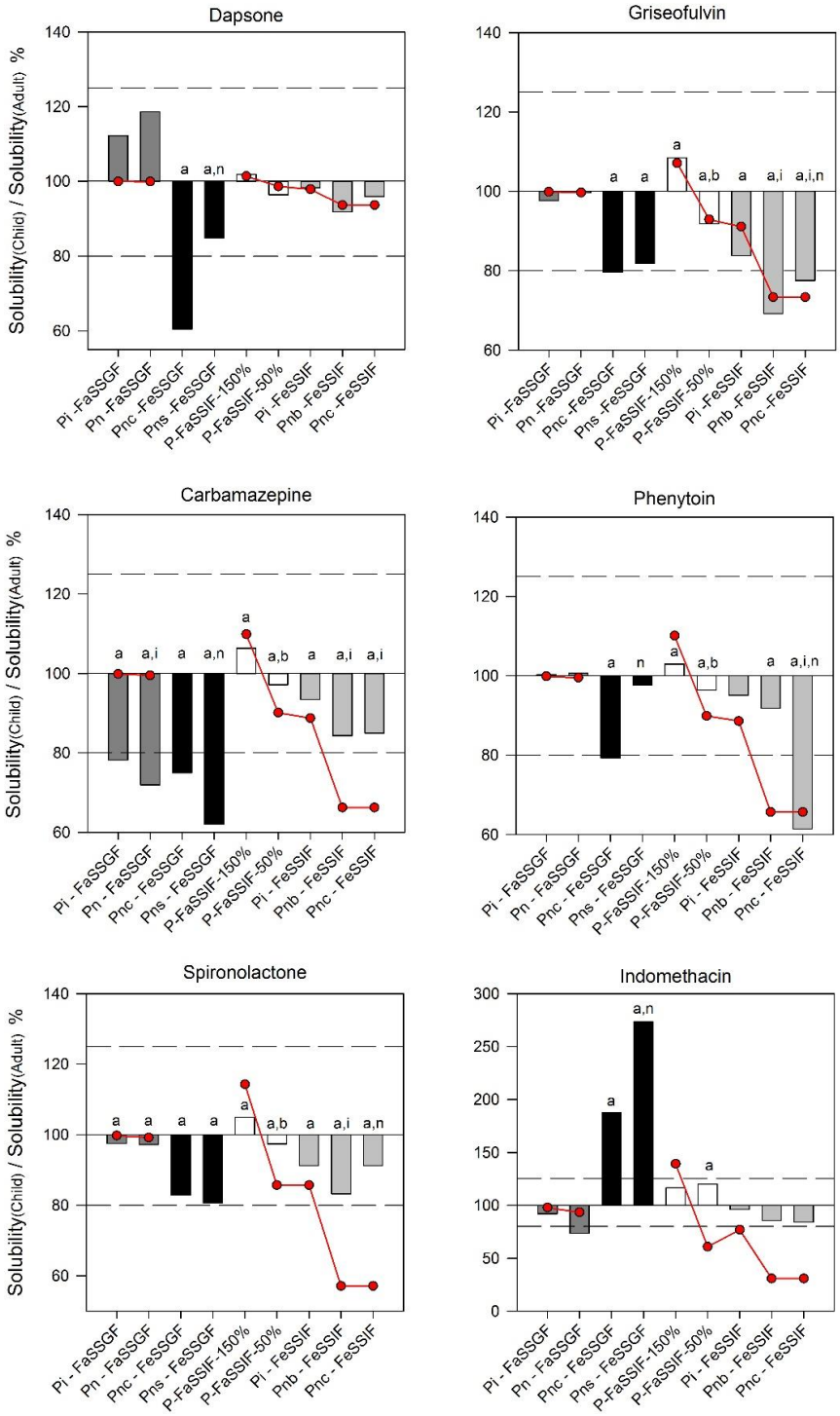
Dapsone
Griseofulvin
Carbamazepine
Phenytoin
Spironolactone
Indomethacin
Solubility(Child) / Solubility(Adult) %
Pi -FaSSGF
Pn -FaSSGF
Pnc -FeSSGF
Pns -FeSSGF
P-FaSSIF-150%
P-FaSSIF-50%
Pi -FeSSIF
Pnb -FeSSIF
Pnc -FeSSIF
Pi - FaSSGF
Pn - FaSSGF
Pnc - FeSSGF
Pns - FeSSGF
Pi - FeSSIF
Pnb - FeSSIF
Pnc - FeSSIF

Figure 4.6 Measured solubility in age-specific biorelevant media expressed as the mean solubility ratio (bars) between each respective pediatric and adult media (i.e. Pi-FaSSGF / $FaSSGF_{Adult}$). Predicted solubility ratios due to differences in media bile acid content were calculated for P-FaSSGF, P-FaSSIF, and P-FeSSIF according Mithani et al.'s equations (red line, dots) [201]. Dashed lines (---) characterizing the bioequivalence criterion (80-125%) are displayed for reference. For a description of media abbreviations and symbols (a,b,n,i), see the footnote to Figure 4.5.

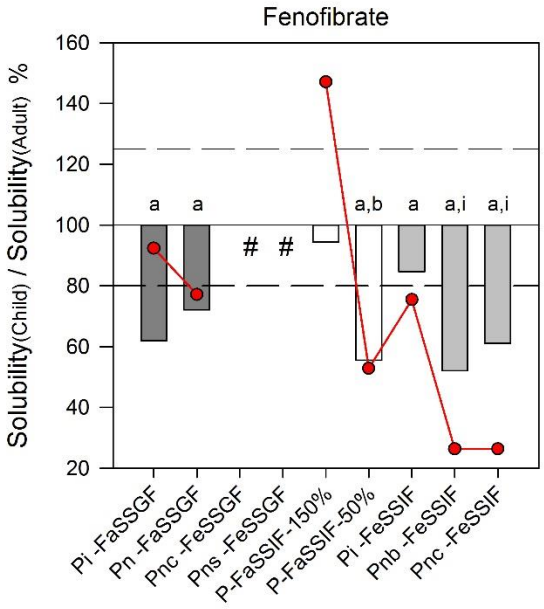

Table 4.9 Predictive performance of Mithani et al.'s [201] equations at characterizing compound specific solubility changes in pediatric media

Compound	RMSE[a]
Dapsone (logP = 0.97)	8.5%
Griseofulvin (logP = 2.18)	3.7%
Carbamazepine (logP = 2.45)	16.9%
Phenytoin (logP = 2.47)	10.9%
Spironolactone (logP = 2.78)	17.4%
Indomethacin (logP = 4.27)	39.1%
Fenofibrate (logP = 5.3)	28.5%

a - Root mean square error (RMSE) was tabulated based on Eq 4.4. Only pediatric media formulated with bile salts (i.e. P-FaSSGF, P-FaSSIF, and P-FeSSIF) were included in the assessment.

4.4 Discussion

Based on an assessment of the current literature, biorelevant media simulating the unique intricacies of the upper gastrointestinal tract (stomach and proximal small intestine) in pediatrics were developed and utilized to estimate compound specific solubility. Preferably, solubility comparisons between pediatrics and adults should be conducted using ex-vivo luminal fluid samples, but due to the numerous logistical and ethical constraints associated with obtaining of such samples in pediatrics, the use of biorelevant media was deemed as a suitable approach. In adults the appropriateness of biorelevant media has been established by investigations depicting strong positive correlations in compound solubility between simulated and human intestinal fluids [272, 273].

Pediatric fed-state gastric media (P-FeSSGF) was formulated using either cow's milk-based or soy-based formula to assess the impact of feed type on compound solubility. The use of human breast milk within the investigation was precluded due to logistic issues associated sample obtainment and uniformity. In terms of uniformity, the composition human breast milk is well known to exhibit both intra- and inter-subject variability in composition [274]. Infant formulas, however, are subject to quality control inspections to ensure batch-to-batch uniformity, ensuring biorelevant media are prepared in a reproducible fashion. Marketed infant formulas are designed to mimic the composition of human breast

milk with regards to the proportions of energy provided from protein, fats, and carbohydrates [275]. In human breast milk, proteins are predominantly comprised of two forms, whey and casein, in a ratio of 60:40, respectively. In contrast, the whey-to-casein ratio of cow's milk is 18:82 [275]. To address this discrepancy, many formulas, including Cow & Gate First Infant Milk (cow's milk based), have introduced additional amounts of whey protein in order to mimic ratios observed in human milk [275]. The influence of casein on compound solubility has previously been depicted for the anticoagulant dicumarol, where increases in casein concentration corresponded to higher dicumarol solubility values [276]. Despite supplementation with vitamins and minerals, infant formula cannot fully reproduce the biological complexity of human breast milk which contains antibodies, enzymes, and growth factors [275]. However, cow's milk formula does provide a suitable approximation in terms of macronutrient composition and protein type that is free from the inherent variability associated with breast milk. As such, solubility studies conducted in neonatal FeSSGF comprised with cow's milk formula may encompass applicability towards breast fed neonates.

Concentrations of media components were formulated to represent the average tendency over a specific age range. To summarize age-specific data from the literature, the investigation utilized non-weighted arithmetic means. Though simplistic in nature, use of the arithmetic mean was preferred over other more robust computational or statistical analyses based on several considerations. First, there is the relative disparity of literature investigations devoted to defining the composition of luminal fluids in pediatrics compared to adults. For many media components only a handful of studies were available to quantify differences between subsequent age groups. Of studies obtained, high degrees of variability were typically noted. This is likely attributed to the dynamic nature of the developmental process, where the composition of luminal fluids continually change as children mature. Due to this disparity of available data and its inherent variability, employment of statistical tests to identify significant differences in component concentrations between adjacent age groups were not applicable. Similarly, the use of regression analyses were typically unable to establish meaningful correlations between parameter values and age. A second consideration for the preferential use of non-weighted arithmetic means was due to the precarious nature of qualifying investigations. A large majority of pediatric studies were completed over three decades ago, where differences in reporting standards and quantitative techniques were wide-ranging. Employment of a non-weighted approach was instituted to simplify the analysis though, understandably, the method lacks the informative capacity of approaches that consider study quality, as frequently adopted by systematic reviews [277]. Finally, studies varied in terms of data presentation, making implementation of weighted averages difficult. Reporting of

variability associated with luminal fluids components was inconsistent between investigations. For example, separate studies utilized a variety of measures including standard deviation, range, or interquartile range. Additionally, the number of subjects allocated to specific age ranges were not identified by some investigators [205]. Due to this lack of consistency between studies, employment of a weighted mean was precluded in favor of a non-weighted approach. As the arithmetic mean does not provide an indication of parameter variability, the analysis is unable to depict expected variations within the population. However, as biorelevant media is developed to represent luminal fluids in an average individual, descriptions of parameter variability were unnecessary.

Due to the disparate nature of available pediatric data, the quantitative value of many media components were based on biological inferences or adoption of adult values. For example pediatric investigations pertaining to luminal concentrations of pepsin, phospholipids, fat digestion products, and osmolality were either scarcely reported or lacking within the literature. The proposed age-specific media attempted to approximate the *in vivo* composition of pediatric luminal fluids based on a current state of knowledge. As future investigations are obtained, such formulations should undoubtedly be modified to provide greater degrees of biological relevance.

In addition to its primary goal of facilitating suitable IVIVC, biorelevant media should demonstrate a practical degree of stability. Apart from noticeable changes in visual appearance, media stability can be formally evaluated by assessing for alterations in physicochemical parameters under ambient and test conditions. In Jantratid et al.'s original publication [182], which described the reference adult media utilized by this investigation, stability was evaluated through measurements of media pH, buffering capacity and osmolality. For adult FeSSGF and FeSSIF-v2, consistency in physicochemical parameters were observed under ambient conditions over a 72 hour study period. In addition, with the exception of minor changes in osmolality, the abovementioned media demonstrated stability under test conditions of 37^{o}C over the same time period. Changes in media physicochemical properties (i.e. poor stability) during solubility assessments may lead to corresponding changes in compound specific saturation solubility. In the current investigation, solubility assessments in fed-state simulated gastric media comprised of cow's milk (FeSSGF) and infant formula (neonatal FeSSGF) were conducted at 37^{o}C after 48 hours for most compounds. Though stability studies were not conducted within the developed pediatric FeSSGF, it was inferred that stability would be similar to that of adult FeSSGF. However, if large scale implementation of the depicted pediatric media is desired, future research evaluating media stability will certainly be required.

For the majority of study compounds, solubility assessments proceeded without issue. However for fenofibrate, the most lipophilic compound evaluated (logP = 5.3), logistic issues materialized with solubility determinations in biorelevant media reflective of the fed gastric state. For FeSSGF media, the study employed equilibrium dialysis to assess compound solubility. Though this technique proved effective for most compounds, it was unsuitable for fenofibrate. Following a 96 hour dwell period, fenofibrate concentrations within the membrane were below the limit of quantification. This result may indicate inadequate permeation of the dialysis membrane by fenofibrate in milk or formula-based samples. A congruent example is demonstrated by the *in vivo* pharmacokinetics of fenofibrate. In humans, fenofibrate exhibits extensive protein binding (~99%) and, as such, filtration by hemodialysis is not considered effective [278, 279]. Based on this assessment, use of equilibrium dialysis was not considered feasible for determination of fenofibrate solubility in fed state gastric media. These values were correspondingly excluded from the analysis.

Solubility assessments were confined to BCS Class II compounds, where limitations in absorption are primarily attributed to inadequate drug solubility. For such compounds, differences in luminal solubility may signify alterations in oral drug performance [48]. To maintain a degree of biological relevance, the analysis was further limited to compounds where documented or investigational uses in both children and adults have been depicted. To identify relevant changes in age-specific solubility, the study utilized the same threshold as depicted by the US-FDA for attainment of *in vivo* bioequivalence (i.e. 80-125%) [200]. It should be noted however that solubility is only one parameter which can exert an effect on oral compound absorption. Other parameters including gastric emptying time, small intestinal transit time, intestinal permeability, gut metabolism, luminal degradation and presence of intestinal transporters may also impart an influence *in vivo*. In order to fully elucidate the impacts of growth and development on oral compound absorption, a more comprehensive analyses such as physiologically-based pharmacokinetic (PBPK) modeling would be required to integrate age-dependencies in all the aforementioned parameters. The presented analysis which focusses on biorelevant solubility as a surrogate for oral compound performance was therefore an overt simplification. However, this approach was justified based on the cohort of compounds assessed, which was confined to solubility-limited (BCS Class II) drugs.

Compared to adult media, solubility in pediatric fasted-state gastric media (i.e. P-FaSSGF) was both statistically different ($p \leq 0.05$) and outside the purported bioequivalence criterion for two compounds, fenofibrate and carbamazepine. For fenofibrate, mean solubility values in adult FaSSGF and pure water were comparable at 0.281 and 0.206 mcg/mL, respectively. In contrast, solubility within

adult fasted-state intestinal media (i.e. FaSSIF) was considerably greater (2.42 mcg/mL). The discrepancy in solubility values between FaSSGF and FaSSIF provides an indication of the relative influence of each state on modulating oral absorption. In this case, due to its poor solubility in comparison to intestinal fluids, fasted state gastric fluids are unlikely to play an influential role on modulating the extent of fenofibrate absorption. Solubility alterations observed in P-FaSSGF were therefore not postulated to impact the oral performance of fenofibrate in children. Differences in solubility between neonatal and infant FaSSGF reached a statistically significant threshold for only one compound, carbamazepine. However for both media, the mean solubility fell outside the bioequivalence threshold when compared to adult values. Based on this analysis, an argument may be formed as to the need for separate pediatric media since solubilities in neonate and infant FaSSGF appear to be similar in most cases. The current investigation focused on solubility, a compound specific property. However, in terms of establishing IVIVC for solid dosage forms, biorelevant media is typically employed within dissolution tests to assess formulation properties [280]. In addition to modulating solubility, media components that are age-specific may also exert an influence on the rate of compound release and subsequent dissolution from a formulation. For example, the addition of pepsin into biorelevant media has been demonstrated to decrease surface tension [183]. For specific formulations, such changes can exert of an effect on the rate of compound dissolution [281]. Also, the presence of pepsin within dissolution media can facilitate effective compound release from cross-linked gelatin capsules [282]. Therefore, although comparable solubilities were observed for neonatal and infant FaSSGF media, use of separate age-specific media may be justified for use in dissolution testing.

Solubility assessments in age-specific FeSSGF media were conducted for six compounds. For the majority of compounds (5/6), the mean solubility in neonatal media, comprised of either cow's milk-based or soy-based formula, fell outside the 80-125% bioequivalence criterion in relation to adult media comprised of milk. In addition, statistically significant differences in compound solubility between pediatric media comprised with cow's milk-based and soy-based formula were observed in four compounds. These results infer that differences in feed composition between children as well as between children and adults can impart relevant changes in gastric solubility and, potentially, affect oral compound performance.

Of the limited pediatric investigations examining luminal fluids within the fasted-state proximal intestine, bile salt concentrations were found to exhibit a high degree of variability without any apparent age dependency. To explore the impact of such variations, two FaSSIF media were developed with bile salt concentrations of 50% (1.5 mM) and 150% (4.5 mM) of adult values. For the

majority of compounds (6/7), mean solubility values within the two proposed P-FaSSIF media fell within an 80-125% range from adult values. However for the most lipophilic compound, fenofibrate (logP = 5.3), solubility in P-FaSSIF media containing 1.5 mM NaTc was 56% of adult values. If such a media is reflective of *in vivo* luminal fluids in children, the observed change in solubility may signify an alteration in fenofibrate oral performance compared to adults. Prospectively, hydrophobic compounds are expected to play an increasingly important role in therapeutics as use of drug discovery techniques such a high-throughput screening typically produces candidate compounds of higher lipophilicity [283]. To provide an accurate depiction of luminal solubility for such compounds, a consensus regarding intestinal bile salt concentrations in pediatrics is needed. This demonstrates a need for more high quality studies characterizing gastrointestinal physiology in pediatrics.

Solubility assessments conducted in fed-state intestinal media representative of infants were within 80-125% of adult values for all 7 compounds tested. Such a result was unsurprising as infant and adult media were compositionally similar, aside from small deviations in bile salt content, lecithin, and osmolality. Two neonatal media were formulated to reflect differences in intestinal fluid composition following administration of breast milk or cow's milk-based formula. Mean compound solubility values in neonatal media fell outside the 80-125% criterion from adult values for 3 of the 7 compounds examined. Statistically significant differences in solubility between media reflective of breast-fed and formula-fed neonates was observed for 3 compounds. The relative magnitude of these differences appeared to be compound specific. For example, spironolactone solubility in intestinal media reflective of breast and formula fed neonates were 83% vs. 91% of adult values, respectively. In contrast, for phenytoin a larger discrepancy between solubility ratios was observed (92% vs. 61% of adult values, respectively). These findings demonstrate the potential impact of different feed types on intestinal compound solubility.

The study also included an evaluation the relative importance of bile salts in modulating compound solubility within the developed pediatric media. Predictive equations presented by Mithani et al. [201] were used to estimate the impact of alterations in bile salt content on compound solubility. Measured solubility values, which are influenced by all media components, were compared to estimated values, which only account for differences in media bile salts, using RMSE. The analysis demonstrated a decreased predictive capacity of the aforementioned equations (ie. larger RMSE values) as compound lipophilicity (logP) increased. This indicates that as compound lipophilicity increases, other media components, aside from bile salts, exert a more pronounced role in modulating compound solubility. For example, the capacity of media components such as buffer (sodium phosphate), fat digestion

products (sodium oleate) and salt (sodium chloride) to modify compound solubility has previously been demonstrated within the literature [44].

4.5 Conclusion

The current investigation strove to appropriately depict the *in vivo* composition of pediatric luminal fluids based on the current literature and represents an initial foray into the development of pediatric biorelevant media. To increase the biological applicability of future iterations of such media, it is clear prospective studies focused on defining the composition of the pediatric lumen under varying conditions is required. For 6 of the 7 BCS Class II compounds investigated, solubility fell outside an 80-125% range from adult values in at least one of the developed pediatric media. This result demonstrates the impact of age-related alterations in GI fluid composition on compound solubility. Solubility represents an integral component of the BCS, a framework which is extensively utilized by both industry and regulatory bodies to guide drug development in adults. The utility of a similar classification system in pediatrics is in part contingent on our understanding of how developmental differences between children and adults translates to alterations in definable properties such as compound solubility. The investigation sought to address this concern and, in turn, provides a dialogue surrounding the future development of a pediatric-focused BCS.

Chapter 5: Improving Pediatric Protein Binding Estimates: An Evaluation of α1-acid glycoprotein (AAG) Maturation in Healthy and Sick Populations

The contents of this chapter are reflective of an original manuscript submitted by the Ph.D. candidate (Anil R Maharaj) to the journal Clinical Pharmacokinetics in Nov 2016. All pertinent research analyses was conducted by the Ph.D. candidate.

5.1 Introduction

Plasma protein binding is a key physiological process capable of imparting influence on both pharmacokinetic (PK) and pharmacodynamic (PD) properties of xenobiotics. As such, measures of plasma protein binding are typically considered an intrinsic component for scaling PK data from preclinical species or *in vitro* systems towards humans [284]. Between children and adults, developmental differences in the concentration of plasma proteins have been documented [51]. As the extent of xenobiotic-protein binding exhibits a direct relationship to the concentration of plasma proteins, differences in protein binding between children and adults are expected [52]. Correspondingly, quantitative descriptions of the ontogeny of plasma proteins represent a central component of scaling PK between different maturational stages (i.e. intraspecies scaling) [66].

Human serum albumin (HSA) and α-1-acid glycoprotein (AAG) are the two major proteins present in serum with binding capacities towards a wide variety xenobiotics [285]. Whereas HSA is typically associated with binding acidic exogenous compounds, AAG displays a high affinity towards basic lipophilic compounds [49, 50]. AAG is comprised of a highly glycosylated single polypeptide chain [285] with a molecular weight ranging between 41-43 kDa [286]. Binding of xenobiotics is facilitated by the presence of a single ligand-binding site per AAG molecule [49, 287]. In humans, the majority of AAG is present as either 2 or 3 genetic variants [288]. Furthermore, differences in ligand binding properties between specific variants have been documented in the literature [289, 290]. For several therapeutic compounds including imipramine, propranolol, lidocaine, methadone, and chlorpromazine, AAG represents the major constituent modulating plasma binding [52]. In healthy subjects, plasma concentrations of AAG range from ≈50-130 mg/dL [285]. However, as an acute-phase reactant, AAG concentrations can increase 3-5 fold in response to pathologies such as Crohn's disease,

myocardial infarction, infection, burns, and malignancy [50, 291]. In comparison, decreased AAG concentrations are associated with pregnancy, oral contraceptive use, and infancy [291].

An evaluation of the degree of change in plasma AAG concentrations associated with normal growth and development was published by McNamara and Alcorn [51]. Using data compiled from three separate publications, the authors derived a quantitative equation (i.e. linear model) describing the relationship between postnatal age (PNA) and plasma AAG concentrations from birth to adulthood. Despite providing suitable estimates for older subjects, the use of a linear model appeared to overestimate AAG concentrations amongst the most developmentally immature subjects (i.e. newborns) [51]. In addition, the aforementioned work exclusively focused on normal/healthy subjects; whereas, utilization of therapeutic compounds is typically focused towards diseased subjects. As AAG is an acute-phase reactant, it is unclear whether the equations presented by McNamara and Alcorn provide a suitable modality for estimating differences in AAG concentrations between pediatric and adult subjects with disease.

This work will serve to quantitatively describe the ontogeny of serum AAG in normal (healthy) individuals as well as an additional cohort of subjects diagnosed or suspected of bacterial infection (infected). Pediatric fraction unbound in plasma (fu) data for compounds exhibiting preferential binding to AAG will be used to compare the predictive capacity of the ontogeny equation derived from this work to McNamara and Alcorn's [51] previously proposed equation.

5.2 Methods

The present analysis evaluating the ontogeny of AAG in humans (from birth to adulthood) was divided into three corresponding subsections: (i) evaluation of AAG ontogeny in normal subjects, (ii) evaluation of AAG ontogeny in subjects with known or suspected infections, and (iii) comparison of the predictive performance of our prospectively derived ontogeny equation to a previously proposed model [51].

5.2.1 Ontogeny of AAG in healthy (normal) subjects

To assess the relationship between age and plasma AAG concentrations in healthy (normal) subjects, the analysis utilized data compiled from the literature. Investigations quantitatively denoting the age of participants in addition to plasma/serum AAG concentrations expressed in terms of central tendency (i.e. mean or median) and spread (i.e. standard deviation, standard error of the mean, or percentiles) were included. Investigations reporting AAG levels among different subject groups were permitted to

contribute multiple data points to the analysis. Publications that expressed data graphically were converted to numerical values using GetData Graph Digitizer (v2.26).

To introduce a degree of consistency between studies conducted over various publication dates, protein concentrations were normalized toward certified reference material (CRM) 470 values, a widely circulated serum protein calibrant developed in 1993 [292], using the following process. For investigations conducted between 1973 to 1993 or those utilizing protein standards manufactured during these aforementioned years, protein standards were assumed to conform to United States National Reference Preparation for Serum Proteins (USNRP) lot 12-0575C values. AAG concentrations were subsequently normalized towards CRM470 values using a proportional transfer value [293]. For investigations conducted after 1993, protein standards were assumed to conform to CRM470 values. As such, no adjustment was made. Studies conducted prior to 1973 were excluded from the analysis due to the assumed diversity in protein standards available prior to this year [294]. Quantitative assays utilized between studies varied and included radial immunodiffusion, nephelometry, turbidimetry, HPLC, and immunoelectrophoresis. Due to the inherent difficulty of assessing quantitative equivalence between specific assays conducted in different laboratories over various periods of time, an overarching assumption that AAG concentrations were equivalent between assay types was used.

In human plasma, AAG concentrations are log-normally distributed [295]. Considering this distributional assumption, the analysis, which compiled data obtained from various investigations, required AAG concentrations to be expressed using log-normal parameters such as the geometric mean and log-normal standard error (log-normal standard deviation/$\sqrt{n}$). For the majority of investigations, AAG concentrations were reported using an arithmetic mean and standard deviation. For these studies, estimates of the geometric mean (μ_{geo}) and log-normal standard error (SE_{LN}) were determined using the following equations [296]

$$\mu_{geo} = \frac{m}{\sqrt{1+\frac{SD^2}{m^2}}} \quad \text{(Equation 5.1)}$$

$$SE_{LN} = \sqrt{\frac{ln\left(1+\frac{SD^2}{m^2}\right)}{n}} \quad \text{(Equation 5.2)}$$

where m is the arithmetic mean, SD is arithmetic standard deviation, and n is the number of individuals examined. Two investigations [297, 298] expressed AAG concentrations in terms of percentiles (5^{th}, 50^{th}, and 95^{th}; or 2.5^{th}, 50^{th} and 97.5^{th}). For these studies, the median (i.e. 50^{th} percentile) was assumed to be equivalent to the geometric mean [299]. Using the assumption that log-transformation of plasma AAG concentrations results in a normal distribution, the log-normal standard error was estimated using the following equation

$$SE_{LN} = \frac{ln(Upper) - ln(Lower)}{2 * T_{\#,n-1} * \sqrt{n}} \qquad \text{(Equation 5.3)}$$

where *Upper* refers to the 95^{th} or 97.5^{th} AAG percentile, *Lower* refers to the 2.5^{th} or 5^{th} AAG percentile, and $T_{\#,n-1}$ is the one-sided critical t-value (probability 0.95 or 0.975) associated with n-1 degrees of freedom. One investigation [300] graphically expressed neonatal AAG concentrations using arithmetic means and standard errors of the mean (SEM) without denoting the number of subjects assessed at each time-point. For this study, the geometric mean was estimated using equation 5.1 with an approximate SD value derived from additional figures from the same manuscript depicting the upper limit of normal for AAG values (mean +2SD). Based on the approximation that the coefficient of variation (CV=SD/m) of a log-normally distributed variable is equal to the log-normal standard deviation [301], an estimate of the log-normal standard error was derived using the right-hand component of equation 5.4.

$$SE_{LN} \sim \frac{CV}{\sqrt{n}} = \frac{SD/m}{\sqrt{n}} = \frac{SEM}{m} \qquad \text{(Equation 5.4)}$$

Prior to evaluating AAG ontogeny, a preliminary graphical assessment was instituted to illustrate the of range of age-specific AAG concentrations, normalized to the CRM470 standard and expressed using geometric mean values, among the complied dataset (Figure 5.1). For one investigation, published by Philip and Hewitt [302], the researchers provided plasma AAG levels among 244 neonatal inpatients between birth and 7 days old. Although subjects were deemed to be 'noninfected' based on bacterial cultures and clinical determinants of infection, all were initially admitted with suspected sepsis. Despite this, AAG concentrations expressed by this investigation appeared to be visually congruent to similar aged subjects expressed by other studies (Figure 5.1). Data pertaining to this study was, therefore, maintained within the analysis although subjects did not meet a prototypical definition of healthy. Based on Figure 5.1, it was also noted that AAG concentrations contributed by Malvy at

al.'s publication [298], which examined plasma protein concentrations within 5 different pediatric age groups, were notably higher than other studies depicting similar aged subjects. For example, the estimated μ_{geo} of AAG concentrations from Malvy et al.'s publication, who examined children over an age range where plasma AAG levels appear to be stable (3 to 16 years) (Figure 5.1), was 131 mg/dL. Comparatively, the estimated μ_{geo} of AAG concentrations in 9 groups of children within a similar age range (3-16 years) from 5 different investigations was 91.9 mg/dL [303-307]. Further stratifying studies based on geographic location and assay type did not address the observed difference in AAG concentrations documented by Malvy et al. For example, based on 3 investigations conducted in the same geographic location as Malvy et al.'s study (i.e. France), the $\mu_{geo}$of AAG concentrations was 91.5 mg/dL for 5 groups of children within a comparable age range [304, 306, 307]. In addition, 106 mg/dL was the μ_{geo} of AAG concentrations in 2 groups of comparably aged children observed in 1 investigation [304] using a similar assay type (nephelometry) as employed by Malvy et al. Based on the aforementioned assessment, AAG concentrations obtained from Malvy et al.'s study were subsequently removed from the dataset.

To quantitatively describe the functional relationship between age and plasma AAG levels, a variety of models were assessed: linear, power, exponential, linear-log, and sigmoid Emax. Gestational ages (GA) for neonatal (preterm and term) and infant subjects' were not a universally reported among all investigations. As such, PNA was utilized as the primary age descriptor within this analysis. The functional form of each model is denoted in Table 5.1. Parameter estimation was conducted using a maximum likelihood estimation (MLE) technique with minimization of the objective function value (the negative two log-likelihood) achieved via the fminunc algorithm in Matlab R2015a (The Mathworks Inc., Natick, MA). Model fits were weighted using the squared reciprocal of log-normal standard errors associated with each study group ($1/{SE_{LN}}^2$). To impart a log-normal error structure, parameter estimation was performed using log-transformed values for observed (i.e. study specific μ_{geo}) and predicted AAG concentrations with PNA, in days, serving as the sole covariate for all fitted models (Table 5.1). Since predicted plasma AAG concentrations at birth (i.e. PNA = 0 days) under the power and sigmoid Emax model return a value of 0, the fitting algorithm, which log-transforms predictions, fails to compute (i.e. Ln(0) = undefined). In addition, the linear-log model is undefined at birth. To circumvent these operational issues, the PNA for subject groups assessed at birth (PNA = 0) were adjusted to a PNA of 1 day. This modification was deemed defensible as the μ_{geo} of AAG concentrations observed among subjects assessed at birth and those observed during the first day

of life were similar within our dataset (19.92 vs. 17.67 mg/dL, respectively). Model selection was performed using a combination of the Akaike Information Criterion (AIC) and a visual inspection of observed study data overlaid with predicted AAG concentrations to assess curve shape.

Figure 5.1 Plasma AAG concentrations among publications examining healthy subjects. Concentrations, normalized to CRM470 values, are depicted using estimated geometric mean values (o) for each study group. Geometric error bars depict the log-normal SE associated with each study cohort. AAG values contributed by Philip and Hewitt [302] (◊) and Malvy et al. [298] (□) are denoted separately.

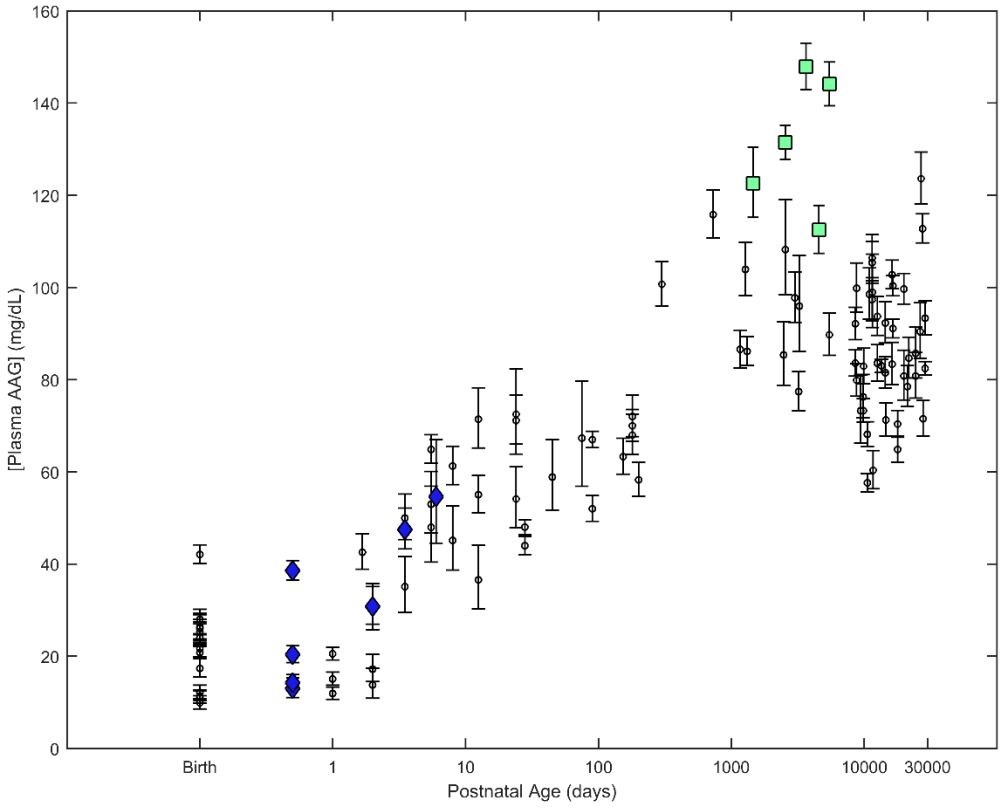

Table 5.1 Ontogeny models investigated

Model	Equation[1]
Linear[2]	$(a * \boldsymbol{AGE}) + b$
Power[2]	$b * \boldsymbol{AGE}^{a}$
Exponential[2]	$b * e^{a*\boldsymbol{AGE}}$
Linear-Log[2]	$b + [a * ln(\boldsymbol{AGE})]$
Sigmoid Emax[3]	$\frac{AAG_{max} * \boldsymbol{AGE}^{P}}{TM_{50}{}^{P} + \boldsymbol{AGE}^{P}}$

[1]the covariate AGE was specified using either postnatal age (days) or postmenstrual age (weeks)

[2]a and b denote estimable parameters associated with the linear, power, exponential, and linear-log models

[3]AAG_{max} (maximum plasma AAG concentration [mg/dL]), TM_{50}(age at 50% AAG_{max}[days]), and P (Hill coefficient) denote estimable parameters associated with the sigmoid Emax model

5.2.2 Ontogeny of AAG in subjects with diagnosed or suspected of infection

To evaluate of the relationship between age and plasma AAG concentrations in patients diagnosed or suspected of infection, individual subject data were compiled over three clinical trials: The Pharmacokinetics of Anti-Staphylococcal Antibiotics in Infants Clinical Trial (Staph Trio; NICHD-2012-STA01, ClinicalTrials.gov NCT01728363; IND 115,396) [308], Pharmacokinetics of Understudied Drugs Administered to Children per Standard of Care (PTN POPS; NICHD-2011-POP01, ClinicalTrials.gov NCT01431326; IND 113,645) [309], and Safety and Pharmacokinetics of Multiple-Dose Intravenous and Oral Clindamycin Pediatric Subjects With BMI ≥ 85th Percentile (CLIN01; NICHD-2012-CLN01, ClinicalTrials.gov NCT01744730; IND 115,396) [310]. The dataset consisted of a subset subjects being treated with the antibiotic clindamycin in whom plasma AAG concentrations were ascertained. Age was denoted as PNA; however, gestational age was also recorded for subjects less than 3 months old.

A similar assessment as described in the previous section was instituted to select the most suitable quantitative equation (Table 5.1) to describe the relationship between plasma AAG levels and PNA. Parameter estimates were obtained via MLE using a log-normal error model with

minimization of the objective function value achieved using the previously described computational approach. Confidence intervals associated with estimated AAG concentrations were tabulated using the delta method (asymptotic theory) [301].

An evaluation of the use of an alternative age descriptor, post-menstrual age (PMA = PNA + GA), was also conducted using this dataset. Parameter estimates were obtained in a similar manner as depicted above but using PMA, in weeks, instead of PNA. For subjects greater than 3 months of age, PMA was calculated assuming a GA of 40 weeks. The AIC and standard deviation of log-normalized residuals (≈RMSE) between models utilizing PMA and PNA were utilized to assess the goodness of fit associated with each age descriptor.

5.2.3 Prediction of pediatric fraction unbound (fu): a comparison of the AAG ontogeny equation derived from this study to a previously proposed model

Estimates of pediatric fu (fu_{ped}) were tabulated from observed adult fu (fu_{adult}) values and the ratio of pediatric-to-adult plasma protein concentrations ($\frac{P_{ped}}{P_{adult}}$) using the following equation proposed by McNamara and Alcorn [51].

$$fu_{ped} = \frac{1}{1+\frac{P_{ped}}{P_{adult}}\frac{(1-fu_{adult})}{fu_{adult}}} \qquad \text{(Equation 5.5)}$$

To obtain $\frac{P_{ped}}{P_{adult}}$ ratios as required by equation 5.5, the derived AAG ontogeny equations, which were formulated in terms of absolute plasma concentrations (mg/dL), were simply divided by estimated adult AAG values.

A set of experimentally determined fu_{ped} values also complied by McNamara and Alcorn [51] were utilized to assess the predictive accuracy of estimates. The dataset consisted of 17 pairs of age-specific fu values (pediatric and adult) for 11 xenobiotics exhibiting specific affinity towards AAG. Observed fu values were predominantly determined in plasma samples from healthy or control subjects. Correspondingly, estimates of fu_{ped} were derived using observed fu_{adult} values from the dataset and $\frac{P_{ped}}{P_{adult}}$ ratios pertaining to the ontogeny of AAG in healthy subjects. Overall predictive performance was evaluated using the average-fold error (AFE) and absolute average-fold error (AAFE) as measures of bias and precision, respectively. The equations for both measures are given below

$$AFE = 10^{\frac{1}{n}\sum \log(\frac{pred}{obs})} \quad \text{(Equation 5.6)}$$

$$AAFE = 10^{\frac{1}{n}\sum \left|\log(\frac{pred}{obs})\right|} \quad \text{(Equation 5.7)}$$

where obs is the observed fu_{ped} value from the dataset and $pred$ is the predicted fu value based on equation 5.5. In addition, the predictive accuracy of fu_{ped} estimates derived using McNamara and Alcorn's [51] seminal AAG ontogeny equation was tabulated for comparison.

5.3 Results

The ontogeny of plasma AAG in healthy (control) subjects was evaluated using data from 25 separate studies complied from the literature [291, 295, 297, 300, 302-307, 311-325]. The analysis included AAG concentrations from 84 subject groups that ranged in average (postnatal) age from 0 days (i.e. newborns) to 79 years. Data from each subject group was weighted by observed log-normalized standard error values ($weight = 1/{SE_{LN}}^2$). In comparison to other models fit using PNA, the sigmoid Emax model was associated with the lowest AIC value (21.81) and depicted a curve shape that was visually congruent with observed AAG concentrations (Figure 5.2). AIC values associated with competing models were as follows: 149.99 (linear), 63.01 (power), 163.78 (exponential), and 37.25 (linear-log). Table 5.2 denotes parameter estimates and associated standard errors for the sigmoid Emax model. The AAG_{max} (89.50 mg/dL) depicts the geometric mean (or median) of plasma AAG concentrations in healthy adults. Comparatively, the model estimates median AAG concentrations to be approximately 3.6 fold lower (i.e. 24.90 mg/dL) during the first day of life (day =1).

Figure 5.2 Ontogeny of AAG among healthy subjects. Concentrations, normalized to CRM470 values, are depicted using estimated geometric mean values (o) for each study group. Geometric error bars depict the log-normal SE associated with each study cohort. Predicted AAG concentrations based on a sigmoid Emax model (solid line - red), as derived from this work, and a linear model (dashed line - blue), as proposed by McNamara and Alcorn (assuming adult plasma AAG concentrations ≈ 89.50 mg/dL) [51], are denoted. Observed data were compiled from the following publications: [291, 295, 297, 300, 302-307, 311-325].

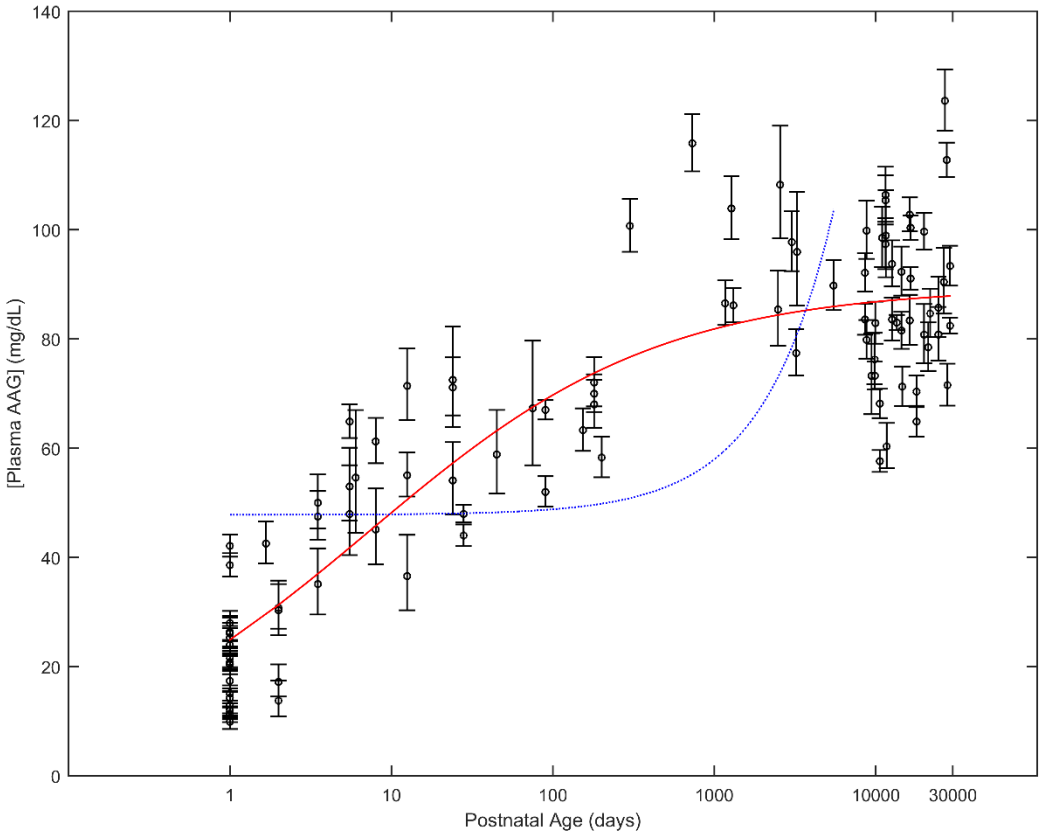

Table 5.2 Parameter estimates (sigmoid Emax model) describing the relationship between postnatal age (days) and AAG (mg/dL) in healthy subjects

Parameter	Estimate	SE[a]	CV[b]
AAG_{max} [mg/dL]	89.50	2.87	3.21%
TM_{50} [days]	7.26	2.28	31.40%
P	0.481	0.0645	13.41%

[a] Standard-Error

[b] Coefficient of Variation

Two-hundred and fourteen individual AAG concentrations complied over 3 separate clinical trials were utilized to evaluate the ontogeny of AAG in subjects diagnosed or suspected of infection. The dataset included 20 subjects from the CLIN01 trial, 177 from the PTN POPS trial, and 17 from the Staph Trio trial. Individuals ranged in PNA from 5 days to 20.5 years. As in healthy subjects, the sigmoid Emax model provided the best fit between PNA and AAG concentrations as determined by the AIC (319.24) and visual examination of curve shape (Figure 5.3A). In comparison, AIC values associated with the linear, power, exponential, and linear-log models were 359.87, 334.61, 360.34, and 329.76, respectively. Parameter estimates and standard errors associated with the sigmoid Emax model using the covariate PNA are denoted in Table 5.3. In subjects diagnosed or suspected of infection, the estimated geometric mean of AAG concentrations among adults (AAG_{max} ; 254.71 mg/dL) was comparatively higher than values observed in healthy (normal) adults. This trend towards increased AAG concentrations was depicted throughout the entire developmental age range. For example, at 5 days old, median AAG concentrations were estimated to be 89.41 mg/dL in infected individuals compared to 40.75 mg/dL in healthy subjects. On average, AAG concentrations from the Staph-Trio trial, which contributed data pertaining to premature born (< 30 weeks GA) neonates and infants less than 3 months PNA, appeared to be overestimated by the sigmoid Emax model fit using PNA (□ in Figure 5.3A). A similar pattern was also seen for children from the CLIN01 trial, all of whom were either overweight or obese (≥85th percentile of weight for age and sex) (Δ in Figure 5.3A).

Table 5.3 Parameter estimates (sigmoid Emax model) describing the relationship between postnatal age (days) and AAG (mg/dL) in subjects with confirmed or suspected infections

Parameter	Estimate	SE[a]	CV[b]
AAG_{max} [mg/dL]	254.71	12.25	4.81%
TM_{50}[days]	11.53	3.11	26.97%
P	0.735	0.167	22.72%

[a] Standard-Error

[b] Coefficient of Variation

Figure 5.3B depicts the ontogeny of AAG derived using a sigmoid Emax model employing PMA as its primary covariate for subjects diagnosed or suspected of infection. The model was associated with an AIC value of 291.02, which was comparatively lower than the previous model fit using PNA. In addition, use of PMA was associated with a lower standard deviation of log-normalized residuals (≈RMSE) in comparison to PNA (0.4710 vs. 0.5031, respectively). Correspondingly, PMA was deemed as the preferable age descriptor for defining the ontogeny of AAG within this subset of subjects. Parameter estimates and standard errors for the sigmoid Emax model fit to PMA are denoted in Table 5.4. The estimated AAG_{max} (254.37 mg/dL) was similar in value to that of the PNA model; however, estimates of the age at 50% AAG_{max} (TM_{50}) and the hill coefficient (P) were expectedly different between models due to the use of varying age descriptors. Additionally, use of PMA decreased the degree of overprediction associated with AAG estimates for premature born children from the Staph-Trio trial (□ in Figure 5.3B). Though, similar to the PNA model, AAG estimates for subjects from the CLIN01 trial tended to be overestimated using the PMA model (Δ in Figure 5.3B).

Figure 5.3 AAG ontogeny with respect to (A) PNA and (B) PMA in subjects diagnosed or suspected of infection. Median (i.e. geometric mean) AAG concentrations (solid lines) and associated 95% CI (dashed lines) as estimated using a sigmoid Emax model are depicted. Subjects from the each clinical trial (Staph Trio, □; PTN POPS ●;CLIN01 Δ) are denoted separately.

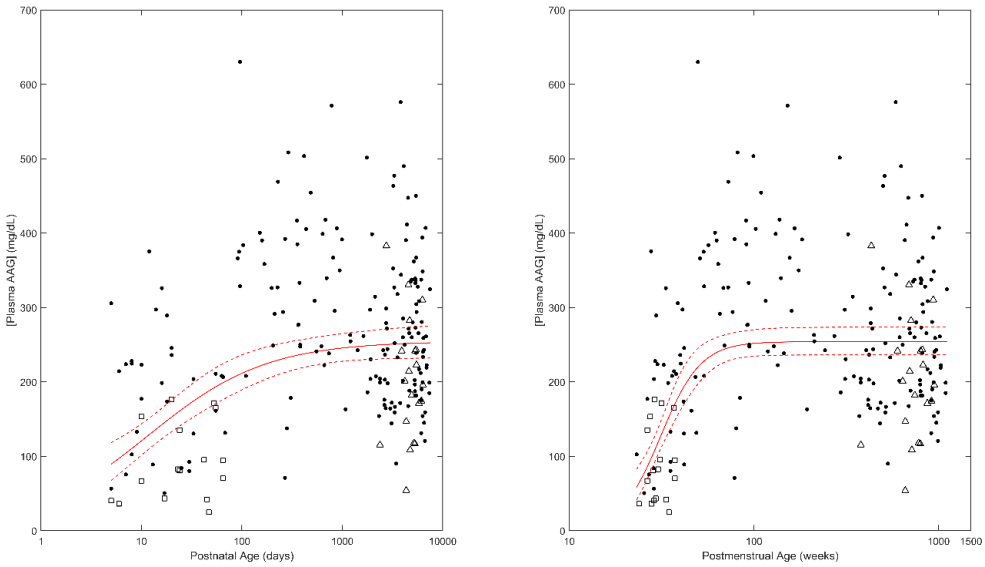

Table 5.4 Parameter estimates (sigmoid Emax model) describing the relationship between postmenstrual age (weeks) and AAG (mg/dL) in subjects with confirmed or suspected infections

Parameter	Estimate	SE[a]	CV[b]
AAG_{max} [mg/dL]	254.37	9.49	3.73%
TM_{50} [weeks]	31.33	1.31	4.18%
P	3.97	0.714	17.98%

[a] Standard-Error

[b] Coefficient of Variation

A graphical comparison of model predicted AAG concentrations between healthy subjects and those diagnosed or suspected of infection is displayed in Figure 5.4A. The comparison employed models parameterized in terms of PNA as the analysis in healthy subjects did not assess ontogeny with regards to PMA. The span of postnatal ages depicted were limited to the age range of purportedly infected subjects (i.e. 5 days to 20.5 years). Normalizing AAG concentrations towards the adult levels provides an estimate of the fractional attainment of adult AAG concentrations (i.e. $\frac{P_{ped}}{P_{adult}}$). Average estimates of $\frac{P_{ped}}{P_{adult}}$ ratios in healthy subjects fell within the 95% CI of values associated with subjects diagnosed or suspected of infection for the assessed age range (5 days to 20.5 years). As a result, it was asserted that the developmental trajectory of the $\frac{P_{ped}}{P_{adult}}$ ratio was not substantially different between healthy and infected subjects (Figure 5.4B).

Figure 5.4 (A) Comparison of median (geometric mean) AAG concentrations with respect to PNA in healthy (dotted line) and infected subjects (Median-solid line; 95% CI –dashed line), as estimated by separate sigmoid Emax models. (B) Comparison of normalized estimates of AAG concentrations (i.e. normalized to adult AAG values) with respect to PNA in healthy (dotted line) and infected subjects (Median-solid line; 95% CI –dashed line). AAG estimates are depicted for postnatal ages ranging between 5 days and 20.5 years.

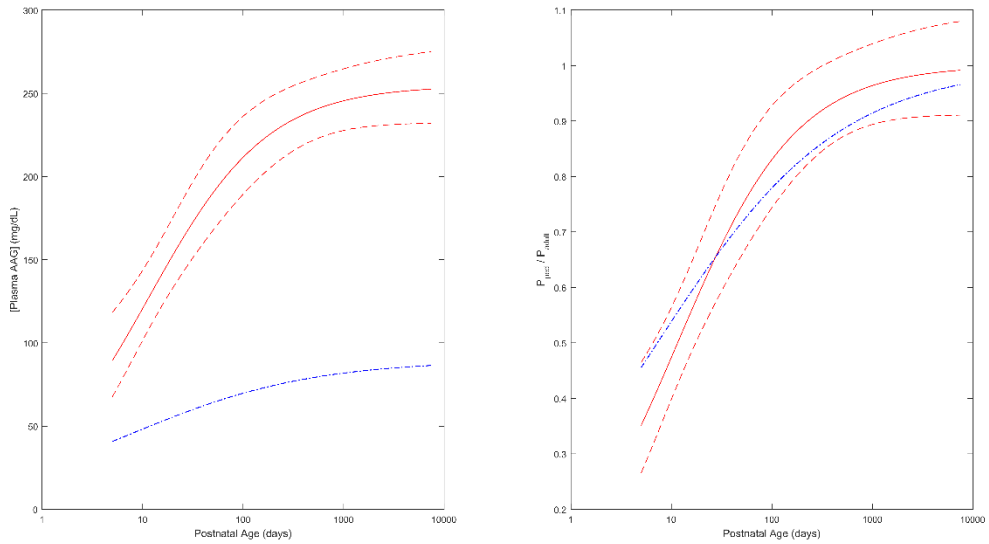

Overall bias associated with use of the derived AAG ontogeny model among healthy subjects, parameterized using PNA, at estimating 17 separate fu_{ped} values was relatively low. On average, estimates underpredicted observed values by 3% (AFE = 0.97). The model was associated with a precision (AAFE) of 1.24, indicating that on average individual predictions were within 24% of observed values. In comparison, use of the ontogeny equation proposed by McNamara and Alcorn [51] for estimating fu_{ped} was associated with a larger degree of underprediction (AFE = 0.74) and poorer precision (AAFE = 1.45). Individual predictions garnered by each respective model are displayed in relation to observed values in Figure 5.5. fu_{ped} estimates derived from the sigmoid Emax model were in closer agreement to observed values in comparison to estimates derived from the linear model as denoted by the concordance correlation coefficient (0.852 vs. 0.652, respectively) [326]. In addition, a higher coefficient of determination (R^2) was associated with estimates from the sigmoid Emax model (0.727 vs. 0.600).

Figure 5.5 Individual fu_{ped} predictions vs. Observed fu_{ped}. Lines of best fit as determined by linear regression are displayed for both the sigmoid Emax (red-solid) and linear models (blue-dashed). The line of identity (black-dotted) is superimposed for reference.

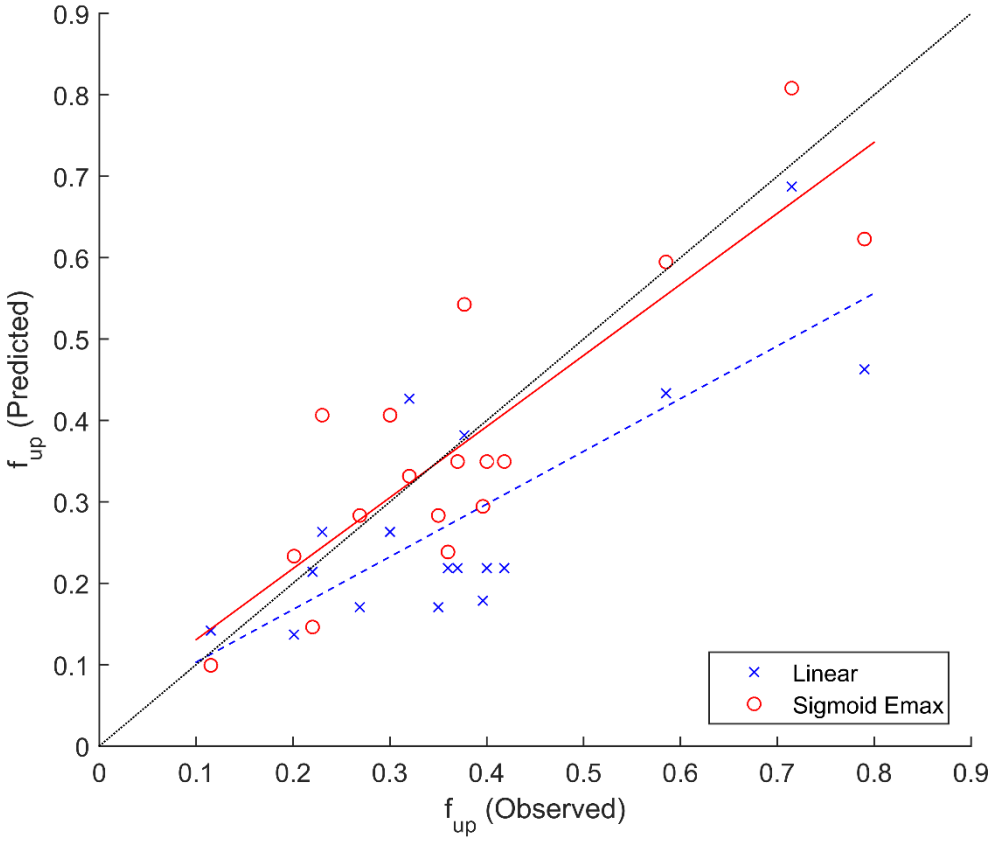

5.4 Discussion

For estimation of AAG concentrations among subjects diagnosed or suspected of infection, the analysis supported use of PMA as a comparatively better age descriptor than PNA. With use of PMA, estimated AAG concentrations were notably less biased for the subset of premature children from the Staph-Trio trial (Figure 5.3). Furthermore, model parameter estimates were relatively more precise (i.e. decreased coefficients of variation; CV%) (Table 5.3 & 5.4). Most notably, the CV% associated with TM_{50} was 26.97% vs. 4.18% for models using PNA and PMA, respectively. Use of PMA as an alternative age descriptor for assessment of the ontogeny of AAG among healthy individuals was precluded as not all studies with neonatal subjects reported GA, thus preventing tabulation of PMA [311, 319]. Several

investigations, however, have documented lower AAG concentrations among premature newborns in comparison to purportedly normal term newborns [300, 302, 305]. As use of PMA provides some capacity to account for prematurity, it is postulated that models using this age descriptor among healthy/normal subjects will exhibit a better fit to AAG concentrations in comparison to PNA. Therefore, it is prudent that prospective studies exploring the trajectory of AAG in healthy individuals document GA among their youngest subjects to permit for PMA calculation. The span of postnatal ages used for comparison of the ontogeny of AAG between the subject groups (healthy vs. infected) was restricted to 5 days to 20.5 years, the age range of purportedly infected subjects (Figure 5.4). Therefore, the analysis was unable to examine the acute-response of AAG associated with infection among extremely young children (i.e. less than 5 days PNA) or older adults (i.e. geriatric).

As an acute-phase reactant, AAG levels increase in response to injury, inflammation, or infection [286]. The magnitude of increase has been related to factors such as the severity of disease [307] and type of infection (i.e. meningitis vs. pneumonia) [327]. Furthermore, normalization of AAG levels appear to follow the clinical course of infection [300]. Data utilized to evaluate the ontogeny of AAG in subjects diagnosed or suspected of infection did not provide sufficient information to stratify individuals based on infection type, severity, or time course of infection. As such, assessed subjects displayed a high degree of inter-subject variability in terms of AAG concentrations, thus making prediction of individual AAG levels precarious. However, for the purposes of scaling PK parameters from adults to pediatrics, the relative difference in AAG concentrations between these two age groups is the measure of interest [66, 127]. The current work demonstrates that, on average, the relative ontogeny profile of $\frac{P_{ped}}{P_{adult}}$ in infected subjects followed a similar trajectory to that observed among healthy subjects (Figure 5.4B). Correspondingly, it could be asserted that scaling of fu, as determined according to equation 5.5, from healthy or infected adults toward pediatric subjects within the same respective clinical state (e.g. infected adult → infected child) could be determined using a single ontogeny profile for $\frac{P_{ped}}{P_{adult}}$ (e.g. use of the profile pertaining to healthy subjects) . The high inter-subject variability observed among subjects diagnosed or suspected of infection could, indeed, result in individual predictions of fu_{ped} that deviate from the average tendency. In terms of subsequent predictions of pediatric PK, this would result in individualized estimates of total compound exposure in plasma (i.e. AUC) that deviate from observed values. However, provided estimates of pediatric intrinsic clearance are sufficient, predictions of unbound plasma exposure (unbound AUC) - a metric

related to pharmacologic effect - should be congruent with observed data for low extraction ratio or orally administered high hepatic extraction ratio compounds [284].

Median AAG estimates among purportedly infected, overweight and obese children from the CLIN01 trial (n=20) were slightly over-predicted by sigmoid Emax models incorporating PNA or PMA. This raises the notion of AAG concentrations differing between overweight and normal weight children - an observation that has been documented among 'healthy' adults [328]. However, as the dataset pertaining to infected subjects did not contain information relating to potential confounders (e.g. infection type, severity, and time course of infection), establishing an association between the attributes (i.e. obesity) of subjects from one specific trial (CLIN01) and AAG may lack external validity and was, therefore, was not pursued. Notably, removal of subjects from the CLIN01 trial from the analysis of AAG ontogeny among infected individuals did not result in a substantial change in model parameters (e.g. AAG_{max}(266.38 mg/dL), TM_{50}(32.18 weeks), and *P* (3.79) – sigmoid Emax model [PMA]).

Based on an observed dataset containing 17 fu_{ped} values, estimates of fu derived using the proposed AAG ontogeny equation from healthy (control) subjects were associated with a low bias (*AFE* = 0.97) and relative accurate precision (*AAFE* = 1.24). Discontinuity between observed and predicted fu values can be related to numerous etiologies; however, an understanding of the assumptions associated with fu prediction in pediatrics can provide some insight. Predictions of fu_{ped} were derived using equation 5.5, as previously depicted by McNamara and Alcorn [51]. With use of this equation, several assumptions are inherently presumed: 1, plasma protein binding is linear (i.e. nonsaturable ligand concentrations); 2, ligand-protein binding properties are the same between children and adults (i.e. number of binding sites per protein and affinity constants are constant with age), and 3, AAG is the principal protein responsible for plasma protein binding. Violation of any of these assumptions can result in deviation between observed and predicted values. With plasma concentrations up to 50-fold lower than albumin and exhibiting only a single binding site [285], AAG is frequently termed as a low capacity protein [52]. Resultantly, therapeutic concentrations that drugs are commonly dosed towards (i.e. 1 – 10 μM) may result in saturation of AAG [285]. This propensity for saturation is expected to be especially prominent among neonatal subjects, where concentrations of AAG are considerably lower than adults. One previous study exploring protein binding of lidocaine among pediatric plasma samples asserted that age-related differences in the binding capacity of AAG between neonates and older children could be responsible for the inconsistency of fu values between the groups [305]. However, this postulation requires further study to be corroborated. Differential protein binding properties between variants of AAG have been documented in the literature [289, 290]. Unfortunately, the datasets

utilized within this analysis did not stratify AAG into specific genetic variants; therefore, developmental changes in variant concentrations and their influence on protein binding estimation were not assessed. Furthermore, some xenobiotics may display affinity for more than one plasma protein. For example, the opioid antagonist naloxone displays affinity for both albumin and AAG [311]. As equation 5.5 only considers changes to a single protein, estimates of fu_{ped} for such compounds may be biased.

Compared to the ontogeny model proposed in this study, fu_{ped} estimates derived from McNamara and Alcorn's [51] AAG ontogeny equation were associated with a higher degree of bias and lower precision. On average, McNamara and Alcorn's equation underpredicted observed fu values by 26% (AFE = 0.74). The authors' utilized a linear equation to describe the ontogeny of AAG (Figure 5.2; age is displayed on a log scale). Unfortunately, this functional form does not provide an appropriate depiction of AAG concentrations among the most developmentally immature subjects. For example, in neonates, the equation provided estimates of AAG concentrations that were well above observed data points. Therefore, considering that ≈80% (14/17) of fu values within the observed dataset were from neonatal subjects, the finding that fu_{ped} estimates derived using McNamara and Alcorn's equation were associated with an underprediction bias was not unexpected.

With ever widening acceptance of the use of physiologically-based pharmacokinetic (PBPK) models for scaling xenobiotic exposures from adults to pediatrics [66, 329], the findings of this analysis can be readily integrated into common practice. PBPK models represent a bottom-up approach that integrates components of organism physiology with xenobiotic-specific parameters to foster *a priori* predictions of systemic as well as tissue-specific exposures [127]. Thus, within such models there exists an intuitive link between the quality of input parameters (i.e. physiological and xenobiotic-specific parameters) and the accuracy of model-predicted exposures. PBPK models typically parameterize the magnitude of xenobiotic-protein binding using fu. This critical parameter can exert profound influences towards the processes of clearance and distribution [49], thus, modulating estimates of xenobiotic exposure. By providing superior estimates of fu_{ped}, the ontogeny model derived from this work can be used in conjunction with PBPK modeling techniques to improve their predictive capacity for pediatrics.

The use of a sigmoid Emax model for defining the ontogeny of AAG concentrations is not unique to this investigation. Johnson et al. [330] previously conducted an analysis of plasma AAG levels using select literature sources. The authors' found that a sigmoid Emax model suitably described the data. Derived parameter estimates were not considerably different from parameters reported among

healthy subjects from the current study. Estimates of AAG_{max}, TM_{50}, and P were 88.7 mg/dL, 8.89 days, and 0.38, respectively, as reported by Johnson et al. Compared to this aforementioned publication, our analysis offered a more comprehensive examination of the available literature with data compiled over 25 separate investigations. The present study also considered a wider variety of prospective models and provided an evaluation of the predictive performance of the derived ontogeny equation at estimating fu, an important parameter utilized for PK scaling. In addition, the assessment of AAG ontogeny among subjects diagnosed or suspected of infection represents a component unique to the current work.

This analysis represents one of the most comprehensive examinations of published literature characterizing plasma AAG levels in healthy subjects from birth to adulthood. However, despite compiling AAG data from 25 studies conducted over a wide range of countries, the majority of data was assumedly directed towards a Caucasian population. For example, only one study was conducted in a country where the population is primarily of Asian descent (i.e. Japan) [317]. The remaining investigations conducted in France, Canada, the Netherlands, USA, Australia, Greece, Denmark, Germany, England, and Belgium, were postulated to contain a high proportion of Caucasian subjects. Within adults, inter-ethnic differences in AAG levels have been documented. In one study, AAG concentrations were denoted to be 20% higher in Caucasians compared to African Americans [331]. Another investigation measuring AAG concentrations in Chinese and Caucasian volunteers found 25% higher levels among Caucasians [332]. Considering the demographics of individuals within the examined studies, the analysis was incapable of investigating for the presence of inter-ethnic differences among healthy subjects; therefore, presented results are primarily reflective of AAG concentrations within a Caucasian population. Racial demographics of individuals included in the analysis of AAG ontogeny among subjects diagnosed or suspected of infection was 76% White, 16% African American, and 8% Other. A secondary analysis was conducted based on the depicted sigmoid Emax model using the covariate PMA (base model) to assess whether inclusion of a binary race covariate (Non-White 0; White 1) could enhance model fit. However, inclusion of race in a proportional manner resulted in a similar AIC to the base model (291.84 vs. 291.02, respectively). As such, use of the covariate race was not considered to be beneficial for estimation of AAG among our sample of purportedly infected subjects.

In this study, the ontogeny of AAG among healthy subjects was assessed using AAG concentration data averaged over multiple subjects from separate publications. Analyses of this type of can be influenced by the presence of an aggregation bias (ecological fallacy). This bias arises from the

loss of information associated with aggregating individual data, leading to distortion of the relationship that exists between individual subjects and the variable of interest [333]. Despite this, use of aggregated data within the analysis was deemed reasonable as the majority of publications failed to report individualized data. In addition, the ontogeny models derived from this investigation should not be considered to entail wider applicability towards other plasma proteins (e.g. albumin), which can follow alternative ontogeny patterns [51].

5.5 Conclusion

The current investigation sought to quantitatively describe the ontogeny of AAG in both healthy subjects and those diagnosed or suspected of infection. A sigmoid Emax model was found to best describe the developmental trajectory of AAG in both groups of subjects (healthy and infected). As an acute-phase reactant, plasma AAG levels increase in response injury, inflammation, and infection [50]. Though a profound dissimilarity in median AAG concentrations between healthy and infected subjects was observed, the analysis depicted a similar ontogeny pattern when AAG levels were normalized toward adult values. Furthermore, the derived ontogeny equation demonstrated a proficient predictive capacity for estimation of fu_{ped}. As developmental changes in plasma protein binding (i.e. fu) can translate into significant alterations in compound distribution and clearance, this work will aid in reducing uncertainty associated with pediatric PK predictions.

Chapter 6: Parameterization of Small Intestinal Water Volume using PBPK Modelling

The contents of this chapter are reflective of an original manuscript published by the Ph.D. candidate (Anil R Maharaj) in the European Journal of Pharmaceutical Sciences. All pertinent research analyses was conducted by the Ph.D. candidate.

Maharaj A, Fotaki N, Edginton A. Parameterization of small intestinal water volume using PBPK modeling. European journal of pharmaceutical sciences : official journal of the European Federation for Pharmaceutical Sciences. 2015;67:55-64. doi:10.1016/j.ejps.2014.10.016.

6.1 Introduction

The integration of physiologically-based pharmacokinetic (PBPK) modelling into the drug development and regulatory review process has increased in frequency over recent years. From 2008 to 2013, 84 Investigational New Drug/ New Drug Applications submitted to the US Food and Drug Administration (FDA) contained PBPK modelling techniques [22]. In addition, a recent drug monograph approved by the FDA utilized PBPK models to assess the clinical implications of specific drug-drug combinations [334]. PBPK modelling is an appealing option for users as it provides a rational framework for generating *a priori* predictions of compound disposition. Accordingly, use of PBPK modelling has been well documented in a variety of settings, from industry to academia, as well as many research areas including drug-drug interactions [335], genetic polymorphism [336], and investigations of altered organ function [337]. Models are mechanistic in nature, combining information based on organism physiology and anatomy with compound physico-chemical properties to predict the time-course of drug disposition. When effectively parameterized, PBPK models facilitate an understanding of compound pharmacokinetics by quantitatively estimating the contribution of absorption, distribution, metabolism and excretion.

In general, the predictive accuracy of PBPK modelling for predicting plasma concentration-time values following intravenous drug administration in adult humans is well-established [28]. In constrast, estimation of the systemic exposure following oral drug administration is comparatively less accurate [28]. This discrepancy in predictive performance can be linked to the complex milieu of

physiological and environmental factors that interact within the gastrointestinal tract to facilitate oral absorption. As such, prediction of oral absorption requires a fundamental understanding of several processes including drug dissolution, degradation, gastric emptying, intestinal transit, drug diffusion/permeation, and first pass metabolism [32]. Commercially, several PBPK modelling software products have integrated oral absorption models into their platforms. These include the advanced compartmental absorption and transit model (ACAT) incorporated into GastroPlus® (Simulations Plus Inc., Lancaster, CA), the advanced dissolution, absorption, and metabolism (ADAM) model incorporated into the Simcyp® simulator (Simcyp Ltd., Sheffield, UK), and the compartmental gastro-intestinal model included in PK-Sim 5® (Bayer Technology Services GmbH, Leverkusen, Germany). Notwithstanding specific inter-model structural intricacies, all models are conceptually based on the compartmental absorption and transit (CAT) model, originally proposed by Yu and Amidon [35], which depicts the gastrointestinal tract as a series of linked compartments.

Organism specific data required for parameterization of compartmental oral absorption models include gastrointestinal geometry (i.e. length, radius), gastric emptying time, intestinal transit, luminal pH, intestinal permeability, gastrointestinal fluid volumes, and enzyme/transporter abundance. With the quality of input parameters intuitively linked to model predictive accuracy, there is an overwhelming need to ensure that model parameters are optimally assigned.

With regards to oral drug delivery, the small intestine is generally considered the primary site of drug absorption due to the presence of several surface structures (folds, villi, microvilli) which serve to increase the absorptive surface area several fold [34]. Since only dissolved drug is permitted to permeate the intestinal membrane, defining of the amount of fluid available within the small intestine is imperative to facilitate predictions of oral drug disposition. Among CAT models presented in the literature, wide variation exists in the amount of fluid allocated to the small intestine, ranging from 250 to 600 mL [55-58]. Conversely, *in vivo* estimates of small intestinal fluid volume within adults denote a central tendency between 86-167 mL [59-61]. As PBPK models should reflect a biological basis in terms of structure and parameterization, this discrepancy raises concerns regarding the physiologic fidelity of such simulations. In addition, use of PBPK models to extrapolate PK information towards unstudied populations require models to exhibit a biological resemblance. For example, procedural workflows for developing pediatric PBPK models capable of estimating age-specific PK alterations are predicated on established adult models [23, 329]. Adult models displaying appropriate agreement with observed data are subsequently scaled towards a pediatric population. This process leverages the relative abundance of adult PK data to establish confidence in model predictions prior to extrapolating

to children. Extrapolations utilize the mechanistic framework of PBPK simulations, allowing model parameters to be modified using *in vivo* measures of anatomy, physiology, and biochemistry of the developmental age group of interest. Adult models incorporating parameters not consistent with known *in vivo* measures are, therefore, limited in terms of performing such extrapolations. As such, demonstration of a PBPK model's physiologic applicability is a crucial step in establishing confidence in simulated results.

The current investigation will serve to assess the biological relevance of the commonly utilized CAT model in terms of small intestinal water volume (SIWV). Using a generic CAT model integrated into a whole-body PBPK model, an optimal value for SIWV will be generated using pharmacokinetic data sets obtained from the literature. To evaluate physiologic fidelity, model derived volume estimates will be compared to experimentally-based SIWV determinations.

6.2 Methods

6.2.1 CAT model structure

A CAT model, developed in Matlab-Simulink® (The Mathworks Inc., Natick, MA), based on the works of Yu and Amidon [35] was implemented within the study to simulate oral drug absorption. Compared to proprietary software packages, creation of a customizable absorption model within the Matlab® environment was deemed necessary as it permitted for flexibility in terms of model analysis and parameterization. A schematic representation of the model is displayed in Figure 6.1. The small intestine is characterized as a series of 7 well-mixed compartments. Drug progresses aborally between compartments following linear transfer kinetics. Anatomically, each compartment represents an equal length of the small intestine with the first-half of the initial compartment pertaining to the duodenum. The subsequent half of the first compartment along with the second and third pertains to the jejunum, and the fourth to seventh compartments represent the ileum [33]. A stomach compartment was added to the model which functioned as a holding compartment, with no absorption occurring, before compound introduction into subsequent intestinal compartments. Colon mediated drug absorption was not incorporated in the model.

Figure 6.1 Schematic Representation of the Developed Compartmental Absorption and Transit (CAT) model [ks – first-order gastric emptying rate; kt – first-order intestinal transit rate; Amp_1 – corrective factor associated with intestinal PxSA for the duodenum and jejunum; and Amp_2 – corrective factor associated with intestinal PxSA for the ileum]

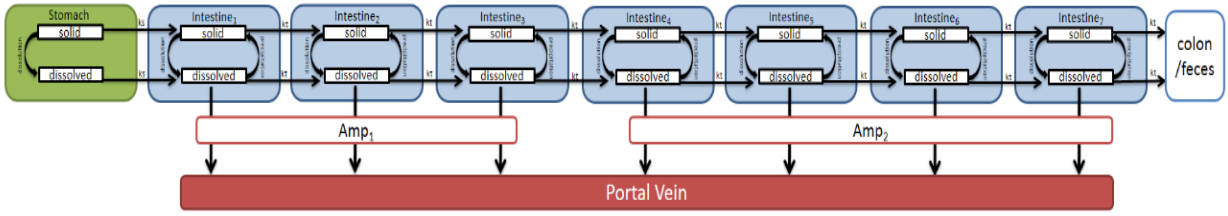

Drug was permitted to exist in two states: solid and dissolved. Dissolution in the stomach and intestine was modelled using the following equation [56] where,

$$R_d = K_d M_i \left(\frac{S_i - C_i}{S_i}\right) \quad \text{(Equation 6.1)}$$

R_d is the rate of dissolution (mg/hr), K_d is the dissolution rate constant (hr^{-1}), M_i is the time dependent mass (mg) of solid drug present within the compartment, S_i is the compartmental solubility limit, and C_i is the time dependent concentration of dissolved drug within the compartment. Precipitation was modelled as an instantaneous process within intestinal compartments. Supersaturation of intestinal fluids was not considered as luminal concentrations were not permitted to exceed compartmental solubility limits. However, the model did permit for precipitated drug to undergo dissolution when drug concentrations fell below the compartmental saturation limit.

The simulated rate of drug absorption into the portal circulation was calculated as follows,

$$R_a = \sum_{i=1}^{3} P \; x \; SA_i \; x \; Amp_1 \; x \; C_i + \sum_{i=4}^{7} P \; x \; SA_i \; x \; Amp_2 \; x \; C_i \quad \text{(Equation 6.2)}$$

where R_a is the rate of drug absorption (mg/hr), P is the intestinal permeability (cm/hr), and SA_i is the geometric compartmental surface area (cm^2). Amp_1 and Amp_2 pertain to corrective amplification factors associated with the permeability x surface area product (P x SA) of the upper (compartments 1 - 3) and lower (compartments 4 - 7) small intestine, respectively. Compartmental surface areas were derived

geometrically assuming a conical (flat) frustum and incorporated literature reported physiologic values of small intestinal radii [338] and length [339]. Permeability was set to a predefined value of 0.001 cm/hr within all intestinal compartments. This initial parameterization was relatively arbitrary as compartmental P x SA values were subsequently refined through the inclusion of amplification factors (Amp_1 and Amp_2). These factors introduced additional degrees of flexibility into the CAT model, allowing for optimization of compartmental P x SA values based on *in vivo* pharmacokinetic data. Use of two amplification factors permitted the model to independently account for PxSA differences between the upper (duodenum and jejunum) and lower (ileum) small intestine.

Gastric fluid volume was defined as 300 mL which approximates the fasted fluid volume of the stomach, 45 mL [61], in addition to the 200-250 mL of water co-ingested with dosages in many pharmacokinetic studies. Allocation of fluid amongst the seven intestinal compartments was based on the relative difference in geometric volume of each compartment. Geometric volumes were calculated using congruent data [338, 339] as that used to estimate compartmental surface areas. Compartment volumes were calculated based on a conical frustum with the total geometric volume of the small intestine estimated to be 931 cm^3. Compartments were assigned an equivalent fraction of fluid per geometric volume. For example, to simulate an intestinal fluid volume of 100 mL, each compartment would be assigned 0.107 ml (100 mL/931cm^3) of fluid per cm^3 of geometric volume. Experimental values for pH specific compound solubility were extracted from the literature. If required, solubility was extrapolated from literature values using the Henderson-Hasselbalch equation [340]. CAT model parameters utilized within the study are displayed in Table 6.1.

Table 6.1 Compartmental Absorption and Transit (CAT) model parameters

Compartment	*pH*[a]	*First Order Transit Rate Constant (hr $^{-1}$)*[b]	*Geometric Surface Area (cm^2)*[c]	*Geometric Volume (cm^3)*[c]	*Permeability (cm/hr)*	*Fluid Volume (ml)*	*Acyclovir pH dependent solubility (mg/mL)*	*Chlorothiazide pH dependent solubility (mg/mL)*[g]
Stomach	1.5	2.8	n/a	n/a	0.001	300[d]	12.98[e]	0.417
Intestine-1	6.5	2.1	303.92	183.81	0.001	-	2.42[f]	0.7696
Intestine-2	6.5	2.1	281.24	157.45	0.001	-	2.42 [f]	0.7696
Intestine-3	6.5	2.1	257.11	131.61	0.001	-	2.42 [f]	0.7696
Intestine-4	7.5	2.1	243.79	118.24	0.001	-	2.71 [f]	2.3397
Intestine-5	7.5	2.1	241.27	115.81	0.001	-	2.71 [f]	2.3397
Intestine-6	7.5	2.1	238.76	113.41	0.001	-	2.71 [f]	2.3397
Intestine-7	7.5	2.1	236.25	111.04	0.001	-	2.71 [f]	2.3397

a - values derived from [237]
b – values derived from [33, 341, 342]
c – values derived from [338, 339]
d – value derived from [61] plus addition of 200-250 mL of fluid ingested with dosages
e – value obtained using Henderson- Hasselbalch equation
f – values derived from [343]
g – values derived from [344, 345]

6.2.2 Drug selection

To effectively parameterize SIWV using PBPK model-based simulations, compound specific pharmacokinetic data sets following oral administration were required. In addition, compound selection was restricted based on several criteria. First, to provide estimates of fluid volumes reflective of the entire small intestine, compounds were required to display poor intestinal permeability. Poor permeability was defined as a fraction of absorption less than 90%, which is consistent with the Biopharmaceutics Classification System (BCS) [346]. To minimize the effects of dissolution within the model, compounds were required to either meet the FDA criterion for rapid dissolution when

administered a an immediate release formulation [346] or be administered as a solution. Pharmacokinetic literature pertaining to candidate compounds were required to be conducted in healthy adults and depict time-dependent drug excretion or plasma profiles following oral absorption at a minimum of two different dosage levels. Parameterization of SIWV necessitated the selection of compounds which displayed non-proportional changes in absorption between increasing dosage strengths. Furthermore, the etiology of this non-linearity should be correlated to saturation of intestinal fluids. As such, compounds displaying non-linear clearance kinetics following intravenous administration or those whose absorption is largely mediated via transporter-based uptake were excluded.

6.2.3 PBPK model parameterization

Estimates of systemic compound disposition following oral absorption was modelled using PK-Sim 5.2® (Bayer Technology Services, Leverkusen, Germany), a whole-body PBPK modelling platform. Tissue-to-plasma partition coefficients (Kp) were derived using the tissue composition based approach as proposed by Rodgers and Rowland [80-82]. Acyclovir and chlorothiazide were selected as candidate compounds based on the criteria stipulated in the previous section. Compound specific physicochemical properties required for model parameterization were obtained from the literature and are displayed in Table 6.2. Parameterization of clearance and distribution were derived using two different modalities depending on the availability of literature data. For acyclovir, where PK studies depicting plasma concentration time values following intravenous compound administration were available, clearance and distribution were simultaneously fit based on minimization of an objective function between simulated (PBPK derived) and observed data. The process of parameter optimization required a mean individual to be generated based on the demographics (race, age, weight, height) of the *in vivo* pharmacokinetic study [79]. Computational optimizations of clearance, in the form of intrinsic clearance (Cl_{int}), and distribution, in the form of lipophilicity, were conducted using the mean study subject while incorporating similar conditions (i.e. dose, infusion time, study duration) as those imposed within the *in vivo* investigation. Since acyclovir exhibits competing clearance processes (i.e. renal and hepatic), pathway specific Cl_{int} values were constrained in order to provide similar proportions of systemic clearance as those observed *in vivo*.

For chlorothiazide, where pharmacokinetic studies following intravenous administration in healthy adults were not available, clearance and distribution were derived using alterative

methodologies. Since chlorothiazide is primarily renally excreted, clearance was tabulated using pharmacokinetic studies containing time-dependent rates of urinary excretion and plasma concentration values following extravascular (oral) drug administration in healthy adults. Alternatively, distribution was tabulated using literature data pertaining to intravenous compound administration in a pre-clinical species (i.e. rat). In this case, lipophilicity, a surrogate measure of distribution, was tabulated using a similar methodology as previously described for acyclovir. The lipophilicity (i.e. distribution) value fitted within the pre-clinical species was used for parameterization of the adult human PBPK model.

Table 6.2 PBPK model parameters

Parameter	*Acyclovir*	*Chlorothiazide*
Cl_{int} (hepatic) (ml/min – per gram intracellular hepatic tissue)	0.104732[a]	-
Cl_{int} (tubular renal secretion) (ml/min – per gram of kidney tissue)	0.906355[a]	6.11 [e]
f_{GFR} [b]	1	1
Lipophilicity (LogP)	-0.56[a]	-0.25[f]
Molecular Weight (g/mol)	225.21	295.72
Fraction unbound (plasma)	0.846[c]	0.177[g]
pKa (acid)	9.04[d]	6.7[g]
pKa (base)	2.16[d]	-

a – values derived from model-based optimization using intravenous data from adult humans [347]
b – proportion of free drug susceptible to passive elimination via glomerular filtration
c – value derived from [348]
d – values derived from [349]
e – value was fitted to provide a systemic clearance of 4.36 ml/min/kg
f – value derived from model-based optimization using intravenous data from rats [350]
g – values derived from [351]

6.2.4 Estimation of SIWV

Compound specific oral pharmacokinetic data sets derived from healthy adult subjects depicting different dosage strengths were utilized to estimate SIWV. Integration of the developed CAT model

with the PK-Sim® created whole-body PBPK model provided predictions of systemic drug disposition (plasma concentration or fraction urinary excreted) following oral absorption. This was accomplished by using the rate of absorption, as quantified by the developed CAT model, as an input into the portal vein within the whole-body PBPK model.

Compound data pertaining to lower dosage strengths, where permeability is postulated to be the rate-limiting step of absorption, were used to calculate amplification factors pertaining to the upper and lower small intestine. To account for the apparent impact of SIWV selection on estimation of intestinal PxSA, a wide range of intestinal fluid volumes were assigned within the CAT model. Volumes between 52.5 mL to 420 mL were allocated using increments of 10.5 mL. Amplification factors were optimized with respect to each SIWV to provide a minimized objective function value between simulated and observed time-dependent pharmacokinetic measures (i.e. 'concentration vs. time' or 'cumulative fraction excreted vs. time'). Simulations utilized congruent conditions (i.e. dose, dosage form, subject demographics) to those stipulated in the observed pharmacokinetic studies. Derived amplification factors from the lower dosage levels were considered to reflect the difference between the naïve model estimate and the true *in vivo* PxSA value.

Observed pharmacokinetic data sets pertaining to higher dosage strengths, where non-proportional changes in compound absorption were observed, were utilized to evaluate SIWV estimates. Based on simulations conducted at the lower dosage level, SIWV values and their corresponding amplification factors were incorporated into the CAT model. Models were further parameterized in accordance with observed study conditions (i.e. dose, dosage form, subject demographics) at the higher dosage level. Optimal model-based estimates of SIWV were determined by comparing simulated predictions of oral compound disposition to observed pharmacokinetic data using a predefined objective function.

6.2.5 Objective function

Parameter optimizations were conducted using MoBi® Toolbox for MATLAB® (Bayer Technology Services GmbH, Leverkusen, Germany/ The Mathworks Inc., Natick, MA), which permitted for iterative assessment of simulation results with observed data. Absolute average fold-error (AAFE) was selected as the objective function of choice to assess model predictive performance.

$$AAFE = 10^{\frac{1}{n}\Sigma\left|log\frac{predicted}{observed}\right|} \qquad \text{(Equation 6.3)}$$

The above objective function was utilized to compare predictions of time-dependent compound disposition (plasma concentration or fraction urinary excreted) to observed pharmacokinetic data sets. Models incorporating SIWV(s) which result in lower AAFE values were considered to possess a greater predictive capability.

To minimize the potential contribution of colonic mediated absorption, all optimizations and assessments were conducted using observed plasma concentrations up to 8 hours following oral absorption of acyclovir. Urinary fraction excretion data pertaining to chlorothiazide was sampled at a lower intensity and, as such, assessments and optimizations were conducted up to 12 hours.

6.3 Results

Based on the restrictive inclusion criteria, which limited the range of appropriate compounds from which rational estimates of SIWV could be attained, acyclovir and chlorothiazide were selected. Briefly, acyclovir is a guanosine-based antiviral drug, whereas chlorothiazide is a diuretic [24]. Pharmacokinetic data following oral administration of 200 and 400 mg of acyclovir in immediate release tablets were acquired from the literature [347]. At a dose of 200 mg, acyclovir bioavailability is 32%, while at 400 mg, oral bioavailability decreases to 23%. The major clearance pathways of acyclovir were denoted as renal clearance (fe = 0.707) and hepatic metabolism (fm = 0.293) [347]. Pharmacokinetic data following oral administration of chlorothiazide solutions at doses of 50, 100, and 250 mg were obtained from the literature [352]. At a dose of 50 mg, the bioavailability of chlorothiazide is 56%, while at doses of 100 and 250 mg the bioavailability decreases to 47% and 33%, respectively. Chlorothiazide elimination was primarily attributed to renal clearance (fe = 1) [352].

Parameter values for acyclovir and chlorothiazide utilized by the whole-body PBPK model are displayed in Table 6.2. Acyclovir clearance and distribution (i.e. lipophilicity) were optimized using pharmacokinetic data depicting a 250 mg intravenous dose to a cohort of 24 healthy adult subjects [347]. For chlorothiazide, pharmacokinetic profiles following intravenous drug administration in healthy adult humans were unavailable. Since renal excretion contributes to the majority of chlorothiazide elimination, clearance was alternatively calculated using data pertaining to extravascular (oral) administration. Pharmacokinetic data following oral administration of 500 mg of chlorothiazide in cohort of 9 healthy adult males was acquired [353]. An average clearance estimate of 4.36 ml/min/kg was derived from time-dependent urinary excretion and plasma concentration data. Distribution (i.e. lipophilicity) was fitted based on pharmacokinetic profiles attained following intravenous

administration of chlorothiazide to Sprague-Dawley rats [350]. PBPK model-based predictions of acyclovir and chlorothiazide disposition following intravenous administration are depicted in Figure 6.2.

Figure 6.2 Fitted estimates of plasma concentration (log) vs. time profiles following intravenous administration of (A) acyclovir and (B) chlorothiazide in an adult human and rat, respectively (lines). Mean observed data is superimposed for reference (circles). Acyclovir, administered at a dose of 250 mg to a cohort of 24 healthy adult subjects [347]. Chlorothiazide, administered at a dose of 10 mg/kg to a cohort of 5 Sprague-Dawley rats [350].

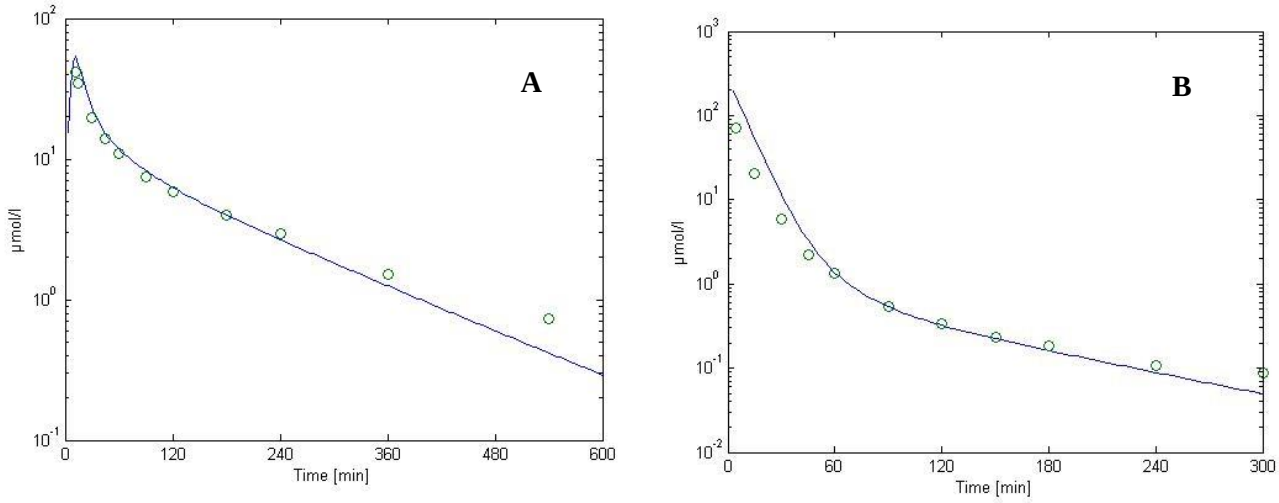

Amplification factors for the upper (Amp_1) and lower (Amp_2) small intestine pertaining to different SIWV were derived from the CAT integrated PBPK model using the lowest dosages of acyclovir (200 mg) and chlorothiazide (50 mg) (Figure 6.3). Figure 6.4 displays model-based predictions of acyclovir and chlorothiazide disposition following oral administration at these respective dosages. The depicted simulations utilize a SIWV of 252 mL. For both compounds, changes in SIWV did not produce any visual effect on model predictions at the lower dosing level. This is the result of fitting drug specific amplification factors (Amp1, Amp2) in relation to SIWV at these dosages.

Figure 6.3 Drug specific amplification factors for the upper (Amp1) and lower (Amp2) small intestine pertaining to different SIWV estimates. Values derived using the lowest dosages of (A) acyclovir [200 mg] and (B) chlorothiazide [50 mg].

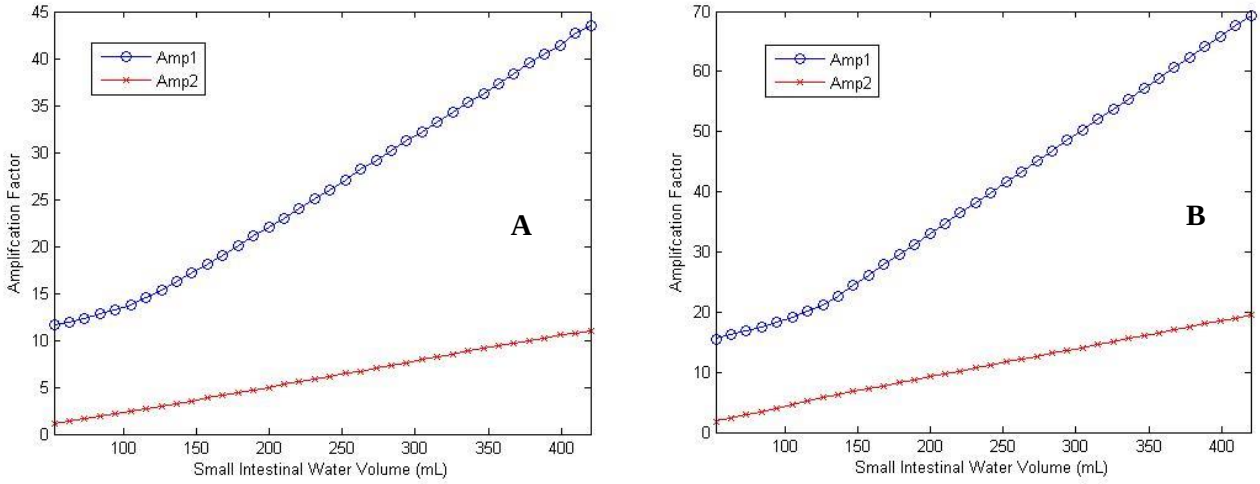

Figure 6.4 Estimates of oral compound disposition in adult humans generated from the developed CAT model incorporating a SIWV of 252 mL (lines). (A) Acyclovir plasma concentration (linear) vs. time estimates following a 200 mg dose. (B) Acyclovir plasma concentration (log) vs. time plot. (C) Chlorothiazide cumulative urinary excretion (linear) vs. time estimates following a 50 mg dose. (D) Chlorothiazide cumulative urinary excretion (log) vs. time plot. Mean observed data is superimposed for reference [347, 352] (circles).

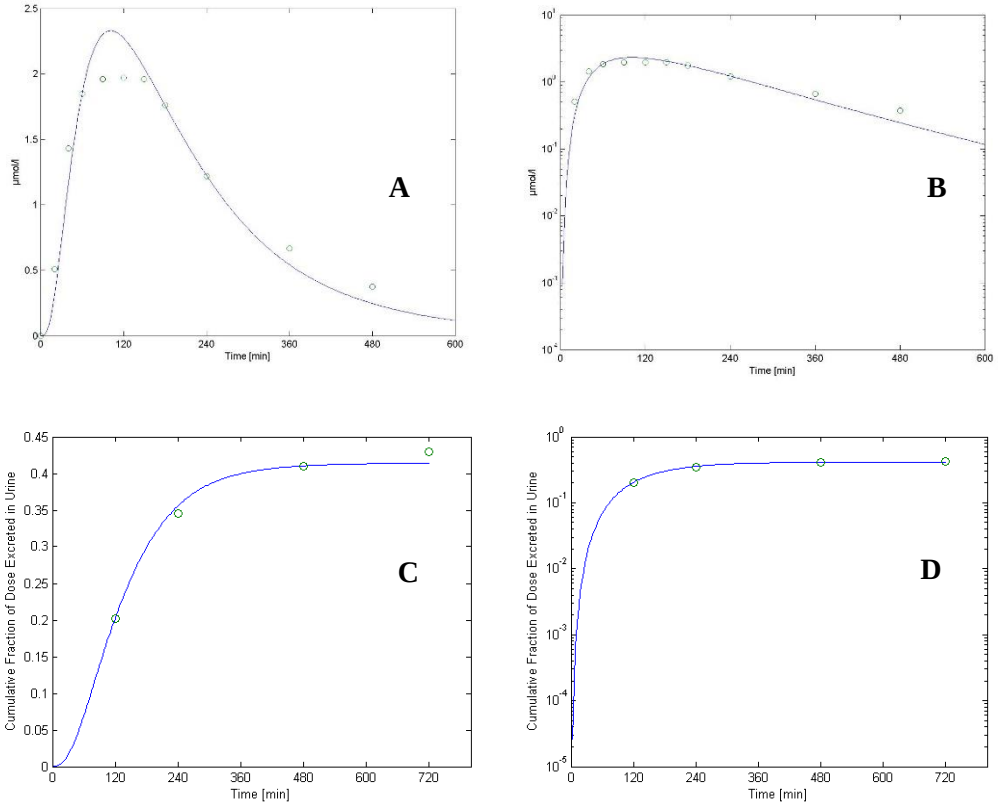

Predictive performance of models incorporating different SIWV values, and their associated amplification factors (Figure 6.3), were assessed using observed data pertaining to oral administration at higher dosages. For acyclovir dosed at 400 mg (Figure 6.5), a CAT model parameterized with a SIWV of approximately 116 mL provided the best estimate of plasma concentration values, as denoted by the AAFE. At a dose of 100 mg (Figure 6.6A), models incorporating SIWV values between 94.5 mL and 136.5 mL provided optimum estimates of chlorothiazide urinary excretion. However, at dosages of 250 mg, urinary excretion of chlorothiazide was most appropriately modelled using a SIWV

of 189 mL (Figure 6.6B). As a comparison, *in vivo* estimates of small intestinal fluid volume within adults denote a central tendency between 86-167 mL [59-61].

Figure 6.5 Absolute average fold error (AAFE) vs. SIWV for a 400 mg dose of acyclovir. AAFE values were tabulated based the discrepancy between observed [347] and predicted (model derived) plasma concentration vs. time values.

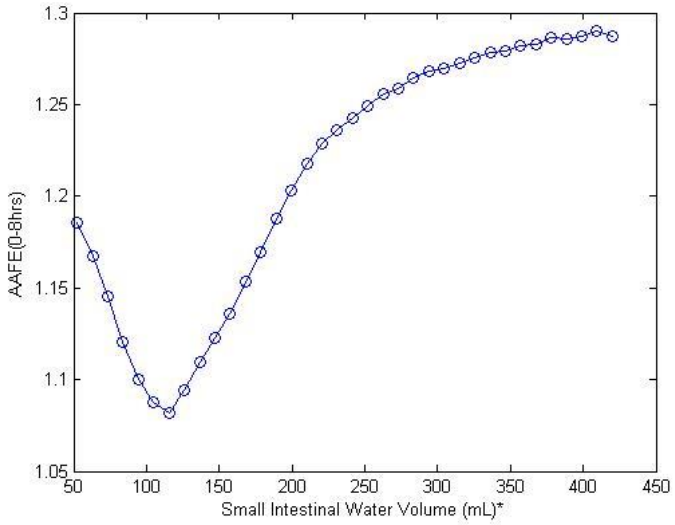

*SIWV with associated P x SA values (Amp1 and Amp2) as depicted in Figure 6.3A.

Figure 6.6 (A) Absolute average fold error (AAFE) vs. SIWV for a 100 mg dose of chlorothiazide. (B) AAFE vs. SIWV for a 250 mg dose of chlorothiazide. AAFE values were tabulated based the discrepancy between observed [352] and predicted (model-derived) cumulative urinary excretion vs. time values.

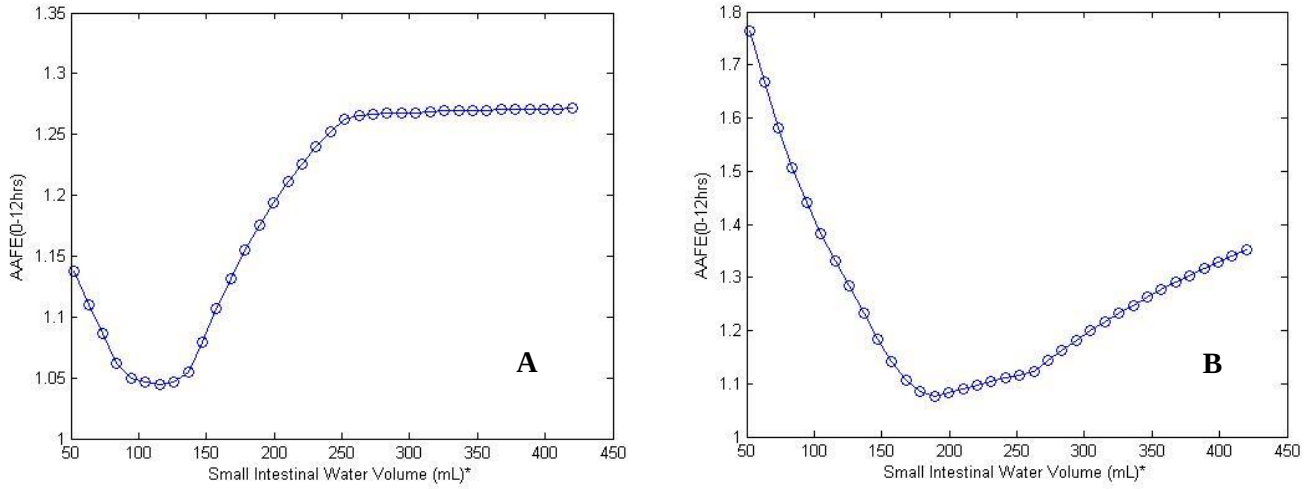

*SIWV with associated P x SA values (Amp1 and Amp2) as depicted in Figure 6.3B

6.4 Discussion

By integrating the developed CAT model into the PBPK modeling framework, optimal simulation-based estimates of SIWV were derived. Based on the described methodology, estimation of SIWV required a restrictive compound selection process to ensure non-linear changes in fraction absorbed, noted within *in vivo* investigations, were predominantly reflective of drug saturation of the intestinal fluids. The confounding presence of Michaelis-Menten absorption kinetics were mitigated by exclusion of compounds that exhibited an affinity for transport mediated intestinal absorption. Studies investigating low permeability compounds (i.e. fraction absorbed < 90%) administered as either a rapidly dissolving solid formulation or in solution permitted for estimation of intestinal permeability at lower dosages while minimizing the effects of dissolution. Although colonic absorption may play a critical role in oral drug bioavailability, especially for controlled release products, this study included only immediate release formulations with low permeability. As a result, compared to the small intestine, the effects of colonic absorption was deemed to be negligible. The study utilized *in vitro* aqueous solubility values obtained from the literature to parameterize the developed CAT model. Though

solubility estimates derived from biorelevant media are considered to be the most physiologically applicable, use of aqueous values were considered appropriate due to the hydrophilic nature of the studied compounds (logP < 0). As such, the presence of bile acids within intestinal fluids were considered to have a minimal influence on compound solubility *in vivo* [201].

The ability of compounds to form supersaturated solutions within intestinal fluids can largely influence *in vivo* oral absorption. Despite this, an accurate method for predicting compound specific supersaturation has yet to be developed. Simple molecular descriptors such as molecular weight, logP and pKa do not appear to allow for identification of compounds that readily establish supersaturated solutions (i.e. chasers) from those that do not (i.e. non-chasers) [354]. Furthermore, if supersaturated solutions are attained, estimation of the time course during which concentrations are sustained above the saturation solubility are not available. Slow precipitation kinetics and the resultant formation of supersaturated solutions can enhance drug bioavailability, especially for poorly soluble weak bases [355]. Within this study, drug precipitation was depicted as an instantaneous process. This assumption was deemed appropriate since both acyclovir and chlorothiazide were considered to possess low intestinal permeabilities. As such, the effects of temporal instances of supersaturation of the intestinal fluids were considered to be less influential with regards to drug absorption. To demonstrate this assertion, estimates of SIWV were derived from acyclovir data using a similar methodology as previously described with one alteration; precipitation was added to the CAT model using 1^{st} order precipitation half-lives of 20, 10, and 5 minutes. The results of this assessment denote models parameterized with SIWV values of 94.5 mL, 94.5 mL and 105 mL as the most applicable for simulating acyclovir oral absorption in conjunction with the aforementioned precipitation half-lives, respectively (Figure 6.7). Comparatively, these estimates are similar to 116 mL, the value obtained using the assumption of instantaneous intestinal precipitation.

While PBPK models can provide estimates of systemic exposure for compounds displaying non-linear clearance, parameterization (i.e. V_{max} and K_m) of these models require either intravenous dose escalation studies or detailed *in vitro* transporter/metabolic based assays. Due to limitations of available data within the literature, compounds exhibiting non-linear clearance in adult humans were excluded from the analysis. Intravenous bolus [356] and multi-dose studies [357] have demonstrated acyclovir clearance to be dose-independent. Though one report identifying the presence of non-linear clearance in rhesus monkeys (n=3) was located [358], intravenous chlorothiazide studies refuting the notion of dose-independent clearance were not obtained with regards to adult humans. Due to a lower dose per kg ratio and poor oral bioavailability, systemic plasma concentration values observed in human

studies [353, 359] were several fold lower than those achieved within the aforementioned primate study, minimizing the likelihood of observing clearance nonlinearities amongst humans. As a result, chlorothiazide was deemed as an acceptable candidate compound for our analysis.

Figure 6.7 Absolute average fold error (AAFE) vs. SIWV for a 400 mg dose of acyclovir. Intestinal precipitation was modelled using a half-lives of (A) 20 minutes, (B) 10 minutes and (C) 5 minutes. AAFE values were tabulated based the discrepancy between observed [347] and predicted (model-derived) plasma concentration vs. time values.

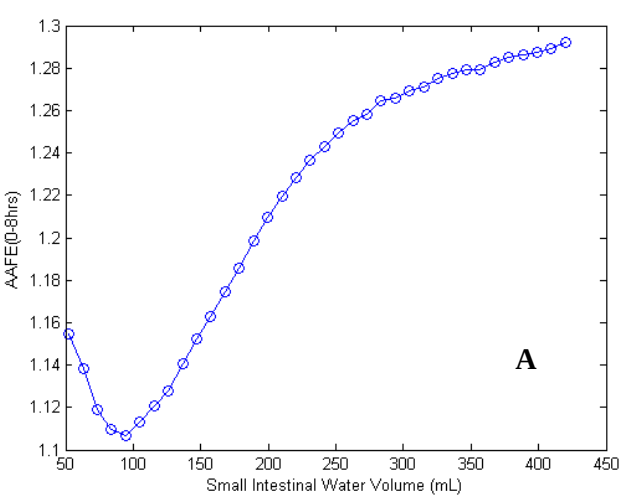

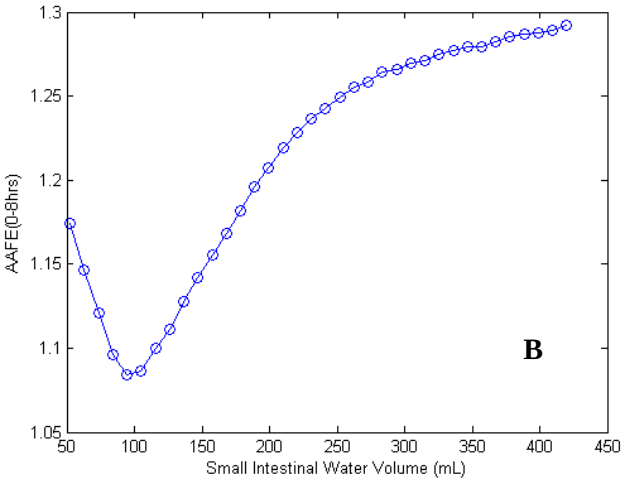

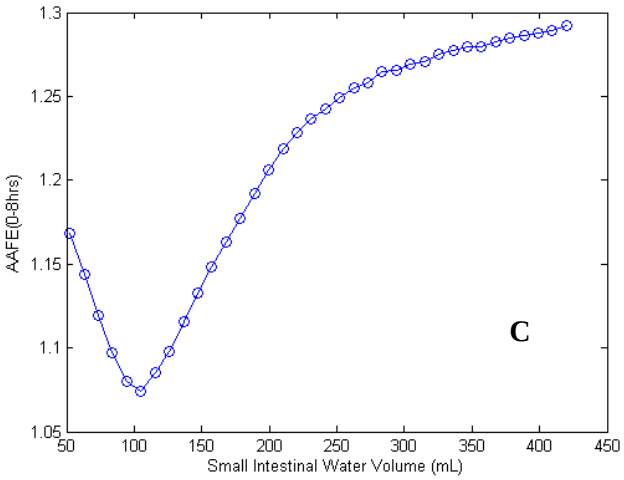

Study results indicate a SIWV of approximately 116 mL best predicted the non-linear absorption pattern of acyclovir between doses of 200 and 400 mg (Figure 6.5). For chlorothiazide, simulations indicated an approximate SIWV of 116 mL best described the non-proportionate absorption pattern at oral doses between 50 and 100 mg, though SIWV values between 94.5 mL and 136.5 mL provided similar degrees of accuracy (Figure 6.6A). In contrast, at doses of 250 mg, simulations indicated a SIWV of 189 mL provided the best estimates of chlorothiazide absorption (Figure 6.6B). This discrepancy with previous results may be explained by the pH dependent solubility of chlorothiazide in acidic mediums. At pH values representative of gastric media (i.e. pH = 1), chlorothiazide exhibits a low solubility (0.417 mg/ml) [345]. This increases the potential of gastric precipitation of drug from orally administered solutions, especially at higher dosages. Assuming a gastric media volume of approximately 250-300 mL (basal gastric volume plus fluid administered with dosage), chlorothiazide doses of 50 and 100 mg in solution would drive gastric concentrations below the solubility limit. Conversely, at doses of 250 mg, chlorothiazide concentrations would exceed the gastric solubility limit and, thus, be subject to precipitation. The effects of gastric precipitation on overall gastrointestinal transit can be profound, leading to increased gastric retention and protracted absorption. Since the developed CAT model utilized within this study assumed a simple first-order gastric emptying rate congruent with *in vivo* emptying kinetics of non-caloric liquids [342], the effects of gastric precipitation and subsequent gastric retention were not accounted for. SIWV values derived using data from orally administered compounds influenced by the effects of gastric precipitation are, therefore, anticipated to lack appropriate specificity. Consequently, estimates of SIWV using observed data pertaining to administration of 250 mg of chlorothiazide in solution may be inappropriately assigned within the context of our model. SIWV estimates obtained from acyclovir and chlorothiazide doses of 400 and 100 mg, respectively, approximate an average of 116 mL. These estimates are derived from dosage strengths where the potential of gastric precipitation is attenuated and, as such, allow for effective parameterization of SIWV within the model.

The results of our analysis are well corroborated by *in vivo* investigations examining small intestinal water content in humans. In two separate studies, Marciani et al. examined SIWV amongst separate cohorts of healthy adult subjects using serial MRI scans. One study quantified the average fasting SIWV as 86 mL (interquartile range 46–134 mL) among 16 subjects [59]. A median fasting SIWV of 167 mL (interquartile range 103-209 mL) was determined among 16 adults in the second study [60]. In a separate investigation, Schiller et al. assessed in-situ SIWV values using MRI scans among 12 healthy adult subjects [61]. The mean (± standard deviation) fasting SIWV was determined

to be 105 ± 72 mL. Within the study, intestinal fluid was not observed to be uniformly distributed throughout the intestine but instead contained within several discrete watery pockets. As a result, solid drug traversing the small bowel may not be in continuous contact with intestinal fluids. Due to the innate complexity of modelling the hydrodynamic movement of fluids within sequestered pockets along the intestine, the developed CAT model utilized a simplified approach with regards to the allocation of intestinal fluid. Compartmental fluid volumes were allocated using a consistent proportion of the geometric volume of each compartment. Despite this simplification, the results of our analysis indicate a SIWV of 116 mL as optimal for CAT model parameterization, a value which is consistent with *in vivo* investigations. Due to this agreement, the CAT model is considered to provide a biologically accurate depiction with regards to SIWV. This finding provides confidence in the potential use of such simulations for predicting oral drug disposition in populations where SIWV may differ (i.e. children). Additionally, results from the current investigation challenge the appropriateness of models incorporating larger SIWV (i.e. 250-600 mL) for simulating oral absorption [55-58].

In terms of solubility, the BCS utilizes 250 mL as its apparent physiologically relevant volume for classifying compounds as high vs. low solubility. At doses between 200 and 400 mg, acyclovir falls within the classification of a highly soluble compound [360]. By convention, compound absorption should not be limited by solubility. However, study results refute this notation as oral absorption of acyclovir at doses of 400 mg was limited due to solubility restrictions within the intestinal fluids, as exemplified by the presence of non-linear absorption when compared to oral doses of 200 mg.

An alternative model-based assessment of gastrointestinal fluid volumes using data from four solubility limited compounds was conducted by Sutton [361]. The analysis found multiple combinations of SIWV (i.e. ranging from 65-260 mL) and drug precipitation half-lives (T_{ppt}) provided appropriate fits with observed data. This result is a reflection of the compounds assessed, which predominantly included high permeability compounds. In such cases, the effect of precipitation on oral absorption is more pronounced and, therefore, requires implicit parameterization within the model. Since the study fit estimates of T_{ppt} following selection of SIWV, it is unsurprising that many combinations of SIWV and T_{ppt} were applicable. A SIWV of 130 mL was subsequently selected based on its agreement with physiologic values derived from the literature. In contrast, the current investigation incorporated only low permeability compounds which attenuated the confounding effects of intestinal precipitation on SIWV selection. In addition, our analysis utilized a quantitative methodology to identify an optimal SIWV for model parameterization. Physiologic values reported in

the literature did not influence selection of SIWV but were merely used as comparative index to assess the biological relevance of the model.

In a separate investigation, Sugano used an approximation of a one compartment absorption model to assess intestinal fluid volumes [362]. The analysis utilized fraction absorbed (Fa%) data from four orally administered compounds (acyclovir, chlorothiazide, lobucavir and ganciclovir). Despite considerable variability surrounding observed Fa% values, a mean intestinal fluid volume of 130 mL was ascertained. Though this value may be valid to predict Fa% in the context of a one compartment model, its applicability towards multi-compartment absorption models, as utilized by many software platforms, is not definitive. Based on the developed CAT model, the results of our analysis converged to a comparable estimate of SIWV (116 mL). To maximize reproducibility, the current study employed a quantitative methodology to assess the appropriateness of SIWV estimates based on observed pharmacokinetic data. In addition, model parameters such as compartmental fluid allocation were clearly defined.

Although computationally complex in comparison to traditional compartmental models, the use of a whole body PBPK model to provide estimates of systemic compound exposure was deemed necessary. For chlorothiazide, development of a systemic compartmental model was hampered due to a lack of intravenous human data amongst the literature. As a result, data depicting intravenous administration of chlorothiazide to rodents [350] was used to refine estimates of compound distribution (Figure 6.2B). Refined distribution parameters were subsequently scaled to humans using PBPK modelling techniques. For acyclovir, plasma profiles following intravenous administration to adult humans were available [347], permitting for the development of traditional compartmental models. However, to maintain consistency with regards to the analysis of the two candidate compounds, whole-body PBPK modelling was selected as the preferable technique.

The current investigation depicts a unique modality to estimate an appropriate SIWV for CAT model parameterization but is not without limitations. The reliance of the methodology on simplifying assumptions regarding gastrointestinal dissolution, transit, precipitation, and permeability are imperative for appropriate estimation of SIWV. Failure of compounds to conform to these specifications would decrease model applicability. To mitigate this potential, drug selection was conducted using a highly restrictive criteria. The derived SIWV represents an average value for parameterizing simulations for healthy adult humans. The analysis did not evaluate SIWV variability within the population, limiting use of our findings in facilitating appropriate population-based estimates of oral compound disposition. Finally, observed pharmacokinetic data sets were exclusively derived

from studies depicting dose administration under fasting conditions. As such, SIWV values derived from this investigation may preclude modeling of drug administration during fed states.

6.5 Conclusion

Using a model-based approach, we quantified an average SIWV of 116 mL using observed pharmacokinetic data from the literature. Compared to other model-based analyses, the methodology employed within the current investigation permitted for identification of SIWV independent of experimentally-based determinations. The estimate represents the optimal value for parameterization of the developed CAT model. The ability of PBPK models to extrapolate predictions of drug exposure between species as well as developmental age groups is predicated on its physiologically relevant framework. The study establishes a correlation between *in vivo* SIWV estimates in adults and parameterization of the widely used CAT model. Based on this finding, the use of CAT models for facilitating predictions of systemic drug exposure in unique and underserved research populations such as pediatrics will be an area of future research.

Chapter 7: Discussion, Summary Example, Conclusion, and Future Directions

Portions of this chapter are reflective of an original manuscript published by the Ph.D. candidate (Anil R Maharaj) in the journal CPT: Pharmacometrics & Systems Pharmacology. All pertinent dialogue included in this chapter was written by the Ph.D. candidate.

Maharaj AR, Edginton AN. Physiologically based pharmacokinetic modeling and simulation in pediatric drug development. CPT Pharmacometrics Syst Pharmacol. 2014;3:e150. doi:10.1038/psp.2014.45.

7.1 Discussion

The collective narrative of this thesis seeks to improve the parameterization of mechanistic oral disposition models in pediatrics, increasing the level of confidence associated with model predictions. As both the structure and parameterization of PBPK models are entrenched upon the notion of biological fidelity, a fundamental understanding of human anatomy and physiology are essential for the development of informative models. Children represent a heterogeneous population in terms of growth and development. Owing to the disparate nature of literature examining age-related changes in oral absorption, parameterization of mechanistic oral disposition models within this population is quite challenging. The current dissertation expands our understanding of the ontogeny of key physiological aspects regulating oral absorption and serves to highlight differences between children and adults. In particular, the thesis provided focused analyses pertaining to the ontogeny of small intestinal transit time (SITT), gastrointestinal (GI) solubility, and α-1-acid glycoprotein (AAG). In addition, complimentary chapters defined the currently accepted modality for the development pediatric PBPK models as well as demonstrated the use of PBPK models as tools for identification of human physiological values.

Chapter 2 of this dissertation provided an explicit example of how structured workflows can be implemented to facilitate the rational development pediatric PBPK models to support clinical investigations. The benzodiazepine lorazepam was used as an illustrative example to demonstrate how each step of the proposed workflow was executed. The end result of the modeling exercise provided age-specific pediatric doses from birth to adulthood that approximated similar plasma exposures ($AUC_{0\text{-}inf}$) to a 2 mg intravenous dose in adults. Similar to workflows presented by other research groups

[21, 23], the workflow proposed in chapter 2 also recommends the initial development, evaluation, and refinement of an adult PBPK model prior to extrapolation towards pediatrics. Based on this methodology, informative pediatric models can be developed in a fashion that leverages the relative wealth of adult PK information available. The importance of evaluating the adult PBPK model should not be understated. As demonstrated in Figure 2.2, misspecification of the adult model can translate into similar discrepancies within subsequently developed pediatric models. As a result, only adult models displaying appropriate agreement with observed PK data should be considered as candidate models for pediatric model development.

One interesting finding that highlighted the intuitive nature of PBPK modeling arose when estimates of lorazepam CL and V_{ss} derived via PBPK modeling were compared to estimates garnered using Population PK (PopPK) modeling [88] for 15 pediatric subjects in whom intensive serial sampling was performed. For this subset of patients, the resolution of plasma concentration-time data was adequate to permit for CL and V_{ss} to be calculated via non-compartmental analysis (NCA). When PK estimates derived via PBPK and PopPK techniques were compared, a similar predictive capacity was noted between the two techniques in terms of the proportion of CL and V_{ss} values falling within a 1.5 fold-error (i.e. ~60% and ~80%, respectively) from observed values (i.e. NCA). This finding was rather remarkable as the PopPK model was built on a dataset that included the abovementioned 15 subjects, yet its predictive capacity was similar to that of a PBPK model that was derived independently of any pediatric PK data.

The research in chapter 2 demonstrated a practical example of the utility of such workflows for extrapolating PK information from adults to pediatrics using PBPK modeling. Within the example, estimates of lorazepam PK derived from the pediatric PBPK model were deemed to be relatively accurate in comparison to a competing PopPK model [88]. However, the research precipitates the question, “Does the use of a structured workflow ensure that pediatric PBPK models deliver accurate estimates of PK in children?” Unfortunately, the simple answer to this question is “no”. As previously described in the introduction, within PBPK models there exists an intuitive relationship between the biological relevance of its input parameters and confidence bestowed upon model predictions. What this means is that in order to have confidence in PBPK model predictions, model parameters should reflect the anatomy and physiology of the organism under study. Thus, a lack of knowledge regarding the ontogeny of processes regulating oral absorption will result in the development of pediatric models with insufficient predictive capacities. An example of this is highlighted in a recent publication that described the development of pediatric PBPK models for simulating the oral disposition of sotolol and

acetaminophen [30]. Simulations performed in older children (2-11 years) fit observed concentration-time data well for both compounds; however, for infants (1 month – 2 years) and neonates (0 to 1 month), the simulations tended to overestimate C_{max} while underestimating t_{max}. The authors attributed this lack of fit to be the result of misspecification of gastric emptying time (GET) within infants and neonates. In fact, when the parameter GET was increased, *post-priori*, PBPK simulations displayed improved predictive accuracy in both age groups. In a separate study, PBPK modeling was utilized to simulate the oral disposition of voriconazole among children (2-11 years) [31]. The initially developed pediatric PBPK model displayed concentration-time values that were incongruent with observed data. In addition, the model predicted oral bioavailability (i.e. 60–94%) was greater than values observed among children (i.e. 44-66%). The authors' postulated the poor fit was a result of a lack of incorporation of intestinal metabolism into the pediatric model. When intestinal first-pass was incorporated, pediatric simulations exhibited an improved fit with the observed data.

To facilitate improved PBPK model parameterization, chapters 3, 4, and 5 of this thesis provided focused assessments of the relationship between age and key physiological parameters (e.g. SITT, intestinal solubility, and AAG) responsible for modulating oral drug disposition. Much of the depicted work leverages data from the current literature to provide a consensus regarding the developmental trajectories of these parameters. Chapter 3 examined the relationship between age and SITT. The analysis, which aggregated data pertaining to children and adults over 40 published investigations, utilized meta-regression techniques to quantitatively examine SITT as a function of age. Based on the results of the analysis, age was not found be a significant modulator of SITT. This finding deviates from previously held assertions that older children exhibit faster intestinal transit times than adults [97, 98]. Such assertions have been linked to previous PK investigations of sustained release (SR) theophylline in asthmatic children who typically display large degrees of inter-individual variability in systemic concentrations [99, 100]. To demonstrate that changes in SITT are unlikely to contribute to inconsistencies in theophylline SR disposition in children, a PBPK model-based approach was employed. From this assessment it was found that alterations in SITT lacked influence on the oral absorption of SR theophylline. Of note, discernable changes in theophylline absorption were only observed when total intestinal transit time (i.e. SITT and LITT) was greatly altered (i.e. ↓ 50%). These results, therefore, downplay decreased SITT as a primary factor contributing to PK variability of SR theophylline in children.

Chapter 4 of this thesis provided a comprehensive literature-based assessment of age-related changes in GI fluid composition. The physicochemical nature of GI fluids exhibits a direct relationship

to compound specific solubility values. Considering the importance of luminal solubility towards oral drug performance, determination of the relationship between age and GI fluid composition is critical to facilitate accurate predictions of pediatric oral absorption. The analysis, which aggregated data depicting GI fluid compositions from children to adults, served to quantitatively evaluate the influence of age on specific physicochemical and compositional properties including pH, buffering capacity, pepsin concentrations, osmolality, bile salt concentrations, and the presence of fat digestion products. The results of this chapter represent the most detailed evaluation of age-specific GI fluid compositions available in the current literature. Of note, the assessment depicted fasting gastric pH in neonates, with the exception of the first few hours after birth, to be similar to that of adults. Fasting gastric pH was maintained at adult levels thereafter. This finding contrasts with a previously published review article that denoted fasting gastric pH in neonates to fall shortly after birth to adult levels, followed by an increase in pH to values between 6-7 [184]. However, the findings expressed by the review article were derived from tertiary sources without an evaluation of the primary literature. Comparatively, results reported in this dissertation incorporated a wide breath of primary literature sources and should, therefore, be viewed as a more comprehensive assessment. In addition to quantitatively denoting developmental differences in GI fluid composition between children and adults, the chapter extended the applicability of this research by formulating a set of novel pediatric biorelevant media. This research represents one of the first reported attempts to develop biorelevant media reflective of children in the literature. In total, 9 different age-specific media were developed to represent the luminal fluids of the stomach and proximal small intestine in both fasted and fed states. Pediatric media were reflective of the unique physicochemical nature of GI fluids in neonates (0-1 month) and younger infants (1-12 months). To assess the impact of developmental changes in fluid composition, solubility assessments were conducted for seven BCS Class II compounds in each pediatric media. Additionally, solubility assessments were conducted in a set of biorelevant media representative of adults [182]. The analysis defined relevant changes in solubility in relation to the adult media using the FDA's *in vivo* bioequivalence criterion (i.e. 80-125%). The absorption of BCS Class II compounds is primarily assumed to be limited by solubility. As such, compounds exhibiting relevant solubility changes within pediatric media could be at increased risk for displaying age-related alterations in oral drug absorption. For six of the seven compounds investigated, solubility fell outside an 80-125% range from adult values in at least one of the developed pediatric media. These findings infer that relevant differences in luminal solubility between pediatric and adult subjects could persist *in vivo*. This inference contrasts with a long

employed assumption – pediatric and adult luminal solubility values are identical - adopted by several research groups investigating oral drug absorption in children [38, 363].

Defining the relationship between age and plasma AAG concentrations was the focus of chapter 5. Although plasma protein binding is typically perceived to alter systemic PK parameters such as clearance (CL) and volume of distribution (V_{ss}) [364, 365], it can also be culpable in influencing oral drug disposition. For the subset of high extraction ratio (ER) compounds, the fraction unbound in blood - which is proportional to the fraction unbound in plasma - exhibits an inverse relationship to hepatic bioavailability (i.e. first-pass) [366]. Thus, increases in the degree of protein binding (i.e. $\downarrow f_{u,p}$) will result in higher hepatic availability; whereas, decreases in the degree of protein binding (i.e. $\uparrow f_{u,p}$) will result in the opposite. Within the chapter, the ontogeny of plasma AAG was quantitatively defined in healthy subjects, using a literature-based dataset, and subjects suspected of infection (i.e. sick subjects), using data aggregated over 3 clinical trials. Compared to other models, the sigmoid Emax model provided the best approximation of the ontogeny of AAG along the entire developmental age range for both subject groups. When utilized to estimate $f_{u,p}$ values in children, the derived Emax equation (from healthy subjects) exhibited a lower degree of bias and higher precision in comparison to a previously proposed approach [51]. Within PBPK models, $f_{u,p}$ represents a key parameter with ramifications towards several processes such as hepatic first-pass (for high ER drugs), CL (low ER drugs), and V_{ss} (for all compounds that distribute outside the plasma space). Thus, by providing more accurate estimates of pediatric $f_{u,p}$, use of the derived AAG ontogeny equation will serve to reduce uncertainty associated with pediatric PK predictions. In addition, the analysis of AAG ontogeny within infected subjects denotes one of the first attempts to quantitatively model plasma AAG levels from neonates to adults in this subject group. This is quite pertinent as drug administration in pediatrics is principally focused towards sick patients.

Chapter 6 demonstrated an alternative use of PBPK modeling to serve as a framework for generating estimates of human physiology. Plasma-concentration time data depicting oral administration of acyclovir and chlorothiazide in adults were utilized to generate model-based estimates of SIWV. The results of this modeling exercise defined a value of ~116 mL as the optimal SIWV for CAT model parameterization in adults. In comparison, CAT models implemented by other research groups have utilized a wide range of SIWV values (250-600 mL) to facilitate predictions of oral compound absorption [55-58]. In terms of *in vivo* estimates of SIWV, the results of one representative investigation from the literature, which examined SIWV among 12 healthy adult subjects using MRI scans, depicted an average volume of 105 mL [61] . This value was closely approximated by the model-

derived value reported in chapter 6, thus confirming the biological fidelity of the depicted CAT model with regards to SIWV parameterization. The work also explicitly denoted how the parameter SIWV can be distributed throughout the multiple compartments of the CAT model, an important consideration in the use of such models for simulating oral drug absorption. Within the depicted CAT model, water volumes were allocated using a consistent proportion of the geometric volume of each compartment with the sum of all compartments equaling the total SIWV (~116 mL). This represents an overt simplification of *in vivo* conditions, where small intestinal water is not uniformly distributed throughout the intestine but instead contained within several discrete watery pockets [61]. Nevertheless, the depicted parameterization scheme was deemed as appropriate based on the congruent relationship between model-based and *in vivo* derived estimates of SIWV. Additionally, the implemented simplification was considered as preferable as it circumvented the innate complexity associated with modeling the hydrodynamic movement of fluids within sequestered pockets along the intestine.

Despite focusing on the parameterization of SIWV within an adult model, the depicted research in chapter 6 encompasses implications towards pediatric model development. Based on the dialogue of chapter 2, the importance of adult model development and evaluation prior to extrapolation to pediatrics was highlighted. An essential component in establishing confidence in PBPK models focuses on evaluating the model's biological relevance in terms of structure and parameterization [39]. The reliability of adult models incorporating parameters not consistent with known *in vivo* measures is considered questionable in terms of performing extrapolations towards pediatrics. The research in chapter 6 confirms the biological fidelity of the CAT model with regards to SIWV, thus instilling confidence in the prospective use of such models for estimation oral drug disposition in pediatrics. The depicted methodology exploits the mechanistic and physiologic framework of PBPK models to facilitate predictions of human physiology using compound specific PK datasets. This demonstrates an alternative use of PBPK modeling that could be of potential benefit in children. Children are considered as a vulnerable population and, as such, may be prohibited from participating in clinical investigations that lack direct benefit towards individual study subjects [367]. As such, invasive assessment techniques that have been employed in adults to quantitatively define aspects of human physiology may be precluded in children, making appropriate parameterization of pediatric PBPK models difficult. Provided the recorded measure (i.e. plasma-concentration time data) is sensitive to the parameter of interest, the methodology presented in chapter 6 could be applied to estimate a variety of anatomical and physiological parameters. In children, the described methodology could be employed to increase our understanding of pediatric physiology in cases where *in vivo* determinations are prohibited.

Quantitative assessments of pediatric physiology, as depicted in this dissertation, will aid in the development of informative pediatric PBPK models with improved capacities for estimating oral compound disposition in children. The findings of a recent publication assessing the age-dependency of gastric emptying (GET) time can also serve to support pediatric model parameterization. In the investigation by Bonner et al. [179], a nonlinear mixed-effects based approached was employed to assess the influence of age on GET using data from 49 studies denoting gastric transit in children, including neonates, and adults. The analysis found meal type (e.g. aqueous, breast milk, formula, semi-solid, and solid) to be a significant covariate of GET; however, age was not. Through use of the final nonlinear mixed-effects model derived from the analysis, GET can be quantitatively defined for pediatric PBPK model parameterization.

Although the research presented in this dissertation strives to increase the knowledge base of pediatric physiological attributes that regulate the oral drug disposition, there is still a need for additional investigations to fully elucidate the age-dependency of the oral absorption process. Knowledge gaps particularly endemic in children with regards to GI anatomy and physiology have been denoted in a 2012 publication by the Pediatric Biopharmaceutics Classification System (P-BCS) Working Group [186]. The group was assembled to assess whether a similar classification system as utilized in adults (i.e. BCS) could be developed for children. Of note, the P-BCS Working Group recognized that significant knowledge gaps with regards to pediatric GI physiology, including intestinal permeability and ontogeny of drug transporters, needs to be addressed prior to establishing a pediatric focused BCS [186]. With regards to the development of informative pediatric PBPK models, these same knowledge gaps are also of relevance.

Intestinal permeability is a measure of the mucosal membrane's inherent resistance to movement of substances across the epithelium. As a surrogate measure, the absorption and subsequent rapid urine excretion of non-metabolizable sugars such as lactulose, mannitol, and L-rhamnose, can be used to provide relative estimates of intestinal barrier function. Mannitol and L-rhamnose are monosaccharaides that can transverse the intestinal membrane via the transcellular pathway; whereas, lactulose permeates across the intestinal membrane through the tight junctions in-between the enterocytes (paracellular) [368]. Based on such tests, it has been noted that intestinal permeability is enhanced during the first few days after birth due to an increased capacity for paracellular transport. With initiation of enteral feeds, permeability rapidly declines as transport via the paracellular route becomes attenuated [369-371]. Mature levels of intestinal permeability are normally attained during the first weeks of life [372]. These findings can be viewed as qualitative indicators of intestinal

permeability; however, they do not provide a capacity to quantitatively discern how the permeability of specific compounds will change with age. Therefore, data derived from the abovementioned tests are of little value for parameterizing PBPK models that are focused on simulating the disposition of specific compounds. In adults, *in vivo* estimates of drug specific intestinal permeability have been determined through the use of intestinal perfusion techniques. These techniques serve to provide regional specific (i.e. jejunum) estimates of compound permeability [122]. Ideally, to examine the age-dependency of permeability, such tests should be employed in developmentally unique cohorts of children (e.g. neonates, infants, toddlers, etc.). However, considering the status of children as a vulnerable population and the invasiveness of this technique, studies among pediatrics would likely be prohibited. PBPK modeling may offer an alternative modality for quantitatively defining intestinal permeability in children. As depicted in chapter 6, the biologically relevant structure and parameterization of PBPK models can be exploited to define optimal values for parameters pertaining to human physiology. For compounds whose oral disposition is sensitive to intestinal permeability, *in vivo* PK measures (e.g. plasma concentration-time data) can be used to facilitate model-based estimates of permeability. To fully evaluate the influence of age on intestinal permeability using this approach, compound-specific PK datasets depicting oral drug administration in children from different development stages as well as adults would be required. In addition, a robust analysis would entail inclusion of a wide range of compounds that vary in terms of physiochemical properties (e.g. logP, molecular weight, pKa). This would permit for an analysis to evaluate whether potentially observed age-specific differences in intestinal permeability are related to specific aspects of compound physico-chemistry.

The presence of transporters along the gut wall can significantly influence compound absorption. Absorptive transporters mainly function to transport their substrates from the gastrointestinal lumen into the intracellular space of the enterocytes. Examples of absorptive transporter families located along the intestine include oligopeptide transporters (PEPT), organic anion-transporting polypeptides (OATP), monocarboxylate transporters (MCT), and organic cation transporters (OCT) [373]. ATP-binding cassette (ABC) transporters are efflux proteins that prevent intracellular accumulation of their substrates by transporting them either apically (back into the intestinal lumen) or basolaterally (into the bloodstream). Examples include P-glycoprotein (P-gp) (transcoded by the MDR1 gene), multi-drug resistance-associated protein 2 (MDR2), and breast cancer resistance protein (BCRP) [373]. Several currently marketed drugs known to be substrates of P-gp include digoxin, tamoxifen, tacrolimus, and nifedipine [374]. Literature reports regarding the ontogeny

of intestinal drug transporters are in relative short supply. Of the few studies published, most have focused on P-gp. Fakhoury et al. [375] observed highly variable levels of P-gp mRNA from duodenal biopsies taken from children of varying ages. No relationship between age and mRNA expression was established. Unlike the previous study, Miki et al. [376] observed a trend towards higher MDR1 (gene responsible for encoding P-gp) mRNA levels with increasing age. Small intestinal samples from fetuses and neonates had lower mRNA expression levels than older children/adults though these differences were not significant. Therefore, in order to increase confidence in estimates of oral drug disposition garnered from pediatric PBPK models, additional investigations defining the ontogeny of P-gp as well as other intestinal transporters are needed.

7.2 Summary Example

This section will demonstrate how specific elements of this thesis can be employed to facilitate the development of pediatric PBPK models for prediction of oral drug absorption. PBPK models were developed for two BCS class II compounds: carbamazepine (antiepileptic) and griseofulvin (antifungal). These compounds were selected based on the results from chapter 4, where both exhibited relevant age-dependent alterations in GI solubility. The objective of this modeling exercise was to use PBPK modeling to discern whether these age-related changes in GI solubility would translate into alterations in oral drug absorption between children and adults.

PK-Sim 6.3® (Bayer Technology Services GmbH, Leverkusen, Germany) was utilized to develop all prospectively described PBPK models for both compounds. To generate age-specific predictions of oral carbamazepine absorption, pediatric PBPK models were developed based on the workflow presented in chapter 2 with one exception. As PK data (e.g. plasma concentration-time profiles) depicting the disposition of carbamazepine following IV administration in adult humans was unavailable, an initial PBPK model was developed based on IV data from a preclinical species (i.e. rhesus monkey) [377]. This was similar to the approach employed in chapter 6 for chlorothiazide. Carbamazepine fraction unbound in plasma ($f_{u,p}$) among rhesus monkeys was parameterized as 0.32 [378]. For all models, tissue-to-plasma partition coefficients were predicted *in silico* using the tissue-composition based approach proposed by Rodgers and Rowland [80-82]. Concentration-time data describing IV administration from the abovementioned preclinical investigation was utilized in conjunction with a preclinical species (i.e. rhesus monkey) PBPK model to derive an estimate of *in vivo* lipophilicity for carbamazepine. This value was subsequently used for parameterization of all

prospective PBPK models (e.g. children and adult). Estimates of intestinal permeability were derived from PK-Sim's proprietary algorithm, which tabulates permeability based on compound specific physicochemical properties. Drug dissolution within all oral absorption models was described using a Noyes-Whitney based approach, as depicted by equation 6.1. Models utilized the assumption that hepatic metabolism represented the primary process regulating carbamazepine clearance [379]. Adult biorelevant solubility values pertaining to the appropriate feeding state, as derived in chapter 4, were employed to parameterize GI solubility within the initially developed adult PBPK models (Table 7.1). SIWV was defined using a congruent method as stated in chapter 6, which assumes a constant proportion of geometric volume of each small intestinal compartment to be comprised of water (e.g. 0.107 mL of fluid per cm^3 of geometric volume). A $f_{u,p}$ of 0.24 was used for parameterization of adult simulations [380]. PK data depicting oral administration of a carbamazepine suspension to a cohort of healthy adult subjects under fasting conditions was utilized to parameterize the *in vivo* dissolution rate constant (K_d) and hepatic intrinsic clearance (Cl_{int}) [381] within the model. Following qualification of the adult PBPK model within the fasted state, an additional simulation was instituted to estimate adult oral disposition under fed-state conditions. The effect of feeding on carbamazepine bioavailability (i.e. no change in $AUC_{0\text{-}inf}$) as described by the simulation was similar to the findings of an *in vivo* investigation examining the influence of enteral feed administration on carbamazepine PK [382]. This fed-state simulation in adults was conducted to provide a like-for-like comparison with prospectively developed pediatric models for which drug administration was exclusively simulated in the fed-state. As children, especially those within the youngest age groups, are typically fed on a more consistent basis than adults during waking hours, it was inferred that fed-state simulations in children would provide the most appropriate reflection of pediatric oral disposition. Once the adult model was finalized, pediatric model development, as depicted in chapter 2, commenced. SITT was parameterized similarly for all age-groups. Pediatric simulations utilized the same K_d value as previously derived for adults. Age-specific models were developed to provide estimates of fraction absorbed (Fa) vs. time in developmentally distinct subjects: neonate (5 days), infant (3 months), child (3 years), and adult (30 years). As described above, all simulations were reflective of drug administration within the fed-state; age-specific GI solubility values used within each model are stated in Table 7.1. Doses ascribed in each simulation were representative of age-specific initial dosing recommendations for primary treatment of epilepsy [24]. Daily doses were divided to represent the typical dosing frequency of a carbamazepine suspension, which is recommended to be administered at least three times a day.

Table 7.1 Carbamazepine biorelevant solubility values utilized for PBPK model parameterization

	Neonate	Infant	Child	Adult
Gastric Solubility (mcg/mL)	592[a] (fed-state)	592[a] (fed-state)	790 (fed-state)	346 (fasted-state) 790 (fed-state)
Intestinal Solubility (mcg/mL)	276[b] (fed-state)	305 (fed-state)	326 (fed-state)	236 (fasted-state) 326 (fed-state)

a - Solubility in simulated fed-state gastric media representative of neonates fed cow's milk-based formula (Pnc-FeSSGF)

b - Solubility in simulated fed-state intestinal media representative of neonates fed cow's milk-based formula (Pnc-FeSSIF)

Development of pediatric and adult PBPK models for predicting griseofulvin oral absorption followed a similar trajectory as presented above. However, in this case, data depicting IV administration of griseofulvin in adults was available [383]. Adult simulations incorporated a $f_{u,p}$ of 0.16 [384]. Estimates of *in vivo* lipophilicity and hepatic Cl_{int}, the primary clearance pathway of griseofulvin [385], were generated using concentration-time data describing IV administration to humans [383] in conjunction with an adult PBPK model. The optimized lipophilicity value was employed in all forthcoming models (e.g. pediatric and adult); whereas, the optimized hepatic Cl_{int} value served to exclusively parameterize subsequently developed adult oral absorption models. Adult PK data describing oral administration of a micronized griseofulvin suspension under fasting conditions was employed to estimate the *in vivo* dissolution rate constant (K_d) for micronized griseofulvin [386]. Biorelevant solubility values used for adult model parameterization are presented in Table 7.2. Similar to above, a fed-state adult model was developed following qualification of the fasted-state model. The results of the fed-state simulation depicted an 80% increase in $AUC_{0\text{-}inf}$ compared to the fasted-state, a finding that correlates well with *in vivo* data (i.e. 70-120% increase in griseofulvin absorption with co-administration of a meal) [387]. Pediatric models were subsequently developed to simulate fed-state administration only. Simulations of Fa vs. time were developed for subjects pertaining to the same age-groups as depicted above. Age-specific GI solubility values used within each model are presented in Table 7.2. Simulated doses were based on age-specific recommendations for the treatment of tinea capitis [24, 388].

Table 7.2 Griseofulvin biorelevant solubility values utilized for PBPK model parameterization

	Neonate	Infant	Child	Adult
Gastric Solubility (mcg/mL)	36[a] (fed-state)	36[a] (fed-state)	45.2 (fed-state)	12.4 (fasted-state) 45.2 (fed-state)
Intestinal Solubility (mcg/mL)	22.1[b] (fed-state)	24 (fed-state)	28.6 (fed-state)	15.2 (fasted-state) 28.6 (fed-state)

a - Solubility in simulated fed-state gastric media representative of neonates fed cow's milk-based formula (Pnc-FeSSGF)

b - Solubility in simulated fed-state intestinal media representative of neonates fed cow's milk-based formula (Pnc-FeSSIF)

PBPK model derived predictions of oral absorption of a carbamazepine suspension under fed conditions is presented for different age groups in Figure 7.1. Despite changes in gastric solubility (~75% of adult values), intestinal solubility, and administration of higher mg/kg doses, both the rate and extent of carbamazepine absorption were largely unchanged in the neonate and infant in comparison to the adult. The child (3 years) simulation, which was parameterized using the same GI solubility values as the adult but incorporated a higher mg/kg dose, also predicted a similar absorption pattern to the adult simulation. Furthermore, model predictions indicated that all age groups would achieve complete absorption (i.e. Fa = 1). In contrast, PBPK model simulations depicting oral administration of a micronized griseofulvin suspension under fed conditions (Figure 7.2) displayed developmental differences in absorption. All pediatric subjects (e.g. neonate, infant, and child), displayed slower rates of absorption in comparison to the adult subject. The extent of absorption in the neonate and infant, who were administered slightly higher weight normalized doses than the adult (i.e. 10 mg/kg vs. 7.35 mg/kg, repectively), was approximately 0.77. In comparison the extent of absorption in the adult model was marginally higher at 0.85. In accordance with pediatric dosing recommendations, the child model was simulated using a dose of 25 mg/kg, which is 3.5x higher than the weight normalized dose commonly prescribed to adults (~7 mg/kg). Simulations from the child model predicted a lower extent of absorption at 0.67.

Figure 7.1 Carbamazepine suspension simulated fraction absorbed in different age groups (Fed State)

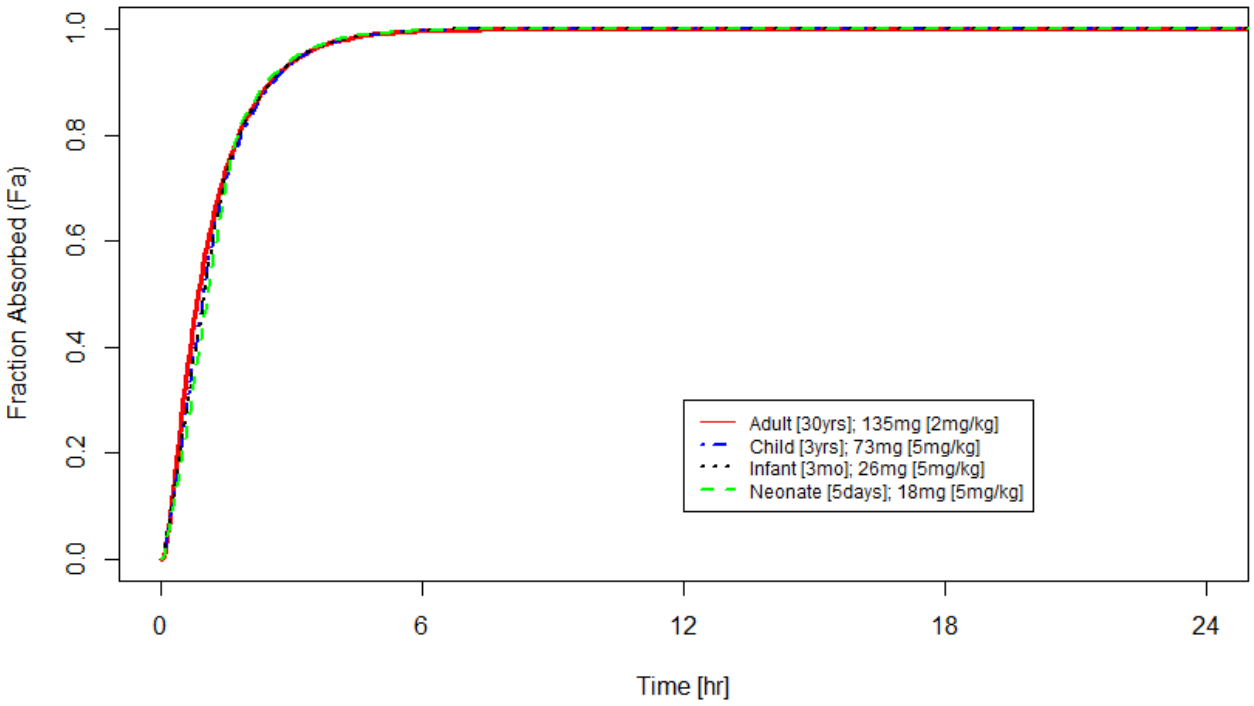

Figure 7.2 Griseofulvin suspension (micronized) simulated fraction absorbed in different age groups (Fed State)

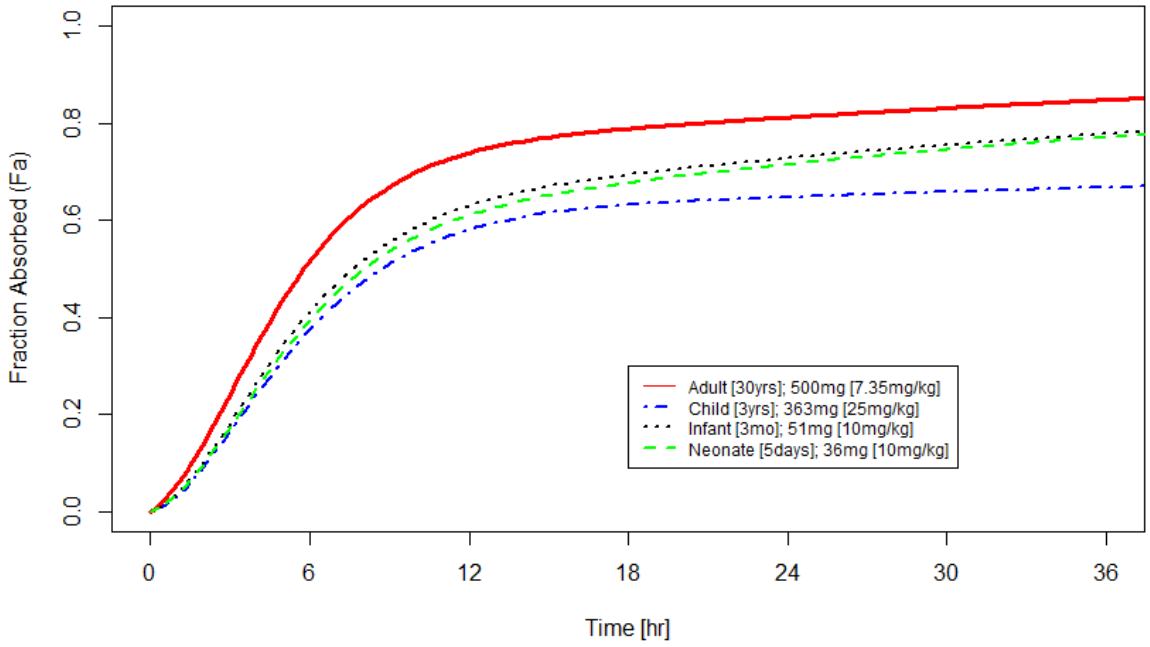

The results of this simulation-based exercise found divergent developmental patterns of absorption for the two BCS class II compounds assessed. For carbamazepine, changes in gastric solubility, intestinal solubility, and administration of different weight normalized doses, failed to induce any discernable changes towards the rate or extent of oral drug absorption. Yet for griseofulvin, changes in the same aforementioned parameters, albeit to different degrees, induced age-specific changes in oral drug performance. The etiology of this discrepancy between the two compounds can be rationalized through an assessment of dose-to-solubility (D/S) ratios. Considering a therapeutic dose of carbamazepine (e.g. 200 mg) and a solubility value pertaining to adult fasted-state intestinal media (0.236 mg/mL), as recommend by the proponents of the Developability Classification System [389], a D/S ratio of 847 can be calculated. For griseofulvin, a similar ratio calculated based on a dose of 500 mg and a biorelevant fasted-state intestinal solubility of 0.015 mg/mL would be ~33000. The magnitude of this value provides an indication of the influence that solubility exerts towards modulating oral

compound absorption. BCS class II compounds with higher D/S ratios are more likely to display solubility limited absorption [389]. In addition, such compounds would be most susceptible to exhibit changes in oral drug absorption due to developmental changes in solubility. However, in order to fully elucidate the impacts of age on oral drug absorption, consideration of GI permeability, transit, and dissolution should also accompany assessments of age-specific GI solubility. To discern why changes in intestinal solubility failed to propagate changes towards oral carbamazepine absorption in pediatric subjects, an understanding of the mechanistic equation employed within PBPK models to describe intestinal absorption can provide some insight. Equation 7.1 presents the factors influencing the rate of intestinal absorption within CAT model compartments,

$$Rate\ (mg/hr) = P_{eff} \cdot SA \cdot C \quad \text{(Equation 7.1)}$$

where P_{eff} represents the intestinal permeability (cm/hr), SA is the intestinal surface area (cm^2), and C is the luminal concentration of drug within intestinal fluids. For all age-groups, PBPK derived simulations denoted luminal concentrations of carbamazepine in the small intestine, the principal site of oral xenobiotic absorption, to fall below the solubility limit. Considering differences in anthropometry between children and adults, it can be inferred that total intestinal SA in children is smaller than that of adults. However, as children were administered larger mg/kg doses, luminal solubility values within the small intestine were higher - yet still below the solubility limit - in comparison to the reference adult subject. Based on equation 7.1, which depicts a compensatory relationship between SA and luminal concentrations, minimal disruptions in the rate of oral carbamazepine absorption would be expected in children. As a result, simulations depicted similar absorption profiles (rate and extent) between pediatrics and adults. This finding is supported by a recent publication depicting the use of PBPK modeling to explore the age-dependency of fluconazole absorption [38]. The analysis denoted a similarity with regards to the absorption profiles (Fa vs. time) of fluconazole in both children and adults. The article asserted a similar etiology as depicted above to explain the lack of age-dependent differences in fluconazole absorption.

Dissimilar to carbamazepine, simulations conducted for griseofulvin indicated the presence of age-specific differences in oral drug absorption. The greater influence of solubility towards modulating oral griseofulvin absorption is conveyed by its high D/S ratio. Based on its mechanistic design, PBPK models, which include parameters for both dose and luminal solubility, can intrinsically account for the impact of specific interrelationships between parameters (e.g. high D/S ratio). Simulations exhibited

luminal concentrations of griseofulvin within the small intestine to be in a state of saturation (i.e. at the solubility limit) for all age groups. Therefore, increased weight-normalized dosages administered to children did not result in higher luminal concentrations. As such, the complimentary relationship described above, where increases in luminal concentrations compensate for decreases in intestinal SA in children, does not exist for griseofulvin. Consequently, age-related changes in intestinal solubility will result in dissimilar oral drug absorption profiles between children and adults. In addition, since drug absorption is already at its upper limit, further increases in the administered dose, as depicted by the simulation pertaining to the child, will result in decreases in Fa. These examples serve to demonstrate the unique capacity of PBPK models to integrate multiple sources of information regarding the age-dependency of human physiology. Within PBPK models, mechanistic equations are employed to quantitatively describe the inter-relationship between model parameters and drug PK. In this regard, PBPK modeling offers a rational approach to discern the effects of changes to a single parameter as well as changes to several parameters on overall drug PK. By incorporating age-specific parameters associated with luminal solubility, intestinal SA, SITT, and intestinal water volume, the derived pediatric PBPK models in this section were able to provide quantitative estimates of the rate and extent of oral absorption specific to each compound. Simulations depicted that despite a similar BCS classification (i.e. class II), age-related differences in oral absorption would be expected for griseofulvin but not carbamazepine. However, the results presented in this section should be viewed with caution since *in vivo* data among pediatric subjects was not available to corroborate them.

7.3 Conclusion

With legislation in both North American and Europe mandating pediatric drug development research, interest in the use of modeling and simulation has increased. Dissimilar to empirically derived modeling techniques (e.g. PopPK), PBPK models offer the unique capacity to generate informative predictions of compound PK in unstudied subpopulations. This attribute is based on their mechanistic design and strategic division of parameters into those that are drug and system-specific. Based on an understanding that parameters pertaining to drug physico-chemistry (i.e. drug-specific) are fixed and those that pertain to anatomy and physiology (i.e. system-specific) can be altered to reflect the age group of interest (e.g. neonate, infant), *a priori* assessments of drug PK in children can be generated. Within PBPK models, the confidence bestowed upon such estimates are intuitively linked to the quality of input parameters. This entails that system-specific parameters should appropriately quantify the underlying anatomy and

physiology of the subject group being modeled. In comparison to adults, there is relative paucity of investigations quantitatively defining key aspects pediatric physiology that influence drug PK, making the parameterization of pediatric PBPK models difficult. Such knowledge gaps particularly persist towards physiological processes governing oral compound disposition in children. As a result, predictions garnered from pediatric PBPK models simulating oral drug absorption may be of questionable reliability. The collective narrative of this thesis sought to improve the parameterization of mechanistic oral disposition models in children. The dissertation offered quantitative assessments pertaining to the ontogeny of small intestinal transit time (SITT), intestinal solubility, and α-1-acid glycoprotein. The results of these analyses both challenged and affirmed long held assumptions regarding pediatric GI physiology as well as improved the accuracy of estimates of pediatric protein binding (i.e. $f_{u,p}$) - a parameter with implications towards hepatic first-pass. Although, this dissertation served to improve the parameterization of PBPK models tasked with simulating oral drug disposition in children, more research is still required to address additional knowledge gaps associated with pediatric GI physiology. For example, quantitative research devoted to assessing intestinal permeability in children and defining the ontogeny of intestinal transporters is lacking. With future advancements in model development there is the potential for PBPK models to shift from being used as a compliment to clinical PK studies to a partial replacement. For example, PBPK models may be used to decrease the number of clinical trials required in children by functioning as the primary exploratory investigation of drug PK. This could potentially eliminate the need for exploratory PK studies in children and permit clinical investigations to function on a confirmatory basis. The capacity of PBPK modeling to support the pediatric drug development process while reducing the burden imposed on study subjects makes it an invaluable tool for improving medication safety and efficacy in children.

7.4 Future Directions

The research portrayed within this thesis represents an initial attempt to consolidate diverse sets of literature sources to provide specific estimates of pediatric physiology that modulate oral drug disposition. With the eventual goal of developing a comprehensive oral absorption model in children, such research should be continually updated to reflect the current literature. In addition, a quantitative understanding of the ontogeny of GI permeability and expression of intestinal transporters needs to be ascertained prior to the development of such a model.

To ensure pediatric PBPK models are developed based on a current state of knowledge, the analyses contained within this thesis should be continually updated to include prospectively conducted research examining pediatric physiology. This process is most pertinent to analyses where physiological information in developmentally immature age groups were sparsely reported. For example, the analysis of small intestinal transit time as a function of age contained data reflective of 52 subject groups of various ages; however, only 2 of these groups pertained to subjects under the age of 2 years. The analysis was therefore compelled to draw conclusions regarding intestinal transit among younger cohorts of subjects using a limited sample. With the inclusion of prospective data from investigations within neonates and infants, reported findings may be amendable to change. This highlights the need for continued revaluation of such research based on the contemporary literature.

To facilitate the effective parameterization of an *in silico* oral disposition model in children, expansion of the research presented in this thesis to include assessments of the age-dependency of GI permeability and intestinal transporters is required. For intestinal permeability, an analysis would normally require *in vivo* determinations conducted in different developmental age-groups (i.e. neonate, infants, children, and adults) using wide array of compounds that vary in terms physicochemistry. However, owing to the myriad of logistic and ethical issues associated with conducting pediatric research, such studies may be prohibited. As an alternative approach, model-based techniques can be employed to provide estimates human intestinal permeability [390]. This process has been depicted in chapter 6 with regards to small intestinal water volume in adults but can be suitably redesigned to provide estimates of GI physiology in children. With regards to intestinal transporters, ongoing research is still required to define both their localization and expression in an age-dependent manner. Most work to date has focussed on the ontogeny of P-glycoprotein [375, 376]. However, several other transporters that can influence oral drug disposition remain unaccounted for (e.g. OCT, OATP, PEPT1, BCRP). In addition, investigations exploring transporter expression/localization should coincide with either the development of new quantitative assays or the adoption of international assay standards in order to reduce inter-laboratory variability associated with transporter protein quantification. This will permit for the integration of data from different research groups, allowing for comprehensive assessments of transporter ontogeny to be conducted.

With an increased legislative demand for pediatric focussed research, the development of a comprehensive and functional *in silico* model capable of providing accurate predictions of pediatric oral absorption is of great interest. However, in order to achieve this goal, ongoing research tasked with deciphering the unique physiology of pediatrics is still required.

Letters of Copyright Permission

Title: A Workflow Example of PBPK Modeling to Support Pediatric Research and Development: Case Study with Lorazepam

Author: A. R. Maharaj

Publication: The AAPS Journal

Publisher: Springer

Date: Jan 1, 2013

Logged in as:
Anil Maharaj
Account #:
3001067132

LOGOUT

Order Completed

Thank you for your order.

This Agreement between Anil R Maharaj ("You") and Springer ("Springer") consists of your license details and the terms and conditions provided by Springer and Copyright Clearance Center.

Your confirmation email will contain your order number for future reference.

Printable details.

License Number	4015710810649
License date	Dec 25, 2016
Licensed Content Publisher	Springer
Licensed Content Publication	The AAPS Journal
Licensed Content Title	A Workflow Example of PBPK Modeling to Support Pediatric Research and Development: Case Study with Lorazepam
Licensed Content Author	A. R. Maharaj
Licensed Content Date	Jan 1, 2013
Licensed Content Volume	15
Licensed Content Issue	2
Type of Use	Book/Textbook
Requestor type	Agency acting on behalf of other industry
Portion	Full text
Format	Print and Electronic
Will you be translating?	No
Print run	6
Author of this Springer article	Yes and you are the sole author of the new work
Order reference number	
Title of new book	Parameterization of in silico Oral Disposition Models: Focus on Pediatrics
Publisher of new book	University of Waterloo
Author of new book	Anil R Maharaj
Expected publication date of new book	Jan 2017
Estimated size of new book (pages)	218
Requestor Location	Anil R Maharaj 396 Wellington St N (Upper) Kitchener, ON N2H5L2 Canada Attn: Anil R Maharaj
Billing Type	Invoice

December 27, 2016

Anil R. Maharaj
University of Waterloo
10 Victoria St. S.
Kitchener, ON N2F 1C5
Canada

Email: a2mahara@uwaterloo.ca

Dear Anil R. Maharaj:

This is to grant you permission to include the following article in your thesis entitled "Parameterization of in silico Oral Disposition Models: Focus on Pediatrics" for the University of Waterloo:

> Anil R. Maharaj and Andrea N. Edginton, Examining Small Intestinal Transit Time as a Function of Age: Is There Evidence to Support Age-Dependent Differences among Children? *Drug Metab Dispos* 2016, 44(7):1080-1089; DOI: https://doi.org/10.1124/dmd.115.068700

On the first page of each copy of this article, please add the following:

> Reprinted with permission of the American Society for Pharmacology and Experimental Therapeutics. All rights reserved.

In addition, the original copyright line published with the paper must be shown on the copies included with your thesis.

Sincerely yours,

Richard Dodenhoff
Journals Director

9650 Rockville Pike | Bethesda | MD | 20814-3995
P: (301) 634-7060 | F: (301) 634-7061 | E: info@aspet.org | www.aspet.org

Title: Assessment of Age-Related Changes in Pediatric Gastrointestinal Solubility
Author: Anil R. Maharaj
Publication: Pharmaceutical Research
Publisher: Springer
Date: Jan 1, 2015

Order Completed

Thank you for your order.

This Agreement between Anil R Maharaj ("You") and Springer ("Springer") consists of your license details and the terms and conditions provided by Springer and Copyright Clearance Center.

Your confirmation email will contain your order number for future reference.

Printable details.

License Number	4015710679998
License date	Dec 25, 2016
Licensed Content Publisher	Springer
Licensed Content Publication	Pharmaceutical Research
Licensed Content Title	Assessment of Age-Related Changes in Pediatric Gastrointestinal Solubility
Licensed Content Author	Anil R. Maharaj
Licensed Content Date	Jan 1, 2015
Licensed Content Volume	33
Licensed Content Issue	1
Type of Use	Book/Textbook
Requestor type	Agency acting on behalf of other industry
Portion	Full text
Format	Print and Electronic
Will you be translating?	No
Print run	6
Author of this Springer article	Yes and you are the sole author of the new work
Order reference number	
Title of new book	Parameterization of in silico Oral Disposition Models: Focus on Pediatrics
Publisher of new book	University of Waterloo
Author of new book	Anil R Maharaj
Expected publication date of new book	Jan 2017
Estimated size of new book (pages)	218
Requestor Location	Anil R Maharaj 396 Wellington St N (Upper) Kitchener, ON N2H5L2 Canada Attn: Anil R Maharaj

Order Completed

Thank you for your order.

This Agreement between Anil R Maharaj ("You") and Elsevier ("Elsevier") consists of your license details and the terms and conditions provided by Elsevier and Copyright Clearance Center.

Your confirmation email will contain your order number for future reference.

Printable details.

License Number	4015710307093
License date	Dec 24, 2016
Licensed Content Publisher	Elsevier
Licensed Content Publication	European Journal of Pharmaceutical Sciences
Licensed Content Title	Parameterization of small intestinal water volume using PBPK modeling
Licensed Content Author	Anil Maharaj,Nikoletta Fotaki,Andrea Edginton
Licensed Content Date	25 January 2015
Licensed Content Volume	67
Licensed Content Issue	n/a
Licensed Content Pages	10
Type of Use	reuse in a thesis/dissertation
Portion	full article
Format	both print and electronic
Are you the author of this Elsevier article?	Yes
Will you be translating?	No
Order reference number	
Title of your thesis/dissertation	Parameterization of in silico Oral Disposition Models: Focus on Pediatrics
Expected completion date	Jan 2017
Estimated size (number of pages)	218
Elsevier VAT number	GB 494 6272 12
Requestor Location	Anil R Maharaj 396 Wellington St N (Upper) Kitchener, ON N2H5L2 Canada Attn: Anil R Maharaj
Total	0.00 USD

Bibliography

1. General Clinical Pharmacology Considerations for Pediatric Studies for Drugs and Biological Products -Guidance for Industry (Draft Guidance). U.S. Department of Health and Human Services. Food and Drug Administration. Center for Drug Evaluation and Research; 2014.
2. Shirkey H. Therapeutic Orphans. J Pediatr. 1968;72(1):119-20.
3. Caldwell PH, Murphy SB, Butow PN, Craig JC. Clinical Trials in Children. Lancet. 2004;364(9436):803-11.
4. Rieder MJ. Better Drug Therapy for Children: Time for Action. Paediatr Child Health. 2003;8(4):210-2.
5. Sachs AN, Avant D, Lee CS, Rodriguez W, Murphy MD. Pediatric Information in Drug Product Labeling. JAMA. 2012;307(18):1914-5.
6. Kimland E, Odlind V. Off-Label Drug Use in Pediatric Patients. Clin Pharmacol Ther. 2012;91(5):796-801.
7. Pandolfini C, Impicciatore P, Provasi D, Rocchi F, Campi R, Bonati M. Off-Label Use of Drugs in Italy: A Prospective, Observational and Multicentre Study. Acta Paediatr. 2002;91(3):339-47.
8. Horen B, Montastruc JL, Lapeyre-Mestre M. Adverse Drug Reactions and Off-Label Drug Use in Paediatric Outpatients. Br J Clin Pharmacol. 2002;54(6):665-70.
9. Turner S, Nunn AJ, Fielding K, Choonara I. Adverse Drug Reactions to Unlicensed and Off-Label Drugs on Paediatric Wards: A Prospective Study. Acta Paediatr. 1999;88(9):965-8.
10. Health Canada Releases Decision on the Labelling of Cough and Cold Products for Children. Health Canada Advisory. Health Canada. 2008. www.hc-sc.gc.ca/ahc-asc/media/advisories-avis/_2008/2008_184-eng.php. Accessed 8/9/2012 2012.
11. Food and Drug Administration Moderization Act. 105th US Congress. 1997;H.R.1411
12. Regulations Requiring Manufacturers to Assess the Safety and Effectiveness of New Drugs and Biological Products in Pediatric Patients--Fda. Final Rule. Fed Regist. 1998;63(231):66631-72.
13. Best Pharmaceuticals for Children Act. 107th Congress. 2002; H.R.2887
14. Pediatric Research Equity Act. 108th Congress. 2003;H.R.2857.
15. Food and Drug Administration Safety and Innovation Act. 112th Congress. 2012;S.3187
16. Paediatric Investigation Plans: Questions and Answers. European Medicines Agency. 2016. http://www.ema.europa.eu/ema/index.jsp?curl=pages/regulation/q_and_a/q_and_a_detail_000015.jsp. Accessed 11/12/2016.
17. Turner MA, Catapano M, Hirschfeld S, Giaquinto C, Global Research in P. Paediatric Drug Development: The Impact of Evolving Regulations. Adv Drug Deliv Rev. 2014;73:2-13.
18. Jadhav PR, Kern SE. The Need for Modeling and Simulation to Design Clinical Investigations in Children. J Clin Pharmacol. 2010;50(9 Suppl):121S-9S.
19. Stockmann C, Barrett JS, Roberts JK, Sherwin C. Use of Modeling and Simulation in the Design and Conduct of Pediatric Clinical Trials and the Optimization of Individualized Dosing Regimens. CPT Pharmacometrics Syst Pharmacol. 2015;4(11):630-40.
20. Jones H, Rowland-Yeo K. Basic Concepts in Physiologically Based Pharmacokinetic Modeling in Drug Discovery and Development. CPT Pharmacometrics Syst Pharmacol. 2013;2:e63.
21. Edginton AN. Knowledge-Driven Approaches for the Guidance of First-in-Children Dosing. Paediatr Anaesth. 2011;21(3):206-13.
22. Pan Y, Grillo J, Hsu V, Zhang L, Sinha V, Huang S. Application of the Fda Pbpk Knowledgebase in Evaluating Model Predictability for Drug-Drug Interactions. Clin Pharmacol Ther.2014.

23. Leong R, Vieira ML, Zhao P, Mulugeta Y, Lee CS, Huang SM et al. Regulatory Experience with Physiologically Based Pharmacokinetic Modeling for Pediatric Drug Trials. Clin Pharmacol Ther. 2012;91(5):926-31.
24. Lexi-Comp Online, Pediatric & Neonatal Lexi-Drugs Online. Lexi-Comp, Inc., Hudson, Ohio. 2012. Accessed 6/18/2012 2012.
25. Kumar P, Walker JK, Hurt KM, Bennett KM, Grosshans N, Fotis MA. Medication Use in the Neonatal Intensive Care Unit: Current Patterns and Off-Label Use of Parenteral Medications. J Pediatr. 2008;152(3):412-5.
26. Twite MD, Rashid A, Zuk J, Friesen RH. Sedation, Analgesia, and Neuromuscular Blockade in the Pediatric Intensive Care Unit: Survey of Fellowship Training Programs. Pediatr Crit Care Med. 2004;5(6):521-32.
27. List of Drugs for Which Pediatric Studies Are Needed. Fed Regist. 2003;68(13):2789-90.
28. Poulin P, Jones RD, Jones HM, Gibson CR, Rowland M, Chien JY et al. Phrma Cpcdc Initiative on Predictive Models of Human Pharmacokinetics, Part 5: Prediction of Plasma Concentration-Time Profiles in Human by Using the Physiologically-Based Pharmacokinetic Modeling Approach. J Pharm Sci. 2011.
29. Khalil F, Laer S. Physiologically Based Pharmacokinetic Models in the Prediction of Oral Drug Exposure over the Entire Pediatric Age Range-Sotalol as a Model Drug. AAPS J. 2014;16(2):226-39.
30. Villiger A, Stillhart C, Parrott N, Kuentz M. Using Physiologically Based Pharmacokinetic (Pbpk) Modelling to Gain Insights into the Effect of Physiological Factors on Oral Absorption in Paediatric Populations. AAPS J. 2016;18(4):933-47.
31. Zane NR, Thakker DR. A Physiologically Based Pharmacokinetic Model for Voriconazole Disposition Predicts Intestinal First-Pass Metabolism in Children. Clin Pharmacokinet. 2014;53(12):1171-82.
32. Huang W, Lee SL, Yu LX. Mechanistic Approaches to Predicting Oral Drug Absorption. AAPS J. 2009;11(2):217-24.
33. Yu L, Crison JR, Amidon GL. Compartmental Transit and Dispersion Model Analysis of Small Intestinal Transit Flow in Humans. Int J Pharm. 1996;140(1):111-8.
34. El-Kattan AV, M. Oral Absorption, Intestinal Metabolism and Human Oral Bioavailability. In: Paxton J, editor. Topics on Drug Metabolism - InTec; 2012. p. 1-34.
35. Yu LX, Amidon GL. A Compartmental Absorption and Transit Model for Estimating Oral Drug Absorption. Int J Pharm. 1999;186(2):119-25.
36. Huang W, Lee SL, Yu LX. Mechanistic Approaches to Predicting Oral Drug Absorption. AAPS J. 2009;11(2):217-24.
37. Kostewicz ES, Aarons L, Bergstrand M, Bolger MB, Galetin A, Hatley O et al. Pbpk Models for the Prediction of in Vivo Performance of Oral Dosage Forms. Eur J Pharm Sci. 2014;57:300-21.
38. Cristofoletti R, Charoo NA, Dressman JB. Exploratory Investigation of the Limiting Steps of Oral Absorption of Fluconazole and Ketoconazole in Children Using an in Silico Pediatric Absorption Model. J Pharm Sci. 2016;105(9):2794-803.
39. Characterization and Application of Physiologically Based Pharmacokinetic Models in Risk Assessment. World Health Organization. International Programme on Chemical Safety 2010. www.inchem.org/documents/harmproj/harmproj/harmproj9.pdf.
40. Jiang XL, Zhao P, Barrett JS, Lesko LJ, Schmidt S. Application of Physiologically Based Pharmacokinetic Modeling to Predict Acetaminophen Metabolism and Pharmacokinetics in Children. CPT Pharmacometrics Syst Pharmacol. 2013;2:e80.

41. Sun D, Yu LX, Hussain MA, Wall DA, Smith RL, Amidon GL. In Vitro Testing of Drug Absorption for Drug 'Developability' Assessment: Forming an Interface between in Vitro Preclinical Data and Clinical Outcome. Curr Opin Drug Discov Devel. 2004;7(1):75-85.
42. Lin JH, Chiba M, Baillie TA. Is the Role of the Small Intestine in First-Pass Metabolism Overemphasized? Pharmacol Rev. 1999;51(2):135-58.
43. Burton PS, Goodwin JT, Vidmar TJ, Amore BM. Predicting Drug Absorption: How Nature Made It a Difficult Problem. J Pharmacol Exp Ther. 2002;303(3):889-95.
44. Khadra I, Zhou Z, Dunn C, Wilson CG, Halbert G. Statistical Investigation of Simulated Intestinal Fluid Composition on the Equilibrium Solubility of Biopharmaceutics Classification System Class Ii Drugs. Eur J Pharm Sci. 2015;67:65-75.
45. Dressman JB, Reppas C. In Vitro-in Vivo Correlations for Lipophilic, Poorly Water-Soluble Drugs. Eur J Pharm Sci. 2000;11 Suppl 2:S73-80.
46. Shono Y, Jantratid E, Janssen N, Kesisoglou F, Mao Y, Vertzoni M et al. Prediction of Food Effects on the Absorption of Celecoxib Based on Biorelevant Dissolution Testing Coupled with Physiologically Based Pharmacokinetic Modeling. Eur J Pharm Biopharm. 2009;73(1):107-14.
47. Amidon GL, Lennernas H, Shah VP, Crison JR. A Theoretical Basis for a Biopharmaceutic Drug Classification: The Correlation of in Vitro Drug Product Dissolution and in Vivo Bioavailability. Pharm Res. 1995;12(3):413-20.
48. Kesisoglou F, Wu Y. Understanding the Effect of Api Properties on Bioavailability through Absorption Modeling. AAPS J. 2008;10(4):516-25.
49. Ascenzi P, Fanali G, Fasano M, Pallottini V, Trezza V. Clinical Relevance of Drug Binding to Plasma Proteins. J Mol Struct. 2014;1077:4-13.
50. Huang Z, Ung T. Effect of Alpha-1-Acid Glycoprotein Binding on Pharmacokinetics and Pharmacodynamics. Curr Drug Metab. 2013;14(2):226-38.
51. McNamara PJ, Alcorn J. Protein Binding Predictions in Infants. AAPS Pharm Sci. 2002;4(1):E4.
52. Routledge PA. The Plasma Protein Binding of Basic Drugs. Br J Clin Pharmacol. 1986;22(5):499-506.
53. Wilkinson GR, Shand DG. Commentary: A Physiological Approach to Hepatic Drug Clearance. Clin Pharmacol Ther. 1975;18(4):377-90.
54. Rowland M, Tozer NT. Clinical Pharmacokinetics and Pharmacodynamics: Concepts and Applications. 4th ed. Baltimore: Lippincott Williams & Wilkins; 2011.
55. Heikkinen AT, Baneyx G, Caruso A, Parrott N. Application of Pbpk Modeling to Predict Human Intestinal Metabolism of Cyp3a Substrates - an Evaluation and Case Study Using Gastroplus. Eur J Pharm Sci. 2012;47(2):375-86.
56. Kortejarvi H, Urtti A, Yliperttula M. Pharmacokinetic Simulation of Biowaiver Criteria: The Effects of Gastric Emptying, Dissolution, Absorption and Elimination Rates. Eur J Pharm Sci. 2007;30(2):155-66.
57. Paixao P, Gouveia LF, Morais JA. Prediction of the Human Oral Bioavailability by Using in Vitro and in Silico Drug Related Parameters in a Physiologically Based Absorption Model. Int J Pharm. 2012;429(1-2):84-98.
58. Peters SA. Evaluation of a Generic Physiologically Based Pharmacokinetic Model for Lineshape Analysis. Clin Pharmacokinet. 2008;47(4):261-75.
59. Marciani L, Cox EF, Hoad CL, Pritchard S, Totman JJ, Foley S et al. Postprandial Changes in Small Bowel Water Content in Healthy Subjects and Patients with Irritable Bowel Syndrome. Gastroenterology. 2010;138(2):469-77, 77 e1.

60. Marciani L, Wright J, Foley S, Hoad CL, Totman JJ, Bush D et al. Effects of a 5-Ht(3) Antagonist, Ondansetron, on Fasting and Postprandial Small Bowel Water Content Assessed by Magnetic Resonance Imaging. Aliment Pharmacol Ther. 2010;32(5):655-63.
61. Schiller C, Frohlich CP, Giessmann T, Siegmund W, Monnikes H, Hosten N et al. Intestinal Fluid Volumes and Transit of Dosage Forms as Assessed by Magnetic Resonance Imaging. Aliment Pharmacol Ther. 2005;22(10):971-9.
62. Bjorkman S. Prediction of Drug Disposition in Infants and Children by Means of Physiologically Based Pharmacokinetic (Pbpk) Modelling: Theophylline and Midazolam as Model Drugs. Br J Clin Pharmacol. 2005;59(6):691-704.
63. Edginton AN, Schmitt W, Willmann S. Development and Evaluation of a Generic Physiologically Based Pharmacokinetic Model for Children. Clin Pharmacokinet. 2006;45(10):1013-34.
64. Johnson TN, Rostami-Hodjegan A. Resurgence in the Use of Physiologically Based Pharmacokinetic Models in Pediatric Clinical Pharmacology: Parallel Shift in Incorporating the Knowledge of Biological Elements and Increased Applicability to Drug Development and Clinical Practice. Paediatr Anaesth. 2011;21(3):291-301.
65. Barrett JS, Della Casa AO, Laer S, Meibohm B. Physiologically Based Pharmacokinetic (Pbpk) Modeling in Children. Clin Pharmacol Ther. 2012;92(1):40-9.
66. Edginton AN, Ritter L. Predicting Plasma Concentrations of Bisphenol a in Children Younger Than 2 Years of Age after Typical Feeding Schedules, Using a Physiologically Based Toxicokinetic Model. Environ Health Perspect. 2009;117(4):645-52.
67. Chin PK, Jensen BP, Larsen HS, Begg EJ. Adult Age and Ex Vivo Protein Binding of Lorazepam, Oxazepam and Temazepam in Healthy Subjects. Br J ClinPharmacol. 2011;72(6):985-9.
68. Crom WR, Relling MV, Christensen ML, Rivera GK, Evans WE. Age-Related Differences in Hepatic Drug Clearance in Children: Studies with Lorazepam and Antipyrine. Clin Pharmacol Ther. 1991;50(2):132-40.
69. Divoll M, Greenblatt DJ. Effect of Age and Sex on Lorazepam Protein Binding. J Pharm Pharmacol. 1982;34(2):122-3.
70. Greenblatt DJ, Schillings RT, Kyriakopoulos AA, Shader RI, Sisenwine SF, Knowles JA et al. Clinical Pharmacokinetics of Lorazepam. I. Absorption and Disposition of Oral 14c-Lorazepam. Clin Pharmacol Ther. 1976;20(3):329-41.
71. Greenblatt DJ, Shader RI, Franke K, MacLaughlin DS, Harmatz JS, Allen MD et al. Pharmacokinetics and Bioavailability of Intravenous, Intramuscular, and Oral Lorazepam in Humans. J Pharm Sci. 1979;68(1):57-63.
72. Verbeeck R, Tjandramaga TB, Verberckmoes R, De Schepper PJ. Biotransformation and Excretion of Lorazepam in Patients with Chronic Renal Failure. Br J ClinPharmacol. 1976;3(6):1033-9.
73. Pyka A, Babuska M, Zachariasz M. A Comparison of Theoretical Methods of Calculation of Partition Coefficients for Selected Drugs. Acta Pol Pharm. 2006;63(3):159-67.
74. Popovic GV, Sladic DM, Stefanovic VM, Pfendt LB. Study on Protolytic Equilibria of Lorazepam and Oxazepam by Uv and Nmr Spectroscopy. J Pharm Biomed Anal. 2003;31(4):693-9.
75. Greenblatt DJ, Comer WH, Elliott HW, Shader RI, Knowles JA, Ruelius HW. Clinical Pharmacokinetics of Lorazepam. Iii. Intravenous Injection. Preliminary Results. J Clin Pharmacol. 1977;17(8-9):490-4.
76. Greenblatt DJ, Divoll M, Harmatz JS, Shader RI. Pharmacokinetic Comparison of Sublingual Lorazepam with Intravenous, Intramuscular, and Oral Lorazepam. J Pharm Sci. 1982;71(2):248-52.

77. Wermeling DP, Miller JL, Archer SM, Manaligod JM, Rudy AC. Bioavailability and Pharmacokinetics of Lorazepam after Intranasal, Intravenous, and Intramuscular Administration. J Clin Pharmacol. 2001;41(11):1225-31.
78. Boxenbaum H. Comparative Pharmacokinetics of Benzodiazepines in Dog and Man. J Pharmacokinet Biopharm. 1982;10(4):411-26.
79. Willmann S, Hohn K, Edginton A, Sevestre M, Solodenko J, Weiss W et al. Development of a Physiology-Based Whole-Body Population Model for Assessing the Influence of Individual Variability on the Pharmacokinetics of Drugs. J Pharmacokinet Pharmacodyn. 2007;34(3):401-31.
80. Rodgers T, Leahy D, Rowland M. Physiologically Based Pharmacokinetic Modeling 1: Predicting the Tissue Distribution of Moderate-to-Strong Bases. J Pharm Sci. 2005;94(6):1259-76.
81. Rodgers T, Leahy D, Rowland M. Tissue Distribution of Basic Drugs: Accounting for Enantiomeric, Compound and Regional Differences Amongst Beta-Blocking Drugs in Rat. J Pharm Sci. 2005;94(6):1237-48.
82. Rodgers T, Rowland M. Physiologically Based Pharmacokinetic Modelling 2: Predicting the Tissue Distribution of Acids, Very Weak Bases, Neutrals and Zwitterions. J Pharm Sci. 2006;95(6):1238-57.
83. Edginton AN, Schmitt W, Voith B, Willmann S. A Mechanistic Approach for the Scaling of Clearance in Children. Clin Pharmacokinet. 2006;45(7):683-704.
84. Sim SM, Back DJ, Breckenridge AM. The Effect of Various Drugs on the Glucuronidation of Zidovudine (Azidothymidine; Azt) by Human Liver Microsomes. Br J ClinPharmacol. 1991;32(1):17-21.
85. Alcorn J, McNamara PJ. Ontogeny of Hepatic and Renal Systemic Clearance Pathways in Infants: Part Ii. Clin Pharmacokinet. 2002;41(13):1077-94.
86. Irwin JJ, Kirchner JT. Anemia in Children. Am Fam Physician. 2001;64(8):1379-87.
87. Hayton WL. Maturation and Growth of Renal Function: Dosing Renally Cleared Drugs in Children. AAPS Pharm Sci. 2000;2(1):E3.
88. Chamberlain JM, Capparelli EV, Brown KM, Vance CW, Lillis K, Mahajan P et al. Pharmacokinetics of Intravenous Lorazepam in Pediatric Patients with and without Status Epilepticus. J Pediatr. 2011.
89. Zhao P. Regulatory Experience in Physiologically-Based Pharmacokinetic (Pbpk) Models in Pediatric Submissions. Food and Drug Administration Advisory Committee for Pharmaceutical Science and Clinical Pharmacology; 3/14/2012.; National Harbor, MD.2012.
90. Chiou WL. Potential Pitfalls in the Conventional Pharmacokinetic Studies: Effects of the Initial Mixing of Drug in Blood and the Pulmonary First-Pass Elimination. J Pharmacokinet Biopharm. 1979;7(5):527-36.
91. Wilson JP. Surface Area of the Small Intestine in Man. Gut. 1967;8(6):618-21.
92. Johnson KC, Swindell AC. Guidance in the Setting of Drug Particle Size Specifications to Minimize Variability in Absorption. Pharm Res. 1996;13(12):1795-8.
93. Levy G, MacGillivray MH, Procknal JA. Riboflavin Absorption in Children with Thyroid Disorders. Pediatrics. 1972;50(6):896-900.
94. Christensen FN, Davis SS, Hardy JG, Taylor MJ, Whalley DR, Wilson CG. The Use of Gamma Scintigraphy to Follow the Gastrointestinal Transit of Pharmaceutical Formulations. J Pharm Pharmacol. 1985;37(2):91-5.
95. Maqbool S, Parkman HP, Friedenberg FK. Wireless Capsule Motility: Comparison of the Smartpill Gi Monitoring System with Scintigraphy for Measuring Whole Gut Transit. Dig Dis Sci. 2009;54(10):2167-74.

96. Miller MA, Parkman HP, Urbain JL, Brown KL, Donahue DJ, Knight LC et al. Comparison of Scintigraphy and Lactulose Breath Hydrogen Test for Assessment of Orocecal Transit: Lactulose Accelerates Small Bowel Transit. Dig Dis Sci. 1997;42(1):10-8.
97. Bartelink IH, Rademaker CM, Schobben AF, van den Anker JN. Guidelines on Paediatric Dosing on the Basis of Developmental Physiology and Pharmacokinetic Considerations. Clin Pharmacokinet. 2006;45(11):1077-97.
98. Strolin Benedetti M, Baltes EL. Drug Metabolism and Disposition in Children. Fundam Clin Pharmacol. 2003;17(3):281-99.
99. Isles AF, Newth CJ. Pharmacokinetics of a Sustained-Release Theophylline Preparation in Infants and Preschool Children with Asthma. J Allergy Clin Immunol. 1985;75(3):377-81.
100. Rogers RJ, Kalisker A, Wiener MB, Szefler SJ. Inconsistent Absorption from a Sustained-Release Theophylline Preparation During Continuous Therapy in Asthmatic Children. J Pediatr. 1985;106(3):496-501.
101. Weinberger M, Hendeles L, Wong L. Relationship of Formulation and Dosing Interval to Fluctuation of Serum Theophylline Concentration in Children with Chronic Asthma. J Pediatr. 1981;99(1):145-52.
102. Grygiel JJ, Ward H, Ogborne M, Goldin A, Birkett DJ. Relationships between Plasma Theophylline Clearance, Liver Volume and Body Weight in Children and Adults. Eur J Clin Pharmacol. 1983;24(4):529-32.
103. Szefler SJ. Erratic Absorption of Theophylline from Slow-Release Products in Children. J Allergy Clin Immunol. 1986;78(4 Pt 2):710-5.
104. Jamei M, Turner D, Yang J, Neuhoff S, Polak S, Rostami-Hodjegan A et al. Population-Based Mechanistic Prediction of Oral Drug Absorption. AAPS J. 2009;11(2):225-37.
105. McConnell EL, Fadda HM, Basit AW. Gut Instincts: Explorations in Intestinal Physiology and Drug Delivery. Int J Pharm. 2008;364(2):213-26.
106. Yuen KH. The Transit of Dosage Forms through the Small Intestine. Int J Pharm. 2010;395(1-2):9-16.
107. Edginton AN, Fotaki N. Oral Drug Absorption in Pediatric Populations. In: Dressman.J.B., Reppas.C., editors. Oral Drug Absorption: Prediction and Assessment. New York, NY: Informa Healthcare USA, Inc.; 2010. p. 108-26.
108. Fallingborg J, Christensen LA, Ingeman-Nielsen M, Jacobsen BA, Abildgaard K, Rasmussen HH. Ph-Profile and Regional Transit Times of the Normal Gut Measured by a Radiotelemetry Device. Aliment Pharmacol Ther. 1989;3(6):605-13.
109. Fallingborg J, Christensen LA, Ingeman-Nielsen M, Jacobsen BA, Abildgaard K, Rasmussen HH et al. Measurement of Gastrointestinal Ph and Regional Transit Times in Normal Children. J Pediatr Gastroenterol Nutr. 1990;11(2):211-4.
110. Borenstein M, Hedges LV, Higgins JPT, Rothstein HR. Meta-Regression. Introduction to Meta-Analysis. John Wiley & Sons, Ltd; 2009.
111. Thompson SG, Sharp SJ. Explaining Heterogeneity in Meta-Analysis: A Comparison of Methods. Stat Med. 1999;18(20):2693-708.
112. Hozo SP, Djulbegovic B, Hozo I. Estimating the Mean and Variance from the Median, Range, and the Size of a Sample. BMC Med Res Methodol. 2005;5:13.
113. Wan X, Wang W, Liu J, Tong T. Estimating the Sample Mean and Standard Deviation from the Sample Size, Median, Range and/or Interquartile Range. BMC Med Res Methodol. 2014;14:135.
114. Brun M, Michalek W, Surjanhata B, Kuo B. Small Bowel Transit Time (Sbtt) by Wireless Motility Capsule (Wmc): Normal Values and Analysis of Pressure Profiles in Different Subgroups of Patients with Slow Sbtt. Gastroenterology. 2011;140(5):S-865.

115. Ishibashi T, Pitcairn GR, Yoshino H, Mizobe M, Wilding IR. Scintigraphic Evaluation of a New Capsule-Type Colon Specific Drug Delivery System in Healthy Volunteers. J Pharm Sci. 1998;87(5):531-5.
116. Bradley RA, Srivastava SS. Correlation in Polynomial Regression. Am Stat. 1979;33(1):11-4.
117. Viechtbauer W. Conducting Meta-Analyses in R with the Metafor Package. J Stat Softw. 2010;36(3):1-48.
118. Pedersen S, Steffensen G. Absorption Characteristics of Once-a-Day Slow-Release Theophylline Preparation in Children with Asthma. J Pediatr. 1987;110(6):953-9.
119. Buss D, Leopold D, Smith AP, Routledge PA. Determinants of the Plasma Protein Binding of Theophylline in Health. Br J Clin Pharmacol. 1983;15(4):399-405.
120. Leopold D, Webb D, Buss DC, Fifield RA, Smith AP, Routledge PA. The Ex Vivo Plasma Protein Binding of Theophylline in Renal Disease. Br J Clin Pharmacol. 1985;19(6):823-5.
121. Parrott N, Lukacova V, Fraczkiewicz G, Bolger MB. Predicting Pharmacokinetics of Drugs Using Physiologically Based Modeling--Application to Food Effects. AAPS J. 2009;11(1):45-53.
122. Lennernas H. Human in Vivo Regional Intestinal Permeability: Importance for Pharmaceutical Drug Development. Mol Pharm. 2014;11(1):12-23.
123. Ginsberg G, Hattis D, Russ A, Sonawane B. Physiologically Based Pharmacokinetic (Pbpk) Modeling of Caffeine and Theophylline in Neonates and Adults: Implications for Assessing Children's Risks from Environmental Agents. J Toxicol Environ Health A. 2004;67(4):297-329.
124. Aslaksen A, Bakke OM, Vigander T. Comparative Pharmacokinetics of Theophylline and Aminophylline in Man. Br J Clin Pharmacol. 1981;11(3):269-73.
125. Horai Y, Ishizaki T, Sasaki T, Chiba K, Suganuma T, Echizen H et al. Bioavailability and Pharmacokinetics of Theophylline in Plain Uncoated and Sustained-Release Dosage Forms in Relation to Smoking Habit. I. Single Dose Study. Eur J Clin Pharmacol. 1983;24(1):79-87.
126. Rovei V, Chanoine F, Strolin Benedetti M. Pharmacokinetics of Theophylline: A Dose-Range Study. Br J Clin Pharmacol. 1982;14(6):769-78.
127. Maharaj AR, Edginton AN. Physiologically Based Pharmacokinetic Modeling and Simulation in Pediatric Drug Development. CPT Pharmacometrics Syst Pharmacol. 2014;3:e150.
128. Bertram F, Andresen V, Layer P, Keller J. Simultaneous Non-Invasive Measurement of Liquid Gastric Emptying and Small Bowel Transit by Combined 13c-Acetate and H2-Lactulose Breath Test. J Breath Res. 2014;8(4):046007.
129. Dalzell AM, Freestone NS, Billington D, Heaf DP. Small Intestinal Permeability and Orocaecal Transit Time in Cystic Fibrosis. Arch Dis Child. 1990;65(6):585-8.
130. Escobar H, Perdomo M, Vasconez F, Camarero C, del Olmo MT, Suarez L. Intestinal Permeability to 51cr-Edta and Orocecal Transit Time in Cystic Fibrosis. J Pediatr Gastroenterol Nutr. 1992;14(2):204-7.
131. Gotze H, Ptok A. Orocaecal Transit Time in Patients with Crohn Disease. Eur J Pediatr. 1993;152(3):193-6.
132. Lewindon PJ, Robb TA, Moore DJ, Davidson GP, Martin AJ. Bowel Dysfunction in Cystic Fibrosis: Importance of Breath Testing. J Paediatr Child Health. 1998;34(1):79-82.
133. Murphy MS, Nelson R, Eastham EJ. Measurement of Small Intestinal Transit Time in Children. Acta Paediatr Scand. 1988;77(6):802-6.
134. Soares AC, Lederman HM, Fagundes-Neto U, de Morais MB. Breath Hydrogen Test after a Bean Meal Demonstrates Delayed Oro-Cecal Transit Time in Children with Chronic Constipation. J Pediatr Gastroenterol Nutr. 2005;41(2):221-4.

135. Vajro P, Silano G, Longo D, Staiano A, Fontanella A. Orocoecal Transit Time in Healthy and Constipated Children. Acta Paediatr Scand. 1988;77(4):583-6.
136. Vreugdenhil G, Sinaasappel M, Bouquet J. A Comparative Study of the Mouth to Caecum Transit Time in Children and Adults Using a Weight Adapted Lactulose Dose. Acta Paediatr Scand. 1986;75(3):483-8.
137. Khin M, Bolin TD, Tin O, Thein Win N, Kyaw-Hla S, Thein Thein M. Investigation of Small-Intestinal Transit Time in Normal and Malnourished Children. J Gastroenterol. 1999;34(6):675-9.
138. Billa N, Yuen KH, Khader MA, Omar A. Gamma-Scintigraphic Study of the Gastrointestinal Transit and in Vivo Dissolution of a Controlled Release Diclofenac Sodium Formulation in Xanthan Gum Matrices. Int J Pharm. 2000;201(1):109-20.
139. Bode S, Dreyer M, Greisen G. Gastric Emptying and Small Intestinal Transit Time in Preterm Infants: A Scintigraphic Method. J Pediatr Gastroenterol Nutr. 2004;39(4):378-82.
140. Bouras EP, Burton DD, Camilleri M, Stephens DA, Thomforde GM. Effect of Cyclooxygenase-2 Inhibitors on Gastric Emptying and Small Intestinal Transit in Humans. Neurogastroenterol Motil. 2004;16(6):729-35.
141. Clarke GM, Newton JM, Short MD. Gastrointestinal Transit of Pellets of Differing Size and Density. Int J Pharm. 1993;100(1–3):81-92.
142. Coupe AJ, Davis SS, Wilding IR. Variation in Gastrointestinal Transit of Pharmaceutical Dosage Forms in Healthy Subjects. Pharm Res. 1991;8(3):360-4.
143. Davis SS, Hardy JG, Taylor MJ, Whalley DR, Wilson CG. The Effect of Food on the Gastrointestinal Transit of Pellets and an Osmotic Device (Osmet). Int J Pharm. 1984;21(3):331-40.
144. Davis S, Hardy J, Wilson C, Feely L, Palin K. Gastrointestinal Transit of a Controlled Release Naproxen Tablet Formulation. Int J Pharm. 1986;32(1):85-90.
145. Davis S, Khosia R, Wilson C. Gastrointestinal Transit of a Controlled-Release Pellet Formulation of Tiaprofenic Acid and the Effect of Food. Int J Pharm. 1987;35(3):253-8.
146. Davis SS, Hardy JG, Fara JW. Transit of Pharmaceutical Dosage Forms through the Small Intestine. Gut. 1986;27(8):886-92.
147. Davis SS, Norring-Christensen F, Khosla R, Feely LC. Gastric Emptying of Large Single Unit Dosage Forms. J Pharm Pharmacol. 1988;40(3):205-7.
148. Davis SS, Hardy JG, Taylor MJ, Whalley DR, Wilson CG. A Comparative Study of the Gastrointestinal Transit of a Pellet and Tablet Formulation. Int J Pharm. 1984;21(2):167-77.
149. Deane AM, Summers MJ, Zaknic AV, Chapman MJ, Di Bartolomeo AE, Bellon M et al. Glucose Absorption and Small Intestinal Transit in Critical Illness. Crit Care Med. 2011;39(6):1282-8.
150. Fadda HM, McConnell EL, Short MD, Basit AW. Meal-Induced Acceleration of Tablet Transit through the Human Small Intestine. Pharm Res. 2009;26(2):356-60.
151. Geypens B, Bennink R, Peeters M, Evenepoel P, Mortelmans L, Maes B et al. Validation of the Lactose-[13c]Ureide Breath Test for Determination of Orocecal Transit Time by Scintigraphy. J Nucl Med. 1999;40(9):1451-5.
152. Khosla R, Feely L, Davis S. Gastrointestinal Transit of Non-Disintegrating Tablets in Fed Subjects. Int J Pharm. 1989;53(2):107-17.
153. Madsen JL. Effects of Gender, Age, and Body Mass Index on Gastrointestinal Transit Times. Dig Dis Sci. 1992;37(10):1548-53.
154. Madsen JL, Jensen M. Gastrointestinal Transit of Technetium-99m-Labeled Cellulose Fiber and Indium-111-Labeled Plastic Particles. J Nucl Med. 1989;30(3):402-6.

155. Wilding IR, Davis SS, Bakhshaee M, Stevens HN, Sparrow RA, Brennan J. Gastrointestinal Transit and Systemic Absorption of Captopril from a Pulsed-Release Formulation. Pharm Res. 1992;9(5):654-7.
156. Zarate N, Mohammed SD, O'Shaughnessy E, Newell M, Yazaki E, Williams NS et al. Accurate Localization of a Fall in Ph within the Ileocecal Region: Validation Using a Dual-Scintigraphic Technique. Am J Physiol Gastrointest Liver Physiol. 2010;299(6):G1276-86.
157. Evans DF, Pye G, Bramley R, Clark AG, Dyson TJ, Hardcastle JD. Measurement of Gastrointestinal Ph Profiles in Normal Ambulant Human Subjects. Gut. 1988;29(8):1035-41.
158. Gelfond D, Ma C, Semler J, Borowitz D. Intestinal Ph and Gastrointestinal Transit Profiles in Cystic Fibrosis Patients Measured by Wireless Motility Capsule. Dig Dis Sci. 2013;58(8):2275-81.
159. Hedsund C, Joensson IM, Gregersen T, Fynne L, Schlageter V, Krogh K. Magnet Tracking Allows Assessment of Regional Gastrointestinal Transit Times in Children. Clin Exp Gastroenterol. 2013;6:201-8.
160. Michalek W, Semler JR, Kuo B. Impact of Acid Suppression on Upper Gastrointestinal Ph and Motility. Dig Dis Sci. 2011;56(6):1735-42.
161. Sarosiek I, Selover KH, Katz LA, Semler JR, Wilding GE, Lackner JM et al. The Assessment of Regional Gut Transit Times in Healthy Controls and Patients with Gastroparesis Using Wireless Motility Technology. Aliment Pharmacol Ther. 2010;31(2):313-22.
162. Van Den Driessche M, Van Malderen N, Geypens B, Ghoos Y, Veereman-Wauters G. Lactose-[13c]Ureide Breath Test: A New, Noninvasive Technique to Determine Orocecal Transit Time in Children. J Pediatr Gastroenterol Nutr. 2000;31(4):433-8.
163. Higgins JP, Thompson SG. Controlling the Risk of Spurious Findings from Meta-Regression. Stat Med. 2004;23(11):1663-82.
164. Iddan G, Meron G, Glukhovsky A, Swain P. Wireless Capsule Endoscopy. Nature. 2000;405(6785):417.
165. Fireman Z, Kopelman Y, Friedman S, Ephrath H, Choman E, Debby H et al. Age and Indication for Referral to Capsule Endoscopy Significantly Affect Small Bowel Transit Times: The Given Database. Dig Dis Sci. 2007;52(10):2884-7.
166. Fireman Z, Paz D, Kopelman Y. Capsule Endoscopy: Improving Transit Time and Image View. World J Gastroenterol. 2005;11(37):5863-6.
167. Ge ZZ, Chen HY, Gao YJ, Gu JL, Hu YB, Xiao SD. Clinical Application of Wireless Capsule Endoscopy in Pediatric Patients for Suspected Small Bowel Diseases. Eur J Pediatr. 2007;166(8):825-9.
168. Nuutinen H, Kolho KL, Salminen P, Rintala R, Koskenpato J, Koivusalo A et al. Capsule Endoscopy in Pediatric Patients: Technique and Results in Our First 100 Consecutive Children. Scand J Gastroenterol. 2011;46(9):1138-43.
169. Oikawa-Kawamoto M, Sogo T, Yamaguchi T, Tsunoda T, Kondo T, Komatsu H et al. Safety and Utility of Capsule Endoscopy for Infants and Young Children. World J Gastroenterol. 2013;19(45):8342-8.
170. Ou G, Svarta S, Chan C, Galorport C, Qian H, Enns R. The Effect of Chewing Gum on Small-Bowel Transit Time in Capsule Endoscopy: A Prospective, Randomized Trial. Gastrointest Endosc. 2014;79(4):630-6.
171. Robinson CA, Jackson C, Condon D, Gerson LB. Impact of Inpatient Status and Gender on Small-Bowel Capsule Endoscopy Findings. Gastrointest Endosc. 2011;74(5):1061-6.
172. Tokuhara D, Watanabe K, Okano Y, Tada A, Yamato K, Mochizuki T et al. Wireless Capsule Endoscopy in Pediatric Patients: The First Series from Japan. J Gastroenterol. 2010;45(7):683-91.

173. Velayos Jimenez B, Fernandez Salazar L, Aller de la Fuente R, de la Calle Valverde F, Del Olmo Martinez L, Arranz Santos T et al. [Study of Gastronitestinal Transit Times with Capsule Endoscopy]. Gastroenterol Hepatol. 2005;28(6):315-20.
174. Westerhof J, Koornstra JJ, Hoedemaker RA, Sluiter WJ, Kleibeuker JH, Weersma RK. Diagnostic Yield of Small Bowel Capsule Endoscopy Depends on the Small Bowel Transit Time. World J Gastroenterol. 2012;18(13):1502-7.
175. Yazici C, Losurdo J, Brown MD, Oosterveen S, Rahimi R, Keshavarzian A et al. Inpatient Capsule Endoscopy Leads to Frequent Incomplete Small Bowel Examinations. World J Gastroenterol. 2012;18(36):5051-7.
176. Sommers DK, van Wyk M, Meyer EC, Snyman JR, Moncrieff J. The Absorption Characteristics of Six Sustained-Release Theophylline Preparations. S Afr Med J. 1992;81(1):20-2.
177. Staib AH, Loew D, Harder S, Graul EH, Pfab R. Measurement of Theophylline Absorption from Different Regions of the Gastro-Intestinal Tract Using a Remote Controlled Drug Delivery Device. Eur J Clin Pharmacol. 1986;30(6):691-7.
178. Bowles A, Keane J, Ernest T, Clapham D, Tuleu C. Specific Aspects of Gastro-Intestinal Transit in Children for Drug Delivery Design. Int J Pharm. 2010;395(1-2):37-43.
179. Bonner JJ, Vajjah P, Abduljalil K, Jamei M, Rostami-Hodjegan A, Tucker GT et al. Does Age Affect Gastric Emptying Time? A Model-Based Meta-Analysis of Data from Premature Neonates through to Adults. Biopharm Drug Dispos. 2015;36(4):245-57.
180. Thompson SG, Higgins JP. How Should Meta-Regression Analyses Be Undertaken and Interpreted? Stat Med. 2002;21(11):1559-73.
181. Galia E, Nicolaides E, Horter D, Lobenberg R, Reppas C, Dressman JB. Evaluation of Various Dissolution Media for Predicting in Vivo Performance of Class I and Ii Drugs. Pharm Res. 1998;15(5):698-705.
182. Jantratid E, Janssen N, Reppas C, Dressman JB. Dissolution Media Simulating Conditions in the Proximal Human Gastrointestinal Tract: An Update. Pharm Res. 2008;25(7):1663-76.
183. Vertzoni M, Dressman J, Butler J, Hempenstall J, Reppas C. Simulation of Fasting Gastric Conditions and Its Importance for the in Vivo Dissolution of Lipophilic Compounds. Eur J Pharm Biopharm. 2005;60(3):413-7.
184. Kaye JL. Review of Paediatric Gastrointestinal Physiology Data Relevant to Oral Drug Delivery. Int J Clin Pharm. 2011;33(1):20-4.
185. Mooij MG, de Koning BA, Huijsman ML, de Wildt SN. Ontogeny of Oral Drug Absorption Processes in Children. Expert Opin Drug Metab Toxicol. 2012;8(10):1293-303.
186. Abdel-Rahman SM, Amidon GL, Kaul A, Lukacova V, Vinks AA, Knipp GT. Summary of the National Institute of Child Health and Human Development-Best Pharmaceuticals for Children Act Pediatric Formulation Initiatives Workshop-Pediatric Biopharmaceutics Classification System Working Group. Clin Ther. 2012;34(11):S11-S24.
187. Hentges DJ, Marsh WW, Petschow BW, Thai WR, Carter MK. Influence of Infant Diets on the Ecology of the Intestinal Tract of Human Flora-Associated Mice. J Pediatr Gastroenterol Nutr. 1992;14(2):146-52.
188. Van Slyke DD. On the Measurement of Buffer Values on the Relationship of Buffer Values to the Dissociation Constant of the Buffer and the Concentration and Reaction of the Buffer Solution. J Biol Chem. 1922;52:525-70.
189. Law V, Knox C, Djoumbou Y, Jewison T, Guo AC, Liu Y et al. Drugbank 4.0: Shedding New Light on Drug Metabolism. Nucleic Acids Res. 2014;42(Database issue):D1091-7.
190. Granero GE, Ramachandran C, Amidon GL. Dissolution and Solubility Behavior of Fenofibrate in Sodium Lauryl Sulfate Solutions. Drug Dev Ind Pharm. 2005;31(9):917-22.

191. Vogt M, Kunath K, Dressman JB. Dissolution Enhancement of Fenofibrate by Micronization, Cogrinding and Spray-Drying: Comparison with Commercial Preparations. Eur J Pharm Biopharm. 2008;68(2):283-8.
192. Juenemann D, Bohets H, Ozdemir M, de Maesschalck R, Vanhoutte K, Peeters K et al. Online Monitoring of Dissolution Tests Using Dedicated Potentiometric Sensors in Biorelevant Media. Eur J Pharm Biopharm. 2011;78(1):158-65.
193. Vertzoni MV, Reppas C, Archontaki HA. Sensitive and Simple Liquid Chromatographic Method with Ultraviolet Detection for the Determination of Nifedipine in Canine Plasma. Anal Chim Acta. 2006;573-574:298-304.
194. Parkin JE, Boddy MR. Development of a Chromatographic Method of Analysis for Glucosyl-Amines Formed from Dapsone. J Liq Chromatogr Relat Technol. 1998;21(14):2131-42.
195. Jain N, Raghuwanshi R, Jain D. Development and Validation of Rp-Hplc Method for Simultaneous Estimation of Atorvastatin Calcium and Fenofibrate in Tablet Dosage Forms. Indian J Pharm Sci. 2008;70(2):263-5.
196. Trotta M, Gallarate M, Carlotti ME, Morel S. Preparation of Griseofulvin Nanoparticles from Water-Dilutable Microemulsions. Int J Pharm. 2003;254(2):235-42.
197. Al Za'abi MA, Dehghanzadeh GH, Norris RL, Charles BG. A Rapid and Sensitive Microscale Hplc Method for the Determination of Indomethacin in Plasma of Premature Neonates with Patent Ductus Arteriousus. J Chromatogr B Analyt Technol Biomed Life Sci. 2006;830(2):364-7.
198. Sanches C, Lopez KV, Omosako CE, Bertoline MA, Pereira MD, Santos S. Micromethod for Quantification of Carbamazepine, Phenobartital and Phenytoin in Human Plasma by Hplc-Uv Detection for Therapeutic Drug Monitoring Application. Lat Am J Pharm. 2008;27(4):485-91.
199. Jain D, Laxman R, Acharya A, Jain V, Bhardwaj S. Development and Validation of Rp-Hplc and Ultraviolet Spectrophotometric Methods for Simultaneous Determination of Sprinolactone and Torsemide in Pharmaceutical Dosage Form. Int J Res Ayurveda Pharm. 2010;1(2):459-67.
200. Guidance for Industry: Bioavailability and Bioequivalence Studies for Orally Administered Drug Products — General Considerations. U.S. Department of Health and Human Services. Food and Drug Administration. Center for Drug Evaluation and Research.; 2003.
201. Mithani SD, Bakatselou V, TenHoor CN, Dressman JB. Estimation of the Increase in Solubility of Drugs as a Function of Bile Salt Concentration. Pharm Res. 1996;13(1):163-7.
202. James LP, Marotti T, Stowe CD, Farrar HC, Taylor BJ, Kearns GL. Pharmacokinetics and Pharmacodynamics of Famotidine in Infants. J Clin Pharmacol. 1998;38(12):1089-95.
203. James LP, Marshall JD, Heulitt MJ, Wells TG, Letzig L, Kearns GL. Pharmacokinetics and Pharmacodynamics of Famotidine in Children. J Clin Pharmacol. 1996;36(1):48-54.
204. Krafte-Jacobs B, Persinger M, Carver J, Moore L, Brilli R. Rapid Placement of Transpyloric Feeding Tubes: A Comparison of Ph-Assisted and Standard Insertion Techniques in Children. Pediatrics. 1996;98(2 Pt 1):242-8.
205. Gharpure V, Meert KL, Sarnaik AP, Metheny NA. Indicators of Postpyloric Feeding Tube Placement in Children. Crit Care Med. 2000;28(8):2962-6.
206. Westhus N. Methods to Test Feeding Tube Placement in Children. MCN Am J Matern Child Nurs. 2004;29(5):282-7; quiz 90-1.
207. Metheny NA, Stewart BJ, Smith L, Yan H, Diebold M, Clouse RE. Ph and Concentrations of Pepsin and Trypsin in Feeding Tube Aspirates as Predictors of Tube Placement. JPEN J Parenter Enteral Nutr. 1997;21(5):279-85.

208. Arvedson JC. Swallowing and Feeding in Infants and Young Children. Goyal and Shaker's Gi Motility Online. New York Nature Publishing Group; 2006.
209. Agunod M, Yamaguchi N, Lopez R, Luhby AL, Glass GB. Correlative Study of Hydrochloric Acid, Pepsin, and Intrinsic Factor Secretion in Newborns and Infants. Am J Dig Dis. 1969;14(6):400-14.
210. Di Maio S, Carrier RL. Gastrointestinal Contents in Fasted State and Post-Lipid Ingestion: In Vivo Measurements and in Vitro Models for Studying Oral Drug Delivery. J Control Release. 2011;151(2):110-22.
211. Armand M, Hamosh M, Mehta NR, Angelus PA, Philpott JR, Henderson TR et al. Effect of Human Milk or Formula on Gastric Function and Fat Digestion in the Premature Infant. Pediatr Res. 1996;40(3):429-37.
212. Armand M, Hamosh M, DiPalma JS, Gallagher J, Benjamin SB, Philpott JR et al. Dietary Fat Modulates Gastric Lipase Activity in Healthy Humans. Am J Clin Nutr. 1995;62(1):74-80.
213. Avery GB, Randolph JG, Weaver T. Gastric Acidity in the First Day of Life. Pediatrics. 1966;37(6):1005-7.
214. Cote CJ, Goudsouzian NG, Liu LM, Dedrick DF, Szyfelbein SK. Assessment of Risk Factors Related to the Acid Aspiration Syndrome in Pediatric Patients-Gastric Ph and Residual Volume. Anesthesiology. 1982;56(1):70-2.
215. Datta S, Houle GL, Fox GS. Concentration of Lidocaine Hydrochloride in Newborn Gastric Fluid after Elective Caesarean Section and Vaginal Delivery with Epidural Analgesia. Can Anaesth Soc J. 1975;22(1):79-83.
216. Ebers DW, Gibbs GE, Smith DI. Gastric Acidity on the First Day of Life. Pediatrics. 1956;18(5):800-2.
217. Euler AR, Byrne WJ, Meis PJ, Leake RD, Ament ME. Basal and Pentagastrin-Stimulated Acid Secretion in Newborn Human Infants. Pediatr Res. 1979;13(1):36-7.
218. Goresky GV, Finley GA, Bissonnette B, Shaffer EA. Efficacy, Duration, and Absorption of a Paediatric Oral Liquid Preparation of Ranitidine Hydrochloride. Can J Anaesth. 1992;39(8):791-8.
219. Griswold CC, Shohl AT. Gastric Digestion in New-Born Infants. Am J Dis Child. 1925;30(4):541-9.
220. Jahr JS, Burckart G, Smith SS, Shapiro J, Cook DR. Effects of Famotidine on Gastric Ph and Residual Volume in Pediatric Surgery. Acta Anaesthesiol Scand. 1991;35(5):457-60.
221. Maekawa N, Mikawa K, Yaku H, Nishina K, Obara H. Effects of 2-, 4- and 12-Hour Fasting Intervals on Preoperative Gastric Fluid Ph and Volume, and Plasma Glucose and Lipid Homeostasis in Children. Acta Anaesthesiol Scand. 1993;37(8):783-7.
222. Maffei HV, Nobrega FJ. Gastric Ph and Microflora of Normal and Diarrhoeic Infants. Gut. 1975;16(9):719-26.
223. Meakin G, Dingwall AE, Addison GM. Effects of Fasting and Oral Premedication on the Ph and Volume of Gastric Aspirate in Children. Br J Anaesth. 1987;59(6):678-82.
224. Miclat NN, Hodgkinson R, Marx GF. Neonatal Gastric Ph. Anesth Analg. 1978;57(1):98-101.
225. Mikawa K, Nishina K, Maekawa N, Asano M, Obara H. Lansoprazole Reduces Preoperative Gastric Fluid Acidity and Volume in Children. Can J Anaesth. 1995;42(6):467-72.
226. Miller BR, Tharp JA, Issacs WB. Gastric Residual Volume in Infants and Children Following a 3-Hour Fast. J Clin Anesth. 1990;2(5):301-5.
227. Nishina K, Mikawa K, Maekawa N, Tamada M, Obara H. Omeprazole Reduces Preoperative Gastric Fluid Acidity and Volume in Children. Can J Anaesth. 1994;41(10):925-9.
228. Omari TI, Davidson GP. Multipoint Measurement of Intragastric Ph in Healthy Preterm Infants. Arch Dis Child Fetal Neonatal Ed. 2003;88(6):F517-20.

229. Rogers IM, Drainer IK, Moore MR, Buchanan KD. Plasma Gastrin in Congenitial Hypertrophic Pyloric Stenosis. A Hypothesis Disproved. Arch Dis Child. 1975;50(6):467-71.
230. Sandhar BK, Goresky GV, Maltby JR, Shaffer EA. Effect of Oral Liquids and Ranitidine on Gastric Fluid Volume and Ph in Children Undergoing Outpatient Surgery. Anesthesiology. 1989;71(3):327-30.
231. Splinter WM, Stewart JA, Muir JG. Large Volumes of Apple Juice Preoperatively Do Not Affect Gastric Ph and Volume in Children. Can J Anaesth. 1990;37(1):36-9.
232. Wakayama Y, Wilkins S, Kimura K. Is 5% Dextrose in Water a Proper Choice for Initial Postoperative Feeding in Infants? J Pediatr Surg. 1988;23(7):644-6.
233. Muller-Lissner SA, Fimmel CJ, Sonnenberg A, Will N, Muller-Duysing W, Heinzel F et al. Novel Approach to Quantify Duodenogastric Reflux in Healthy Volunteers and in Patients with Type I Gastric Ulcer. Gut. 1983;24(6):510-8.
234. Rees WD, Go VL, Malagelada JR. Simultaneous Measurement of Antroduodenal Motility, Gastric Emptying, and Duodenogastric Reflux in Man. Gut. 1979;20(11):963-70.
235. Klein S. The Use of Biorelevant Dissolution Media to Forecast the in Vivo Performance of a Drug. AAPS J. 2010;12(3):397-406.
236. Klein S, Butler J, Hempenstall JM, Reppas C, Dressman JB. Media to Simulate the Postprandial Stomach I. Matching the Physicochemical Characteristics of Standard Breakfasts. J Pharm Pharmacol. 2004;56(5):605-10.
237. Dressman JB, Amidon GL, Reppas C, Shah VP. Dissolution Testing as a Prognostic Tool for Oral Drug Absorption: Immediate Release Dosage Forms. Pharm Res. 1998;15(1):11-22.
238. Kalantzi L, Goumas K, Kalioras V, Abrahamsson B, Dressman JB, Reppas C. Characterization of the Human Upper Gastrointestinal Contents under Conditions Simulating Bioavailability/Bioequivalence Studies. Pharm Res. 2006;23(1):165-76.
239. Dressman JB, Berardi RR, Dermentzoglou LC, Russell TL, Schmaltz SP, Barnett JL et al. Upper Gastrointestinal (Gi) Ph in Young, Healthy Men and Women. Pharm Res. 1990;7(7):756-61.
240. Sondheimer JM, Clark DA, Gervaise EP. Continuous Gastric Ph Measurement in Young and Older Healthy Preterm Infants Receiving Formula and Clear Liquid Feedings. J Pediatr Gastroenterol Nutr. 1985;4(3):352-5.
241. Billeaud C, Senterre J, Rigo J. Osmolality of the Gastric and Duodenal Contents in Low Birth Weight Infants Fed Human Milk or Various Formulae. Acta Paediatr Scand. 1982;71(5):799-803.
242. Thatrimontrichai A, Janjindamai W. Postprandial Osmolality of Gastric Contents in Very Low-Birth-Weight Infants Fed Expressed Breast Milk with Additives. Southeast Asian J Trop Med Public Health. 2009;40(5):1080-6.
243. Fuchs A, Dressman JB. Composition and Physicochemical Properties of Fasted-State Human Duodenal and Jejunal Fluid: A Critical Evaluation of the Available Data. J Pharm Sci. 2014;103(11):3398-411.
244. Fredrikzon B, Olivecrona T. Decrease of Lipase and Esterase Activities in Intestinal Contents of Newborn Infants During Test Meals. Pediatr Res. 1978;12(5):631-4.
245. Gilbertson HR, Rogers EJ, Ukoumunne OC. Determination of a Practical Ph Cutoff Level for Reliable Confirmation of Nasogastric Tube Placement. JPEN J Parenter Enteral Nutr. 2011;35(4):540-4.
246. Metheny NA, Eikov R, Rountree V, Lengettie E. Clinical Research: Indicators of Feeding-Tube Placement in Neonates. Nutr Clin Pract. 1999;14(6):307-14.
247. Boehm G, Bierbach U, Senger H, Jakobsson I, Minoli I, Moro G et al. Activities of Lipase and Trypsin in Duodenal Juice of Infants Small for Gestational Age. J Pediatr Gastroenterol Nutr. 1991;12(3):324-7.

248. Boehm G, Braun W, Moro G, Minoli I. Bile Acid Concentrations in Serum and Duodenal Aspirates of Healthy Preterm Infants: Effects of Gestational and Postnatal Age. Biol Neonate. 1997;71(4):207-14.
249. Brueton MJ, Berger HM, Brown GA, Ablitt L, Iyngkaran N, Wharton BA. Duodenal Bile Acid Conjugation Patterns and Dietary Sulphur Amino Acids in the Newborn. Gut. 1978;19(2):95-8.
250. Challacombe DN, Edkins S, Brown GA. Duodenal Bile Acids in Infancy. Arch Dis Child. 1975;50(11):837-43.
251. Encrantz JC, Sjovall J. On the Bile Acids in Duodenal Contents of Infants and Children. Bile Acids and Steroids 72. Clin Chim Acta. 1959;4:793-9.
252. Glasgow JF, Dinsmore H, Molla A, Macfarlane T. A Comprehensive Study of Duodenal Bile Salts in Newborn Infants and Their Relationship to Fat Absorption. Ir J Med Sci. 1980;149(9):346-56.
253. Jarvenpaa AL. Feeding the Low-Birth-Weight Infant. Iv. Fat Absorption as a Function of Diet and Duodenal Bile Acids. Pediatrics. 1983;72(5):684-9.
254. Norman A, Strandvik B, Ojamae O. Bile Acids and Pancreatic Enzymes During Absorption in the Newborn. Acta Paediatr Scand. 1972;61(5):571-6.
255. Poley JR, Dower JC, Owen CA, Jr., Stickler GB. Bile Acids in Infants and Children. J Lab Clin Med. 1964;63:838-46.
256. Signer E, Murphy GM, Edkins S, Anderson CM. Role of Bile Salts in Fat Malabsorption of Premature Infants. Arch Dis Child. 1974;49(3):174-80.
257. Lavy U, Silverberg M, Davidson M. Role of Bile Acids in Fat Absorption in Low Birth Weights Infants. Pediatr Res. 1971;5(8):387-.
258. Clarysse S, Tack J, Lammert F, Duchateau G, Reppas C, Augustijns P. Postprandial Evolution in Composition and Characteristics of Human Duodenal Fluids in Different Nutritional States. J Pharm Sci. 2009;98(3):1177-92.
259. Srinivasan L, Bokiniec R, King C, Weaver G, Edwards AD. Increased Osmolality of Breast Milk with Therapeutic Additives. Arch Dis Child Fetal Neonatal Ed. 2004;89(6):F514-7.
260. Barbero GJ, Runge G, Fischer D, Crawford MN, Torres FE, Gyorgy P. Investigations on the Bacterial Flora, Ph, and Sugar Content in the Intestinal Tract of Infants. J Pediatr. 1952;40(2):152-63.
261. Boehm G, Bierbach U, Senger H, Jakobsson I, Minoli I, Moro G et al. Postnatal Adaptation of Lipase- and Trypsin-Activities in Duodenal Juice of Premature Infants Appropriate for Gestational Age. Biomed Biochim Acta. 1990;49(5):369-73.
262. Robinson PJ, Smith AL, Sly PD. Duodenal Ph in Cystic Fibrosis and Its Relationship to Fat Malabsorption. Dig Dis Sci. 1990;35(10):1299-304.
263. Rune SJ, Viskum K. Duodenal Ph Values in Normal Controls and in Patients with Duodenal Ulcer. Gut. 1969;10(7):569-71.
264. Challacombe DN, Brown GA, Edkins S. Duodenal Bile Acids in Infants with Protracted Diarrhoea. Arch Dis Child. 1979;54(2):131-4.
265. Harries JT, Muller DP, McCollum JP, Lipson A, Roma E, Norman AP. Intestinal Bile Salts in Cystic Fibrosis: Studies in the Patient and Experimental Animal. Arch Dis Child. 1979;54(1):19-24.
266. Armand M, Borel P, Pasquier B, Dubois C, Senft M, Andre M et al. Physicochemical Characteristics of Emulsions During Fat Digestion in Human Stomach and Duodenum. Am J Physiol. 1996;271(1 Pt 1):G172-83.

267. Hernell O, Staggers JE, Carey MC. Physical-Chemical Behavior of Dietary and Biliary Lipids During Intestinal Digestion and Absorption. 2. Phase Analysis and Aggregation States of Luminal Lipids During Duodenal Fat Digestion in Healthy Adult Human Beings. Biochemistry. 1990;29(8):2041-56.
268. Lindquist S, Hernell O. Lipid Digestion and Absorption in Early Life: An Update. Curr Opin Clin Nutr Metab Care. 2010;13(3):314-20.
269. Lambert DK, Christensen RD, Henry E, Besner GE, Baer VL, Wiedmeier SE et al. Necrotizing Enterocolitis in Term Neonates: Data from a Multihospital Health-Care System. J Perinatol. 2007;27(7):437-43.
270. Lucas A, Cole TJ. Breast Milk and Neonatal Necrotising Enterocolitis. Lancet. 1990;336(8730):1519-23.
271. Penn AH, Altshuler AE, Small JW, Taylor SF, Dobkins KR, Schmid-Schonbein GW. Digested Formula but Not Digested Fresh Human Milk Causes Death of Intestinal Cells in Vitro: Implications for Necrotizing Enterocolitis. Pediatr Res. 2012;72(6):560-7.
272. Clarysse S, Brouwers J, Tack J, Annaert P, Augustijns P. Intestinal Drug Solubility Estimation Based on Simulated Intestinal Fluids: Comparison with Solubility in Human Intestinal Fluids. Eur J Pharm Sci. 2011;43(4):260-9.
273. Augustijns P, Wuyts B, Hens B, Annaert P, Butler J, Brouwers J. A Review of Drug Solubility in Human Intestinal Fluids: Implications for the Prediction of Oral Absorption. Eur J Pharm Sci. 2014;57:322-32.
274. Hibberd CM, Brooke OG, Carter ND, Haug M, Harzer G. Variation in the Composition of Breast Milk During the First 5 Weeks of Lactation: Implications for the Feeding of Preterm Infants. Arch Dis Child. 1982;57(9):658-62.
275. Smith JD, Clinard V, Barnes CL. Pharmacists' Guide to Infant Formulas for Term Infants. J Am Pharm Assoc. 2011;51(3):e28-35; quiz e6-7.
276. Macheras PE, Reppas CI. Studies on Drug-Milk Freeze-Dried Formulations. I: Bioavailability of Sulfamethizole and Dicumarol Formulations. J Pharm Sci. 1986;75(7):692-6.
277. Juni P, Altman DG, Egger M. Systematic Reviews in Health Care: Assessing the Quality of Controlled Clinical Trials. BMJ. 2001;323(7303):42-6.
278. Chapman MJ. Pharmacology of Fenofibrate. Am J Med. 1987;83(5B):21-5.
279. Desager JP, Costermans J, Verberckmoes R, Harvengt C. Effect of Hemodialysis on Plasma Kinetics of Fenofibrate in Chronic Renal Failure. Nephron. 1982;31(1):51-4.
280. Fotaki NV, M.;. Biorelevant Dissolution Methods and Their Applications in in Vitro- in Vivo Correlations for Oral Formulations. Open Drug Deliv J. 2010;4:2-13.
281. Horter D, Dressman JB. Influence of Physicochemical Properties on Dissolution of Drugs in the Gastrointestinal Tract. Adv Drug Deliv Rev. 2001;46(1-3):75-87.
282. Marques MR. Enzymes in the Dissolution Testing of Gelatin Capsules. AAPS Pharm Sci Tech. 2014;15(6):1410-6.
283. Lipinski CA. Drug-Like Properties and the Causes of Poor Solubility and Poor Permeability. J Pharmacol Toxicol Methods. 2000;44(1):235-49.
284. Benet LZ, Hoener BA. Changes in Plasma Protein Binding Have Little Clinical Relevance. Clin Pharmacol Ther. 2002;71(3):115-21.
285. Trainor GL. The Importance of Plasma Protein Binding in Drug Discovery. Expert Opin Drug Discov. 2007;2(1):51-64.
286. Fournier T, Medjoubi NN, Porquet D. Alpha-1-Acid Glycoprotein. Biochim Biophys Acta. 2000;1482(1-2):157-71.

287. Schonfeld DL, Ravelli RB, Mueller U, Skerra A. The 1.8-a Crystal Structure of Alpha1-Acid Glycoprotein (Orosomucoid) Solved by Uv Rip Reveals the Broad Drug-Binding Activity of This Human Plasma Lipocalin. J Mol Biol. 2008;384(2):393-405.
288. Jolliet-Riant P, Boukef MF, Duche JC, Simon N, Tillement JP. The Genetic Variant a of Human Alpha 1-Acid Glycoprotein Limits the Blood to Brain Transfer of Drugs It Binds. Life Sci. 1998;62(14):PL219-26.
289. Eap CB, Cuendet C, Baumann P. Binding of D-Methadone, L-Methadone, and Dl-Methadone to Proteins in Plasma of Healthy Volunteers: Role of the Variants of Alpha 1-Acid Glycoprotein. Clin Pharmacol Ther. 1990;47(3):338-46.
290. Herve F, Gomas E, Duche JC, Tillement JP. Evidence for Differences in the Binding of Drugs to the Two Main Genetic Variants of Human Alpha 1-Acid Glycoprotein. Br J Clin Pharmacol. 1993;36(3):241-9.
291. Veering BT, Burm AG, Souverijn JH, Serree JM, Spierdijk J. The Effect of Age on Serum Concentrations of Albumin and Alpha 1-Acid Glycoprotein. Br J Clin Pharmacol. 1990;29(2):201-6.
292. Zegers I, Keller T, Schreiber W, Sheldon J, Albertini R, Blirup-Jensen S et al. Characterization of the New Serum Protein Reference Material Erm-Da470k/Ifcc: Value Assignment by Immunoassay. Clin Chem. 2010;56(12):1880-8.
293. Baudner S, Bienvenu J, Blirup-Jensen S, Carlstrom A, Johnson AM, Milford Ward A et al. The Certification of a Matrix Reference Material for Immunochemical Measurement of 14 Human Serum Proteins Crm 470. Brussels, Belgium: Community Bureau of References (BCR) of the Commission of the European Communities. 1992; Report No.: BCR/92/92.
294. Whicher JT, Ritchie RF, Johnson AM, Baudner S, Bienvenu J, Blirup-Jensen S et al. New International Reference Preparation for Proteins in Human Serum (Rpphs). Clin Chem. 1994;40(6):934-8.
295. Behr W, Schlimok G, Firchau V, Paul HA. Determination of Reference Intervals for 10 Serum Proteins Measured by Rate Nephelometry, Taking into Consideration Different Sample Groups and Different Distribution Functions. J Clin Chem Clin Biochem. 1985;23(3):157-66.
296. Röst G, Vizi Z, Kiss IZ. Impact of Non-Markovian Recovery on Network Epidemics. In: Mondaini RP, editor. Biomat 2015: Proceedings of the International Symposium on Mathematical and Computational Biology. World Scientific Publishing Company; 2016. p. 40-53.
297. Kanakoudi F, Drossou V, Tzimouli V, Diamanti E, Konstantinidis T, Germenis A et al. Serum Concentrations of 10 Acute-Phase Proteins in Healthy Term and Preterm Infants from Birth to Age 6 Months. Clin Chem. 1995;41(4):605-8.
298. Malvy DJ, Poveda JD, Debruyne M, Montagnon B, Burtschy B, Herbert C et al. Laser Immunonephelometry Reference Intervals for Eight Serum Proteins in Healthy Children. Clin Chem. 1992;38(3):394-9.
299. Ott WR. Environmental Statistics and Data Analysis. Taylor & Francis; 1994.
300. Sann L, Bienvenu J, Lahet C, Divry P, Cotte J, Bethenod M. Serum Orosomucoid Concentration in Newborn Infants. Eur J Pediatr. 1981;136(2):181-5.
301. Bonate PL. Pharmacokinetic-Pharmacodynamic Modeling and Simulation. 2nd ed. New York: Springer; 2011.
302. Philip AG, Hewitt JR. Alpha 1-Acid Glycoprotein in the Neonate with and without Infection. Biol Neonate. 1983;43(3-4):118-24.
303. Bendayan R, Pieper JA, Stewart RB, Caranasos GJ. Influence of Age on Serum Protein Binding of Propranolol. Eur J Clin Pharmacol. 1984;26(2):251-4.

304. Bienvenu J, Sann L, Bienvenu F, Lahet C, Divry P, Cotte J et al. Laser Nephelometry of Orosomucoid in Serum of Newborns: Reference Intervals and Relation to Bacterial Infections. Clin Chem. 1981;27(5):721-6.
305. Lerman J, Strong HA, LeDez KM, Swartz J, Rieder MJ, Burrows FA. Effects of Age on the Serum Concentration of Alpha 1-Acid Glycoprotein and the Binding of Lidocaine in Pediatric Patients. Clin Pharmacol Ther. 1989;46(2):219-25.
306. Meistelman C, Benhamou D, Barre J, Levron JC, Mahe V, Mazoit X et al. Effects of Age on Plasma Protein Binding of Sufentanil. Anesthesiology. 1990;72(3):470-3.
307. Pressac M, Vignoli L, Aymard P, Ingenbleek Y. Usefulness of a Prognostic Inflammatory and Nutritional Index in Pediatric Clinical Practice. Clin Chim Acta. 1990;188(2):129-36.
308. Gonzalez D, Delmore P, Bloom BT, Cotten CM, Poindexter BB, McGowan E et al. Clindamycin Pharmacokinetics and Safety in Preterm and Term Infants. Antimicrob Agents Chemother. 2016;60(5):2888-94.
309. Gonzalez D, Melloni C, Yogev R, Poindexter BB, Mendley SR, Delmore P et al. Use of Opportunistic Clinical Data and a Population Pharmacokinetic Model to Support Dosing of Clindamycin for Premature Infants to Adolescents. Clin Pharmacol Ther. 2014;96(4):429-37.
310. Smith M, Gonzalez D, Goldman J, Yogev R, Sullivan JE, Reed M et al. Pharmacokinetics of Multiple-Dose Intravenous Clindamycin in Obese Children - Poster (#4194.689). Pediatric Academic Societies Annual Meeting; San Diego, CA. 2015.
311. Asali LA, Brown KF. Naloxone Protein Binding in Adult and Foetal Plasma. Eur J Clin Pharmacol. 1984;27(4):459-63.
312. Ballou SP, Lozanski FB, Hodder S, Rzewnicki DL, Mion LC, Sipe JD et al. Quantitative and Qualitative Alterations of Acute-Phase Proteins in Healthy Elderly Persons. Age Ageing. 1996;25(3):224-30.
313. Belpaire FM, Wynant P, Van Trappen P, Dhont M, Verstraete A, Bogaert MG. Protein Binding of Propranolol and Verapamil Enantiomers in Maternal and Foetal Serum. Br J Clin Pharmacol. 1995;39(2):190-3.
314. Blain PG, Mucklow JC, Rawlins MD, Roberts DF, Routledge PA, Shand DG. Determinants of Plasma Alpha 1-Acid Glycoprotein (Aag) Concentrations in Health. Br J Clin Pharmacol. 1985;20(5):500-2.
315. Davis D, Grossman SH, Kitchell BB, Shand DG, Routledge PA. The Effects of Age and Smoking on the Plasma Protein Binding of Lignocaine and Diazepam. Br J Clin Pharmacol. 1985;19(2):261-5.
316. Kawerk N, Succari-Aderschlag M, Foglietti MJ. Microheterogeneity of Alpha 1-Acid Glycoprotein in Healthy Elderly Subjects: Patterns Obtained by Crossed Affino-Immunoelectrophoresis. Clin Chim Acta. 1991;202(1-2):65-72.
317. Kishino S, Nomura A, Di ZS, Sugawara M, Iseki K, Kakinoki S et al. Alpha-1-Acid Glycoprotein Concentration and the Protein Binding of Disopyramide in Healthy Subjects. J Clin Pharmacol. 1995;35(5):510-4.
318. Lee SK, Thibeault DW, Heiner DC. Alpha 1-Antitrypsin and Alpha 1-Acid Glycoprotein Levels in the Cord Blood and Amniotic Fluid of Infants with Respiratory Distress Syndrome. Pediatr Res. 1978;12(7):775-7.
319. Meuldermans W, Woestenborghs R, Noorduin H, Camu F, van Steenberge A, Heykants J. Protein Binding of the Analgesics Alfentanil and Sufentanil in Maternal and Neonatal Plasma. Eur J Clin Pharmacol. 1986;30(2):217-9.
320. Milman N, Graudal N, Andersen HC. Acute Phase Reactants in the Elderly. Clin Chim Acta. 1988;176(1):59-62.

321. Raubenstine DA, Ballantine TV, Greecher CP, Webb SL. Neonatal Serum Protein Levels as Indicators of Nutritional Status: Normal Values and Correlation with Anthropometric Data. J Pediatr Gastroenterol Nutr. 1990;10(1):53-61.
322. Routledge PA, Stargel WW, Kitchell BB, Barchowsky A, Shand DG. Sex-Related Differences in the Plasma Protein Binding of Lignocaine and Diazepam. Br J Clin Pharmacol. 1981;11(3):245-50.
323. Succari M, Foglietti MJ, Percheron F. Microheterogeneity of Alpha 1-Acid Glycoprotein: Variation During the Menstrual Cycle in Healthy Women, and Profile in Women Receiving Estrogen-Progestogen Treatment. Clin Chim Acta. 1990;187(3):235-41.
324. Winkel P, Statland BE, Nielsen MK. Biologic and Analytic Components of Variation of Concentration Values of Selected Serum Proteins. Scand J Clin Lab Invest. 1976;36(6):531-7.
325. Wilson AS, Stiller RL, Davis PJ, Fedel G, Chakravorti S, Israel BA et al. Fentanyl and Alfentanil Plasma Protein Binding in Preterm and Term Neonates. Anesth Analg. 1997;84(2):315-8.
326. Lin LI. A Concordance Correlation Coefficient to Evaluate Reproducibility. Biometrics. 1989;45(1):255-68.
327. Gotoh H, Ishikawa N, Shioiri T, Hattori Y, Nomura H, Ogawa J. Diagnostic Significance of Serum Orosomucoid Level in Bacterial Infections During Neonatal Period. Acta Paediatr Scand. 1973;62(6):629-32.
328. Benedek IH, Blouin RA, McNamara PJ. Serum Protein Binding and the Role of Increased Alpha 1-Acid Glycoprotein in Moderately Obese Male Subjects. Br J Clin Pharmacol. 1984;18(6):941-6.
329. Maharaj AR, Barrett JS, Edginton AN. A Workflow Example of Pbpk Modeling to Support Pediatric Research and Development: Case Study with Lorazepam. AAPS J. 2013;15(2):455-64.
330. Johnson TN, Rostami-Hodjegan A, Tucker GT. Prediction of the Clearance of Eleven Drugs and Associated Variability in Neonates, Infants and Children. Clin Pharmacokinet. 2006;45(9):931-56.
331. Johnson JA, Livingston TN. Differences between Blacks and Whites in Plasma Protein Binding of Drugs. Eur J Clin Pharmacol. 1997;51(6):485-8.
332. Zhou HH, Adedoyin A, Wilkinson GR. Differences in Plasma Binding of Drugs between Caucasians and Chinese Subjects. Clin Pharmacol Ther. 1990;48(1):10-7.
333. Wakefield J. Ecologic Studies Revisited. Annu Rev Public Health. 2008;29:75-90.
334. Imbruvica: Product Monograph. Janssen Biotech Inc. 2013. http://www.imbruvica.com/downloads/Prescribing_Information.pdf. Accessed 17/07/2014.
335. Siccardi M, Marzolini C, Seden K, Almond L, Kirov A, Khoo S et al. Prediction of Drug-Drug Interactions between Various Antidepressants and Efavirenz or Boosted Protease Inhibitors Using a Physiologically Based Pharmacokinetic Modelling Approach. Clin Pharmacokinet. 2013;52(7):583-92.
336. Yeo KR, Kenny JR, Rostami-Hodjegan A. Application of in Vitro-in Vivo Extrapolation (Ivive) and Physiologically Based Pharmacokinetic (Pbpk) Modelling to Investigate the Impact of the Cyp2c8 Polymorphism on Rosiglitazone Exposure. Eur J Clin Pharmacol. 2013;69(6):1311-20.
337. Li GF, Wang K, Chen R, Zhao HR, Yang J, Zheng QS. Simulation of the Pharmacokinetics of Bisoprolol in Healthy Adults and Patients with Impaired Renal Function Using Whole-Body Physiologically Based Pharmacokinetic Modeling. Acta Pharmacol Sin. 2012;33(11):1359-71.

338. Cronin CG, Delappe E, Lohan DG, Roche C, Murphy JM. Normal Small Bowel Wall Characteristics on Mr Enterography. Eur J Radiol. 2010;75(2):207-11.
339. Basic Anatomical and Physiological Data for Use in Radiological Protection: Reference Values. A Report of Age- and Gender-Related Differences in the Anatomical and Physiological Characteristics of Reference Individuals. Icrp Publication 89. Ann ICRP. 2002;32(3-4):5-265.
340. Hansen NT, Kouskoumvekaki I, Jorgensen FS, Brunak S, Jonsdottir SO. Prediction of Ph-Dependent Aqueous Solubility of Druglike Molecules. J Chem Inf Model. 2006;46(6):2601-9.
341. Nicolaides E, Symillides M, Dressman JB, Reppas C. Biorelevant Dissolution Testing to Predict the Plasma Profile of Lipophilic Drugs after Oral Administration. Pharm Res. 2001;18(3):380-8.
342. Steingoetter A, Fox M, Treier R, Weishaupt D, Marincek B, Boesiger P et al. Effects of Posture on the Physiology of Gastric Emptying: A Magnetic Resonance Imaging Study. Scand J Gastroenterol. 2006;41(10):1155-64.
343. Shojaei AH, Berner B, Xiaoling L. Transbuccal Delivery of Acyclovir: I. In Vitro Determination of Routes of Buccal Transport. Pharm Res. 1998;15(8):1182-8.
344. Hsu FH, Prueksaritanont T, Lee MG, Chiou WL. The Phenomenon and Cause of the Dose-Dependent Oral Absorption of Chlorothiazide in Rats: Extrapolation to Human Data Based on the Body Surface Area Concept. J Pharmacokinet Biopharm. 1987;15(4):369-86.
345. Resetarits DE, Bates TR. Apparent Dose-Dependent Absorption of Chlorothiazide in Dogs. J Pharmacokinet Biopharm. 1979;7(5):463-70.
346. Guidance for Industry: Waiver of in Vivo Bioavailability and Bioequivalence Studies for Immediate-Release Solid Oral Dosage Forms Based on a Biopharmaceutics Classification System. U.S.Department of Health and Human Services. Food and Drug Administration. Center for Drug Evaluation and Research.; 2000.
347. Vergin H, Kikuta C, Mascher H, Metz R. Pharmacokinetics and Bioavailability of Different Formulations of Aciclovir. Arzneimittelforschung. 1995;45(4):508-15.
348. de Miranda P, Good SS, Laskin OL, Krasny HC, Connor JD, Lietman PS. Disposition of Intravenous Radioactive Acyclovir. Clin Pharmacol Ther. 1981;30(5):662-72.
349. Balon K, Riebesehl BU, Muller BW. Drug Liposome Partitioning as a Tool for the Prediction of Human Passive Intestinal Absorption. Pharm Res. 1999;16(6):882-8.
350. Jung D, Lam HD, Chu M. Absorption and Disposition Kinetics of Chlorothiazide in Protein-Calorie Malnutrition. Biopharm Drug Dispos. 1990;11(1):53-60.
351. Kratochwil NA, Huber W, Muller F, Kansy M, Gerber PR. Predicting Plasma Protein Binding of Drugs: A New Approach. Biochem Pharmacol. 2002;64(9):1355-74.
352. Osman MA, Patel RB, Irwin DS, Craig WA, Welling PG. Bioavailability of Chlorothiazide from 50, 100, and 250 Mg Solution Doses. Biopharm Drug Dispos. 1982;3(2):89-94.
353. Welling PG, Barbhaiya RH. Influence of Food and Fluid Volume on Chlorothiazide Bioavailability: Comparison of Plasma and Urinary Excretion Methods. J Pharm Sci. 1982;71(1):32-5.
354. Box KJ, Volgyi G, Baka E, Stuart M, Takacs-Novak K, Comer JE. Equilibrium Versus Kinetic Measurements of Aqueous Solubility, and the Ability of Compounds to Supersaturate in Solution--a Validation Study. J Pharm Sci. 2006;95(6):1298-307.
355. Shono Y, Jantratid E, Dressman JB. Precipitation in the Small Intestine May Play a More Important Role in the in Vivo Performance of Poorly Soluble Weak Bases in the Fasted State: Case Example Nelfinavir. Eur J Pharm Biopharm. 2011;79(2):349-56.

356. Laskin OL, Longstreth JA, Saral R, de Miranda P, Keeney R, Lietman PS. Pharmacokinetics and Tolerance of Acyclovir, a New Anti-Herpesvirus Agent, in Humans. Antimicrob Agents Chemother. 1982;21(3):393-8.
357. Whitley RJ, Blum MR, Barton N, de Miranda P. Pharmacokinetics of Acyclovir in Humans Following Intravenous Administration. A Model for the Development of Parenteral Antivirals. Am J Med. 1982;73(1A):165-71.
358. Gustafson JH, Benet LZ. Saturable Kinetics of Intravenous Chlorothiazide in the Rhesus Monkey. J Pharmacokinet Biopharm. 1981;9(4):461-76.
359. Shah VP, Walker MA, Hunt JP, Schuirmann D, Prasad VK, Cabana BE. Thiazides Xi: Partitioning of Chlorothiazide in Red Blood Cells after Oral Administration. Biopharm Drug Dispos. 1984;5(1):55-62.
360. Arnal J, Gonzalez-Alvarez I, Bermejo M, Amidon GL, Junginger HE, Kopp S et al. Biowaiver Monographs for Immediate Release Solid Oral Dosage Forms: Aciclovir. J Pharm Sci. 2008;97(12):5061-73.
361. Sutton SC. Role of Physiological Intestinal Water in Oral Absorption. AAPS J. 2009;11(2):277-85.
362. Sugano K. Fraction of a Dose Absorbed Estimation for Structurally Diverse Low Solubility Compounds. Int J Pharm. 2011;405(1-2):79-89.
363. Gandhi SV, Rodriguez W, Khan M, Polli JE. Considerations for a Pediatric Biopharmaceutics Classification System (Bcs): Application to Five Drugs. AAPS Pharm Sci Tech. 2014;15(3):601-11.
364. Gibaldi M, McNamara PJ. Apparent Volumes of Distribution and Drug Binding to Plasma Proteins and Tissues. Eur J Clin Pharmacol. 1978;13(5):373-80.
365. Rowland M. Protein Binding and Drug Clearance. Clin Pharmacokinet. 1984;9 Suppl 1:10-7.
366. Schmidt S, Gonzalez D, Derendorf H. Significance of Protein Binding in Pharmacokinetics and Pharmacodynamics. J Pharm Sci. 2010;99(3):1107-22.
367. Shaddy RE, Denne SC, Committee on D, Committee on Pediatric R. Clinical Report--Guidelines for the Ethical Conduct of Studies to Evaluate Drugs in Pediatric Populations. Pediatrics. 2010;125(4):850-60.
368. McOmber ME, Ou CN, Shulman RJ. Effects of Timing, Sex, and Age on Site-Specific Gastrointestinal Permeability Testing in Children and Adults. J Pediatr Gastroenterol Nutr. 2010;50(3):269-75.
369. Catassi C, Bonucci A, Coppa GV, Carlucci A, Giorgi PL. Intestinal Permeability Changes During the First Month: Effect of Natural Versus Artificial Feeding. J Pediatr Gastroenterol Nutr. 1995;21(4):383-6.
370. Rouwet EV, Heineman E, Buurman WA, ter RG, Ramsay G, Blanco CE. Intestinal Permeability and Carrier-Mediated Monosaccharide Absorption in Preterm Neonates During the Early Postnatal Period. Pediatr Res. 2002;51(1):64-70.
371. Weaver LT, Laker MF, Nelson R. Intestinal Permeability in the Newborn. Arch Dis Child. 1984;59(3):236-41.
372. Beach RC, Menzies IS, Clayden GS, Scopes JW. Gastrointestinal Permeability Changes in the Preterm Neonate. Arch Dis Child. 1982;57(2):141-5.
373. Dressman JB, Reppas.C. Oral Drug Absorption: Prediction and Assessment. 2nd ed. New York: Informa Healthcare; 2010.
374. Murakami T, Takano M. Intestinal Efflux Transporters and Drug Absorption. Expert Opin Drug Metab Toxicol. 2008;4(7):923-39.

375. Fakhoury M, Litalien C, Medard Y, Cave H, Ezzahir N, Peuchmaur M et al. Localization and Mrna Expression of Cyp3a and P-Glycoprotein in Human Duodenum as a Function of Age. Drug Metab Dispos. 2005;33(11):1603-7.
376. Miki Y, Suzuki T, Tazawa C, Blumberg B, Sasano H. Steroid and Xenobiotic Receptor (Sxr), Cytochrome P450 3a4 and Multidrug Resistance Gene 1 in Human Adult and Fetal Tissues. Mol Cell Endocrinol. 2005;231(1-2):75-85.
377. Levy RH, Lockard JS, Green JR, Friel P, Martis L. Pharmacokinetics of Carbamazepine in Monkeys Following Intravenous and Oral Administration. J Pharm Sci. 1975;64(2):302-7.
378. Levy RH, Moreland TA, Morselli PL, Guyot M, Brachet-Liermain A, Loiseau P. Carbamazepine/Valproic Acid Interaction in Man and Rhesus Monkey. Epilepsia. 1984;25(3):338-45.
379. Pelkonen O, Myllynen P, Taavitsainen P, Boobis AR, Watts P, Lake BG et al. Carbamazepine: A 'Blind' Assessment of Cvp-Associated Metabolism and Interactions in Human Liver-Derived in Vitro Systems. Xenobiotica. 2001;31(6):321-43.
380. MacKichan JJ, Zola EM. Determinants of Carbamazepine and Carbamazepine 10,11-Epoxide Binding to Serum Protein, Albumin and Alpha 1-Acid Glycoprotein. Br J Clin Pharmacol. 1984;18(4):487-93.
381. Wada JA, Troupin AS, Friel P, Remick R, Leal K, Pearmain J. Pharmacokinetic Comparison of Tablet and Suspension Dosage Forms of Carbamazepine. Epilepsia. 1978;19(3):251-5.
382. Bass J, Miles MV, Tennison MB, Holcombe BJ, Thorn MD. Effects of Enteral Tube Feeding on the Absorption and Pharmacokinetic Profile of Carbamazepine Suspension. Epilepsia. 1989;30(3):364-9.
383. Chiou WL, Riegelman S. Absorption Characteristics of Solid Dispersed and Micronized Griseofulvin in Man. J Pharm Sci. 1971;60(9):1376-80.
384. Schafer-Korting M, Korting HC, Mutschler E. Human Plasma and Skin Blister Fluid Levels of Griseofulvin Following a Single Oral Dose. Eur J Clin Pharmacol. 1985;29(1):109-13.
385. Symchowicz S, Wong KK. Metabolism of Griseofulvin-14c; Studies in Vitro. Biochem Pharmacol. 1966;15(10):1601-6.
386. Lin CC, Magat J, Chang R, McGlotten J, Symchowicz S. Absorption, Metabolism and Excretion of 14c-Griseofulvin in Man. J Pharmacol Exp Ther. 1973;187(2):415-22.
387. Ogunbona FA, Smith IF, Olawoye OS. Fat Contents of Meals and Bioavailability of Griseofulvin in Man. J Pharm Pharmacol. 1985;37(4):283-4.
388. Weston WL, Thorne EG. Two Cases of Tinea in the Neonate Treated Successfully with Griseofulvin. Clin Pediatr. 1977;16(7):601-2.
389. Butler JM, Dressman JB. The Developability Classification System: Application of Biopharmaceutics Concepts to Formulation Development. J Pharm Sci. 2010;99(12):4940-54.
390. Sjogren E, Dahlgren D, Roos C, Lennernas H. Human in Vivo Regional Intestinal Permeability: Quantitation Using Site-Specific Drug Absorption Data. Mol Pharm. 2015;12(6):2026-39.

Appendix A

Appendix A Table 1 – Lactulose H2 Breath Tests – 2nd Order Meta-Regression Model

Summary Statistics	k=14	$Q_{M\ (df=2)}$= 0.5693 (p = 0.7523)		I^2 = 92.74%	R^2 = 0.00%
	Estimate	Standard Error	p–Value	95% CI (lower)	95% CI (upper)
Fixed Effects					
Intercept (B_0)	72.2331	7.2767	**<0.0001**	57.9711	86.4951
Age (B_1)	-0.5473	0.8123	0.5005	-2.1395	1.0449
Age^2 (B_2)	0.0202	0.0688	0.7692	-0.1147	0.1551
Random Effects					
Between study variance (τ^2)	265.7347	133.4775	-	-	-
Tau (τ)	16.3014	-	-	-	-

Appendix A Table 2 - Lactulose H2 Breath Tests – 3rd Order Meta-Regression Model

Summary Statistics	k=14	$Q_{M\ (df=3)}$= 2.2215 (p = 0.5277)		I^2 = 92.62%	R^2 = 0.00%
	Estimate	Standard Error	p–Value	95% CI (lower)	95% CI (upper)
Fixed Effects					
Intercept (B_0)	71.9471	7.1014	**<0.0001**	58.0286	85.8656
Age (B_1)	1.0215	1.4616	0.4846	-1.8432	3.8862
Age^2 (B_2)	0.1263	0.1072	0.2388	-0.0838	0.3364
Age^3 (B_3)	-0.0115	0.0090	0.2023	-0.0292	0.0062
Random Effects					
Between study variance (τ^2)	250.4728	132.6760	-	-	-
Tau (τ)	15.8263	-	-	-	-

Appendix A Figure 1 - OCTT as a function of age for investigations employing lactulose H_2 breath testing in normal subjects free of GI disease (open circles). The diameter of each circle is proportional to the $1/(Variance_i)^{1/2}$. Estimates of OCTT based on meta-regression models with age as a (A) 2nd order polynomial and (B) 3rd order polynomial regressor have been superimposed for reference (mean – solid line; 95% CI – dotted lines).

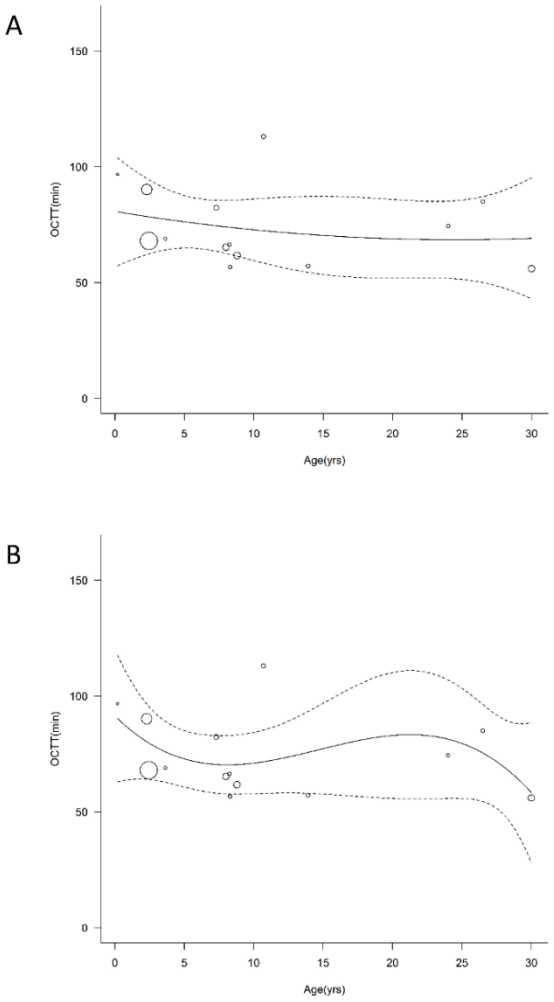

Appendix A Table 3 - Scintigraphy and Other Techniques – 2nd Order Meta-Regression Model

Summary Statistics	k= 38	$Q_{M\ (df=3)}$= 19.1390 (p = 0.0003)		I^2 = 84.69%	R^2 = 38.15%
	Estimate	Standard Error	p–Value	95% CI (lower)	95% CI (upper)
Fixed Effects					
Intercept (B_0)	209.1456	8.7541	**<0.0001**	191.9879	226.3032
Measurement Method (B_1)	63.3489	14.5391	**<0.0001**	34.8527	91.8451
Age (B_2)	0.5571	0.5282	0.2916	-0.4782	1.5925
Age^2 (B_3)	-0.0140	0.0235	0.5510	-0.0601	0.0321
Random Effects					
Between study variance (τ^2)	1193.9761	383.0047	-	-	-
Tau (τ)	34.5540	-	-	-	-

Appendix A Table 4 - Scintigraphy and Other Techniques – 3rd Order Meta-Regression Model

Summary Statistics	k=38	$Q_{M\ (df=4)}$= 18.5941 (p = 0.0009)		I^2 = 85.16%	R^2 = 35.88%
	Estimate	Standard Error	p–Value	95% CI (lower)	95% CI (upper)
Fixed Effects					
Intercept (B_0)	209.1322	8.8842	**<0.0001**	191.7194	226.5450
Measurement Method (B_1)	62.8645	15.1339	**<0.0001**	33.2027	92.5264
Age (B_2)	0.6653	0.9135	0.4664	-1.1252	2.4558
Age^2 (B_3)	-0.0112	0.0307	0.7150	-0.0714	0.0489
Age^3 (B_4)	-0.0002	0.0013	0.8829	-0.0028	0.0024
Random Effects					
Between study variance (τ^2)	1237.7908	399.9655	-	-	-
Tau (τ)	35.1823	-	-	-	-

Appendix A Figure 2 - SITT or OCTT as a function of age for investigations employing scintigraphy (black circles) and other measurement techniques (open circles) in normal subjects free of GI disease. The diameter of each circle is proportional to the $1/(Variance_i)^{1/2}$. Estimates of mean intestinal transit time based on meta-regression models with age as a (A) 2nd order polynomial and (B) 3rd order polynomial regressor have been separately superimposed for studies utilizing scintigraphy (solid line) and other measurement techniques (dotted line).

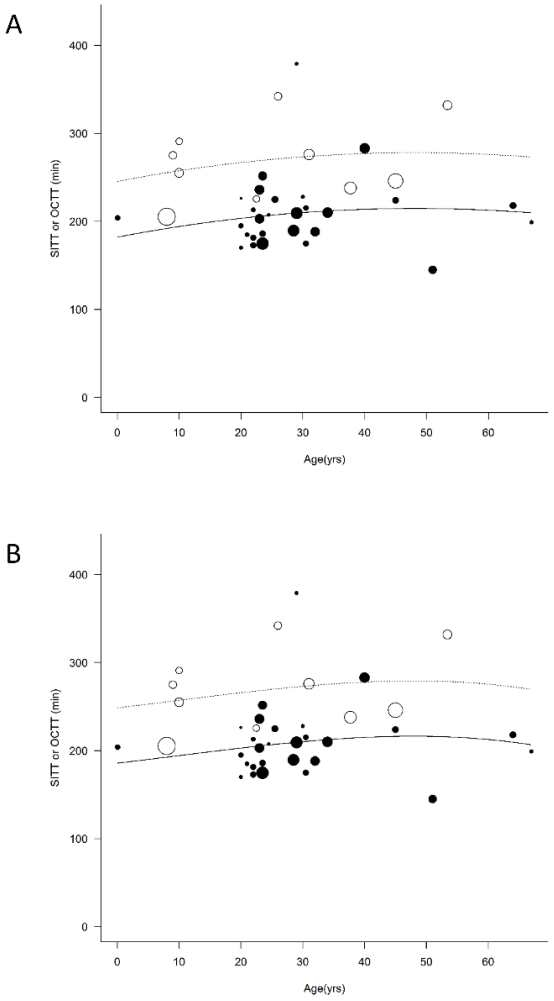

Appendix A Table 5 - Capsule Endoscopy Studies – 2nd Order Meta-Regression Model

Summary Statistics	k=16	$Q_{M\ (df=2)}$= 12.1807 (p = 0.0023)		I^2 = 91.64%	R^2 = 46.87%
	Estimate	Standard Error	p–Value	95% CI (lower)	95% CI (upper)
Fixed Effects					
Intercept (B_0)	230.2096	21.5577	**<0.0001**	187.9573	272.4618
Age (B_1)	-0.8142	0.3922	**0.0379**	-1.5830	-0.0455
Age^2 (B_2)	0.0744	0.0369	**0.0435**	0.0022	0.1466
Random Effects					
Between study variance (τ^2)	825.9859	416.7517	-	-	-
Tau (τ)	28.7400	-	-	-	-

Appendix A Table 6 - Capsule Endoscopy Studies – 3rd Order Meta-Regression Model

Summary Statistics	k=16	$Q_{M\ (df=3)}$= 21.6888 (p < 0.0001)		I^2 = 87.87%	R^2 = 66.18%
	Estimate	Standard Error	p–Value	95% CI (lower)	95% CI (upper)
Fixed Effects					
Intercept (B_0)	210.9497	20.1139	**<0.0001**	171.5273	250.3721
Age (B_1)	1.8768	1.0820	0.0828	-0.2440	3.9976
Age^2 (B_2)	0.0924	0.0325	**0.0045**	0.0286	0.1562
Age^3 (B_3)	-0.0041	0.0015	**0.0085**	-0.0071	-0.0010
Random Effects					
Between study variance (τ^2)	525.6570	295.9862	-	-	-
Tau (τ)	22.9272	-	-	-	-

Appendix A Figure 3 - SITT as a function of age for investigations employing capsule endoscopy (open circles). The diameter of each circle is proportional to the 1/ (Variance$_i$)$^{1/2}$. Estimates of SITT based on meta-regression models with age as a (A) 2nd order polynomial and (B) 3rd order polynomial regressor have been superimposed for reference (mean – solid line; 95% CI – dotted lines).

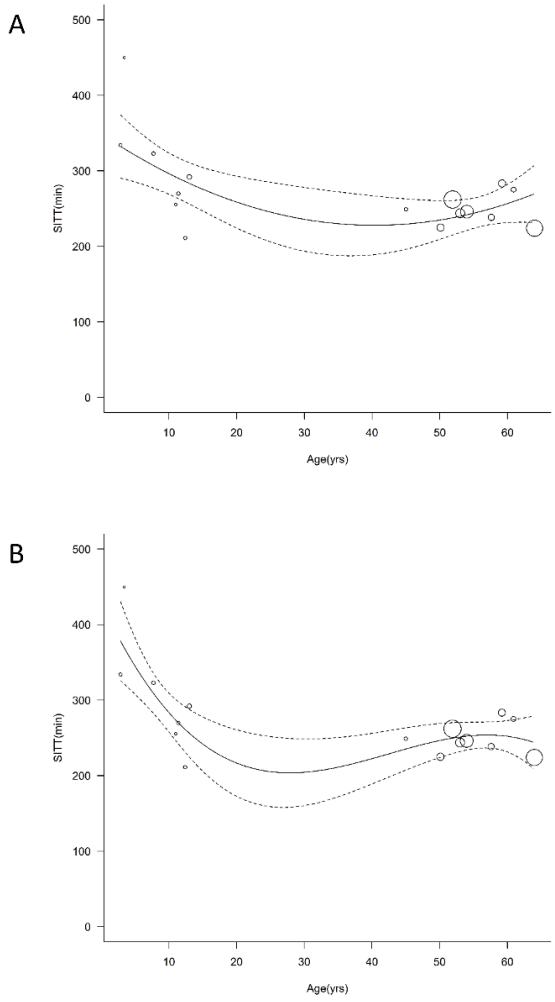

Appendix A Table 7 - Scintigraphy and Other Techniques – 1st Order (Linear) Meta-Regression Model with Interaction Terms

Summary Statistics	k=38	$Q_{M\ (df=3)}$= 19.5837 (p = 0.0002)		I^2 = 84.48%	R^2 = 38.85%
	Estimate	Standard Error	p–Value	95% CI (lower)	95% CI (upper)
Fixed Effects					
Intercept (B_0)	207.4751	7.9619	**<0.0001**	191.8700	223.0802
Measurement Method (B_1)	62.3044	14.1997	**<0.0001**	34.4735	90.1354
Age (B_2)	0.1117	0.6107	0.8549	-1.0854	1.3087
Age*Measurement Method (B_3)	0.7562	0.9599	0.4309	-1.1253	2.6376
Random Effects					
Between study variance (τ^2)	1180.4401	380.7146	-	-	-
Tau (τ)	34.3575	-	-	-	-

Appendix A Table 8 - Scintigraphy and Other Techniques – 2nd Order Meta-Regression Model with Interaction Terms

Summary Statistics	k= 38	$Q_{M\ (df=5)}$= 18.8281 (p = 0.0021)		I^2 = 85.13%	R^2 = 34.49%
	Estimate	Standard Error	p–Value	95% CI (lower)	95% CI (upper)
Fixed Effects					
Intercept (B_0)	209.5920	9.1776	**<0.0001**	191.6043	227.5797
Measurement Method (B_1)	55.4072	21.5381	**0.0101**	13.1933	97.6211
Age (B_2)	0.3505	0.7896	0.6572	-1.1971	1.8981
Age^2 (B_3)	-0.0144	0.0290	0.6207	-0.0713	0.0425
Age*Measurement Method (B_4)	0.5113	1.0988	0.6417	-1.6422	2.6649
Age^2*Measurement Method (B_5)	0.0336	0.0670	0.6157	-0.0977	0.1650
Random Effects					
Between study variance (τ^2)	1264.6466	416.3814	-	-	-
Tau (τ)	35.5619	-	-	-	-

Appendix A Table 9 - Scintigraphy and Other Techniques – 3rd Order Meta-Regression Model with Interaction Terms

Summary Statistics	k=38	$Q_{M\ (df=7)}$= 25.2448 (p = 0.0007)		I^2 = 82.97%	R^2 = 42.44%
	Estimate	Standard Error	p–Value	95% CI (lower)	95% CI (upper)
Fixed Effects					
Intercept (B_0)	209.3306	8.7403	**<0.0001**	192.2000	226.4612
Measurement Method (B_1)	68.6123	21.3590	**0.0013**	26.7495	110.4752
Age (B_2)	0.6738	1.2194	0.5806	-1.7162	3.0637
Age^2 (B_3)	-0.0078	0.0335	0.8162	-0.0735	0.0579
Age^3 (B_4)	-0.0005	0.0014	0.7322	-0.0033	0.0023
Age*Measurement Method (B_5)	-4.6744	2.7732	0.0919	-10.1098	0.7611
Age^2*Measurement Method (B_6)	-0.0474	0.0755	0.5301	-0.1954	0.1006
Age^3*Measurement Method (B_7)	0.0123	0.0060	**0.0391**	0.0006	0.0240
Random Effects					
Between study variance (τ^2)	1111.1671	389.1959	-	-	-
Tau (τ)	33.3342	-	-	-	-

Appendix A Figure 4 - SITT or OCTT as a function of age for investigations employing scintigraphy (black circles) and other measurement techniques (open circles) in normal subjects free of GI disease. The diameter of each circle is proportional to the $1/(Variance_i)^{1/2}$. Mean estimates of SITT based on a meta-regression model with age as a linear regressor and an interaction term (measurement method * age) have been separately superimposed for studies utilizing scintigraphy (solid line) and other measurement techniques (dotted line).

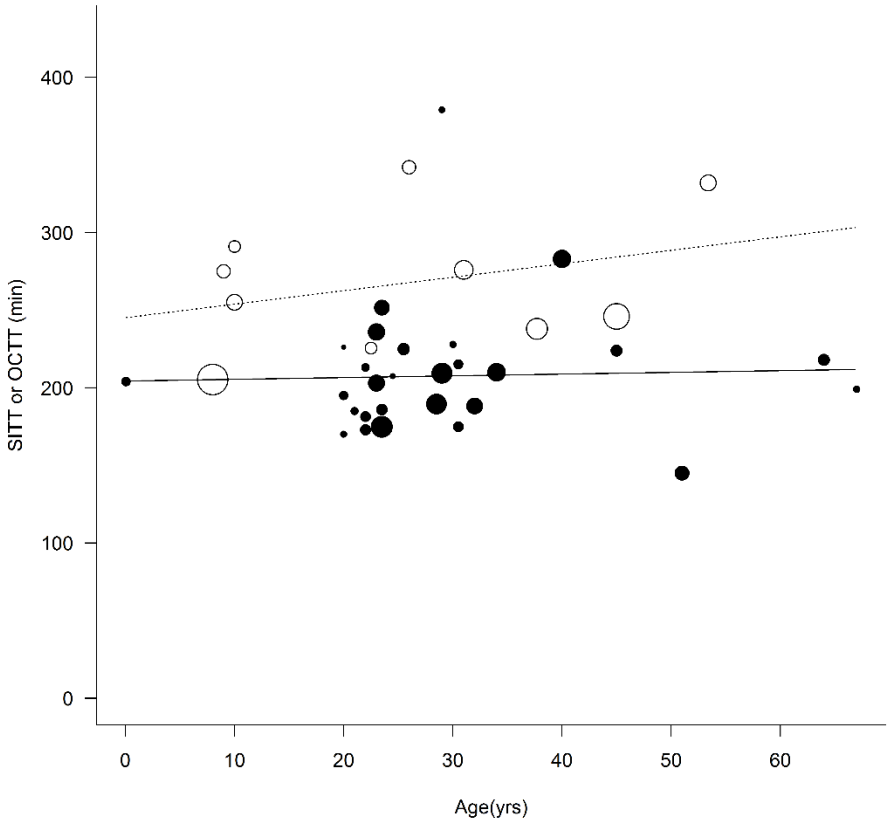

Appendix A Figure 5 - SITT or OCTT as a function of age for investigations employing scintigraphy (black circles) and other measurement techniques (open circles) in normal subjects free of GI disease. The diameter of each circle is proportional to the $1/(Variance_i)^{1/2}$. Mean estimates of SITT based on a meta-regression model with age as a 2nd order regressor and interaction terms between each order of age and measurement method have been separately superimposed for studies utilizing scintigraphy (solid line) and other measurement techniques (dotted line).

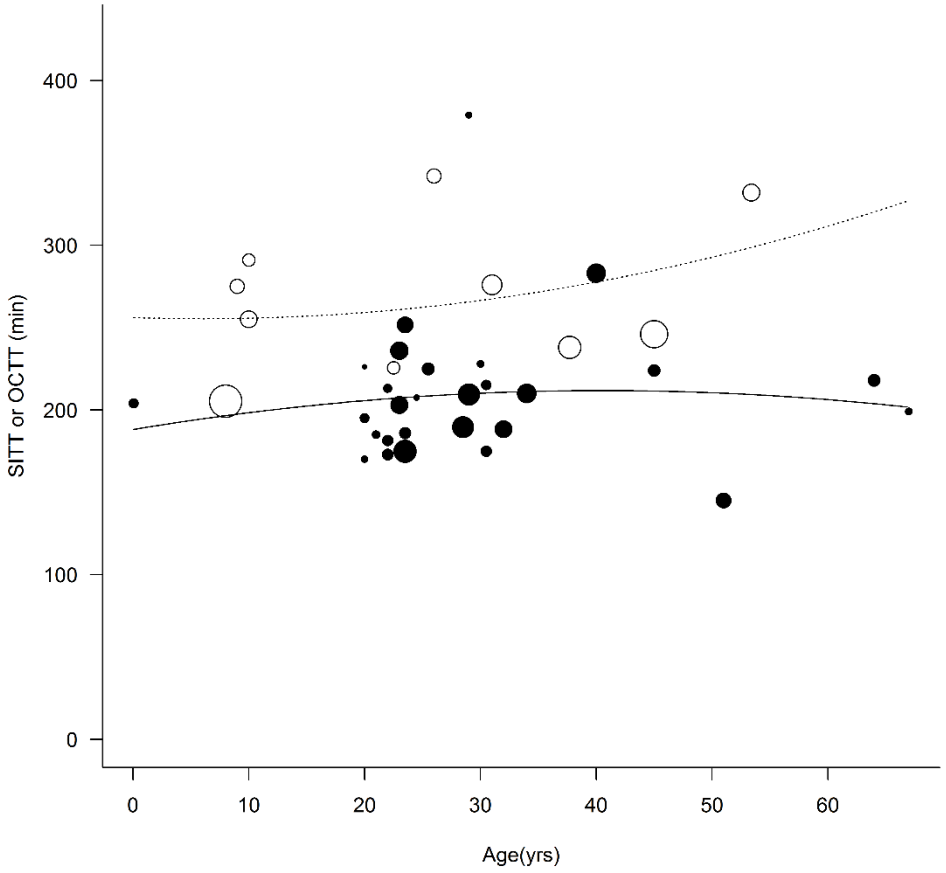

Appendix A Figure 6 - SITT or OCTT as a function of age for investigations employing scintigraphy (black circles) and other measurement techniques (open circles) in normal subjects free of GI disease. The diameter of each circle is proportional to the $1/(Variance_i)^{1/2}$. Mean estimates of SITT based on a meta-regression model with age as a 3rd order regressor and interaction terms between each order of age and measurement method have been separately superimposed for studies utilizing scintigraphy (solid line) and other measurement techniques (dotted line).